UNIVERSIDADE DE LISBOA
FACULDADE DE CIÊNCIAS
DEPARTAMENTO DE QUÍMICA E BIOQUÍMICA

STUDY OF THE MOLECULAR MECHANISM USED BY THE PEPTIDIC VECTOR PEP-1 TO INTRODUCE PROTEINS INSIDE CELLS

Sónia Troeira Henriques

DOUTORAMENTO EM BIOQUÍMICA
(Especialidade de Biofísica Molecular)

2007

UNIVERSIDADE DE LISBOA
FACULDADE DE CIÊNCIAS
DEPARTAMENTO DE QUÍMICA E BIOQUÍMICA

STUDY OF THE MOLECULAR MECHANISM USED BY THE PEPTIDIC VECTOR PEP-1 TO INTRODUCE PROTEINS INSIDE CELLS

Sónia Troeira Henriques

Tese orientada pelo Prof. Doutor Miguel Augusto Rico Botas Castanho

DOUTORAMENTO EM BIOQUÍMICA
(Especialidade de Biofísica Molecular)

2007

Prefácio

O objecto de estudo desta tese foi o mecanismo de acção de um péptido vector, pep-1, capaz de introduzir proteínas dentro de células. Para a realização do trabalho usaram-se essencialmente técnicas espectroscópicas e de microscopia. Do trabalho realizado resultaram os seguintes artigos já publicados:

1) Henriques S.T., Castanho M.A.R.B. (2004) Consequences of nonlytic membrane perturbation to the translocation of the cell penetrating peptide pep-1 in lipidic vesicles, *Biochemistry*, 43, 9716-9724.

2) Henriques S.T., Castanho M.A.R.B. (2005) Environmental factors that enhance the action of the cell penetrating peptide pep-1. A spectroscopic study using lipidic vesicles, *Biochim. Biophys. Acta*, 1669, 75-86.

3) Henriques S.T., Costa J., Castanho M.A.R.B. (2005) Translocation of β-Galactosidase mediated by the cell-penetrating peptide pep-1 into lipid vesicles and human HeLa cells is driven by membrane electrostatic potential, *Biochemistry*, 44, 10189-98.

4) Henriques S.T., Costa J., Castanho M.A.R.B. (2005) Re-evaluating the role of strongly charged sequences in amphipathic cell-penetrating peptides. A fluorescence study using Pep-1, *FEBS Lett*., 579, 4498-502.

5) Henriques S.T., Melo M.N, Castanho M.A.R.B. (2006) Cell-Penetrating Peptides and Antimicrobial Peptides: how different are they?, *Biochem J,* 399*,* 1-7.

6) Henriques S.T., Melo M.N, Castanho M.A.R.B. (2007) How to address CPP and AMP translocation? Methods to detect and quantify peptide internalization *in vitro* and *in vivo*, *Mol Memb Biol,* 24*,* 173-184.

7) Henriques S.T., Quintas A., Bagatolli L.A., Homblé F., Castanho M.A.R.B. (2007) Energy-independent translocation of cell-penetrating peptides occurs without formation of pores. A biophysical study with pep-1, *Mol Memb Biol,* 24, 282-293.

8) Henriques S.T., Castanho M.A.R.B. (2007) Translocation or membrane disintegration? Implication of peptide-membrane interactions in pep-1 activity, *J Pep Science*, no prelo.

Como a maior parte do trabalho experimental relativo ao estudo do pep-1 já foi publicado em revistas internacionais, optou-se pela sua apresentação com recurso aos artigos científicos e pela redacção da tese em língua inglesa.

O manuscrito está dividido em oito capítulos. O primeiro capítulo apresenta uma introdução geral ao tema da internalização de macromoléculas dentro das células, com particular destaque para os péptidos vectores, vulgarmente designados por *cell penetrating peptides* (CPPs) e ao pep-1 como objecto de estudo. No segundo capítulo estão descritos estudos de interacção péptido-membrana realizados com modelos de membrana, os quais foram publicados em dois artigos (artigos 1 e 2, ver lista acima). A totalidade destes estudos foi realizada no laboratório de biofísica da FCUL sob orientação do Prof. Dr. Miguel Castanho onde foram empregues metodologias biofísicas. No terceiro capítulo é apresentado um artigo (artigo 7) onde se explorou a possibilidade de formação de poro induzida pelo pep-1. A parte experimental foi realizada essencialmente em laboratórios estrangeiros sob a orientação do Dr. Fabrice Homblé (Université Libre de Bruxelles, Bruxelas, Bélgica) e do Dr. Luís Bagatolli (Southern Denmark University, Odense, Dinamarca) onde se aplicaram técnicas não disponíveis no laboratório de biofísica da FCUL tais como: espectroscopia de infravermelho; equipamento para a realização de medidas de electrofisiologia; equipamento para preparar vesículas unilamelares grandes por aplicação do método de electroformação e microscopia confocal. No capítulo quatro estão apresentados os estudos realizados com linhas celulares de Humano, os quais foram publicados em dois artigos (artigos 3 e 4). Os estudos *in vitro* foram realizados no laboratório de biofísica na FCUL e os estudos em linhas celulares foram realizadas em colaboração com a Dr. Júlia Costa (ITQB, Oeiras). No capítulo cinco são integrados os resultados e apresentadas as conclusões. Uma comparação do mecanismo de acção do pep-1 com o mecanismo de outros péptidos vectores é apresentada. No capítulo seis estão os anexos onde se encontram três artigos de revisão que foram publicados no decurso do trabalho doutoral e relacionados com o pep-1 e os CPPs em geral (artigos 5, 6 e 8).

Durante o doutoramento foi ainda objecto de estudo um outro péptido, o PrP(106-126), correspondente a um fragmento da proteína de prião que é considerado como o responsável pela toxicidade na doença do prião. Não se sabe se a toxicidade

deste péptido ocorre ao nível da membrana ou se dentro da célula. Como o PrP(106-126) possui uma estrutura anfipática semelhante à do pep-1, a possibilidade do PrP(106-126) atravessar a membrana por um mecanismo semelhante ao do pep-1 foi testada. Os resultados obtidos serão apresentados em dois artigos, ainda em preparação. No capítulo sete está um dos artigos ainda não publicado onde se incluem os resultados obtidos nos estudos com o péptido PrP(106-126). Por último, o capítulo oito compreende a bibliografia.

Gostaria de agradecer a todos aqueles que de alguma forma contribuíram para a realização dos trabalhos aqui apresentados.

Agradeço em primeiro lugar ao Professor Miguel Castanho pela oportunidade para a realização do doutoramento no seu laboratório, pela sua dedicação e empenho, pelos ensinamentos, pela sua formação pessoal e profissional, e sobretudo pela amizade.

Agradeço ao Departamento de Química e Bioquímica e ao Centro de Química e Bioquímica da Faculdade de Ciências da Universidade de Lisboa pelas facilidades concedidas para a realização do trabalho. Agradeço à Fundação para a Ciência e Tecnologia pelo apoio financeiro concedido (bolsa SFRH/BD14337/2003).

Agradeço à Salomé pelo exemplo de trabalho e dedicação, pelo companheirismo nos momentos bons e nos momentos mais difíceis, pelas discussões científicas e em especial pela amizade partilhada ao longo do percurso académico. Agradeço também à Virgínia pela boa disposição, pela amizade diária, pelos momentos de folia partilhados e pelo ombro amigo nos momentos menos alegres.

Agradeço a todos os colegas de grupo que passaram pelo laboratório de biofísica, incluindo os elementos estrangeiros, pela amizade, pelo apoio e pelos momentos de diversão. Quero agradecer em particular ao David Pina pela sua disponibilidade, pela simplicidade e por me ter alargado os horizontes. Agradeço ainda à Marta e ao Henri pela lufada de ar fresco que trouxeram ao laboratório.

Agradeço ao Professor Manuel Prieto e a todo os elementos do seu grupo no Instituto Superior Técnico pelas discussões científicas, pelas facilidades concedidas e pelos momentos de diversão fora das horas de trabalhos. Quero agradecer em particular ao Fábio pela simpatia e disponibilidade constantes que sempre demonstrou.

Agradeço à Doutora Júlia Costa por me ter recebido no seu laboratório. Agradeço os ensinamentos, a orientação, as discussões científicas e as facilidades

concedidas. Quero ainda agradecer a todos os elementos do grupo, em especial à Catarina Brito, à Vanessa Morais, ao Victor Sousa e ao Rui Almeida, por me terem recebido e pela ajuda no laboratório.

Ao Doutor Fabrice Homblé pela boa disposição, pela orientação no trabalho experimental realizado em Bruxelas na Université Libré de Bruxelles e ao Doutor Erik Goormaghtigh pelas dicas no infravermelho. Agradeço ainda ao meu tio Adérito Henriques pelo alojamento e pela companhia durante o estágio realizado em Bruxelas.

Agradeço ao Doutor Luís Bagatolli por me ter recebido no seu laboratório na Dinamarca, pelos seus ensinamentos e pela boa disposição. Aos restantes elementos do grupo pela simpatia com que me acolheram.

Agradeço à Doutora Marie-Isabel Aguilar por me ter recebido no seu laboratório na Monash University, Austrália. Agradeço ainda a todos os elementos do grupo que me integraram, em especial à Sharon Unabia pela simpatia e disponibilidade, ao Doutor Leonard Pattenden pela ajuda com o SPR e pelo entusiasmo, e ao Kristopher Hall pelas dicas no AFM.

Agradeço ao Doutor Cláudio Soares (ITQB-UNL) pela ajuda com o Pymol e ao Doutor Nuno Santos (IMM-FML) pela utilização do espectrofluorímetro. Agradeço ao Doutor Alexandre Quintas pela ajuda na obtenção e tratamento dos espectros de CD.

Agradeço ao Instituto de Odivelas pelo papel determinante na minha formação pessoal e académica e pelo alojamento durante o doutoramento. Agradeço ainda a todas as alunas universitárias que fizeram parte da residência do Instituto e que foram a minha família nos dias de semana.

Por fim quero agradecer à minha família, em especial mãe e irmãos, e ao Nuno, pela compreensão, pela dedicação e pelo amor que sempre me destinaram, o que me encorajou semana após semana. Depois dos momentos bons e momentos menos bons é a eles que dedico esta tese.

Contents

Resumo

A introdução de genes e de proteínas dentro de células é vista como uma possível ferramenta no estudo de processos celulares, bem como no tratamento de doenças genéticas. Esta possibilidade é no entanto limitada pela membrana celular, a qual constitui uma barreira para a entrada de moléculas hidrófilas. Para a possível entrada de moléculas com interesse farmacológico, ou com qualquer outra finalidade, é necessário utilizar um meio de transporte capaz de introduzir moléculas activas dentro de células. Nos últimos anos, têm sido desenvolvidas diferentes estratégias no sentido de contornar a barreira da célula. Como por exemplo: o uso de vectores virais; uso de lipossomas; electroporação ou microinjecção. Os primeiros, apesar de muito eficientes, devem ser evitados devido a reacções imunogénicas. Os restantes apresentam menos imunogenicidade mas são menos eficientes, apresentam uma baixa especificidade com dificuldades em atingir o alvo celular, elevados níveis de toxicidade e de consumo de tempo. Isto traduz-se numa incapacidade para atingir os efeitos bioquímicos desejados.

Algumas proteínas citoplasmáticas, quando adicionadas extracelularmente, são capazes de entrar na célula por um mecanismo não tóxico. A capacidade de internalização destas proteínas deve-se à existência de sequências peptídicas ricas em aminoácidos básicos na proteína. Estas sequências catiónicas, frequentemente designadas por *cell-penetrating peptides* (CPPs), quando acopladas a outras proteínas, funcionam como vectores para a introdução de macromoléculas dentro das células. O mecanismo usado por estes péptidos revelou-se não tóxico e não invasivo. A introdução da proteína ao invés do gene tem ainda a vantagem de conseguir modificar o fenótipo de uma forma rápida e eficiente e com um maior impacto para futuras aplicações. Na maioria dos CPPs o complexo CPP/macromolécula é obtido pela ligação covalente entre CPP e a macromolécula.

Os CPPs mais estudados são a penetratina (16 resíduos de aminoácidos) e o TAT (13 resíduos de aminoácidos), os quais são provenientes da proteína pAntp (proteína de transcrição da *Drosophila*) e da proteína Tat (proteína de transcrição do HIV-1), respectivamente. Estes péptidos foram os primeiros identificados com propriedades de vector. Depois da descoberta do possível potencial destes péptidos, um grande número de outros péptidos têm sido relatados com propriedades semelhantes. Actualmente esta família inclui péptidos provenientes de diferentes fontes: uns derivados de proteínas ou de toxinas, outros são sintéticos e há ainda péptidos que resultam da quimera de duas ou mais sequências provenientes de diferentes fontes. De um modo geral os CPPs podem ser descritos como: pequenos péptidos (não mais do que 35 aminoácidos), solúveis em água, não tóxicos, capazes de translocar através da membrana celular por um mecanismo independente de receptores e de transportar consigo moléculas hidrófilas.

Apesar das muitas possíveis aplicações destes péptidos o mecanismo usado pelos mesmos é tema de debate na literatura. A elucidação da estratégia usada por estes vectores é importante para uma futura distribuição de macromoléculas com interesse biológico em organismos vivos.

Inicialmente foi proposto um mecanismo independente de receptores (sequências L e D foram internalizadas com a mesma eficiência, o que exclui a intervenção de um receptor para mediar a entrada dentro da célula) e independente de endocitose. A possível contribuição da endocitose foi avaliada pela eficiência de internalização a 37ºC e a 4ºC por meio de observações microscópicas. Eficiências semelhantes para as duas temperaturas sugerem que a entrada dos CPPs é independente das vias endossomais (a baixas temperaturas a produção de ATP é inibida e os processos celulares dependentes de energia, tal como a endocitose, são inibidos). Estes resultados sugerem que a translocação dos CPPs envolve a interacção directa do péptido com a membrana, onde as interacções péptido-lípido apresentam um papel central no processo. A observação da translocação directa de CPPs em modelos de membrana, compostos apenas por lípidos, veio apoiar esta hipótese de translocação.

Contudo, observações recentes sugerem que a localização dos CPPs dentro das células a 4ºC é artificial e resulta de procedimentos de fixação das células para poderem ser visualizadas ao microscópio. A possível explicação para esta localização artificial prende-se com a grande afinidade dos CPPs para a membrana, devida à carga positiva dos péptidos e à carga negativa da membrana celular, o que faz com que permaneçam

adsorvidos à superfície da membrana mesmo que não sejam internalizados. Após a fixação, um processo agressivo para as células, o péptido aparece no citoplasma ou no núcleo. Depois desta observação foi realizada uma reavaliação do processo de internalização e houve uma tendência geral para aceitar que o mecanismo fisiológico mais relevante para a internalização dos CPPs é a endocitose. Todavia, resultados contraditórios têm sido publicados e diferentes grupos apoiam uma ou a outra hipótese.

O péptido anfipático pep-1 (Ac-KETWWETWWTEWSQPKKKRKV-cisteamina) inclui-se na família dos CPPs. Este péptido apresenta uma grande eficiência para a introdução de proteínas, péptidos e anticorpos dentro células de uma forma não tóxica e não imunogénica. O pep-1 oferece vantagens relativamente a outros CPPs pois em vez de ligações covalentes entre o péptido e a macromolécula, a formação do complexo CPP/macromolécula é mediada por interacções electrostáticas e hidrófobas.

À semelhança do que acontece com os outros CPPs no início deste projecto havia incerteza no possível mecanismo de translocação usado por este péptido. Para uma aplicação mais generalizada deste transportador, e de outros pertencentes à mesma classe, a elucidação do mecanismo de acção é determinante. Os principais objectivos deste projecto são: a elucidação do mecanismo de translocação do pep-1; avaliar a sua qualidade como vector e comparar a seu modo de acção com os demais do grupo.

A estrutura primária do pep-1 pode ser dividida em três domínios: um domínio hidrófobo rico em resíduos de Trp (Ac-KETWWETWWTEW); um domínio hidrófilo rico em aminoácidos básicos (KKKRKV-cisteamina) e um espaçador entre os dois anteriores (SQP) aumentando a flexibilidade e a integridade dos outros dois domínios. Em condições oxidantes há uma ligação persulfureto entre duas moléculas de péptido devido ao grupo cisteamina na extremidade C. Tendo em conta a anfipaticidade do pep-1 é de esperar que apresente uma elevada afinidade para a membrana celular que poderá ser relevante para a sua actividade biológica. Este foi o ponto de partida para a realização dos nossos estudos.

O trabalho experimental foi desenhado no sentido de crescente complexidade. Numa fase inicial avaliou-se a interacção do pep-1 com modelos de membranas simples compostos apenas por fosfolípidos. Estes modelos lipídicos são simples mas permitem modular as propriedades da membrana, como a fluidez e a carga da membrana, a força iónica e o pH. Em seguida foram realizados estudos em cultura de células humanas

onde se testou a capacidade vector do pep-1 quando complexado com uma proteína. Pela utilização de diferentes metodologias aplicando essencialmente técnicas biofísicas (e.g. espectroscopia de fluorescência e espectroscopia de UV-vis, dicroísmo circular, espectroscopia de infravermelho e electrofisiologia) e técnicas microscópicas (epifluorescência e microscopia confocal) foi possível obter resultados que integrados indicam que o pep-1 é capaz de translocar através da membrana celular por um mecanismo não mediado por endocitose.

Resumidamente, foi possível verificar que a o mecanismo de translocação do péptido é iniciado pela partição do pep-1 na membrana celular. As interacções péptido-lípido são inicialmente governadas por interacções electrostáticas entre o domínio hidrófilo e os grupos polares dos fosfolípidos que compõem a membrana celular. Subsequentemente, dada a proximidade com a membrana, o domínio hidrófobo insere-se na bicamada, adquirindo uma conformação em hélice α. Aquando da inserção, o domínio hidrófobo induz destabilizações locais na membrana mas sem indícios para a formação de poro. A distribuição assimétrica das cargas na membrana celular (relativamente à composição lipídica e a gradiente electroquímico) é responsável pela existência de um potencial transmembranar (negativo dentro da célula) o qual promove a translocação do pep-1 da camada externa para a camada interna da membrana. Este processo é facilitado pelos distúrbios locais promovidos pela inserção do péptido na membrana e pelas interacções electrostáticas entre a molécula de péptido carregada positivamente e o interior da membrana carregada negativamente. Em contacto com o meio intracelular, ambiente redutor em contraste com as condições oxidantes fora da célula, o péptido perde afinidade para a membrana tornando-se mais estável dentro da célula. O processo torna-se praticamente irreversível e o equilíbrio é sempre deslocado no sentido extracelular $\rightarrow$ intracelular o que facilita a internalização do péptido bem como das macromoléculas associadas.

A translocação ocorre por um processo mediado pela afinidade do pep-1 para a membrana onde as interacções de natureza electrostáticas e hidrófoba são determinantes no processo. Pelos estudos *in vivo* foi possível confirmar que este é o único mecanismo com relevância fisiológica, não se tendo identificado indícios para a endocitose como possível via alternativa.

A entrada do pep-1 por um mecanismo independente de endocitose, em desacordo com o verificado para outros CPPs, sugere que o mecanismo de entrada não é

igual para todos os elementos desta família de péptidos e cada caso deverá ser analisado independentemente.

No decurso do nosso trabalho experimental usou-se o pep-1 não derivatizado, fazendo-se uso das suas propriedades fluorescentes intrínsecas. No entanto, um pep-1 derivatizado com uma sonda fluorescente foi também estudado e comparado com o péptido original. O péptido modificado apresentou uma menor afinidade para a membrana bem como uma menor eficiência de penetração nas células. Verificou-se ainda que, a pequena percentagem de péptido que entra na célula fá-lo por endocitose, ao contrário do pep-1 original. Estes resultados sugerem que o mecanismo de internalização utilizado depende especificamente do péptido, das condições experimentais e da sua afinidade para a membrana a qual modula a concentração de péptido particionado na membrana celular. Para baixas concentrações a endocitose é o mecanismo mais provável, ao passo que concentrações elevadas de péptido na membrana activam o processo físico, mais rápido que a endocitose.

Esta hipótese baseia-se na observação de que alguns péptidos, dependendo das condições e em especial da concentração em solução, apresentam uma internalização mediada maioritariamente ou por endocitose (para baixas concentrações) ou pela penetração directa através da membrana (para altas concentrações). A suportar esta hipótese está também a relação entre afinidade e partição observada em vários estudos.

É de referir que, quando os CPPs são internalizados por um mecanismo mediado por endocitose, a macromolécula acoplada ao vector só atingirá o seu alvo final se o CPP conseguir escapar dos endossomas. Para que isto ocorra o CPP terá de atravessar a membrana dos endosomas o que pressupõe um processo físico. O gradiente de pH, que existe entre os endosomas (pH =5) e o citoplasma (pH=7.4), é um possível potenciador da passagem de CPPs através da membrana, em semelhança ao que acontece quando a translocação é mediada pelo potencial transmembranar. CPPs cuja internalização ocorra maioritariamente por um mecanismo mediado por endocitose revelaram-se menos eficientes.

O trabalho aqui apresentado revela os princípios que modulam a translocação do pep-1. A internalização deste vector ocorre por um processo físico, rápido e com elevada eficiência. A aplicação do pep-1 como vector é mais vantajosa que o uso de vectores virais porque não induz imunogeneicidade e é mais eficiente que outros métodos não virais como a electroporação, a microinjecção ou mesmo outros CPPs.

Com este projecto é possível uma orientação mais focada para a utilização de um meio eficaz que consiga ultrapassar a barreira da membrana celular e introduzir fármacos dentro de organismos vivos.

Abstract

The introduction of genetic material or proteins to originate a defined biochemical effect inside the cell has a remarkable potential for the treatment of Human diseases, however this is hampered by the cell membrane barrier for the entry of hydrophilic macromolecules. A possible strategy to overcome the membrane barrier was proposed after the discovery of basic peptidic sequences with ability to pass trough the membrane in a non-toxic and non-immunogenic manner. These peptides are commonly designated as cell-penetrating peptides (CPPs). Pep-1 is a CPP and has been successfully used to introduce several macromolecules biologically active inside cultured cells. The main goal of this thesis is to clarify the mechanism used by this peptide to pass through the membrane and to confirm if its efficiency as a carrier to introduce proteins inside cells. The interaction with membranes was followed *in vitro* with model membranes: large unilamellar vesicles; planar lipid membranes, giant unilamellar vesicles and supported bilayers. HeLa cells were used to follow the translocation of pep-1 associated with a protein. Fluorescence and UV-Vis spectroscopy methodologies, CD and ATR-FTIR spectroscopy, electrophysiological measurements and fluorescence microscopy were used to carry on the experimental work. It was shown that pep-1 is able to interact with and to destabilize the lipidic bilayers without evidence for pore formation at variance with other CPPs that use an endosomal pathway. Although all the evidences show that pep-1 translocates by a physically-mediated mechanism promoted by transmembrane potential with no evidences for the use of endosomal routes as an alternative pathway. Differences between this particular pep-1 and other CPPs can be related with the affinity for membrane. Peptides with higher affinity for membrane have more propensities to be internalized by a non-endocytic mechanism. Lower affinity for membranes favours endocytic uptake.

Keywords

Drug delivery
Cell-penetrating peptides
Translocation
Membrane
Permeability
Transmembrane potential

Abbreviations and Symbols

AMPs	Antimicrobial peptides
ATR-FTIR	Attenuated total reflection Fourier transform infrared
BLMs	Black lipid membranes
CD	Circular dichroism
CF	Carboxyfluorescein
Chol	Cholesterol
CLIC	Clathrin and dynamin-independent carriers
CPPs	Cell-Penetrating Peptides
CTxB	Cholera toxin B
DPPC	Dipalmitoyl-*sn*-glycero-3-phosphocholine
DPPS	1,2-Dipalmitoyl-*sn*-glycero-3-phosphoserine
E_K	Potassium Nernst potential
FITC	Fluorescein isothiocyanate
FRET	Fluorescence resonance energy transfer
GEEC	Early endosomal compartment
GUVs	Giant unilamellar vesicle
I_W	Fluorescence intensities in the absence of lipid
I_L	Fluorescence intensities in presence of lipid
IR	Infrared
IRE	Internal reflection plate
K_0	Extracellular potassium concentration
K_i	Intracellular potassium concentrations
K_P	Partition coefficient
$[L]$	Lipid concentration
L_α	Liquid crystalline phase

L_β	Lamellar gel phase
L_o	Liquid ordered phase
LDL	Low density lipoprotein
LUVs	Large unilamellar vesicles
MAPs	Model amphipathic peptides
MLVs	Multilamellar vesicles
MUG	4-methylumbelliferone-β-D-galacto-pyranoside
NBD	7-nitro-2-1,3-benzoxadiazol-4-il
NLS	Nuclear localization signal
NMR	Nuclear magnetic resonance
ONPG	o-nitrophenyl-β-galactopyranoside
pAntp	Drosophila antennapedia transcription protein
PC	Phosphatidylcholine
PE	Phosphatildylethanolamine
Penetratin	CPP from pAntp
PLMs	Planar lipid membranes
POPC	1-palmitoyl-2-oleoyl-*sn*-glycero-3-phosphocholine
POPG	1-palmitoyl-2-oleoyl-*sn*-glycero-3-phosphoglycerol
PS	Phosphatidylserine
Rh	Rhodamine
SM	Sphingomyelin
SUVs	Small unilamellar vesicles
Tat	HIV-1 transcriptional activator protein
TAT	CPP from Tat
TB	Trypan blue
TRITC	Tetramethylrhodamine
4-MU	4-Methylumbelliferone
5-NS	5-Doxyl-stearic acid
16-NS	16-Doxyl-stearic acid
β-Gal	β-Galactosidase
γ_L	Molar volume of lipid

Chapter 1

Introduction

Chapter 1.

Introduction

1.1. Strategies to introduce macromolecules inside cells

The introduction of genetic material or proteins to originate a defined biochemical effect inside cells has shown tremendous potential as a biological tool for studying cellular processes and is challenging for the treatment of human diseases (see reference [1] and references therein).

Hydrophilic macromolecules that lack specific membrane receptors are not able to cross plasma membranes due to hydrophobic nature of the core of lipid bilayers. An efficient cellular delivery system is of first importance for an insertion of macromolecules of pharmacological interest or other biological potential. Over the last years, several strategies have been developed to introduce material inside the cells for a variety of purposes such as: protein structure/function studies; DNA insertion to modulate expression of proteins; and drug delivery with therapeutic purposes. Some examples of approaches that have been used are: viral vectors; liposomes-based delivery; electroporation and microinjection [2].

Viruses are really efficient infecting a host cell and introducing their DNA or RNA genomes, this observation led to the use of viral particles as vectors to introduce exogenous genetic material to cells. The development of viral vectors for long-term gene delivery to mammalian cells has been the main goal of viral vectorology since early 1980s. Adenoviruses and retroviruses have been used in a broad host range and for multiple applications (see references [3-5] and references therein). These viral associated vectors are efficient, although the possible pathogenic effects against the host organism, the high costs of production, the limit size of the genetic material that can be packaged for viral gene therapy and a lack of desired tissue selectivity has hampered a more extensive and global therapeutic application. So non-viral alternatives have gathered much attention [2, 6].

Non-viral strategies which are potentially less immunogenic have been developed to overcome viral vectors limitations. Microinjection is an example; this approach involves the transfer of macromolecules into a living cell using micropipettes (Figure 1.1).

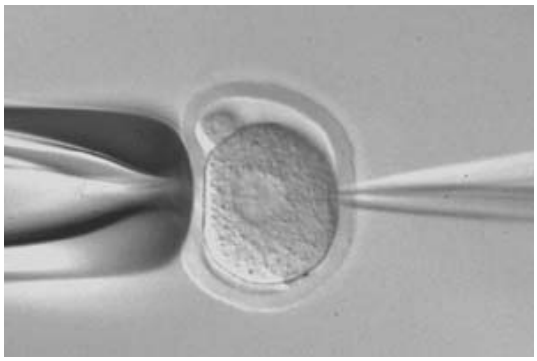

Figure 1.1. Microinjection approach to introduce material inside cells. Macromolecules are injected inside cells by the use of micropipettes; this procedure has to be performed cell by cell. Source: http://transgenese.crchul.ulaval.ca/transgeniques.htm

This technique has no cell-type restriction and there is no apparent limitation on the size or type of macromolecule that can be injected [7]. However, because this technique can only be performed one cell at a time with individual glass micropipettes, it is time consuming, requires specific technical skills and is practical only when treating a small number of cells [8]. There is also a limitation to the cell types that can be readily used for microinjection [8]. An efficient method for transforming a larger number of cells at once should be improved for a more generalized application.

Another non-viral strategy is the use of electric pulses (electroporation), which was first demonstrated with the introduction of DNA in 1982 [9]. When transmembrane

potential is above a threshold, transient pores are formed which allow cellular uptake of hydrophilic molecules (see Figure 1.2) (see reference [10] and references therein for possible applications). This technique can be applied to many cells at once, however it is a non-specific strategy and can become toxic, since molecules can enter or exit the cell without control during transient membrane destabilizations [2]. A large cell death percentage may occur [8].

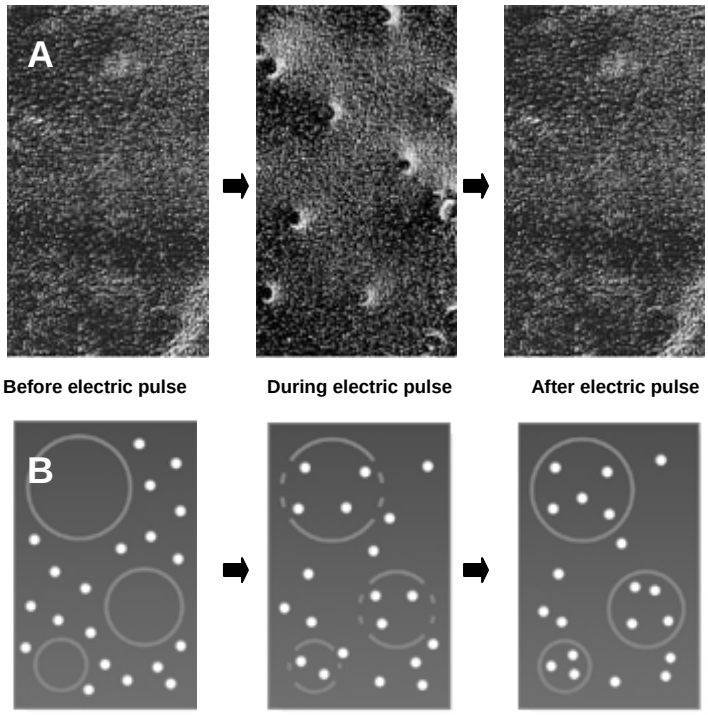

Figure 1.2. Electroporation approach to introduce material inside cells. An electric field induces transient pore formation which enables the entry of material. **A)** Electron micrographs of cells before and after brief electric pulses; opening pores and resealing of membrane is observed. **B)** Illustration of material entrance during electropermeabilization. Source: http://www.inovio.com/technology/electroporation.htm

In 1987 Felgner et al. reported the use of cationic liposomes as an efficient and effective system to deliver DNA [11]. Upon mixing DNA with cationic liposomes, DNA is condensed into small particles called lipoplexes, the process involving an initial rapid association of polycationic liposomes and polyanionic DNA through electrostatic interaction (see reference [2] and references therein). This gene therapy strategy is not immunogenic, does not have size restriction and different types of nucleic acids can be delivered ([6]). It is inexpensive and is relatively easy to use in large-scale [6]. Liposomal carriers have been successfully used to deliver genetic material into cells and can be internalized by endosomal vesicles through endocytosis or by direct fusion with the cell membrane. In endosomal route genetic material may stay enclosed within endosomes and fail to access the cytoplasm and nucleus, leading to inefficient low gene expression (see Figure 1.3). Cell transfection by direct fusion produces increased levels

of gene expression [6]. The uncertainty in the pathway for cell entry, the low efficiency of delivery [6], a possible toxicity related to gene transfer by lipoplexes [2] and potential interference with lipid metabolism [8] hamper a more general application of cationic liposomes as a vehicle to introduce material *in vivo*. Different strategies have been developed in order to improve transfection efficiency of liposomal carriers, some of them involving direct injection [6, 12].

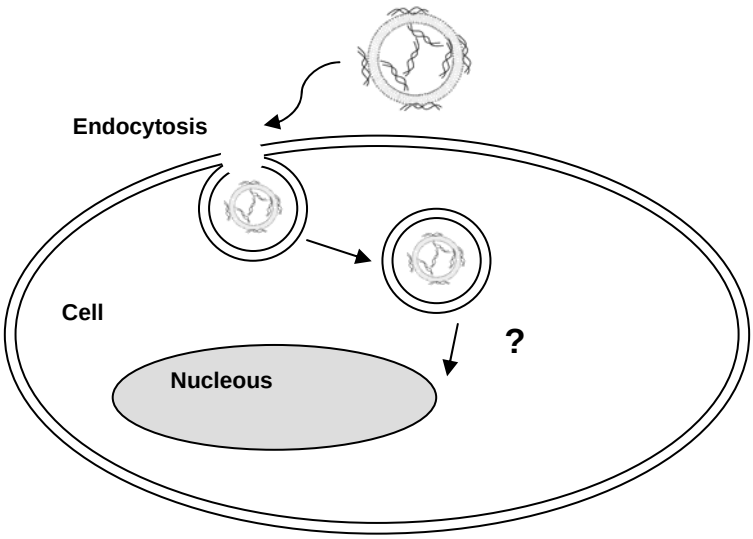

Figure 1.3. Cationic liposomes can be used to introduce genetic material inside the cell. Due to electrostatic interactions between negatively-charged DNA and cationic liposomes, a good delivery system can be obtained. Cationic liposomes are internalized by endocytosis. The escape from endosomes can hamper an efficient delivery.

A non-invasive administration with a better efficiency for a good transfection and application in vivo is of particular interest to the future development of gene therapy [6].

1.2. New strategy to introduce macromolecules inside the cells using peptides as vectors

All the non-viral strategies above mentioned are more focussed and improved for genetic material delivery and all of them have serious drawbacks which result in a transient and varied gene expression with a consequent incapacity to reach the final desired effect [1].

The fact that some intracellular proteins when added to extracellular medium are able to pass through the membrane inspired a new approach. This phenomenon was first observed with Tat (HIV-1 transcriptional activator protein) [13] and pAntp (Drosophila antennapedia transcription protein) [14]. The ability of these proteins to cross the membranes is due to basic amino acid sequences and the minimal peptidic sequences necessary for the translocation to occur within Tat [15] and pAntp [16] were elucidated.

Conjugated molecules such as peptides [17] or proteins [18] coupled to these basic peptides can be delivered into cells; this observation made these basic sequences very attractive and a new class of vectors, initially denoted as Protein Transduction Domains (PTDs) [19] and more recently re-baptized as Cell-Penetrating Peptides (CPPs) [20], emerged.

The CPP derived from pAntp has 16 amino acid residues [16] and is commonly known as penetratin. The Tat (48-60) fragment which include the whole basic regions of the protein and its Nuclear Localization Signal (NLS) is the most efficient in internalization [15].

This strategy prospects a substantial improvement in cellular delivery. The greater advantage of this strategy when compared with the above referred is the possibility to introduce proteins in a non-toxic and non-invasive way. Internalization of proteins instead of genes can modify the phenotype in less than 2 hours in an efficient manner envisaging a fast and effective strategy for drug delivery with a major impact on future treatments [21, 22]. This new approach opens new possibilities for the development of vaccines and protein therapies for cancer and infectious diseases [23].

After the discovery of the potential of Tat peptide (TAT) and penetratin as vectors a larger number of peptides (Table 1.1), including peptides from protein sequences (pVEC [24] and VP22 [25]), synthetic peptides (such as model amphipathic peptides (MAPs) [26], and oligoarginines [27]) or chimera peptides (obtained by the

fusion of sequences from different sources, as transportan [28] and MPG [29]) have been shown to translocate across cellular membrane.

Table 1.1. Source and amino acid sequence of some CPPs. Positively-charged amino acids are highlighted.

Peptide	Source	Sequence
Penetratin	pAntp homeodomain [16]	**R**QI**K**IWFQN**RR**M**K**W**KK**
TAT	HIV-1 Transcriptional activator [15]	G**RKKRR**Q**RRR**PPQ
VP22	Viral protein (HSV-1) [25]	DAATAT**R**G**R**SAAS**R**PTE**RPR**APA**R**SAS**RPRR**PVE
pVEC	Murin VE-Cadherin [24]	LLIIL**RRR**I**RK**QAHAHS**K**
MAP	Synthetic [30]	**K**LAL**K**LAL**K**AL**K**AAL**K**LA
Oligoarginine	Synthetic [31]	**RRRRRRRR**
Transportan	Chimeric (galanin-mastoparan) [28]	GWTLNSAGYLLG**K**INL**K**ALAALA**KK**IL
$S4_{13}$-PV	Chimeric (dermaseptin S4-SV40) [32]	ALW**K**TLL**KK**VLKAP**KKKRK**V-cysteamine
MPG	Chimeric (gp41-SV40) [33]	GALFLGFLGAAGSTMGAWSQP**KKKRK**V

This ability is part of the biological function of many of these peptides, although this does not automatically mean that they can be used as a carrier. In order to distinguish between translocating peptides able to deliver cargoes and others unable to do it, a CPP can be defined as a short (no more that 35 residues) water soluble, non-toxic, peptide able to efficiently translocate through cellular membrane by a mechanism independent from a chiral receptor, able to deliver hydrophilic macromolecules into cells and eventually originating a defined biochemical effect inside the cell [34].

Besides proteins [18, 19, 35-37], several other hydrophilic macromolecules have been efficiently coupled to these CPPs and delivered inside the cells, such as: peptides [17, 38-40]; antisense oligonucleotides [29, 41-44]; SiRNA [45, 46] and plasmid DNA [47, 48]. Nanoparticles [49] and liposomes [50] have also been internalized by means of CPP. Introduction of cargo macromolecules into primary and transformed cultured cells with efficiency close to 100% can be obtained.

The application of CPPs to deliver macromolecules inducing a specific biochemical effect has been efficiently used *in vivo* in rats with a construct of penetratin associated to a peptide nucleic acid [44]. A caveolin-1 scaffolding domain peptide attached to penetratin was also successfully taken up by mouse aorta rings and its

biological effects were detected [51]. The capacity to pass blood brain barrier mediated by a CPP strategy was also shown by a CPP-dexorubicin construct [52] and also with a construct of TAT-β-Galactosidade [23]. This last CPP-cargo construct can also reach mice organs via systemic circulation and transduces in a variety of murine tissues, including liver, kidney, heart, muscle, lung, spleen and brain [23]. This unspecificity can limit the application of these CPP constructs when a single organ or tissue is the target.

1.3. How do CPPs translocate across cell membrane?

The exact mechanism underlying the translocation used by CPPs to pass through cellular membrane still awaits complete understanding; the information available in the literature is scarce and controversial. A mechanism independent on receptors was proposed based on studies with reverse and D-enantiomer sequences, which have similar translocation efficiency as the original peptide [27, 31, 53]. A mechanism independent of endosomal pathway was also purposed supported by the observation that internalization of such peptides is similar at 4ºC and 37ºC [15, 16, 27, 53, 54] (at low temperatures ATP production is inhibited and energy-dependent cellular processes, like endocytosis, are inhibited or greatly diminished).

Recent observations suggesting that the cell localization observed for CPPs is artifactual and occurs during cell fixation for immunochemistry and cell imaging [55], raised the questioned if the translocation of such peptides is really dependent on endocytosis. An artificial cell localization was first reported in 2001 with the structural protein VP22 [55], which also possesses vector properties and can be used to transport other proteins [25]. VP22 binds to surface which allow the protein to remain attached to cells during washing. In the cell fixation process the protein is released and co-localized with nucleus due to affinity of VP22 to DNA [55]. The artifactual cell localization by fixation was confirmed by comparison of the localization of the Histone H1, which does not have cell-penetrating properties, before and after cellular fixation [56]. Biased localization of soluble proteins, during preparation of cells for immunofluorescence, was formerly reported in 1992 [57]. The possibility of an artifactual cell localization was further confirmed in 2003 by Thorén et al [58] and a re-evaluation of the translocation mechanism of several CPPs has been done is the last 4 years.

By the re-evaluation of the translocation mechanism it is clear that penetratin [58, 59], TAT [60-64] and oligoarginine [60, 65-67] among other CPPs, can cross the plasmatic membrane by endocytosis. A tendency to accept this pathway as the main mechanism for internalization of all the CPPs has been generalized in the literature; however, there is no consensus in the specific endocytic pathway used for the uptake of these peptides. The involvement of different pathways has been identified, for instance

raft-dependent pathway involving macropinocytosis [68], clathrin-mediated endocytosis [69, 70] or caveolae-dependent endocytosis [62, 71]. Controversial results are published the dissimilarities being due to different experimental conditions in particular with different cellular lines, labelled-peptides and protein-conjugated peptides, which can inhibit some pathways while favouring other.

The involvement of the basic residues in peptide translocation was tested and it was found that the deletion or substitutions of a single basic amino acid residue dramatically reduced TAT uptake [72]. The importance of the overall charge of the peptide was further confirmed by Wender *et al*., and it was identified that nonaarginine (R9) is more efficiently internalized than Tat fragment [73].

These results suggest that the first interaction with membrane, prior to endocytosis event, appears to be governed by electrostatic interactions between the basic amino acids within CPPs sequence and biological membranes. The heparan sulfate (HS) proteoglycans at the cell membrane were proposed to act as receptors for penetratin [63, 74-76], Tat peptide [63, 70] and also for oligoarginine [66].

The biological activity exhibited by CPPs is consistent with the cargoes macromolecules reaching the cytosol. In a picture where the endosomal pathway emerges as the physiological uptake of CPPs, the escape from endosomes is mandatory for the potential use of CPPs as a strategy to deliver macromolecules with biological relevance inside the cell; this raises the question by which mechanism the internalized CPPs reach the final target?

An escape from endosomes due to acidification was proposed for penetratin, TAT and oligoarginine [61, 65]. This hypothesis is supported by Granslund and co-workers results, where penetratin was encapsulated in liposomes. In the absence of pH gradient no penetratin escape takes place, while when a pH gradient exist (5.5 inside, 7.4 outside), there is a fraction escaping from the liposomes and this occurs without membrane lysis neither pore formation [77]. In opposite to this it was verified that a higher membrane disturbance induced by poliarginines occurs with pH in the average 7.5-9.5 and an escape of endosomes prior to their acidification was suggested [66].

If a mechanism able to permeate membrane for endosomal escape exists, this can also suggest a similar mechanism to pass cell membranes. Direct observation of some CPPs translocation in model membranes systems [78, 79] support the existence of

a possible energy-independent mechanism, governed by peptide-membrane interactions, to cross the membrane. Furthermore, higher amounts of oligoarginine peptide were located in cytosol at 4ºC than at 37ºC. A possible explanation for this phenomenon is that when incubation is held at 37ºC, oligoarginine release in the cytoplasm can be difficult due to endosome entrapment [67], at 4ºC the existence of an alternative pathway which operates when endosomal pathways are inhibited can more easily locate oligoarginine in cytosol. A possibility of an alternative pathway to endocytosis was proposed [80] shortly after the discovery of Tat protein capacity to internalize inside cell.

A translocation dependence on a negative transmembrane potential was observed *in vitro* with liposomes [78] and *in vivo* into HeLa cells [81] for some CPPs. Terrone et al. suggested that a part of the peptide can transverse through the membrane by a mechanism dependent on transmembrane potential (negative inside) and other part is internalized by endosomal pathway. When in endosomes the membrane potential may facilitate translocation of CPPs from endosomal lumen to the cytoplasm, considering that the endocytic compartment exhibit a significant transmembrane potential (lumenal side positive) [78].

Even with direct observation of CPP internalization in membrane model systems, a broadly acceptance that the main cellular internalization mechanism of CPPs involves endocytosis, compromise the usage of these peptides for drug delivery. When entering in the cell via endocytosis the molecules can become entrapped in the endosome and ultimately end in the lysosome, where degradation processes take place. Thus even if efficient cellular uptake via endocytosis is observed, the delivery of intact peptide/protein or other macromolecule is compromised by insufficient endosomal escape and subsequent lysosomal degradation. An inefficient escape from endosomes was verified by the observation that after TAT-Cre peptide uptake the majority of the complex remained entrapped in endosomes even after 24h [68]. One possible solution is to complement CPP with a membrane destabilizing agent (e.g. viral fusogenic peptide or membrane-destabilizing peptide) to improve CPP-mediated protein transfection as has been proposed by Wadia *et al.* [68]. A markedly enhanced CPP-cargo construct escape from endosomes was verified when a fusogenic peptide was associated with the TAT. In a more recent report, Lebleu and co-workers found that a modified penetratin

in which six Arg residues where added to N-terminus make the CPP more efficient to internalize and to target a PNA with a high efficiency [82].

For a generalized application of these peptides as a vehicle with pharmaceutical relevance or other biological/scientific applications, the elucidation of the translocation mechanism is of first importance. The experiments to study CPP internalization are frequently carried on with TAT and Penetratin. In the last years, peptides from diverse sources have been identified with CPP properties, beside the ability to enter cells and the presence of basic amino acid residues, these peptides can vary in size, nature, biological function, secondary structure, hydrophobicity and amphipathicity (see reference [34] and references therein). The mechanism by which CPPs pass through the membrane is far from being completely understood. Taking into account all the information available in the literature regarding the translocation mechanism and the varied nature of the different peptides belonging to the CPP family, a careful and special attention to this topic should be taken and a simplistic comparison with other CPPs should be carefully done.

1.4. Pep-1 a new peptide carrier

In most CPPs so far referred, the CPP-macromolecule complex is obtained due to covalent link between the CPP and the cargo molecule. The strategy to couple cargoes to CPPs can be obtained by production of a CPP-cargo by chemical peptide synthesis, which is generally restricted to short cargoes (e.g. 10-20 amino acids); larger protein cargoes can be produced by recombinant DNA technologies with expression in bacteria and their purification prior to use [83]. Another approach is to synthesize the CPP and the cargo molecule independently and posterior linkage by a reactive residue included in either CPP and cargo molecules (e.g. activated cysteine at CPP N-Terminal with a free cysteine included in the cargo molecule). This approach enables coupling of large proteins (see reference [83] and references therein). After cellular uptake, the reducing environment in the cytosol cleaves the disulfide linkage and frees the cargo molecule from the CPP [26], avoiding interferences with cargo biological function or its cellular localization. All these strategies to couple a cargo have limitations, are time consuming and require specific technical skills; moreover a CPP-cargo may induce desnaturation of the protein due to covalent link to the CPP.

A new approach based on an amphipathic peptide named pep-1 (Chatiot®) has been proposed for protein delivery. Pep-1 delivers a broad range of protein directly into mammalian cells maintaining their biological activity in different cellular lines with lack of toxicity and lack of sensitivity to serum [84]. The advantage of this peptide in comparison with CPPs above referred is that this peptide forms a non-covalent complex with the macromolecule to be delivered, avoiding complicate procedures with covalent links above referred. This complex is easily obtained by mixing the peptide with the macromolecule during about 30 minutes and a complex, stable in physiological buffer, is obtained and ready to use onto cells. The size and the nature of the cargo protein to be delivered can influence the number of pep-1 molecules required to obtain an efficient complex. After cellular uptake the complex dissociates in the cytosol leaving the macromolecule biologically active and free to proceed to its target organelles, while pep-1 localizes in the nucleus and does not affect the final cargo location [84]. The efficiency of translocation can vary in the range 60-95%, depending on the cell type and the cargo molecule [84].

Pep-1 has been efficiently used to introduce several peptides [84-87], proteins [88-93] and biologically active antibodies [85, 94-99] inside cultured cells from different sources. It is noteworthy the capacity to deliver macromolecules in neuronal cells [88, 93, 95, 96], and also plant cells converted into protoplasts [92] producing the expected biochemical effect in the correct localization inside the cell. The biological activity is generally maintained after translocation of the delivered macromolecule, for instance: 1) enzymatic activity was detected after enzyme internalization [84, 90, 91]; 2) pep-1 was efficiently employed to deliver an antibody to clarify the intracellular trafficking of a membrane-anchored enzyme [98], which indicates that after internalization, the antibody diffuses throughout the cells and interacts with the target protein and thus, allows the identification of the subcellular compartment that harbours the target protein. The use of pep-1 in animals has also been reported [100, 101], where pep-1/cargo complexes were intratracheally instilled, for instance Aoshiba *et al.* have used pep-1 to deliver Caspase-3 to the lungs of mice; alveolar wall apoptosis and emphysematous changes were detected as a result of actively internalized Caspase-3 [100].

Altogether these published reports strengthen the use of pep-1 as a vehicle for intracellular deliver of macromolecules with biological interest such as pharmaceutical agents.

1.5. Main goals of the project

Pep-1 (acetyl-KETWWETWWTEWSQPKKKRKV-cysteamine) is an amphipathic peptide with three domains: (i) a Trp-rich "hydrophobic" domain (Ac-KETWWETWWTEW), responsible for "hydrophobic interaction" with proteins and cell membranes; (ii) a hydrophilic domain (KKKRKV-Cys) derived from a nuclear localization signal (NLS) of Simian Virus 40 (SV-40) large T antigen, required to improve solubility; and (iii) a spacer domain (SQP) which improves the flexibility and the integrity of the other two domains [84]. A cysteamine group is present in the C-terminal and an acetyl group caps the N-terminus. In oxidizing conditions a disulfide link is formed between two peptide molecules by the cysteamine group (Figure 1.4).

The term amphipathicity refers to molecules with both hydrophilic and hydrophobic parts [102] and is dependent on the relative abundance of hydrophobic and hydrophilic domains within a peptide. One possible quantitative measure of amphipathicity is the hydrophobic moment [103]. It is possible to distinguish between primary amphipathicity and secondary amphipathicity in peptides. Peptides with primary amphipathicity are made of a hydrophobic and a hydrophilic domain. A peptide with secondary amphipathicity has hydrophobic and only hydrophilic residues however a separation of hydrophilic and hydrophobic parts is only achieved with the peptide secondary structure [102]. The simplest and most common secondary structure in peptides is the amphipathic α-helix [102].

Cell membranes are composed of amphipathic bilayers, therefore an increasing hydrophobic moment of model peptide results in a significant increase in the permeability and haemolytic activities of these peptides in target membranes, which implies a better peptide-membrane affinity (see reference [103] and references therein). Antimicrobial peptides (AMPs) activity is known to be dependent on peptide-membrane interaction and on the capacity to induce membrane leakage. For AMPs the capacity to interact with membranes and the degree of amphipathicity are correlated. For these peptides amphipathic α-helix formation occurs upon membrane interaction, which seems to favour peptide insertion and cellular toxicity [103].

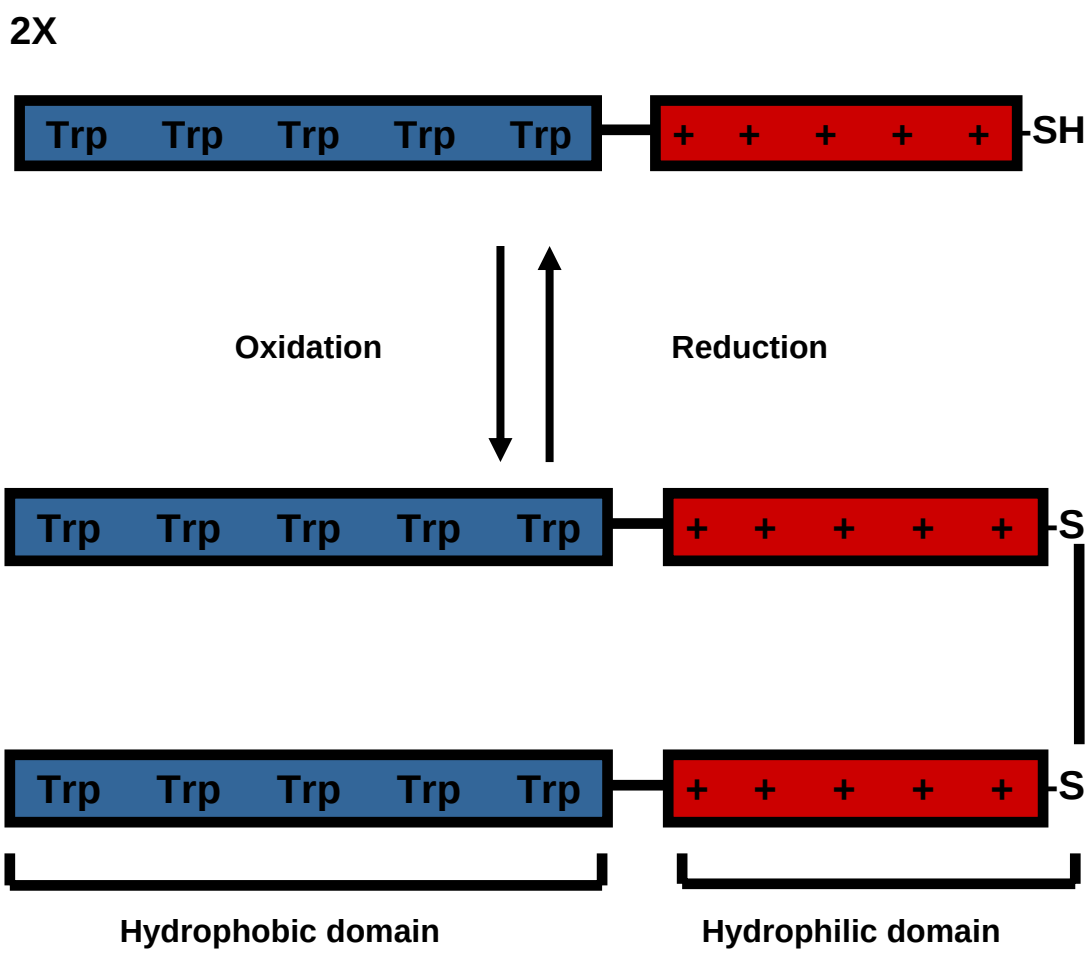

Figure 1.4. Schematic representation of pep-1 molecule. Primary amphipathicity is evident: "hydrophobic" domain (Ac-KETWWETWWTEW) is represented by five Trp residues and hydrophilic domain (KKKRKV-Cys) is represented by five positive charges. In between a spacer domain (SQP) with a Pro residue is responsible by the flexibility and integrity of the other two domains. In oxidizing conditions a disulfide link between two cysteamine groups is expected, reducing environment cleavages this disulfide link.

The use of an amphipathic transporter to deliver cargoes molecules inside cells where the cell membrane is the first barrier seems feasible; in this regard, peptide interacts first with hydrophilic region and then penetrates the hydrophobic interior of the cell membrane [102]. A clear dependence of peptide incorporation upon amphipathicity was demonstrated with MAPs [104]. Reports from Divita and Heitz group demonstrate that peptides with primary amphipathicity are also efficient to interact with lipidic membranes and to translocate across cell membrane [33, 105].

Pep-1 is a promising vehicle to deliver macromolecules with biological relevance into cells. However, for a more generalized and optimized use of this carrier the elucidation of the mechanism of action is mandatory. When I started my PhD, there was not much information regarding the possible mechanisms used by this peptide to translocate across cellular membranes. Morris *et al.* suggested that this peptide translocates by an endocytosis-independent pathway, although, these results were obtained in fixation conditions and with a labelled peptide [84], which can compromise the results, as stated above.

The main objective of this project was to unravel how pep-1 interacts with cells at membrane level. Pep-1 is a peptide with primary amphipathicity, which suggests direct interaction with lipids in biological membranes and this can be the key-feature to explain pep-1 ability to pass through the cell membrane. In order to evaluate this hypothesis, the experimental work was first performed with model membranes to evaluate the possible effect of membrane charge, viscosity and ionic strength. Different model membranes were used depending on the methodology: Large unilamellar vesicles were used with fluorescence methodologies; Giant unilamellar vesicles were used in confocal microscopy and planar lipid membranes for electrophysiological measurements. In order to evaluate the possible effect of a cargo on the translocation mechanism studies with a complex pep-1/protein were also performed. The protein chosen for these experiments was β-Galactosidade (β-Gal) from *E. Coli*. After characterization of pep-1 interaction with model membranes, cultured mammalian cells were used. Results obtained *in vitro* and *in vivo* were compared.

In the following chapters published results are presented in the paper format. An introduction with the specific objectives, model membranes and the methodologies used was included for detailed information.

Chapter 2

Pep-1 and model membranes

Chapter 2.

Pep-1 and model membranes

2.1. Introduction

2.1.1. General membrane remarks

The plasma membrane defines the boundary of the cell and is the surface of contact with its environment [106]. Biological membranes play a central role in both the structure and function of cells and are complex structures where lipid and proteins are the principal components and its relative contribution is dependent on cell type and function. Phospholipids are the most commonly found membrane lipids (essentially glycerophospholipids, Figure 2.1.A) [107] and due to it amphipathic nature and cylindrical shape, the most favourable structure in aqueous environment is the lipidic bilayer, which forms spontaneously by self-assembly of lipid molecules with a hydrocarbon interior and polar groups on either side (Figure 2.1.B). With this bilayer shape, lipids minimize the contact with water and this phenomenon is known as entrotopic effect, also named "hydrophobic effect" designated by hydrophobic force [108].

The hydrophobic core of the lipidic bilayer is the most important structural feature in the role of membranes as a barrier [107]. Proteins for instance are embedded with their hydrophobic surfaces buried in the lipid. Besides its highly dynamic structure where lipids and proteins can rotate or diffuse laterally [106], lipid bilayers are impermeable to several molecules and are responsible for a restrict regulation of molecules passage inward and outward, which is responsible for maintaining the gradient levels essential for vital cellular functions.

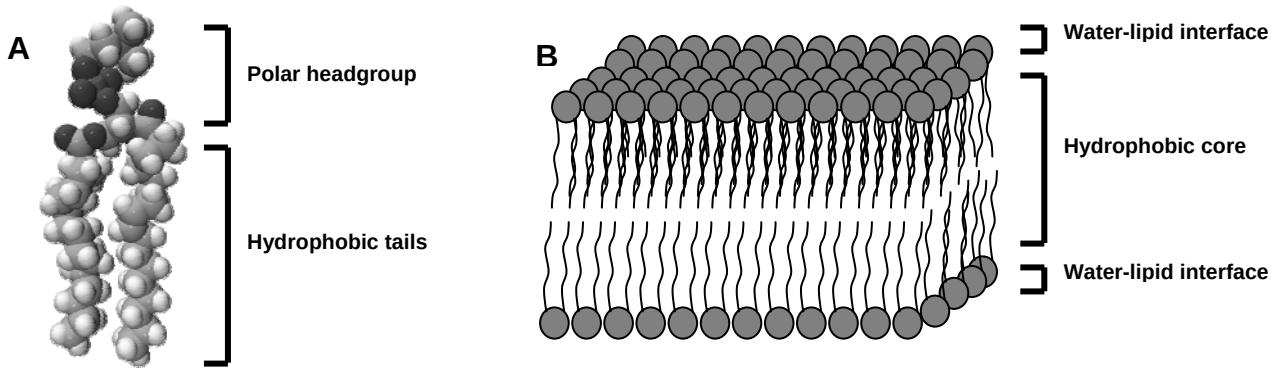

Figure 2.1. A) Schematic representation of 1-Palmitoyl-2-Oleoyl-*sn*-Glycero-3-Phosphocholine (POPC), a glycerophospholipid. **B)** Schematic representation of a lamellar arrangement of a lipidic bilayer. Polar headgroups interface the aqueous environment and shield the hydrophobic core.

Cell membranes are complex structures with an enormous diversity with multiple lipids that appear to play several roles within membranes (see reference [107] for further information). In a simplistic point of view, lipidic mixture can be regard as a stable matrix and cell barrier in which the proteins can function. The amount and nature of membrane proteins vary and are considered the biochemically active components of the membrane, which comprise a diversity of activities such as enzymatic, transporters, receptors, pores, depending on the nature of each particular membrane [107].

2.1.2. Membrane phase behaviour

Depending on the temperature, pressure, hydration and phospholipid nature (hydrocarbon tails and the composition of headgroups) a pure lipidic bilayer can present different thermodynamic phases. In the most common phospholipids the low-temperature phase is designated by a lamellar gel phase (L_β) (Figure 2.2.A). The

molecules are packed more tightly together and the acyl chains are more highly ordered and are maximally extended [107, 109]. At higher temperature, the gel phase undergoes a transition to the L_α phase, which is designated as liquid crystalline or fluid phase (Figure 2.2.B). This form has a considerable disorder in the acyl chains and is usually assumed to be physiologically the most important phase [107, 109]; in the fluid phase the bilayer thickness is shorter than in the gel phase (Figure 2.2).

The major thermodynamic driving force stabilizing hydrated lipid aggregates is the entropic effect, however *van der Waals* forces (short, weak and attractive forces between adjacent hydrocarbon chains) and hydrogen bonding (between polar headgroups of some lipid molecules) are also stabilizing factors of the bilayer structure. At phase transition *van der Waals* forces between fatty acyl chains have an important role; these forces are responsible for the relative stability of the gel and liquid crystalline phases. The stability of the phase increases with the tail length because of the increased *van der Waals* interactions in longer chains [109]. In the presence of a double bond (*trans* or *cis*) the ability of the chains to interact orderly is decreased and so the ability to form a gel phase [107].

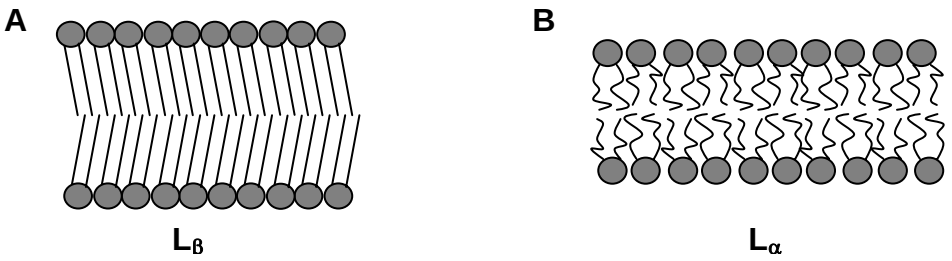

Figure 2.2. Schematic representation of lipidic bilayers in: **A)** Lamellar gel phase (L_β) where the molecules are packed tightly and orderly together; and **B)** Lamellar liquid crystalline phase (L_α) with a considerable disorder in the acyl chains conformation. These structural features were elucidated by X-ray diffraction data. Figures adapted from [107, 109].

Cholesterol is the most common found sterol in animal cell membranes and it constitutes about 30% of the mass of the membrane lipids of many cell plasma membranes [107]. Cholesterol modulates membrane fluidity. When cholesterol is added to a liquid-crystalline phase a more ordered phase, liquid ordered (L_o) phase (less fluid than liquid crystalline phase but more fluid than gel phase), occurs on the membrane [110]. Depending on the cholesterol-phospholipid proportion the membrane has fluid

phase or liquid ordered properties. At low cholesterol concentration lipidic membranes have fluid phase properties, while at high cholesterol concentration membrane is more ordered and L_o phase properties are dominant. For intermediate concentrations the two phases coexist [110].

The fluid mosaic model of biological membranes proposed by Singer and Nicolson [111] emphasizes membrane fluidity and free lateral diffusion of membrane components the fluid phase is considered to be the bulk phase in biological membranes, but the observation of patches of lipids with composition and physical state different from the rest of the membrane suggests the coexistence of phases. This model is referred as "lipid-raft" model and is based on dynamic clustering of sphingolipids and cholesterol to form platforms that move in the fluid bilayer. A role on protein attachment during signal transduction has been proposed by Simons and Ikari [112]. The physical state of these domains is assumed to be similar to a L_o phase [112-114].

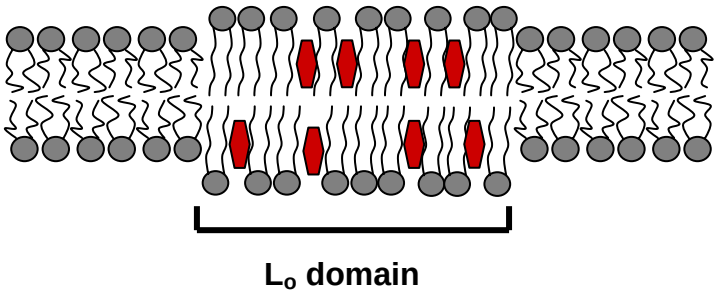

Figure 2.3. Schematic drawing of a liquid ordered domain (L_o) in a fluid phase bilayer (L_α). Hexagon represents cholesterol molecules which modulate membrane viscosity. Figure adapted from [114].

2.1.3. Membrane asymmetry

The membrane is a twofold asymmetric structure. The two leaflets of the membrane bilayer have their specific lipid and protein composition. The asymmetric arrangement of membrane proteins was the first to be discovered [115] which accounts for the differences in the function of the outer and inner surface. The interior of the membrane contains proteins involved in intracellular events while outside may contain proteins involved in the defence mechanism of the cell [115], for instance. The transverse asymmetry of phospholipids has became apparent due to asymmetrical localization of the enzymes involved in phospholipid synthesis [116] and due to the fact that the chemical environment of both bilayers is different [115]. Now is known that the compositional asymmetry of the plasma membrane does not correspond to the

asymmetry of lipid synthesis or hydrolysis. The transbilayer lipid distribution results from a continuous inward and outward movement of lipids between two monolayers (for further information see reference [117]). Hence, lipid asymmetry is formed and afterwards maintained by specific mechanisms that control lipid movement across the bilayer [117].

The asymmetric arrangement of phospholipids in plasma membrane was first established for natural lipids in erythrocytes and confirmed with different techniques [118-120]. Asymmetry in different animal eukaryotic membranes have also been elucidated and in general is possible to assume that the choline-containing lipids, phosphatidylcholine (PC) and sphingomyelin (SM), are primarily on the external leaflet of the plasma membrane, while amino-containing glycerophospholipids, phosphatildylethanolamine (PE) and phosphatidylserine (PS) are located preferentially on the cytoplasmic leaflet [115, 121-123]. The relative molar fraction of each lipid depends on the membrane organelle and species. Noteworthy are the neutral composition of external layer and the negative charge of inner layer of plasma membrane in Human cells. The erythrocyte plasma membrane for instance has about 20% molar of PS in the inner layer [107]).

Besides lipidic and protein transbilayer asymmetry there are also membrane potentials contributing for transmembrane asymmetry. There are three types of electric potential related to membranes [124]: 1) the transmembrane potential, which is associated with gradients of electric charge across the phospholipid membrane (negative inside) and is important in different biological processes; 2) the electrostatic surface potential, which results from the net charge found on the membrane surface; the 3) membrane dipole potential, which results from the net contribution of molecular polarizations arising from the water molecules that adopt an organized structure in the membrane surface and electrical dipoles associated with the carbonyl group of the lipids (see [124] and references therein). The various electrical potentials associated with membranes are involved in a large number of cellular processes [125, 126] and they may also be implicated in protein- and peptide-membrane interaction, structure and function [127-131]; moreover membrane potentials can be modulated when peptides insert in the membrane [128, 132].

2.1.4. Model membranes used in spectroscopy studies

Due to the complexity of biological membrane peptide-membrane interaction studies are usually initiated with simple model membranes so that different properties such as lipid charge, membrane viscosity and the presence of sterols can be modulated. Each of the several model membranes that have been used to study membrane-active peptides has advantages and disadvantages, depending on the techniques to be employed. To start our studies, peptide/membrane interactions were followed using spectroscopic methodologies and liposomes.

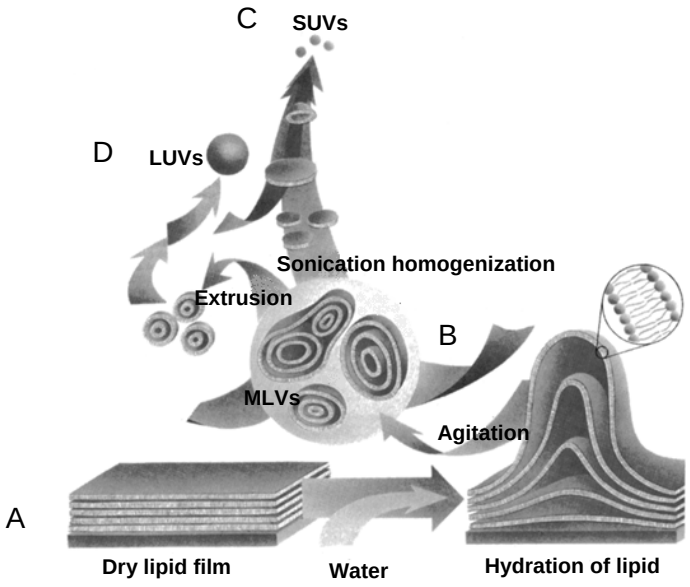

Figure 2.4. Preparation of LUVs and SUVs. **A)** Lipids are dissolved in chloroform and the solvent is removed to yield a lipid film. After addition of water/buffer, hydrated lipid sheets detach spontaneously. **B)** Upon agitation and freeze-thaw cycles, a MLVs suspension is obtained. **C)** Sonication may be used to produce SUVs while **D)** extrusion can be used to obtain LUVs. Image adapted from: http://www.avantilipids.com.

.

When phospholipids are suspended in an excess of aqueous solution they spontaneously form multilamellar vesicles (MLVs). These aqueous dispersions produced by mechanical agitation of an aqueous medium in the presence of a dry lipid film were designated as liposome by Bangham *et al.* [133] (Figure 2.4). Generically the term liposome is applied for hydrated lipid dispersions which can be characterized based on size and number of lamellas [134]. MLVs are large vesicles with two or more lamellas; vesicles with one lamella can be: small unilamellar vesicles (SUVs) with a ~30nm diameter; large unilamellar vesicles (LUVs) with a ~100nm diameter; and giant unilamellar vesicles (GUVs) with a diameter higher than 10μm. The type of liposome obtained is dependent on the preparation procedure, where three phases can be distinguished: lipidic film preparation, lipid hydration and final processing to obtain a

specific liposome (e.g. sonication to obtain SUVs with a diameter of about 30nm [135] and extrusion of MLVs to obtain LUVs with a diameter of about 100nm [134], see Figure 2.4).

SUVs or LUVs are the preferred vesicles used for the application of spectroscopic methodologies; they both have particular advantages and drawbacks. SUVs have smaller size and therefore reduced light scattering, but due to high membrane curvature these liposomes are characterized by a non-ideal lipid packing (less dense packing of phospholipids), which may produces anomalous peptide binding (see reference [136] and references therein). LUVs have a lipid packing close to planar membrane due to their larger radii of curvature relative to molecular dimensions and are more stable than SUVs [136]. Moreover the binding enthalpies and entropies were distinctly different for the two membrane systems; the binding to SUVs is enthalpy-driven whereas the binding to LUVs is entropy-driven [137]. Even with higher scattering artefacts associated (which can be easily corrected) LUVs are more suitable models of biological membranes [136] and they were chosen for the first characterization of the pep-1/membrane interactions.

2.2. Interaction of Pep-1 with model membranes followed by spectroscopy methodologies

Characterization of pep-1 interaction with model membranes carried in this project is published in two articles with the following titles: 1) *Environmental factors that enhance the action of the cell penetrating peptide pep-1. A spectroscopic study using lipidic vesicles* and 2) *Consequences of nonlytic membrane perturbation to the translocation of the cell penetrating peptide pep-1 in lipidic vesicles*, which are presented afterwards. Experiments presented in these two reports were mainly obtained by fluorescence methodologies and using LUVs as model membranes.

2.2.1. *Environmental factors that enhance the action of the cell penetrating peptide pep-1. A spectroscopic study using lipidic vesicles*

2.2.1.1. Motivation and methodologies

In the paper *Environmental factors that enhance the action of the cell penetrating peptide pep-1. A spectroscopic study using lipidic vesicles* a characterization of pep-1 interaction with model membranes was performed, where peptide affinity for different model membranes and in-depth location in the lipidic bilayer was determined.

Fluorescence spectroscopy is a powerful technique for peptide/membrane interactions analysis; peptides containing aromatic amino acids enable the use of fluorescence spectroscopy with no need for chemical derivatization with fluorescent probes. Pep-1 is intrinsically fluorescent due to its five Trp residues. Trp fluorescence emission is environmental-sensitive: when Trp residues are totally exposed to aqueous environment its fluorescence emission has a spectral maximum at ~350nm; at variance, in a more hydrophobic environment there is a blue shift in fluorescence emission spectrum with a concomitant increase in quantum yield and a decrease in emission band width at half-height (see references [138, 139] and references therein).

To carry on these studies a photophysical characterization of pep-1 was performed in the absence and in the presence of lipid membranes: i.e., quantum yields, excited states, red-edge excitation shifts and anisotropies were quantified (for a detailed information on these photophysical parameters see reference [138]). Altogether pep-1 photophysical parameters gave information about peptide organization in aqueous solution and affinity for model membranes. The influence of environmental factors such as: pH, ionic strength, and reducing environment were addressed.

In the study of the interaction of a peptide with model membranes systems, the determination of peptide extension of insertion in lipidic bilayers is of first importance to obtain information on the peptide affinity to membranes [140]. The extension of interaction of pep-1 with lipid membranes was quantified by means of the molar ratio partition coefficient, K_P

$$K_P = \frac{[Pep-1]_{Lipid}}{[Pep-1]_{Aqueous}} \quad \text{(eq.2.1)}$$

The increase in the fluorescence intensity (I) with lipid concentration was used to determine K_P by means of eq.2.2:

$$I = \frac{I_W + K_P \gamma_L [L] I_L}{1 + K_P \gamma_L [L]} \quad \text{(eq.2.2)}$$

where I_W and I_L are the fluorescence intensities in the absence of lipid and limit value for increasing lipid concentrations, respectively, γ_L is the molar volume of lipid and [L] is the lipid concentration – for more details see reference [140]).

In-depth location when pep-1 inserts in lipidic membrane was studied by acrylamide quenching and by differential quenching of 5-Doxyl-stearic acid (5-NS) and 16-Doxyl-stearic acid (16-NS) using Fernandes *et al.* formalism [141]. Fluorescence quenching refers to the phenomena of fluorescence quantum yield decrease due to direct interaction between the fluorophore and a quencher molecule; this can result from a static and/or a dynamic mechanism – for more details see reference [139].

Acrylamide is a quencher of Trp fluorescence emission, soluble in aqueous solution [138]. At variance, it is unable to efficiently quench the fluorescence of Trp residues deeply buried in the bilayer [142]. With this quencher one has information about the sub-population of fluorophores that is accessible to the aqueous environment [142] (Figure 2.5). The population of fluorophores that inserts in the lipidic membrane can be assessed by 5-NS and 16-NS, which are derivatized fatty acids, able to partition in lipidic bilayers, with a doxyl group ($NO^{\bullet}$) in position 5 and 16, respectively. This group is able to quench Trp residues and its in depth location in the membrane is near the interface for 5-NS or deeply buried in hydrophobic core for 16-NS (Figure 2.5). Stern-Volmer formalism was used to determine K_{SV} (more details in references [138, 139, 141]), which provides information about the quenching efficiency and ultimately about the in-depth location of fluorophores [142] (see Figure 2.5).

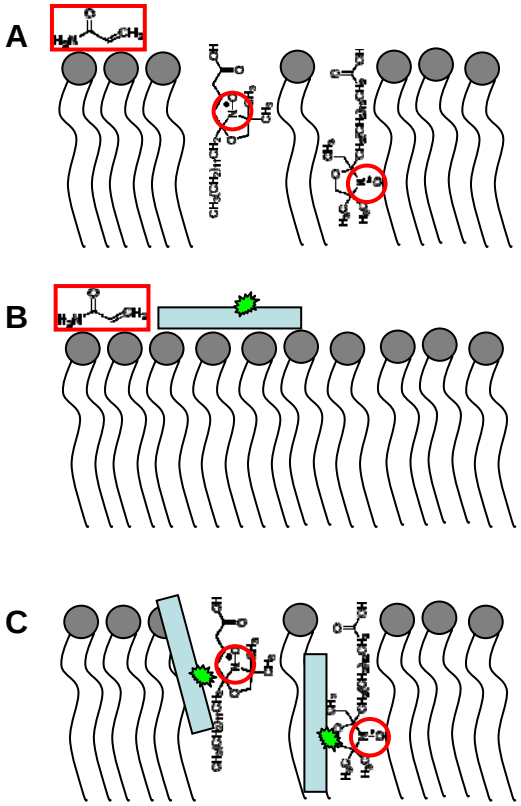

Figure 2.5. Peptide in depth location determined by quenching of acrylamide, 5-NS and 16-NS. **A)** Quenchers location in the presence of lipidic membranes: acrylamide is soluble in aqueous medium and is unable to insert extensively in the membrane; the doxyl group ($NO^{\bullet}$) in 5-NS fatty acid locates close to the water-lipid interface but the doxyl group in 16-NS molecule has deeper location, in the hydrophobic core. **B)** Fraction of fluorophores not inserted in the membrane or that adsorbs at membrane surface are quenched by acrylamide. **C)** When peptide inserts in the membrane close to the water-lipid interface 5-NS is a more efficient quencher than 16-NS; if the fluorophore inserts more deeply in hydrophobic phase 16-NS is a more efficient quencher.

Phospholipids with a phosphatidylcholine (PC) headgroup are the major component in animal cell membranes. The most common acyl chains are C16, C18 and C20; the degree of unsaturation varies widely [107]. Our studies were started with liposomes composed by 1-palmitoyl-2-oleoyl-*sn*-glycero-3-phosphocholine (16:0-18:1; POPC). This lipid forms bilayers in fluid phase at room temperature and can be used to represent the bulk phase in cell membrane. Inner leaflet of plasma membrane is considered to have 20% of negatively-charged phospholipids [107]; in order to evaluate the charge effect in pep-1 affinity and to mimic the inner leaflet, liposomes with POPC and different percentages of a negatively-charged phospholipid with similar acyl chains, 1-palmitoyl-2-oleoyl-*sn*-glycero-3-phosphoglycerol (POPG), were used. The more abundant negatively-charged phospholipid in mammalian cells is PS, the use of PG instead of PS does not compromise the objective to evaluate electrostatic interaction effect, since previous reports demonstrate that interactions mediated by electrostatic forces are independent on the lipid headgroup (PG *vs.* PS) and the basic amino acids (Arg *vs.* Lys) within the peptide [143, 144].

A possible effect of viscosity and the interaction of pep-1 with more rigid domains within plasma membrane were tested with vesicles composed by POPC/Chol (2:1 molar ratio). With this lipidic composition homogeneous membranes with a liquid ordered-like phase are obtained [145, 146].

More rigid membranes were obtained with liposomes composed by 1,2-dipalmitoyl-*sn*-glycero-3-phosphocholine (16:0-16:0; DPPC). This lipid forms a gel phase at room temperature due to saturated acyl chains which favour *van der Waals forces* between molecules and a more highly ordered bilayer. Charge effect in gel-like phase was evaluated with 1,2-Dipalmitoyl-*sn*-glycero-3-phosphoserine (DPPS); different DPPC/DPPS mixtures were compared.

These lipidic systems were used and compared through the studies presented in the following manuscripts.

2.2.1.2. Declaration on authorship of published manuscript: *Environmental factors that enhance the action of the cell penetrating peptide pep-1. A spectroscopic study using lipidic vesicles*

I, Sónia Troeira Henriques declare that the experimental design, the laboratory work, data analysis and discussion were carried on by me under guidance of Dr. Miguel ARB Castanho.

The manuscript was written by me and by my supervisor Dr. Miguel ARB Castanho. Theoretical deduction of peptide fluorescence emission spectrum completely inserted in lipid bilayers and partition formalism accounting for self-quenching presented in Appendix A and Appendix B of the paper were performed by Dr. Miguel ARB Castanho.

I, Miguel ARB Castanho, as Sónia T Henriques supervisor, hereby acknowledge and confirm the information above is correct.

_____ _____

Sónia Troeira Henriques Miguel ARB Castanho

Available online at www.sciencedirect.com
SCIENCE DIRECT
Biochimica et Biophysica Acta 1669 (2005) 75–86
BIOCHIMICA ET BIOPHYSICA ACTA
BBA
http://www.elsevier.com/locate/bba

Environmental factors that enhance the action of the cell penetrating peptide pep-1 A spectroscopic study using lipidic vesicles

Sónia Troeira Henriques, Miguel A.R.B. Castanho*

Centro de Química e Bioquímica, Faculdade de Ciências da Universidade de Lisboa, Ed. C8, Campo Grande, 1749-016 Lisboa, Portugal

Received 2 September 2004; received in revised form 18 November 2004; accepted 19 November 2004
Available online 5 March 2005

Abstract

Pep-1 is a cell penetrating peptide (CPP) derived from the nuclear localization sequence of Simian Virus 40 large antigen T and from reverse transcriptase of Human Immunodeficiency Virus. Although it has been successfully used to transport proteins into cells, its action at the molecular level is not yet clear, mainly the local environmental factors that condition partition and translocation. Characterization in aqueous medium and quantification of partition into bilayers were carried out. Dynamic light scattering studies show that pep-1 self-associates in aqueous medium. The role of the bilayer phase, anionic lipids, ionic strength of the medium, reducing agents and pep-1 concentration on the extent and kinetics of partition were studied. Unlike others cationic CPP (e.g. penetratin) pep-1 has a high affinity to neutral vesicles ($K_p = 2.8 \times 10^3$), which is enhanced by anionic lipids. In a reduction environment partition is strongly inhibited ($K_p = 2.2 \times 10^2$), which might be a key-feature in the biological action of pep-1. Peptide incorporation takes place in the millisecond time-range to the lipidic interfaces. These environmental factors are systematized to enlighten how they help cellular uptake.

Keywords: Translocation; Vector; Peptide carrier; Fluorescence; Vesicle

1. Introduction

The observation that some intracellular proteins translocate naturally across the plasmatic membrane and the identification of basic peptidic sequences responsible for this ability, lead to novel techniques of protein transduction [1–6]. These peptidic sequences, also known as protein transduction domains (PTDs), have been used and optimized as carriers. The three most investigated PTDs are derived from the Human Immunodeficiency Virus 1 (HIV-1) transcriptional activator (tat), the *Drosophila* homeotic transcription factor Antennapedia (Antp), and the Herpes Simplex Virus (HSV) protein VP22 [1,2,5,7]. These PTDs require covalent coupling with the target protein [3,7]. However, this kind of interaction induces alterations in the native form of protein, which can limit the technology [7].

Pep-1 is a synthetic peptide carrier forming non-covalent hydrophobic interactions with the cargo, capable of introducing a great variety of proteins in different cellular lines, without the need to denature proteins [7–10]. This kind of interaction stabilizes the protein, avoiding degradation and preserving its natural characteristics [7,9]. Pep-1 delivers proteins into mammalian cells [7,8,10–12], or in plant cells converted in protoplasts [13], and maintains at least 80% of the viability of different cellular cultures in concentrations up to 1 mM [7] at an average efficiency of 60–95%, depending on the cell type and the protein being transduced [8]. Since it is a non-toxic and non-invasive method with results in less than 2 h, pep-1 is an attractive vehicle to introduce functional proteins in cells [7,8]. This method can potentially: 1) correct genetic diseases by altering the phenotype; 2) function like a vaccine by the introduction of antibodies and 3) be used for research on the study of the function/structure of proteins.

* Corresponding author. Tel.: +351 217500931; fax: +351 217500088.
E-mail address: castanho@fc.ul.pt (M.A.R.B. Castanho).

0005-2736/$ - see front matter © 2005 Elsevier B.V. All rights reserved.
doi:10.1016/j.bbamem.2004.11.017

Pep-1 has 21 amino acids residues (KETWWETWWTEWSQPKKKRKV) with three different domains: the so-called hydrophobic, rich in Trp residues (KETWWETWWTEW), the hydrophilic one rich in basic amino acids (KKKRKV) and a spacer sequence with a Pro (SQP), between the other two [7]. The peptide is acetylated in the N terminal and has a cysteamine group on the C terminal [7] and has a tendency to form disulfide bonds in aqueous solution. The hydrophobic domain is from HIV-1 reverse transcriptase [14] and is responsible for both forming hydrophobic interactions with proteins and for an efficient targeting to the cell membrane [7]. The hydrophilic sequence is a nuclear localization signal (NLS) from the large antigen T of Simian Virus 40 (SV40) [7] and has been used in other peptide carriers [9,15]. This domain improves solubility and intracellular distribution of the peptide [7]. The presence of the Pro residue in spacer sequence promotes a large flexibility and the integrity of other two domains [7].

The understanding of the mechanism of Pep-1 action and the local environmental factors that affect such a mechanism is of first importance for a generalized application and optimization of the process. The amphipaticity of the carrier suggests a strong interaction with the lipidic biomembranes. Despite some molecular-level details, biochemical and biophysical actions of pep-1 are still unknown; Silvius and co-workers recently demonstrated that translocation of cell penetrating peptides is intimately related to the transmembrane potential across lipidic membranes [16]. For pep-1, dependence on membrane potential for translocation occurrence was also verified [17]. Deshayes et al. [18] addressed several specific points relative to pep-1 translocation. Our aim in this paper is to give insight on additional environmental processes that furthermore favour translocation. The presence of five residues of Trp enables the application of fluorescence spectroscopy techniques with no need for derivatization with a fluorescent probe.

2. Material and methods

2.1. Materials

Chariot™, the commercial name of pep-1, was obtained from Active Motif (Rixensart, Belgium) with purity higher than 95%, carboxyfluorescein-labelled pep-1 (pep-1-CF; linked by a Lys in C terminal and blocked with a Ser) was obtained from GenScript Corporation (Piscataway, New Jersey) with purity higher than 95%; 2-(4-(2-Hydroxyethul)-1-piperazinyl) ethanesulfonic acid (HEPES), sodium chloride, L-Tryptophan, acrylamide, ethanol and chloroform spectroscopic were from Merk (Darmstadt, Germany); 1-Palmitoyl-2-Oleoyl-*sn*-Glycero-3-Phosphocholine (POPC), 1-Palmitoyl-2-Oleoyl-*sn*-Glycero-3-(Phospho-rac-(1-glycerol)) (POPG), 1,2-Dipalmitoyl-*sn*-Glycero-3-phosphocholine (DPPC) and 1,2-Dipalmitoyl-*sn*-Glycero-3-(phospho-L-serine) (DPPS), from Avanti Polar-Lipids (Alabaster, Alabama); 5-Doxyl-stearic acid (5DS) and 16-Doxyl-stearic acid (16DS) from Aldrich Chem Co. (Milwaukee, Wisconsin); Cholesterol (chol) and DL-Dithiothreitol (DTT) from sigma (St. Louis, Missouri), *tris*-(2-cyanoethyl)phosphine (phosphine) from molecular probes (Eugene, Oregon), and Oxidized glutathione (GSSG) from Boehringer Manheim (Germany).

Pep-1 solutions were prepared in HEPES buffer (10 mM HEPES, pH 7.4 containing 10 mM (low ionic strength) or 150 mM NaCl (the so-called physiologic ionic strength)). The assays were performed at room temperature in a UV-Vis spectrophotometer Jasco V-530 and in a spectrofluorometer SLM Aminco 8100, equipped with 450 W Xe lamp, Glan-Thompson polarizers, and double monochromators. Fluorescence intensity values were corrected for inner filter effect [19].

2.2. Characterization of pep-1 in aqueous solution

Spectral characterization was performed and fluorescence steady-state anisotropy was used to study red-edge effects (details have been published elsewhere, see Ref. [20]). Quantum yield-dependence on peptide concentration, ionic strength and reduction effects in the presence of phosphine (1 mM) were also evaluated.

A light scattering apparatus equipped with a He–Ne laser (632.8 nm; 35 mW) model 127 from Spectra-Physics and a 72 channels UNICOR autocorrelator was used to study the aggregation of pep-1 in aqueous solution. Peptide solutions were filtered through a sterile 0.22 μM pore Millipore filter. Data was fitted with a tri-exponential function; the average diffusion coefficient, D, was determined (λ=632.8 nm; right angle geometry) and hydrodynamic radius, R_h, was calculated by means of the Stokes–Einstein equation (details have been published elsewhere, see Ref. [21]).

Pep-1-CF solutions (0.023, 0.058, 0.12, 0.17, 0.23 and 0.58 μM) at low ionic strength, were titrated with small volumes of a pep-1 stock solution (688 μM). Pep-1-CF fluorescence was followed with λ_{exc}=490 nm.

2.3. Reduction effect and fluorescence quenching in aqueous solution

Quenching assays were followed by fluorescence intensity with excitation at 280 nm and emission at 350 nm unless stated otherwise. Fluorescence quenching by acrylamide was carried out using λ_{exc}=290 nm to minimize the relative quencher/fluorophore light absorption ratio. Nevertheless, the quenching data were corrected for the simultaneous light absorption of fluorophore and quencher [22]. Quenching assays data with negative deviation from the Stern–Volmer representation Eq. (1) were analysed using Eq. (2),

$$\frac{I_0}{I} = 1 + K_{SV}[Q] \quad (1)$$

(I and I_0 are the fluorescence intensity of the sample in the presence and absence of quencher, respectively, K_{SV} is the Stern–Volmer constant and $[Q]$ the concentration of quencher) [20,23],

$$\frac{I_0}{I} = \frac{1 + K_{SV}[Q]}{(1 + K_{SV}[Q])(1 - f_B) + f_B} \quad (2)$$

($f_B = \frac{I_{0,B}}{I_0}$ is the fraction of light accessible to the quencher and $I_{0,B}$ is the fluorescence intensity of the accessible population to the quencher, when $[Q]=0$ [20,23]).

2.4. Preparation of lipid vesicles

Large unilamellar vesicles (LUVs), with typical 100 nm diameter [24] were prepared by the extrusion method described elsewhere [25] and used as models of biological membranes.

2.5. Extent and kinetics of partition in LUV

The extent and kinetics of partition assays of pep-1 (6.88 μM) in the absence or presence of phosphine (1 mM), were carried out with LUVs of POPC and POPG (liquid-crystal phase), DPPC and DPPS (gel phase) or POPC and chol (2:1) (liquid-ordered phase). Titrations of pep-1 with lipidic suspensions (final concentrations ranges from 0 to 3.75 mM), both in low and physiologic ionic strength, were used to evaluate the extent of the partition. Samples were left to incubate for 10 min after each addition of lipid suspension. The partition coefficient, K_p, is calculated from the fit of experimental data with Eq. (3) as described elsewhere [26]

$$\frac{I}{I_W} = \frac{1 + K_p\gamma_L \frac{I_L}{I_W}[L]}{1 + K_p\gamma_L[L]} \quad (3)$$

where I_W and I_L are the fluorescence intensities in aqueous solution and in lipid solution, respectively, γ_L is the molar volume of lipid and $[L]$ is the lipidic concentration) [26] γ_L used was 7.63×10^{-1} dm^3 mol^{-1} for vesicles containing POPC [27] and 6.89×10^{-1} dm^3 mol^{-1} for vesicles containing DPPC [28]. Pep-1 is restricted to the outer leaflet of bilayers in the absence of a transbilayer potential [17], so data analysis was carried out considering the effective lipid concentration as half of the total lipid concentration [26].

Kinetic assays were followed by fluorescence emission intensity (λ_{ex}=280 nm and λ_{em}=340 nm; pep-1 in lipidic vesicles has a 10 nm blue-shifted emission spectrum, by application of Eq. (AI.8), see Appendix B). Lipidic suspensions (final concentration of 3.75 mM; this concentration ensures that the molar fraction of partitioned peptide in lipidic phase, X_L, is ≥0.8, calculated using Eq. (4) [29]) were added to the peptide solutions (6.88 μM) with physiologic ionic strength.

$$X_L = \frac{K_p\gamma_L[L]}{1 + K_p\gamma_L[L]} \quad (4)$$

The Eq. (AIII.11) deduced in Appendix C was used to fit the kinetics data.

2.6. Location in lipidic membranes

The membrane in-depth location of the pep-1 Trp residues was studied by differential quenching methodologies. 5DS and 16DS are quenchers of Trp fluorescence, which have different locations in the lipidic bilayer. 5DS is located near the interface while 16DS buries more deeply into the bilayer core [30]. Titration of peptide samples (6.88 and 1.45 μM), in the presence of LUVs composed of different lipid mixtures (3.5 mM lipid in buffer with low or physiologic ionic strength), was carried out with ethanolic solution of 5DS and 16DS (final ethanol concentration was kept below 2%). The assays were followed by fluorescence emission intensity (λ_{ex}=280 nm, λ_{em}=340 nm). Data were corrected for simultaneous absorption of fluorophore and quencher [22]. Effective concentration of quencher in the lipidic bilayer matrix, $[Q]_L$,

$$[Q]_L \approx \frac{K_{p,Q}[Q]_T}{1 + K_{p,q}\gamma_L[L]} \qquad \gamma_L[L] << 1 \quad (5)$$

was used in the Stern–Volmer plots; $[Q]_T$ is the quencher concentration in total solution volume and $K_{p,Q}$ is the quencher partition coefficient [29]. For gel phase vesicles $K_{p,Q}$ equals 12,570 and 3340 for 5 DS and 16 DS, respectively. In crystal-liquid-like phase the values used for 5 DS and 16 DS were 89,000 and 9730, respectively [31].

Acrylamide is unable to efficiently quench the fluorescence of Trp residues deeply buried in the bilayer; titration of peptide in the presence of LUVs with this quencher also gives insight on peptide in-depth location [19]. Fluorescence emission quenching (λ_{exc}=290 nm, λ_{em}=340 nm) with acrylamide was carried out with different lipidic mixtures (3.5 mM lipid concentration) in the absence and presence of phosphine (1 mM).

3. Results and discussion

3.1. Aqueous solution

The organization of pep-1 may be potentially influenced by the ionic strength (pep-1 is a charged peptide at pH 7.4) and reduction agents (via inter-molecular disulfide bonds at the cysteamine terminal). Pep-1 has five Trp residues located in its so-called hydrophobic region, which enable structural characterization by fluorescence spectroscopy. The fluorescence spectra of peptide and free Trp in aqueous media present equal vibrational progression (Fig. 1A), this is true both in low and physiologic ionic strength.

At low ionic strength the peptide quantum yield is slightly concentration-dependent (Fig. 1B). Dynamic light scattering correlograms (data not shown) show evidence for the presence of aggregates with mean (weight-averaged) hydro-

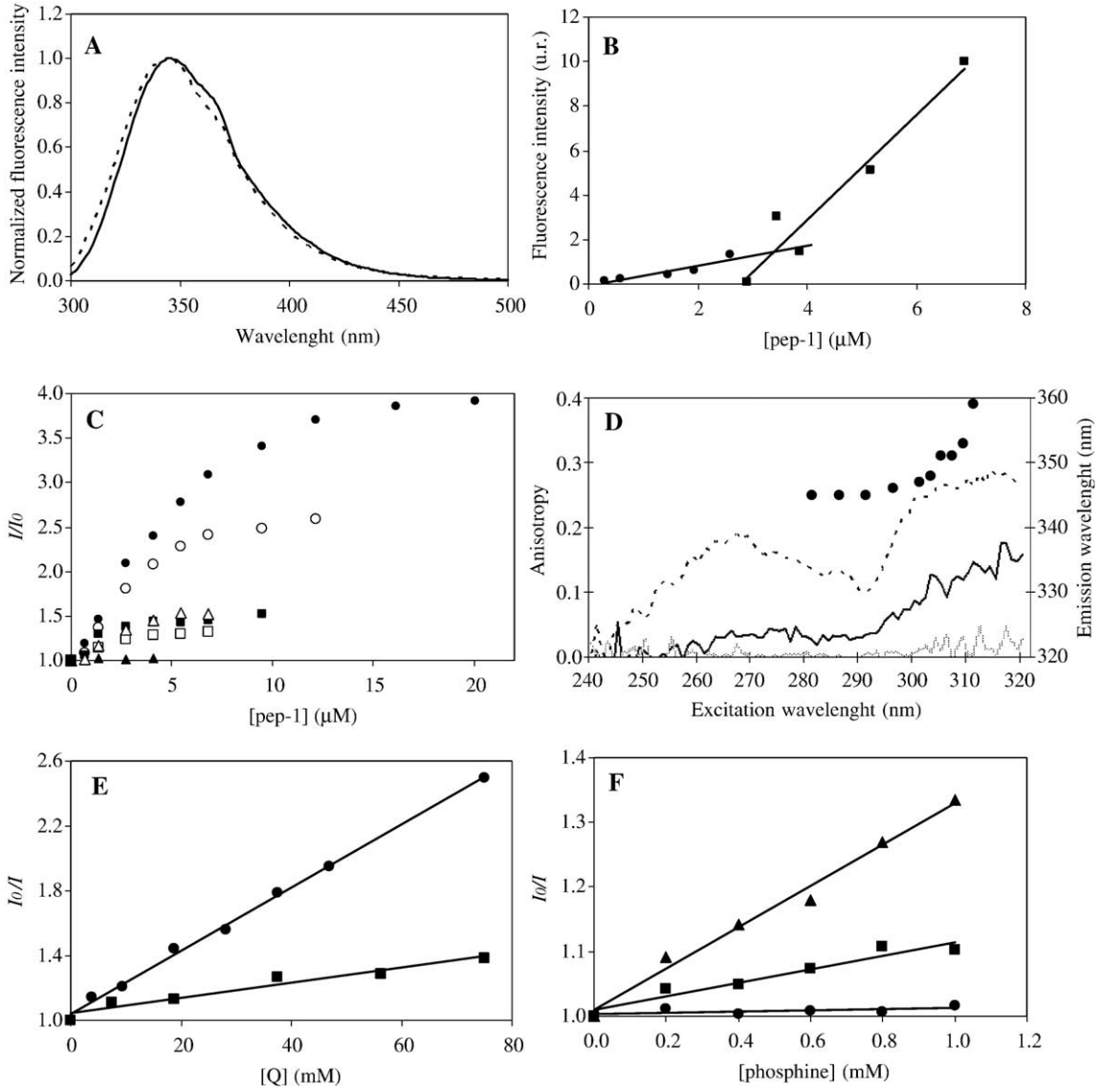

Fig. 1. Characterization of Pep-1 in aqueous solution. Pep-1 (or free Trp) in 10 mM HEPES buffer pH 7.4 containing 10 mM NaCl. (A) Fluorescence emission spectra (λ_{exc}=280 nm) of free Trp (solid line) and pep-1 (dashes) in aqueous solution. (B) Fluorescence intensity (λ_{exc}=280 nm and λ_{em}=350 nm) dependence on pep-1 concentration. There are two linear zones with different slopes, that intersect at an apparent critical concentration (3.4 ± 1.7 μM); below (circles) and above (squares) it, the peptide has different quantum yields. (C) Titration of 0.023 (solid circle), 0.058 (open circles), 0.12 (solid square), 0.17 (open square), 0.23 (open triangle) and 0.58 μM (solid triangle) pep-1-CF with non-labelled pep-1 followed by fluorescence emission at λ_{exc}=490 nm λ_{em}=520 nm. (D) Red-edge excitation shift of 6.88 μM pep-1: variation of maximum emission wavelength (circles) and variation of anisotropy for pep-1 (black solid line), free Trp in buffer (control 1; grey solid line) and free Trp in glycerol (control 2; dashes) with the excitation wavelength. (E) Quenching of fluorescence emission of free Trp by GSSG (circles) and by GSH (squares), notice that hydrolysis of one GSSG molecule forms two GSH molecules. (F) Effect of reducing agent phosphine on free Trp (control; circles), 6.88 μM pep-1 (squares) and 1.45 μM pep-1 (triangles).

dynamic radius of $<R_h>$ ≈ 60 nm in both 1.45 μM and 6.88 μM pep-1 solutions (i.e. below and above the apparent critical concentrations of 3.4 ± 1.7 μM (Fig. 1B)). However these averaged values do not exclude the presence of smaller aggregates in suspension (light scattering techniques have very low sensitivity for smaller aggregates in polydispersed systems) [32]. It is not possible to conclude from Fig. 1B alone if the "critical concentration" is a monomer/micelle transition or reflects the clustering of previously formed n-mers (similarly to what was concluded for polyene antibiotics [33]). Fig. 1C shows that, when pep-1-CF is titrated with unlabelled peptide, fluorescence emission intensity of the carboxy-fluorescein moiety increases when low concentrations of labelled peptide are used. This may be explained on the basis of fluorescence re-absorption ("trivial effect" energy transfer) caused by self-aggregation and closely packed chromophores. Trapping photons in the oligomers increase the probability of non-radiative decay of the fluorophores to the ground state. Therefore, oligomeric forms of the amphipathic peptide occur in solution.

Non-linear Stern–Volmer plots for the fluorescence quenching of the aggregates by the hydrophilic molecule

acrylamide (f_B=0.59 and 0.61 for 1.45 and 6.88 μM, respectively) are evidence that Trp residues sense heterogeneous local micro-environments [26]. Moreover, there is a fraction of the fluorophores not in contact with the aqueous solvent (hydrophobic "pockets" in the aggregates). This result is further confirmed by the occurrence of red-edge excitation shift in the fluorescence spectra of 6.88 μM pep-1 (Fig. 1D), which supports the hypothesis of a reduced mobility on the Trp side chain [34]. A complete depolarization of clustered pep-1 at $\lambda_{excitation}$<280 nm at variance to what is observed with immobilized Trp residues in glycerol (Fig. 1D) is a consequence of Trp–Trp energy migration (homotransfer), which is favoured by adjacent Trp residues in the peptide sequence. Energy migration is known to play a role in red-edge phenomena since red-shifting of Trp emission leads to a decrease in the absorption/emission spectral overlap [23]. Depolarization by migration is not efficient and anisotropy raises at the red-edge. The large ratio of anisotropies taken at 310/270 nm is a consequence of energy migration. Largely shifted emission spectra of Trp (Fig. 1D) are not common but other cases have been reported before [26,35].

It should be stressed that -SH group is a quencher of Trp fluorescence (Fig. 1E). Moreover disulfide bonds are also efficient quenchers (Fig. 1E). The differential effect of the reducing agent phosphine on the fluorescence quantum yield of the aggregates below and above the apparent critical concentration (Fig. 1F) is an evidence of an alteration of the internal molecular structure of the aggregate. Reduction of the -S-S- bonds implies a more pronounced effect at lower concentration (quenching is enhanced with the addition of phosphine; reduction of -S-S- induces a larger diffusional freedom of pep-1, resulting in improved quenching of Trp residues by -SH groups). At higher concentrations, the addition of phosphine does not induce a pronounced alteration in the contact of -S-S- or -SH groups with Trp residues. The fraction of fluorophores accessible to acrylamide in the presence of reducing agent phosphine is bigger for 1.45 μM pep-1 (f_B=0.80) than for 6.88 μM (f_B=0.71). The red-edge excitation shift for 6.88 μM pep-1 is not significantly influenced by the reducing agent phosphine.

At physiologic ionic strength the pep-1 quantum yield is independent of concentration and is not altered in the presence of reducing agent (data not shown). These results suggest that the organization of pep-1 is similar in the range of concentrations evaluated. A non-linear Stern–Volmer (f_B=0.73 for 1.45 μM and 0.63 for 6.88 μM pep-1) and a red-edge excitation shift was also observed for physiologic ionic strength, indicating that peptide aggregates in aqueous solution, but organization of these aggregates is not dependent on concentration.

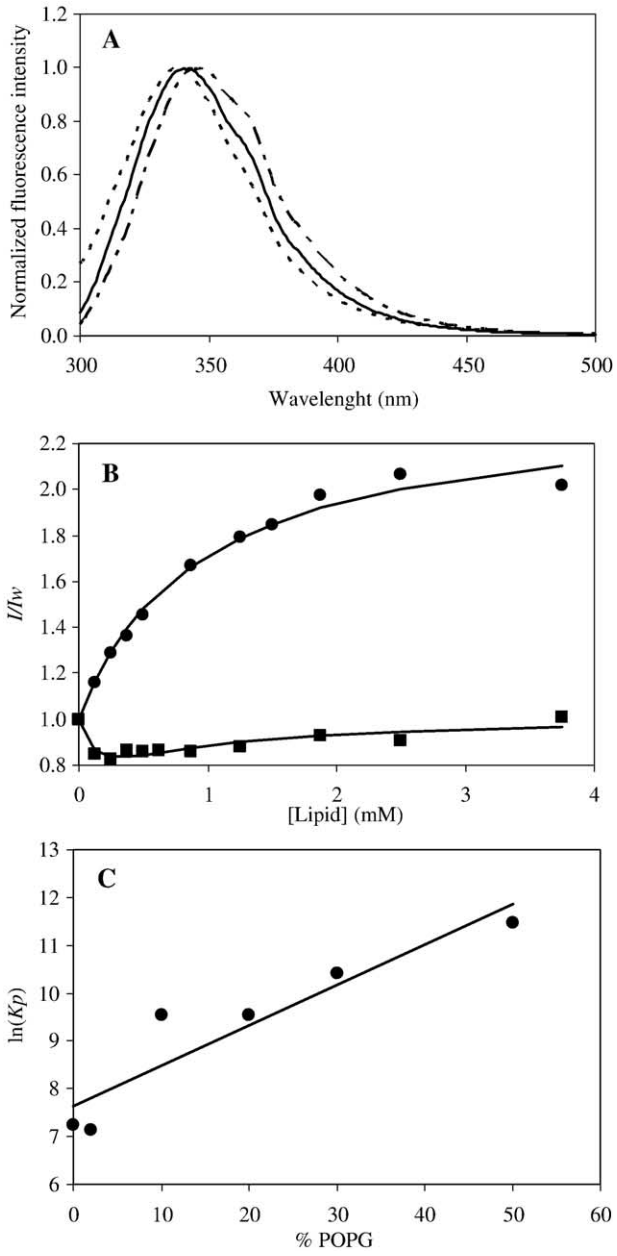

Fig. 2. Partition of pep-1 in LUVs. 6.88 μM pep-1 in 10 mM HEPES buffer pH 7.4 containing 10 mM NaCl. (A) Fluorescence emission spectra of pep-1 in aqueous solution (long and short dashes), in the presence of 0.5 mM POPC LUVs (solid line) and when is completely inserted in lipidic phase (short dashes; spectra calculated using Eq. (AI.8), Appendix A); fluorescence emission spectra were recorded for other lipidic concentrations but only one is represented for the sake of simplicity. (B) Fluorescence emission intensity of pep-1 normalized to [L]=0 (I/I_W) upon titration with LUVs of POPC (circles) or DPPC (squares)—Eq. (3) and Eq. (AII.10) (see Appendix B), respectively, were fitted to data. (C) K_p (logarithmic scale) of pep-1 in vesicles with different molar ratios of POPC:POPG.

3.2. Extent of partition into liquid-crystal bilayers

Titration of aqueous suspensions of the peptide (1.45 or 6.88 μM) with lipidic vesicles leads to blue-shifted emission spectra (Fig. 2A) and an increase in the fluorophore quantum yield (Fig. 2B). The fluorescence intensity is related to K_p by Eq. (3). When POPC large unilamellar vesicles are used ([pep-1]=6.88 μM), $K_p=(2.8\pm0.6)\times10^3$ for low ionic strength, which leads to $\Delta G=-1.9\times10^4$ J mol^{-1}. The calculated molar fraction of the peptides

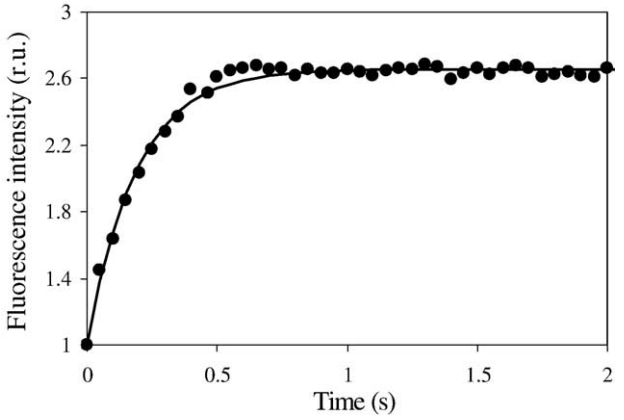

Fig. 3. Partition kinetics of 6.88 μM pep-1 (10 mM HEPES buffer pH 7.4 containing 150 mM NaCl) in 3.75 mM DPPC:DPPS (4:1) LUVs. Fit was realized with Eq. (A.III.11) (see Appendix C).

inserted in the lipidic matrix at 3.5 mM POPC (close to the reference value in biological systems [36]) is X_L=0.80 (Eq. (4)). This value is not sensitive to the ionic strength of the medium (K_p=(3.4 ± 0.6) × 10^3 for physiologic strength), because POPC is globally a neutral lipid. K_p increases exponentially with the molar fraction content of the negatively charged lipid POPG in the POPC bilayer (Fig. 2C). Such exponential behaviour is predicted under the framework of simple theories [37]. For 20% negative lipids (the expected natural occurrence in most cells [38]) and [L]=3.5 mM, X_L is very close to 100% (K_p=2.8 ± 0.4) × 10^4), i.e. virtually all the peptide is inserted in biological membranes. Naturally, at higher ionic strengths, partition coefficient values are decreased (K_p=2.2 ± 0.4) × 10^4), but the difference is not significant and for [L]=3.5 mM X_L is also close to 100%. When phosphine is added to the POPC suspension, K_p is remarkably reduced to (4.8 ± 1.2) × 10^2, showing that the aggregate formed by monomeric peptides in aqueous solution is more stable than the aggregates formed by the dimers. In other words, the reducing environment stabilizes the peptide in aqueous solution. A similar phenomenon was reported for a magainin analogue [39]. When POPG (20%) is present, K_p is also decreased in reducing conditions ((7.2 ± 2.4) × 10^2 for physiologic ionic strength), which means that peptide organization effects superimpose to electrostatic ones in partition.

3.3. Extent of partition into gel phase bilayers

The importance of biomembranes lateral heterogeneity (membrane domains) in the occurrence and control of several biochemical phenomena [40] prompted us to study gel-phase membranes in addition to fluid liquid-crystal ones. DPPC, a neutral lipid at pH 7.4, forms gel bilayers in aqueous environment at room temperature. In the presence of DPPC, the fluorescence spectrum of the peptide is blue-shifted relative to aqueous solution (data not shown). Nevertheless, the fluorescence quantum yield decreases at low lipid concentrations, increasing afterwards (Fig. 2B). We explored the hypothesis that this could be due to self-quenching because at low lipidic concentrations the peptide/lipid molar ratio is high. Eq. (AII.10) was derived (see Appendix B) assuming self-quenching occurrence in partition plots and it fits the experimental data (Fig. 2B). There is no significant difference in partition coefficients of [pep-1]=6.88 μM, for low and physiologic ionic strength (K_p=(1.3 ± 0.4) × 10^4 and (0.6 ± 0.2) × 10^4, respectively). As partition to gel phase bilayers occurs as surface adsorption and/or insertion in line defects in the lipidic palisades, a direct and quantitative comparison with K_p obtained in POPC is prevented. Yet, it should be stressed that K_p is also quite big in rigid lipidic areas of heterogeneous membranes. As before, in the presence of phosphine K_p decreases at both ionic strength ((8.0 ± 1.6) × 10^3 for low ionic strength and (8.0 ± 2.3) × 10^3 for physiologic ionic strength). DPPS, a negatively charged lipid which keeps gel phase properties in the DPPC matrix, causes an increase in K_p up to 10% molar (K_p=(1.4 ± 0.6) × 10^5 for low ionic strength). In the 10–50% range K_p is broadly constant (data not shown). This saturation is probably related to a saturation of the line defects in the gel. Likewise, increasingly blue-shifted emission fluorescence spectra are observed up to 5% DPPS, the wavelength of the emission maximum remaining constant after that.

3.4. Extent of partition into cholesterol-containing bilayers

POPC bilayers having 33% molar cholesterol are homogeneous [41] and can be regarded as model compositions to study liquid-ordered-like patches in biological membranes [42]. Both blue-shifted emission spectra and increased fluorescence quantum yield are detected when pep-1 is in the presence of POPC/cholesterol vesicles. Evidence for self-quenching at high peptide/lipid ratios is obtained (data not shown), as before with DPPC. Nevertheless, the apparent extent of partition is close to the one measured when only POPC was used, (K_p=(3.4 ± 0.4) × 10^3 for low ionic strength and (2.2 ± 0.6) × 10^3 for physiologic ionic strength). Cholesterol affects the partition patterns but not significantly its extent i.e. it favours sulfur/indole interactions, whether by modulation of its organ-

Table 1
Parameters of 6.88 μM pep-1 kinetic incorporation in LUVs, determined by non-linear regression fitting of Eq. (AIII.11) (see Appendix C)

Lipid[a]	$t_{1/2}$ (× 10^2 ms)	K_p (× 10^4)
POPC	6.9 ± 5.2	1.2 ± 0.7
POPC:POPG (4:1)	0.5 ± 0.3	3.4 ± 1.8
POPC:col (2:1)	1.9 ± 0.3	1.5 ± 0.5
DPPC	2.4 ± 0.8	1.4 ± 0.4
DPPC:DPPS (4:1)	1.2 ± 0.3	2.6 ± 0.6

[a] The final lipidic concentration in each case is 3.75 mM (10 mM HEPES buffer pH 7.4 containing 150 mM NaCl).

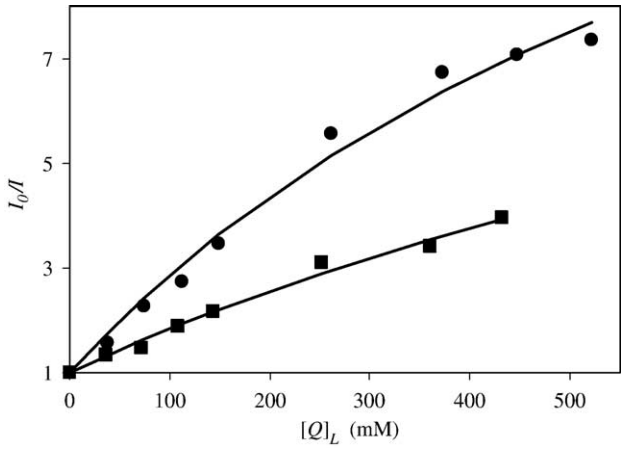

Fig. 4. Pep-1 location in POPC LUVs. Stern–Volmer plot of the fluorescence quenching of 6.88 μM Pep-1 by 5DS (circles) and 16DS (squares) concentration. Effective quencher concentration in lipidic phase was determined using Eq. (5). Eq. (2) was fitted to data by means of non-linear regression. Lipidic concentration is 3.5 mM in a 10 mM HEPES buffer pH 7.4 containing 10 mM NaCl.

ization, or by forcing peptide location in a narrower space of the membrane. The second hypothesis seems more reasonable, on the account of the results obtained with DPPC.

3.5. Kinetics

Partition of pep-1 into lipid bilayers occurs in the second time range, presenting an hyperbolic-like dependence of fluorescence intensity with time (Fig. 3).This dependence was rationalized in terms of a simple partition model (Appendix C) and $t_{1/2}=\ln 2/k_{in}$, as well as K_p, were calculated by fitting Eq. (AIII.11) to the experimental data (Table 1). Partition is faster for gel-phase and liquid-ordered membranes relative to liquid-crystal ones. Anionic lipids decrease $t_{1/2}$. There is a correlation between partition extent and velocity. In spite of differences in methodologies to determine the K_p's, the ones obtained from kinetic data are in fair agreement with those obtained in steady-state experiments (the effect of negative lipids is well pronounced).

Table 3
Emission fluorescence quenching of 6.88 μM pep-1, incorporated in LUVs, by acrylamide[a]

Lipid	[phosphine] (mM)	K_{SV} (M^{-1})
POPC	0	3.1 ± 0.5
	1	17 ± 4.5
POPC:POPG (4:1)	0	2.7 ± 0.4
	1	30.9 ± 9.9
DPPC	0	3.1 ± 0.2
	1	69.4 ± 16.2
DPPC:DPPS (4:1)	0	3.8 ± 0.2
	1	19.3 ± 3.5

[a] Total lipidic concentration was 3.5 mM. Assays were performed in 150 mM (the so-called physiologic ionic strength) NaCl. f_B and K_{SV} were determined by fitting Eq. (2) to experimental data.

3.6. Pep-1 location in the lipid palisade

In-depth location on the pep-1 Trp residues was carried out by means of fluorescence quenching with doxyl derivatized stearic acid. The closer the Trp residues are to the quencher group, the more efficient is the quenching. Thus 5DS probes the bilayer interface while 16DS probes its core. More refined methods [30] are difficult to apply because the Trp residues span a 9-amino acids sequence in the peptide. Stern–Volmer plots show downward deviation from linearity (Fig. 4). This can be due to the existence of fluorescence sub-populations with differential accessibility to the quencher [23]. In the limit, a fraction of the fluorophores may be completely segregated from the quenchers [43]. For instance incomplete partition into membranes ($X_L<1$) renders a fraction of fluorophores completely inaccessible to lipophilic quenchers. Thus, Eq. (2) was used for data analysis. f_B should be equal to the fraction of light emitted from the incorporated peptide, f_L, which can be calculated from K_p [29]

$$f_L = \frac{(I_L/I_W)K_p\gamma_L[L]}{1+(I_L/I_W)K_p\gamma_L[L]} \quad (6)$$

The results are presented in Table 2. Regardless of the lipidic systems or peptide concentrations, 5DS is a more efficient quencher than 16DS. This is evidence of a shallow position of the so-called hydrophobic region of

Table 2
Emission fluorescence quenching of pep-1, incorporated in LUVs, by 5DS and 16DS[a]

[pep-1] (μM)	Lipid	Ionic strength	f_L	$f_{B,5DS}$	$K_{SV,5DS}$ (M^{-1})	$f_{B,16DS}$	$K_{SV,16DS}$ (M^{-1})
6.88	POPC	low	0.90	0.95 ± 0.43	22.1 ± 2.6	0.92 ± 0.45	9.7 ± 1.1
		physiologic	0.94	1	12.3 ± 0.5	1	3.6 ± 0.1
	POPC:POPG (4:1)	physiologic	0.99	0.96 ± 0.24	29.4 ± 1.9	1	6.3 ± 0.1
	DPPC	low	0.94	0.95 ± 0.22	70.4 ± 6.3	1	15.7 ± 0.4
		physiologic	0.98*	0.97 ± 0.30	207 ± 28	1	16.5 ± 0.7
	DPPC:DPPS (4:1)	physiologic	0.99*	0.92 ± 0.33	374 ± 61	1	8.8 ± 0.4
1.45	POPC	physiologic	0.95*	0.74 ± 0.24	27.2 ± 3.8	1	3.0 ± 0.1
	POPC:POPG (4:1)	physiologic	0.98*	0.78 ± 0.33	29.9 ± 5.2	1	6.3 ± 0. 4
	DPPC:DPPS (4:1)	physiologic	0.99*	0.81 ± 0.45	262 ± 67.9	0.77 ± 0.20	22.4 ± 2.4

[a] Total lipidic concentration was 3.5 mM. Assays were performed in 10 mM HEPES buffer containing 10 mM (low ionic strength) or 150 mM (the so-called physiologic ionic strength) NaCl. f_B and K_{SV} were determined by fitting Eq. (2) or Eq. (1) (f_B=1) to experimental data. f_L was determined by application of Eq. (6) using K_p values obtained by the steady-state or kinetic methodologies (marked with *).

pep-1 at the membrane interface. f_L is in agreement with $f_{B,5DS}$ and $f_{B,16DS}$, given the intrinsic experimental error. It is interesting to notice that the quenching efficiency using lipophilic doxyl probes is bigger in gel-phase membranes. This may be due to segregation of both fluorophore and quenchers to defect lines in the gel matrix, favouring static quenching mechanisms at high local concentrations in a molecular scale.

To further search the membrane insertion extent of pep-1, fluorescence quenching experiments using the hydrophilic quencher acrylamide were carried out at 6.88 μM pep-1 and 150 mM NaCl. Results presented in Table 3 demonstrate that fluorescence emission of pep-1 in the presence of LUVs is not efficiently quenched by acrylamide. Although Trp residues are located near the water–lipid interface, they are protected from aqueous environment. In the presence of a reducing agent the quenching efficiency was markedly improved, which suggests that pep-1 is not so extensively incorporated in lipidic vesicles. These results are in agreement with partition data.

4. Conclusions

In a recently published work [17] the capacity of pep-1 to translocate across a lipidic bilayer was demonstrated. Translocation in vesicles only occurs in the presence of a transmembrane potential. The nature of cell membrane (negatively charged inside and neutral outside) prompted us to evaluate the pep-1 affinity for lipidic bilayers in different conditions. The information gathered in the present study highlights some important features of environmental factors that may be crucial to pep-1 molecular action at the biological membrane level. Fig. 5 gathers the information into a mechanistic model. Most biomembranes are asymmetrically charged (neutral at the outer surface and negative inside [38]). The present study shows that Pep-1 in the outer aqueous environment inserts extensively into membranes, whether at high or low concentration, even when no transbilayer potential is present. After anchorage at the bilayer surface, electrostatic attraction combined with lipid bilayer perturbation probably causes translocation into the inner leaflet of the membrane [17]. Being an anionic interface, the release into the cellular environment could be problematic if it was not for the pep-1 reduction (Fig. 5), which turns the peptide aggregates into stable structures with low K_p. This makes the process irreversible in practice inside cells and pep-1 is then available for uptake by cellular compartments.

Results obtained with DPPC suggest that the liquid heterogeneity boundaries in biological membranes may serve as gateways for pep-1 crossing. Membrane fusion may also facilitate translocation, as addressed by Terrone et al. (2003) [16].

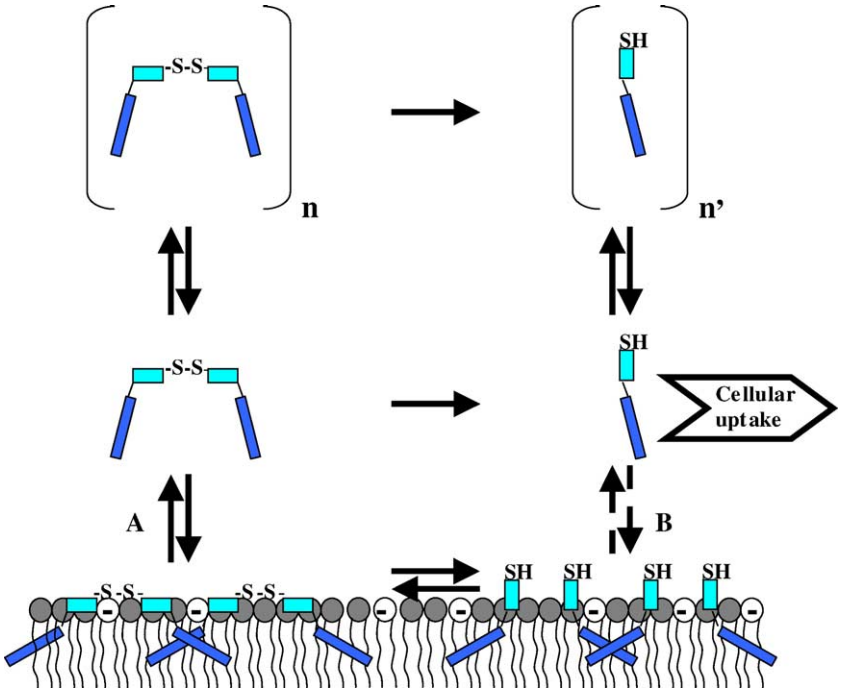

Fig. 5. Mechanistic model for the environmental factors that lead to cellular uptake of pep-1. Pep-1 in the outer aqueous environment incorporates extensively in lipidic bilayers (see text) and translocation occurs, mainly due to membrane perturbation and electrostatic interaction [17]. This sketch depicts the influence of a reducing environment at the cell interior, which is responsible for membrane detachment of pep-1 (thus, it is a crucial factor in pep-1 functionality). Although partition equilibrium of the dimerized peptide to the negatively charged inner leaflet of the mammals' model membranes (A) greatly favours lipidic phase (see text), reduction of pep-1 in the cell interior combined with a partition equilibrium (B) which favours aqueous phase for the monomeric peptide (see text) results in availability of free pep-1 inside the cell. Light blue fragments represent the Lys-rich hydrophilic domain. In dark blue are the Trp-rich domains.

Acknowledgements

We thank Drs. Manuel L. M. Lopes and Lara Penedo for helping with the dynamic light scattering, and Dr. Manuel Prieto (UTL, Portugal) for valuable discussions. Fundação para a Ciência e Tecnologia is acknowledged for funding and a grant to S. T. Henriques.

Appendix A. Theoretical calculation of the peptide fluorescence emission spectrum when it is completely inserted in lipid bilayers

The Trp emission fluorescence is very sensitive to the polarity of the surrounding solvent. The total emission spectrum of pep-1, $I_t(\lambda)$, is dependent both on the spectrum of pep-1 sub-population incorporated in lipid, $I_L(\lambda)$, and the spectrum of the sub-population of the fluorophore present in aqueous solution, $I_W(\lambda)$,

$$I_t(\lambda) = n_L i_L(\lambda) + n_W i_W(\lambda) = I_L(\lambda) + I_W(\lambda) \quad \text{(AI.1)}$$

where $i_i(\lambda)$ is the spectrum of one molecule and n_i the number of molecules in lipid, L, or in water, W. Eq. (AI.1) can be rewritten,

$$I_t(\lambda) = n_L \Phi_L I_{L,N}(\lambda) + n_W \Phi_W I_{W,N}(\lambda) \quad \text{(AI.2)}$$

where $I_{i,N}(\lambda)$ is the normalized emission spectrum; Φ_L and Φ_W are the quantum yield in lipid and water, respectively. Eq. (AI.2) can be rewritten in terms of the molar fraction of peptide in lipid, X_L, and in water, X_W,

$$\frac{I_t(\lambda)}{n_L + n_W} = X_L \Phi_L I_{L,N}(\lambda) + X_W \Phi_W I_{W,N}(\lambda) \quad \text{(AI.3)}$$

$I_t(\lambda)$, can be expressed in terms of the average quantum yield of peptide, $\langle \Phi \rangle_{L,W}$,

$$I_t(\lambda) = (n_L + n_W)\langle \Phi \rangle_{L,W} I_{t,N}(\lambda) \quad \text{(AI.4)}$$

$$\langle \Phi \rangle_{L,W} = X_L \Phi_L + X_W \Phi_W = (1 - X_W)\Phi_L + X_W \Phi_W \quad \text{(AI.5)}$$

Combining Eqs. (AI.3), (AI.4) and (AI.5):

$$I_{L,N}(\lambda) = \left(1 + \frac{X_W}{1 - X_W}\frac{\Phi_W}{\Phi_L}\right) I_{t,N}(\lambda) - \frac{X_W}{1 - X_W}\frac{\Phi_W}{\Phi_L} I_{W,N}(\lambda) \quad \text{(AI.6)}$$

Considering the Eq. (4) (see text),

$$\frac{X_W}{1 - X_W} \approx \frac{1}{K_p \gamma_L [L]} \quad \text{(AI.7)}$$

Therefore, the peptide emission spectrum when totally inserted in lipid membranes, is obtained,

$$I_{L,N}(\lambda) = \left(1 + \frac{1}{K_p \gamma_L [L]}\frac{\Phi_W}{\Phi_L}\right) I_{t,N}(\lambda) - \frac{1}{K_p \gamma_L [L]}\frac{\Phi_W}{\Phi_L} I_{W,N}(\lambda) \quad \text{(AI.8)}$$

Appendix B. Partition formalism accounting for self-quenching in membranes

The quantum yield of a fluorophore population is a linear combination of its components,

$$\Phi = X_L \Phi_L + X_W \Phi_W \quad \text{(AII.1)}$$

Eq. (4) (see text) can be applied to most experimental conditions (lipidic volume very small relative to the total sample volume, $\gamma_L[L] << 1$). Combining Eqs. (AII.1) and (4):

$$\Phi = \frac{\gamma_L K_p [L]}{1 + \gamma_L K_p [L]} \Phi_L + \frac{1}{1 + \gamma_L K_p [L]} \Phi_W \quad \text{(AII.2)}$$

Considering that there is no significant spectral shift influence on the measured fluorescence intensity, I:

$$I = \frac{\gamma_L K_p [L]}{1 + \gamma_L K_p [L]} I_L + \frac{1}{1 + \gamma_L K_p [L]} I_W \quad \text{(AII.3)}$$

where I_L is the emission intensity of the fluorophore molecules incorporated in lipid, in the case of self-quenching absence. I_L is constant if the fluorophore concentration is maintained throughout the experiment. In the case of existing self-quenching, I_L is dependent on lipidic concentration. When lipid concentration is low, the fluorophore concentration in the membrane is high, and the self-quenching notable. In the case of self-quenching, I_L is the intensity that would be recorded in case all fluorophores had the quantum yield of molecules incorporated in lipid at infinite dilution.

In homogeneous solution, *self-quenching* can be described by, [1]

$$\frac{1}{I} = \frac{k_f + k_{nr}}{I_{exc} \varepsilon l k_f [F]} + \frac{k_q}{I_{exc} \varepsilon l k_f} \quad \text{(AII.4)}$$

where I_{exc} is the excitation light intensity, k_q is the kinetic constant of the quenching process, k_f is the radiative fluorescence constant, and $[F]$ is the fluorophore concentration. Considering $k_1 = I_{exc} \Phi \varepsilon l$ and $k_2 = \frac{k_q}{k_f}\frac{1}{\varepsilon l}$, the fluorescence intensity of flurophore can be described by Eq. (AII.5),

$$I = \frac{k_1 [F]}{1 + k_2 k_1 [F]} \quad \text{(AII.5)}$$

In a partition experiment, self-quenching is a consequence of fluorophore compartmentalization inside the lipidic matrix. Imagining that all illuminated volume is occupied by lipidic matrix (limit condition for I_L) and that the lipidic concentration is constant, the fluorescence

intensity dependence on fluorophore concentration, $I_L([F])$ is dictated by Eq. (AII.5), where $[F]$ stands for the fluorophore concentration in the lipidic matrix ($[F]_L$).

In this limit situation, $[F]_L = n_t/v_t$, where n_t is the total number of solute moles and v_t is the total illuminated volume. However, in attainable experimental conditions, only a fraction of the lipid is being illuminated. This fraction equals the fraction of fluorophores being illuminated (n_i/n_t, where n_i and n_t are the illuminated and total moles of fluorophore, respectively). Thus,

$$I([L]) = \frac{k_1[F]_L}{1 + k_2 k_1 [F]_L} \frac{n_i}{n_t} = \frac{k_1[F]_t}{1 + k_2 k_1 [F]_L} \quad \text{(AII.6)}$$

($[F]_t$ is the fluorophore concentration over the whole volume). Taking Eq. (3) (see text), $[F]_L$ is related with $[F]_t$,

$$[F]_L = \frac{K_p}{1 + K_p \gamma_L [L]} [F]_t \quad \text{(AII.7)}$$

So, fluorescence intensity dependence on lipid concentration is:

$$I([L]) = \frac{k_1[F]_t}{1 + k_2 k_1 \dfrac{K_p[F]_t}{1 + k_p \gamma_L [L]}}$$

$$= k_1[F]_t \frac{1 + K_p \gamma_L [L]}{1 + K_p \gamma_L [L] + k_2 K_p k_1 [F]_t} \quad \text{(AII.8)}$$

$k_1[F]_t = I_L$ is the fluorescence emission intensity recorded in the absence of self-quenching, so,

$$I([L]) = I_L \frac{1 + K_p \gamma_L [L]}{1 + K_p \gamma_L [L] + k_2 K_p I_L} \quad \text{(AII.9)}$$

Combining Eqs. (AII.3) and (AII.9),

$$I = \frac{\gamma_L K_p [L] I_L}{1 + K_p \gamma_L [L] + k_2 K_p I_L} + \frac{I_W}{1 + \gamma_L K_p [L]} \quad \text{(AII.10)}$$

Appendix C. Kinetic of partition formalism

If the limit conditions are,

$$n_W(t = 0) = n_t, \quad n_L(t = 0) = 0$$

$$n_L(t = \infty) \approx \gamma_L [L] K_p n_W$$

$$0 < t < \infty \; n_W(t) = n_t - n_L(t)$$

the fluorescence intensity dependence on time can be described by:

$$I(t) \propto \Phi_L n_L + \Phi_W n_W$$

$$I(t = 0) \propto \Phi_W n_t$$

$$0 < t < \infty$$

therefore,

$$\frac{I(t)}{I(t = 0)} = \frac{\Phi_L}{\Phi_W} \frac{n_L(t)}{n_t} + \frac{n_W(t)}{n_t} \quad \text{(AIII.1)}$$

The relative intensity, $I_R(t) = I(t) \neq I(t = 0)$, can be rewritten:

$$I_R(t) = \left(\frac{\Phi_L}{\Phi_W} - 1 \right) \frac{n_L(t)}{n_t} + 1 \quad \text{(AIII.2)}$$

At $t = \infty$,

$$\frac{n_L(t = \infty)}{n_W(t = \infty)} = \gamma_L [L] K_p \quad \text{(AIII.3)}$$

$$\frac{n_L(t = \infty)}{n_t - n_L(t = \infty)} = \gamma_L [L] K_p \quad \text{(AIII.4)}$$

$$\frac{n_L(t = \infty)}{n_t} = \frac{\gamma_L [L] K_p}{1 + \gamma_L [L] K_p} \quad \text{(AIII.5)}$$

K_p can be expressed in terms of kinetic constants,

$$K_p = \frac{k_{in}}{k_{out}} \quad \text{(AIII.6)}$$

where k_{in} and k_{out} are the first-order velocity constants of the fluorophore entering and leaving the lipidic matrix, respectively. Under the framework of our kinetic model, [2]

$$k_{in} t = \frac{n_L(t = \infty)}{n_t} \ln \left(\frac{n_L(t = \infty)}{n_t(t = \infty) - n_L(t)} \right) \quad \text{(AIII.7)}$$

Therefore,

$$\exp \left(k_{in} t \frac{n_t}{n_L(t = \infty)} \right) = \frac{n_L(t = \infty)}{n_t(t = \infty) - n_L(t)} \quad \text{(AIII.8)}$$

But

$$\frac{n_L(t)}{n_L(t = \infty)} = 1 - \exp \left(- \frac{n_t}{n_L(t = \infty)} k_{in} t \right) \quad \text{(AIII.9)}$$

combining Eq. (AIII.5) with Eq. (AIII.9),

$$\frac{n_L(t)}{n_t} = \frac{\gamma_L [L] K_p}{1 + \gamma_L [L] K_p} \left(1 - \exp \left(- \frac{n_t}{n_L(t = \infty)} k_{in} t \right) \right) \quad \text{(AIII.10)}$$

when this term is applied in Eq. (AIII.2),

$$I_R(t) = \left(\frac{\Phi_L}{\Phi_W} - 1 \right) \frac{\gamma_L [L] K_p}{1 + \gamma_L [L] K_p} \times \left(1 - \exp \left(- \frac{1 + K_p [L] \gamma_L}{\gamma_L [L] K_p} \right) k_{in} t \right) + 1 \quad \text{(AIII.11)}$$

References

[1] M.J.E. Prieto, M. Castanho, A. Coutinho, A. Ortiz, F.J. Aranda, J.C. Gómez-Fernández, Fluorescence study of a derivatized diacylglycerol incorporated in model membranes, Chem. Physics of Lipids 69 (1994) 75–85.

[2] K.J. Laider, Chemical Kinetics, 3rd Ed., Harper Collins Publishers, NY, 1987.

References

[1] J.S Wadia, M. Becker-Hapak, S.F. Dowdy, Protein transport, in: Ü. Langel (Ed.), Cell-Penetrating Peptides, Processes and Applications, CRC Press Pharmacology and Toxicology Series, CRC press, NY, 2002, pp. 365–375.
[2] A. Eguchi, T. Akuta, H. Okuyama, T. Senda, H. Yokoi, H. Inokuchi, S. Fujita, T. Hayakama, K. Takeda, M. Hasegawa, M. Nakanisshi, Protein transduction domain of HIV-1 Tat Protein promotes efficient delivery of DNA into mammalian cells, J. Biol. Chem. 247 (2001) 27205–27210.
[3] M.A. Bogoyevitch, T.S. Kendrick, C.H. Dominic, R.K. Barr, Taking the cell by stealth or storm? Protein transduction domain (PTDs) as versatile vectors for delivery, DNA Cell Biol. 21 (2002) 879–894.
[4] J.P. Richard, K. Melikov, E. Vives, C. Ramos, B. Verbeure, M.J. Gait, L.V. Chernomordik, B. Lebleu, Cell-penetrating peptides, a reevaluation of the mechanism of cellular uptake, J. Biol. Chem. 278 (2003) 585–590.
[5] S.R. Schwarze, K.A. Hruska, S.F. Dowdy, Protein transduction: unrestricted delivery into all cells? Trends Cell Biol. 10 (2000) 290–295.
[6] L. Chaloin, N.V. Mau, G. Divita, F. Heitz, Interactions of cell-penetrating peptides with membranes, in: Ü. Langel (Ed.), Cell-Penetrating Peptides, Processes and Applications, CRC Press Pharmacology and Toxicology Series, CRC press, NY, 2002, pp. 23–51.
[7] M.C. Morris, J. Depollier, J. Mery, F. Heitz, G. Divita, A peptide carrier for the delivery of biologically active proteins into mammalian cells, Nat. Biotechnol. 19 (2001) 1143–1147.
[8] http://www.activemotif.com/products/cell/chariot. php, 2004.
[9] C.M. Morris, L. Chalion, F. Heitz, G. Divita, Signal sequence-based cell-penetrating peptides and their applications for gene delivery, in: Ü. Langel (Ed.), Cell-Penetrating Peptides, Processes and Applications, CRC Press Pharmacology and Toxicology Series, CRC press, NY, 2002, pp. 93–113.
[10] A. Ikari, M. Nakano, K. Kawano, Y. Suketa, Up-regulation of sodium-dependent glucose transporter by interaction with heat shock protein 70, J. Biol. Chem. 277 (2002) 33338–33343.
[11] M. Coulpier, J. Anders, C.F. Ibáñez, Coordinated activation of autophosphorilation sites in the RET receptor tyrosine kinase, J. Biol. Chem. 277 (2002) 1991–1999.
[12] J. Zhou, J.-T. Hsieh, The inhibitory role of DOC-2/DAB2 in growth factor receptor mediated signal cascade, J. Biol. Chem. 276 (2001) 27793–27798.
[13] Y. Wu, M.D. Wood, F. Katagiri, Direct delivery of bacterial avirulence proteins into resistant *Arabidopsis* protoplasts leads to hypersensitive cell death, Plant J. 33 (2003) 131–137.
[14] M. Morris, V. Robert-Hebmann, L. Chaloin, J. Mery, F. Heitz, C. Devaux, R.S. Goody, G. Divita, A new potent HIV-1 reverse transcriptase inhibitor, J. Biol. Chem. 274 (1999) 24941–24946.
[15] L. Chaloin, N.V. Mau, G. Divita, F. Heitz, Interactions of cell-penetrating peptides with membranes, in: Ü. Langel (Ed.), Cell-Penetrating Peptides, Processes and Applications, CRC Press Pharmacology and Toxicology Series, CRC press, NY, 2002, pp. 163–186.
[16] D. Terrone, S.L. W. Sang, L. Roudaia, J.R. Silvius, Penetratin and related cell-penetrating cationic peptides can translocate across lipid bilayers in the presence of transbilayer potential, Biochemistry 42 (2003) 13787–13799.
[17] S.T. Henriques, M.A.R.B. Castanho, Consequences of nonlytic membrane perturbation to the translocation of the cell penetrating peptide pep-1 in lipidic vesicles, Biochemistry 43 (2004) 9716–9724.
[18] S. Deshayes, A. Heitz, M.C. Morris, P. Charnet, G. Divita, F. Heitz, Insight into the mechanism of internalization of the cell-penetrating carrier peptide pep-1 through conformational analysis, Biochemistry 43 (2004) 1449–1457.
[19] G.A. Caputo, E. London, Using a novel dual fluorescence quenching assay for measurement of tryptophan depth within lipid bilayers to determine hydrophobic α-helix location within membranes, Biochemistry 42 (2003) 3265–3274.
[20] N.C. Santos, M.A.R.B. Castanho, Fluorescence spectroscopy methodologies on the study of proteins and peptides. On the 150th anniversary of protein fluorescence, Trends Appl. Spectrosc. 4 (2002) 113–125.
[21] N.C. Santos, M.A.R.B. Castanho, Teaching light scattering spectroscopy: the dimension and shape of tobacco mosaic virus, Biophys. J. 71 (1996) 1641–1650.
[22] A. Coutinho, M. Prieto, Ribonuclease T1 and alcohol dehydrogenase fluorescence quenching by acrylamide, J. Chem. Educ. 70 (1993) 425–428.
[23] J.R. Lakowics, Principles of Fluorescence Spectroscopy, 2nd ed., Kluwer Academic/Plenum publishers, NY, 1999.
[24] T. Wieprecht, M. Beyermann, J. Seeling, Thermodynamics of the coli-α-helix transition of amphipathic peptides in a membrane environment; the role of the curvature, Biophys. Chem. 96 (2002) 191–201.
[25] L.D. Mayer, M.J. Hope, P.R. Cullis, Vesicles of variable sizes produced by a rapid extrusion procedure, Biochim. Biophys. Acta 858 (1986) 161–168.
[26] N.C. Santos, M. Prieto, M.A.R.B. Castanho, Quantifying molecular partition into model systems of biomembranes: an emphasis on optical spectroscopic methods, Biochim. Biophys. Acta 1612 (2003) 123–135.
[27] S.W. Chiu, E. Jakobsson, S. Subramanian, H.L. Scott, Combined Monte Carlo and molecular dynamics simulation of fully hydrated dioleyl and palmitoyl-oleyl-phosphatidylcholine lipid bilayers, Biophys. J. 77 (1999) 2462–2469.
[28] J.F. Naigle, M.C. Weiner, Structure of fully hydrated bilayer dispersions, Biochim. Biophys. Acta 942 (1988) 1–10.
[29] N.C. Santos, M. Prieto, M.A.R.B. Castanho, Interaction of the major epitope of HIV gp41 with membrane novel systems. A fluorescence spectroscopy study, Biochemistry 37 (1998) 8674–8682.
[30] M.X. Fernandes, J.G. Torre, M.A.R.B. Castanho, Joint determination by brownian dynamics and fluorescence quenching of the in-depth location profile of biomolecules in membranes, Anal. Biochem. 307 (2002) 1–12.
[31] J.R. Wardlaw, W.H. Sawyer, K.P. Ghiggino, Vertical fluctuations of phospholipid acyl chains in bilayers, FEBS Lett. 223 (1987) 20–24.
[32] S.E. Harding, D.B. Sattelle, V.A. Bloomfield (Eds.), Laser Light Scattering in Biochemistry, Royal Soc. Chemistry, Cambridge, 1992.
[33] M. Castanho, W. Brown, M. Prieto, Filipin and its interaction with cholesterol in aqueous media studied using static and dynamic light scattering, Biopolymers 34 (1994) 447–456.
[34] C. Mangavel, R. Maget-Dana, P. Tauc, J.-C. Brochon, D. Sy, A. Reynaud, Structural investigations of basic amphipathic model peptides in the presence of lipid vesicles studied by circular dichroism, fluorescence monolayer and modelling, Biochim. Biophys. Acta 1371 (1998) 265–2983.
[35] L.A. Falls, B.C. Furie, M. Jacobs, B. Furie, A.C. Rigby, The ω-loop region of the human prothrombin γ-carboxyglutamic acid domain penetrates anionic phospholipid membranes, J. Biol. Chem. 276 (2001) 23895–23902.
[36] J.R. Silvius, Lipidated peptides as tools for understanding the membrane interactions of lipid-modified proteins, in: S.A. Simon, T.J. McIntosh (Eds.), Peptide–Lipid Interactions, Academic Press, California, 2002, pp. 371–395.
[37] D. Murray, A. Arbuzova, B. Honig, S. McLaughlin, The role of electrostatic and nonpolar interactions in the association of peripheral proteins with membranes, in: S.A. Simon, T.J. McIntosh

(Eds.), Peptide–Lipid Interactions, Academic Press, California, 2002, pp. 277–307.
[38] R.B. Gennis, Biomembranes, Molecular Structure and Function, Springer-verlag, NY, 1989.
[39] C.E. Dempsey, S. Ueno, M. Avison, Enhanced membrane permeabilization and antibacterial activity of a disulfide–dimerized magainin analogue, Biochemistry 42 (2003) 402–409.
[40] K. Simons, E. Ikonen, Functional rafts in cell membranes, Nature 387 (1997) 569–572.
[41] C.R. Mateo, J.-C. Brochon, M.P. Lillo, A.U. Acuña, Liquid-crystalline phases of cholesterol/lipid bilayers as revealed by the fluorescence of *trans*-parinaric acid, Biophys. J. 65 (1993) 2237–2247.
[42] J.R. Silvius, Role of cholesterol in lipid raft formation: lessons from lipid model systems, Biochim. Biophys. Acta 1610 (2003) 174–183.
[43] S. Lehrer, Solute perturbation of protein fluorescence. The quenching of the tryptophyl fluorescence of model compounds and of lysozyme by iodide ion, Biochemistry 10 (1971) 3254–3263.

2.2.2. *Consequences of nonlytic membrane perturbation to the translocation of the cell penetrating peptide pep-1 in lipidic vesicles.*

2.2.2.1. Motivation and methodologies used

After characterization of environmental factors that improve pep-1 affinity for lipidic membranes and the possible location of this peptide in the membrane, functional abilities of pep-1 and the effects on membrane integrity were aimed. The possibility of vesicle aggregation and fusion of lipids; induction of phospholipid flip-flop; segregation of anionic phospholipids; ability to induce pore formation and to translocate across cell membrane were evaluated. The results and conclusions were published in the article titled: *Consequences of nonlytic membrane perturbation to the translocation of the cell penetrating peptide pep-1 in lipidic vesicles*.

The stability of liposomes dispersion is mainly governed by three types of forces: electrostatic repulsion, *van der Waals* attraction and hydration forces [147]. The electrostatic force is affected by charge density of the vesicles and the electrolyte concentration, while *van der Waals* interactions can be modulated by modification of the vesicle size. The magnitude of hydration force is related to the energy required to remove water from the surface. The presence of polyvalent cations is able not only to charge surface density upon adsorption to the membrane but also to dehydrated the lipid headgroup and thereby induce aggregation of phospholipid vesicles. Pep-1 has 7 positive charges and a positive global charge (+3) at physiological conditions. Regarding this positive global charge and peptide affinity for lipidic membranes it would be expected that this peptide could work as a destabilising agent, as observed for penetratin [147]. Optical density was employed to monitor vesicle aggregation induced by pep-1. Turbidity is directly proportional to the R^2 (R, particle size) [148], consequently, small increases in the size of the liposomes due to aggregation originate a high increase in turbidity which can be followed by optical density. The possibility of vesicle aggregation was further confirmed with fluorescence microscopy with vesicles doped with a Rhodamine B-labelled phospholipid.

Vesicle fusion may result from a variety of stimuli able to destabilize lipidic membranes [149]. Some examples of propitious conditions for fusion events occurrence

are discussed in the reference [150]. Pep-1 is amphipathic, which is a common characteristic among fusiogenic peptides [151]; the possibility of vesicle fusion induced by this peptide was evaluated by the use of Förster Resonance Energy Transfer (FRET) methodology. FRET is referred to the process in which the energy associated with electronic excitation in a molecule (donor) is "shared" with a nearby molecule (acceptor) trough dipole-dipole coupling. The energy shared is dependent on distance between dipoles [152] and is strongly dependent on the overlap of emission spectrum of donor molecule and excitation spectrum of acceptor molecule.

To follow vesicle fusion induced by pep-1 FRET between 7-nitro-2-1,3-benzoxadiazol-4-il (NBD; acceptor) and Rhodamine (Rh; donor) was followed. NBD is a fluorophore with an emission at about 463nm and Rh is excited around 470nm. Vesicles doped with NBD-PE and with Rh-PE were mixed with non-labelled vesicles. In the case of fusion of vesicles induced by pep-1, NBD and Rh molecules become more separated on average and a decrease in FRET efficiency is monitored (Figure 2.6).

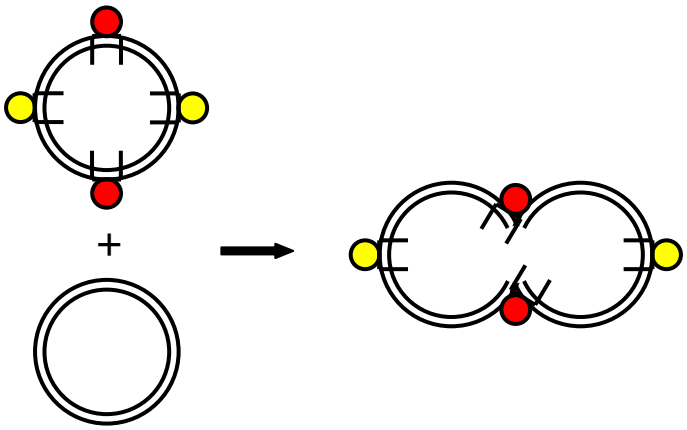

Figure 2.6. Fusion of vesicles can be followed by FRET between NBD (yellow, donor) and Rh (red, acceptor). A decrease in FRET efficiency is expected upon fusion of labelled vesicles (doped with Rh and NBD) with non-labelled vesicles. A decrease in FRET efficiency results from an increase in the distance between donor and acceptor. Image adapted from http://probes.invitrogen.com/handbook/.

Pep-1 affinity to lipidic membranes increases in the presence of anionic phospholipids [153] (see section 2.2.1); results obtained with other CPPs suggest that the internalization mechanism is dependent on the interaction with anionic lipids or other negatively-charged molecules at cell surface [63, 66, 70, 154]. A specific interaction with anionic phospholipids and the possibility of pep-1-induced anionic lipid segregation were tested. This was also followed by FRET between NBD and Rh by the use of vesicles labelled with C6-NBD-PG (anionic phospholipid) and Rh-PE

(zwitterionic phospholipid). In the case of segregation of anionic phospholipids due to peptide-inducing clustering, the average distance between Rh and NBD would increase and a decrease in FRET efficiency upon peptide addition should be notorious.

Some basic peptides are able to induce membrane perturbation that provokes membrane leakage and ultimately membrane lyses. This is a common feature among AMPs such as Melitin [155, 156], Magainin 2 [157] and Buforin 2 [158]. The possibility of pore formation induced by pep-1 was tested by means of NBD fluorescence emission quenching in the presence of Co^{2+} ions [159]. This quencher can not access the inner core of membranes but is able to quench NBD molecules attached to phospholipid headgroups in the water-lipid interface [159]. When vesicles are doped with NBD-labelled phospholipid (N-NBD-PE), NBD molecules are homogenously distributed in the two layers. Upon Co^{2+} addition, fluorescence emission of NBD molecules in the outer layer is quenched, while NBD molecules in the inner layer are inaccessible to the quencher because Co^{2+} ions are notable to transverse the lipid bilayer. In the case of pore formation upon peptide addition, the membrane becomes permeable to Co^{2+} ions, which will result in quenching of the fluorescence emission of NBD molecules in the inner layer (Figure 2.7).

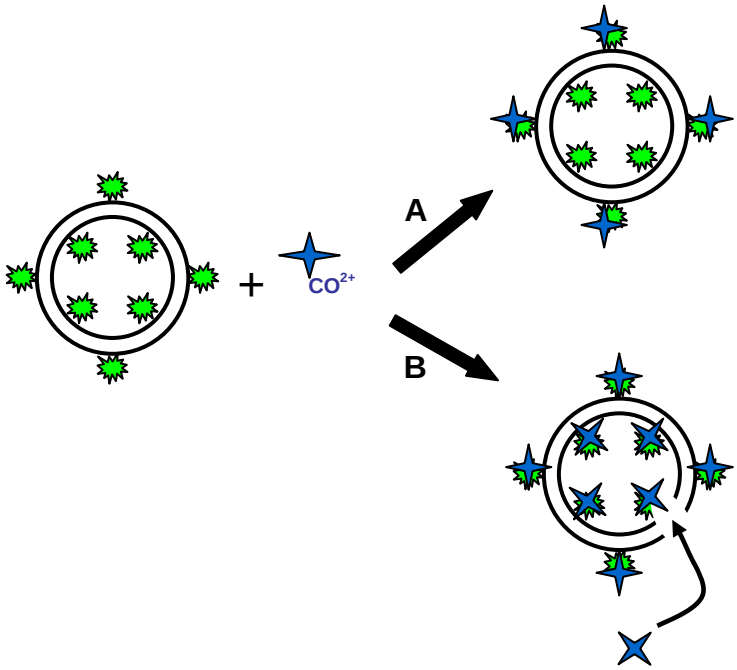

Figure 2.7. Pore formation followed by quenching of NBD with Co^{2+} ions. NBD fluorophores are homogeneously distributed trough inner and outer layers. Upon Co^{2+} addition **A)** fluorescence emission of NBD fluorophores in the outer layer will be quenched; **B)** in the case of pore formation, the membrane becomes impermeable to Co^{2+} ions, which in addition will quench NBD molecules in the inner layer.

The pore formation was also evaluated by means of Rh fluorescence, which is quenched by pep-1 molecules. Vesicles were prepared with Rh B-containing buffer in the absence or in presence of pep-1. Then, non-encapsulated Rh B was removed by exclusion chromatography. For this particular study MLVs instead of LUVs were used to enable a gradual effect in the case of pore formation due translocation through the various lamellae. In the sample prepared with peptide, pep-1 is accessible to encapsulated Rh B molecules, serving as control; in the samples prepared without peptide, pep-1 was added later than and the quenching efficiency was compared to the control. If pep-1 does not form pores, it does not quench the Rh B molecules encapsulated in the vesicles. In the case of pore formation, pep-1 quenches the Rh B fluorophores inside the liposomes and the Rh fluorescence intensity is similar to the one obtained when pep-1 was added prior to vesicle formation.

Peptide incorporation in lipidic vesicles can promote flip-flop (transbilayer movement) of phospholipids due to lipidic bilayer perturbation [160-162]. Peptide mediated "flop" is primarily the results of local disturbances of the bilayer structure in the vicinity of the peptide [161].
If pore formation is not observed, flip-flop can be evaluated with a methodology similar to the one used to evaluate pore formation (see Figure 2.7) but with C6-NBD-PG instead of N-NBD-PE (in the former molecule NBD fluorophore is in the acyl chain while in N-NBD-PE the fluorophore is attached to the headgroup). C6-NBD-PG can undergo flip-flop [161, 163, 164], whereas NBD-PE cannot (NBD fluorophores derivatized in the polar group of the phospholipids inhibit flip-flop due to hydrophilic nature of the probe and its location [165]). In the case of flip flop an increase in NBD fluorescence emission quenching induced by Co^{2+} ions is expected after peptide addition.

The biological activity of Pep-1 is dependent on its capacity to translocate across cell membrane. The possibility of pep-1 to translocate through model membranes was tested. The methodology used took advantage from the pep-1 quencher properties relative to Rh fluorescence. For these studies the fluorophore was placed in the lipidic bilayers attached to a phospholipid (Rh-PE) and two approaches were used. In the first one MLVs doped with Rh-PE were prepared with buffer in the presence or absence of

pep-1. In this later sample, pep-1 was added afterwards and the Rh fluorescence quenching induced by the pep-1 was compared with the value obtained with the sample where the pep-1 was added prior to vesicle formation. In the second approach LUVs doped with Rh-PE were used, where the fluorophore is distributed homogeneously in the two layers. Upon peptide addition Rh fluorophores outside the membrane will be quenched; in the case of translocation pep-1 will became accessible to Rh molecules in the inner layer and a more efficient quenching will be notice (similar to what is represented in Figure 2.7).

Terrone et al. [78] verified that penetratin and related CPPs are able to translocate across model membranes by a physical mechanism dependent on transmembrane potential. The transmembrane potential similar to the one presented in cellular membranes (negative inside) can be mimetized with liposomes loaded with K^+-containing buffer and dispersed in a Na^+-containing buffer after valinomycin addition. Valinomycin forms highly specific pores for potassium ions (at variance with sodium ions, for instance) in the cell membrane. It works as a potassium-specific carrier facilitating the passage of potassium ions across membranes and modifying the electrochemical potential gradient [166, 167], creating a net charge with an excess of positive charges in of the bilayer sides.

The methodologies above referred were used to evaluate the functional features of pep-1 with model membranes; the manuscript with the results obtained is presented afterwards.

2.2.2.2. Declaration on authorship of published manuscript: *Consequences of nonlytic membrane perturbation to the translocation of the cell penetrating peptide pep-1 in lipidic vesicles*

I, Sónia Troeira Henriques declare that the experimental design, the laboratory work, the data analysis and discussion were carried on by me under guidance of Dr. Miguel ARB Castanho. Dr. Fernando Antunes and Nuno MV Pedroso helped me in the first contact with fluorescence microscopy.

The manuscript was written by me and by my supervisor Dr. Miguel ARB Castanho.

I, Miguel ARB Castanho, as Sónia T Henriques supervisor, hereby acknowledge and confirm the information above is correct.

_____ _____

Sónia Troeira Henriques Miguel ARB Castanho

Consequences of Nonlytic Membrane Perturbation to the Translocation of the Cell Penetrating Peptide Pep-1 in Lipidic Vesicles†

Sónia Troeira Henriques and Miguel Augusto Rico Botas Castanho*

Centro de Química e Bioquímica, Faculdade de Ciências da Universidade de Lisboa, Ed. C8, Campo Grande, 1749-016 Lisboa, Portugal

Received December 29, 2003; Revised Manuscript Received April 27, 2004

ABSTRACT: The action of the cell penetrating pep-1 at the molecular level is not clearly understood. The ability of the peptide to induce (1) vesicle aggregation, (2) lipidic fusion, (3) anionic lipid segregation, (4) pore or other lytic structure formation, (5) asymmetric lipidic flip-flop, and (6) peptide translocation across the bilayers in large unilamellar vesicles was studied using photophysical methodologies mainly related to fluorescence spectroscopy. Neflometry and turbidimetry techniques show that clustering of vesicles occurs in the presence of the peptide in a concentration- and anionic lipid content-dependent manner. Results from Forstër resonance energy transfer-based methodologies prove lipidic fusion and anionic lipid segregation, but no evidence for pores or other lytic structures was found. Asymmetric lipid flip-flop was not detected either. A specific method related to the quenching of the rhodamine-labeled lipids by pep-1 was developed to study the eventual translocation of the peptide. Translocation does not occur in symmetrical neutral and negatively charged vesicles, except when a valinomycin-induced transmembrane potential exists. Our work strongly suggests that the main driving force for peptide translocation is charge asymmetry between the outer and inner leaflet of biological membranes and reveals that pep-1 is able to perturb membranes without being cytotoxic. This nonlytic perturbation is probably mandatory for translocation to occur.

The molecular ability to cross the biomembrane barrier and introduce material into cells is a recent matter of interest in research. So far, gene delivery technologies are most used, but these kinds of delivery systems have some drawbacks, such as low efficiency, poor specificity, poor bioavailability, and toxicity (*1*). Introduction of proteins directly into a cell is a better alternative because the posttranslation modification is critical for the biological function of the protein (*2*). Nevertheless traditional methods to introduce proteins have low efficiency; the transduced protein often enters the endocytic pathway and traffics to the lysosome where it will be degraded and inactivated (*2*). New strategies for protein transduction have been developed that use peptide carriers designated as protein transduction domains (PTDs)[1] (*1*−*7*). These "vectors" are basic sequences capable of translocating across the plasmatic membranes in a manner independent of receptors or the endosomal pathway, carrying proteins covalently linked (*1*−*7*).

Pep-1, a synthetic peptide carrier capable of introducing active proteins into cells, has advantages over "genetic therapy" because phenotype can be altered in less than 2 h (*3*, *8*, *9*), as well as over other PTDs since the interaction with proteins is independent of covalent links; the complex pep-1/protein is promoted by hydrophobic forces (*3*, *8*, *10*). The pep-1 has 21 amino acid residues (KETWWETWW-TEWSQPKKKRKV), which can be divided into three different domains: a "so-called" hydrophobic one, rich in tryptophans (KETWWETWWTEW), a hydrophilic domain with basic residues (KKKRKV), and a spacer between them (SQP) (*3*, *8*). The hydrophobic sequence is responsible for the hydrophobic interactions with proteins (*3*, *8*) and for the intrinsic fluorescence of the peptide. The hydrophilic domain improves intracellular distribution and the solubility of peptide (*3*, *8*). The spacer sequence is a link between the other two domains (*3*, *8*). Peptide is acetylated on the N terminus and has a cysteamine group on the C terminus (*8*); at physiological pH (7.4), the peptide has a global charge of +3.

Like others PTDs, pep-1 translocates along biological membranes in a manner independent of the endosomal pathway (*8*), which suggests a physical process dictated by the lipid bilayer. Pep-1 has high affinity for lipid bilayers, and the presence of negative charges in the vesicles enhances the partition to lipid bilayers, showing a strong electrostatic interaction (*11*).

In the present paper, our aim is to present functional abilities of the peptide (vesicle aggregation, dissociation, and

† This work was supported by Fundação para a Ciência e Tecnologia (Portugal).

* To whom correspondence should be addressed. Tel.: +351217500931. Fax: +351217500088. E-mail: castanho@fc.ul.pt.

[1] Abbreviations: PTDs, protein transduction domains; HEPES, 2-(4-(2-hydroxyethyl)-1-piperazinyl)ethanesulfonic acid; POPC, 1-palmitoyl-2-oleoyl-*sn*-glycero-3-phosphocholine; POPG, 1-palmitoyl-2-oleoyl-*sn*-glycero-3-(phospho-*rac*-(1-glycerol)); DPPC, 1,2-dipalmitoyl-*sn*-glycero-3-phosphocholine; DPPS, 1,2-dipalmitoyl-*sn*-glycero-3-(phospho-L-serine); C6-NBD-PC, 1-myristoyl-2-[6-[(7-nitro-2−1,3-benzoxadiazol-4-yl)amino]caproil]-*sn*-glycero-3-phosphocholine; C6-NBD-PG, 1-myristoyl-2-[6-[(7-nitro-2−1,3-benzoxadiazol-4-yl)amino]caproil]-*sn*-glycero-3-phosphoglycerol; N-NBD-PE, 1,2-dipalmitoyl-*sn*-glycero-3-phosphoethalonamine-*N*-(7-nitro-2-1,3-benzoxadiazol-4-yl); N-Rh-PE, 1,2-dipalmitoyl-*sn*-glycero-3-phosphoethalonamine-*N*-(lissamine rhodamine B sulfonyl); Rh B, rhodamine B; TX-100, Triton X-100; LUVs, large unilamellar vesicles; MLVs, multilamellar vesicles; FRET, Forstër resonance energy transfer; OD, optical density.

10.1021/bi036325k CCC: $27.50
Published on Web 07/07/2004

fusion, pore formation in the lipidic bilayer, induction of phospholipid flip-flop, segregation of anionic phospholipid, and the ability to translocate) and to propose a molecular model of action.

EXPERIMENTAL PROCEDURES

Reagents and Apparatus. Chariot, the commercial name of pep-1, was obtained from Active Motif (Rixensart, Belgium) with purity >95%; 2-(4-(2-Hydroxyethyl)-1-piperazinyl)ethanesulfonic acid (HEPES), sodium chloride, and chloroform (spectroscopic grade) were from Merk (Darmstadt, Germany); 1-palmitoyl-2-oleoyl-*sn*-glycero-3-phosphocholine (POPC), 1-palmitoyl-2-oleoyl-*sn*-glycero-3-(phospho-*rac*-(1-glycerol)) (POPG), 1,2-dipalmitoyl-*sn*-glycero-3-phosphocholine (DPPC), 1,2-dipalmitoyl-*sn*-glycero-3-(phospho-L-serine) (DPPS), 1-myristoyl-2-[6-[(7-nitro-2-1,3-benzoxadiazol-4-yl)amino]caproil]-*sn*-glycero-3-phosphocholine (C6-NBD-PC), 1-myristoyl-2-[6-[(7-nitrro-2-1,3-benzoxadiazol-4-yl)amino]caproil]-*sn*-glycero-3-phosphoglycerol (C6-NBD-PG), 1,2-dipalmitoyl-*sn*-glycero-3-phosphoethalonamine-*N*-(7-nitro-2-1,3-benzoxadiazol-4-yl) (N-NBD-PE), and 1,2-dipalmitoyl-*sn*-glycero-3-phosphoethalonamine-*N*-(lissamine rhodamine B sulfonyl) (N-Rh-PE) were from Avanti Polar-Lipids (Alabaster, Alabama); Triton X-100 (TX-100), rhodamine B (Rh B), and valinomycin were from Sigma (St. Louis, Missouri); cobalt(II) chloride hexahydrate ($CoCl_2 \cdot 6H_2O$) was from Acrós organics (Geel, Belgium), and tris-(2-cyanoethyl)phosphine (phosphine) was from molecular probes (Eugene, Oregon).

The assays were performed at room temperature in a UV−vis spectrophometer, Jasco V-530, in a spectrofluorometer, SLM Aminco 8100 (equipped with a 450 W Xe lamp, Glan−Thompson polarizers, and double monochromators), and in a fluorescence microscope, Olympus BX41 (using band-pass filters). The microscopy results were recorded in a digital camera, Olympus camedia 4040 zoom. Solutions were prepared in 10 mM HEPES buffer, pH 7.4, containing 150 mM NaCl (the so-called physiologic ionic strength). Osmolalities were measured in a freezing-point depression osmometer (Osmometer Automatic; Knauer, Berlin, Germany).

Preparation of Lipid Vesicles. Large unilamellar vesicles (LUVs) are a good model of biological membranes having no significant curvature effects (typical 100 nm diameter) (*12*). LUVs were prepared by the extrusion method described elsewhere (*13*). To obtain multilamellar vesicles (MLVs), the extrusion step was not performed. To study the effect of transmembrane potential in translocation, LUVs were prepared in HEPES buffer with 150 mM KCl or with 150 mM NaCl and passed through a 10 mL Econo-Pac 10DG column (Bio-Gel P-6DG gel with 6 kDa molecular weight exclusion) packed in buffer containing 150 mM NaCl or 150 mM KCl, respectively (determined dilution factor of vesicles is 1.2). Addition of valinomycin immediately induces a negative potential in K^+-loaded vesicles in Na^+-buffer and a positive one in Na^+-loaded vesicles in K^+-buffer (*14*).

Vesicle Aggregation Induced by Pep-1. Vesicle aggregation was monitored by optical density (OD) at 436 nm as described elsewhere (*15*). Briefly 6.88 μM pep-1 was added to a LUV suspension; additional lipid suspension aliquots were added after signal stabilization. LUVs of POPC or of different molar ratios of POPC and POPG (4:1 and 1:1) were prepared. Initial and final lipidic concentrations used in the assays were 25 and 106 or 106 and 222 μM, respectively. The pep-1 concentration effect was tested with POPC/POPG (1:1) vesicles; 0.54, 1.45, 3.40, and 6.88 μM pep-1 concentrations were used. Fluorescence microscopy studies were carried out with POPC vesicles doped with 1% of N-Rh-PE, a 510−550 nm excitation filter, and a 590 nm band-pass filter. The final lipidic and pep-1 concentrations used were 0.1 and 1.45 or 6.88 μM, respectively.

LUV Fusion and Anionic Lipid Segregation Induced by Pep-1. Fusion was tracked using the Forstër resonance energy transfer (FRET)-based methodology described before by others (*16*−*18*). Briefly, vesicles doped with both 1% N-NBD-PE (donor) and 1% N-Rh-PE (acceptor) and unlabeled vesicles were mixed; after that, 0.54, 1.45, or 6.88 μM pep-1 was added. If fusion between unlabeled vesicles and donor/acceptor-labeled vesicles occurs, the average distance between donors and acceptors increases, that is, FRET efficiency decreases. POPC, POPC/POPG (4:1), and POPC/POPG (1:1) were used (final lipid concentrations of 50 and 100 μM). Fluorescence intensity was followed with λ_{exc} = 463 nm (NBD absorption) and λ_{em} = 590 nm (Rh emission). Control experiments were carried out in all cases. Fluorescence quenching of Rh by pep-1 was evaluated by adding pep-1 (0−6.88 μM) to 1% N-Rh-PE doped vesicles to establish the minimal fluorescence intensity decrease expected (i.e., corresponding to fusion absence). The other end of the fusion scale (100%) was calculated by adding excess TX-100 surfactant (0.2% v/v) to the vesicle suspension. Fusion extent was calculated by linear interpolation between these limits.

Pep-1-induced anionic lipid segregation was also followed by FRET between NBD and Rh. Fluorescence emission intensity of Rh B dependence on pep-1 concentration (0−6.88 μM) was monitored in LUVs of POPC and POPC/POPG (4:1) containing 1% C6-NBD-PG and 1% N-Rh-PE. Final lipidic concentrations of 0.05, 0.1, and 1 mM were used. Control assays were carried out with C6-NBD-PC (zwiterionic) instead of C6-NBD-PG.

Pore Formation and Phospholipid Flip-Flop. Co^{2+} is an aqueous quencher of NBD fluorescence (*19*, *20*) and is accessible to N-NBD-PE and C6-NBD-PC inserted in vesicles (*20*). Pore formation was tested as described previously by others (*20*). Briefly vesicle suspensions of POPC, POPC/POPG (4:1), DPPC, and DPPC/DPPS (4:1) containing 1% N-NBD-PE were prepared in the absence and presence of 20 mM $CoCl_2$. In vesicles prepared without Co^{2+}, the quencher was added after LUV formation to guarantee that Co^{2+} is accessible only to NBD present in the external layer. No significant shrinkage was detected by turbidimetry in agreement with the small effect expected for vesicles upon osmolality variation due to 20 mM Co^{2+} (in/out osmolality ratio = 0.83; see Figure 1 in ref *21*). NBD fluorophores derivatized in the polar group of phospholipids inhibit flip-flop (*17*, *22*) given the hydrophilic nature of the probe and its localization (*17*). The same methodology was used to study flip-flop, but LUVs were doped with 1% C6-NBD-PC or 1% C6-NBD-PG. Phospholipids derivatized in short acyl chains can undergo flip-flop (*23*−*25*). Flip-flop was studied in POPC and DPPC LUVs. Fluorescence emission intensity (λ_{exc} = 460 nm and λ_{em} = 531 nm; excitation wavelength is optimized for best NBD/Co^{2+} absorbance

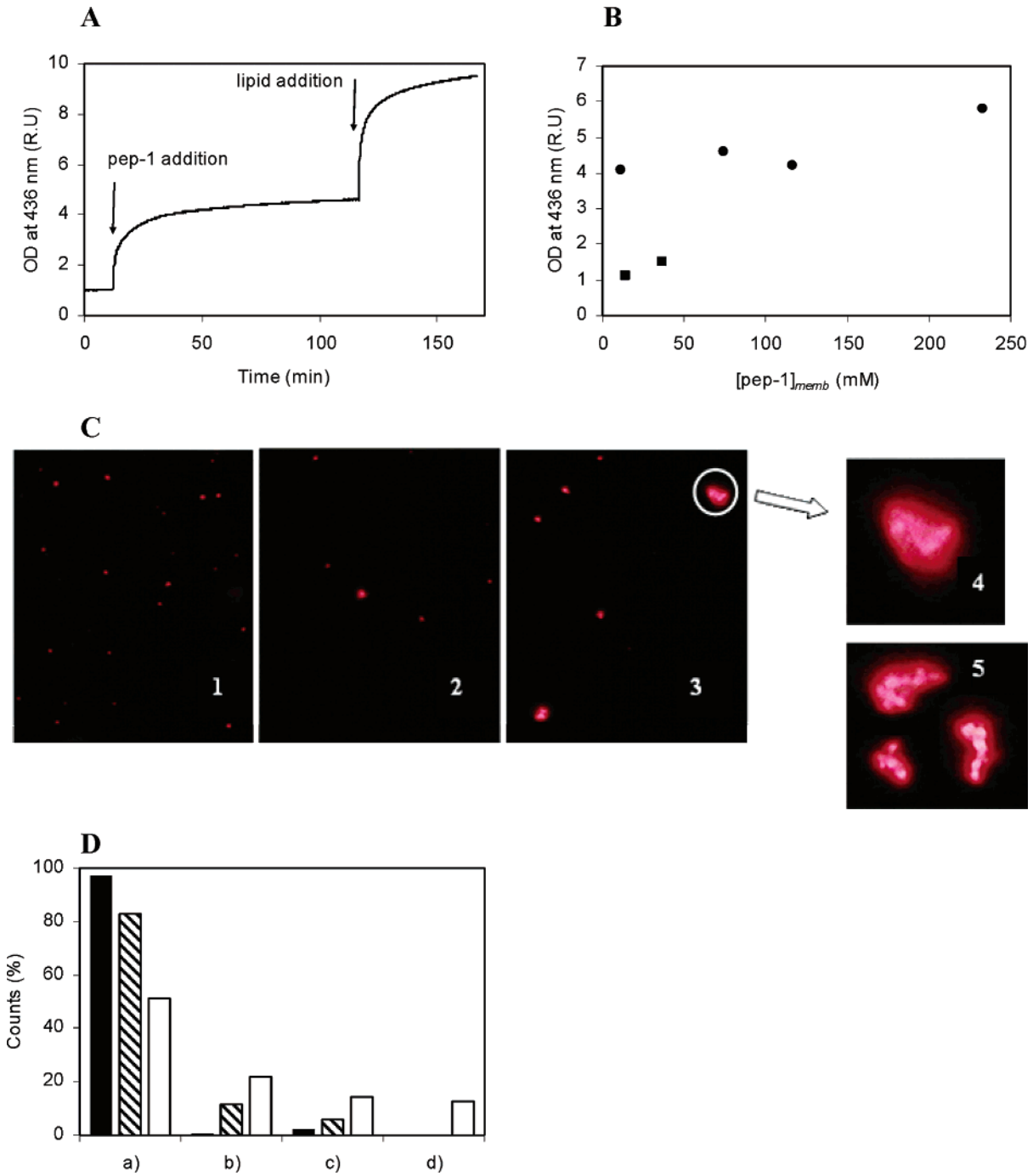

FIGURE 1: Vesicle aggregation induced by pep-1. Panel A shows the time course of the optical density (OD) at 436 nm showing aggregation of POPC/POPG (4:1) LUVs. After signal stabilization, 6.88 μM pep-1 was added to the 25 μM lipidic suspension in 10 mM HEPES buffer, pH 7.4, containing 150 mM NaCl. Peptide addition induced vesicle aggregation. Further addition of vesicle suspension to a 106 μM lipidic concentration induces more vesicle aggregation. Panel B shows the dependence of the normalized OD at 436 nm of a 25 μM lipidic suspension of POPC, POPC/POPG (4:1), and POPC/POPG (1:1) LUVs on pep-1 effective concentration in the membrane (eq 10 in ref *26*) below (■) and above (●) critical concentration for aggregate organization (3.4 ± 1.7 μM; ref *11*) (see Table 1). Panel C shows micrographs of POPC LUVs doped with 1% N-Rh-PE obtained by fluorescence microscopy with a 510−550 nm excitation filter and a 1000× amplification (1) in the absence and in the presence of (2) 1.45 and (3) 6.88 μM pep-1. In micrograph 3, less and larger bright units (aggregated vesicles) are presented. Fusion of subunits occurs as seen in amplifications 4 and 5 (6.88 μM pep-1). It is possible to identify different LUV subunits that constitute the aggregates. Panel D shows the percentage of bright units in preparations of POPC LUVs doped with 1% N-Rh-PE observed by fluorescence microscopy with a 510−550 nm excitation filter (filled columns refer to control, hatched to 1.45 μM pep-1 addition, and unfilled to 6.88 μM pep-1): (a) bright units where only one LUV could be noticed, (b) aggregates where fusion already occurred, and (c,d) aggregates formed by 2−3 and 4 or more units, respectively.

ratios) was recorded before and after 1.45 and 6.88 μM (final concentrations) pep-1 addition. Control assays without Co^{2+} were performed. The lipid concentration used was 100 μM. The data values were corrected for the inner filter effect (*19*).

Pore formation was also evaluated in LUVs loaded with 30 μM rhodamine B. Buffer containing the desired Rh B concentration was added to the lipidic film prior to MLV formation; after the extrusion step, the vesicle suspension

was eluted through a 10 mL Econo-Pac 10DG column (Bio-Gel P-6DG gel with 6 kDa molecular weight exclusion) packed with buffer (without Rh B) to remove nonencapsulated Rh B. Encapsulated Rh B fluorescence intensity was recorded ($\lambda_{exc} = 554$ nm and $\lambda_{em} = 576$ nm) prior to and after addition of 1.45 and 6.88 μM peptide.

Translocation Assays. Vesicles doped with 1% N-Rh-PE (100 μM total lipid concentration) were used to evaluate fluorescence emission quenching of Rh by pep-1. The Rh emission fluorescence intensity was monitored at $\lambda_{exc} = 570$ nm and $\lambda_{em} = 590$ nm.

To study translocation in absence of transmembrane potential, POPC and POPC/POPG (4:1) MLVs were prepared in the absence and presence of 1.45 or 6.88 μM peptide. Vesicles prepared directly in pep-1 suspensions are controls because in this case pep-1 is accessible to Rh fluorophores present in all lamellae. In the other experiments, pep-1 was added to MLVs prepared in absence of pep-1 to a final concentration of 1.45 or 6.88 μM. The assays were repeated in the presence of 1 mM phosphine. Usage of MLVs enables a gradual effect in case translocation occurs.

Transbilayer potentials were created in POPC, POPC/POPG (4:1), and POPC/POPG (1:1) vesicles (see Preparation of Lipid Vesicles). Pep-1 was added to vesicles to a final concentration of 6.88 μM. After the fluorescence signal was constant, valinomycin was added to vesicles at a $1:10^4$ molar ratio (mol/mol lipid; *14*; from ethanolic solution; final ethanol concentration 0.2%). Controls without valinomicin (i.e., in the absence of a transmembrane potential) were also prepared. Pore formation (in POPC/POPG (4:1) LUVs) and flip-flop (of C6-NBD-PC and C6-NBD-PG in POPC LUVs) were also evaluated (see methodology in previous section) in the presence of negative transmembrane potential. Valinomycin was added after addition of 6.88 μM pep-1.

RESULTS AND DISCUSSION

Pep-1 Induced Vesicle Aggregation. Vesicle aggregation is dependent on three main forces (*15*): electrostatic repulsion, van der Waals attraction, and hydration. Multivalent cations may alter the charge density at the vesicles surfaces, as well as dehydrate the lipid polar groups, and therefore eventually lead to aggregation of vesicles. Pep-1 is a multivalent cation that anchors at the lipidic membrane interface (*11*): this prompted us to study the effect of pep-1 on aggregation of vesicles. When the peptide is added to LUVs of POPC/POPG 4:1 (molar), the optical density of the solution slowly increases (Figure 1A) until a plateau is reached ~100 min later. Further addition of lipids results in a second increase in optical density (Figure 1A), that is, lipid addition does not revert the vesicle aggregation, at variance to penetratin-induced aggregation (*15*). Table 1 presents data that account for the effect of anionic lipids, total lipidic concentration, and peptide concentration on vesicle aggregation ability. Effective concentration of the peptide at the lipidic environment was calculated in all cases to enable direct comparisons (see ref *11* and eq 10 in ref *26*). The main experimental evidences from Table 1 are as follows: (1) Anionic lipids favor aggregation, although the effect is relatively weak (Figure 1B). (2) Addition of lipids to increase the total lipid concentration also leads to further aggregation (Figure 1A); when penetratin is used, the opposite effect is observed (*15*), suggesting that pep-1 and penetratin do not coincide in their mode of action at molecular level. (3) The optical density obtained upon peptide addition when the initial lipidic concentration is 106 μM is different from the one obtained when initial lipidic concentration is 25 μM and is increased to 106 μM after peptide addition. The final dimension of vesicle aggregates does not depend on the lipidic concentration, only. Stepwise addition of lipid results in bigger aggregates (in terms of light scattering intensity, the effect of volume change superimposes to the simultaneous process of scattering particle concentration decrease). One possible explanation is the ability of pep-1 to add isolated vesicles to previously formed aggregates but inability to cluster large previously formed aggregates. Stepwise addition of vesicles enlarges previously formed aggregates rather than create new small aggregates. (4) Pep-1 organization in the aqueous environment (i.e., 1.45 vs 6.88 μM in Table 1) influences vesicle aggregation (Figure 1B).

Table 1: Vesicle Aggregation Induced by Pep-1

lipid	[lipid] (μM)[a] initial/final	X_L[b] initial/final	$[pep\text{-}1]_T$ (μM)	$[pep\text{-}1]_{memb}$ (mM)[c] initial/final	OD[d] peptide/lípid
POPC	25/106	0.03/0.12	6.88	11.3/10.3	4.1/7.9
		0.12/0.23	6.88	10.3/9.08	4.8/8.2
POPC/POPG (4:1)	25/106	0.17/0.47	6.88	74.1/69.5	4.6/9.5
	106/222	0.47/0.65	6.88	69.5/63.8	4.4/6.9
POPC/POPG (1:1)	25/106	0.49/0.80	0.54	13.8/5.35	1.1/1.2
			1.45	37.1/14.7	1.5/1.9
		0.65/0.89	3.44	117/37.7	4.2/6.0
			6.88	233/75.4	5.8/8.8

[a] Before peptide addition, lipid concentration was 25 or 106 μM; after more lipid was added, the final concentration became 106 or 222 μM, respectively. [b] The molar fraction of peptide inserted in lipid (X_L) was determined by eq 3 in ref *34* using partition coefficients for pep-1 (*11*). [c] Pep-1 concentration in lipidic bilayer by application of eq 10 in ref *26*. [d] Optical density (OD) at 436 nm (normalized to [pep-1] = 0) of POPC and POPC/POPG vesicles (prepared in 10 mM HEPES, pH 7.4, buffer containing 150 mM NaCl) after peptide, first number, and more lipid addition, second number (see Figure 1B).

Fluorescence microscopy studies using POPC vesicles doped with N-Rh-PE confirm aggregation (Figure 1C). Pep-1 addition results in less and bigger bright units relative to the control in the micrographs. At higher pep-1 concentration, aggregation of smaller units is noticeable with a magnification of 1000× (Figure 1C,D). Because turbidity is proportional to the squared volume of scattering entities, a small fraction of big aggregates may lead to high optical density values.

Peptide-induced vesicle aggregation implies a severe reduction in vesicle stability due to a decrease in electrostatic repulsion and interference with the hydration layer. This second factor seems dominant since POPC vesicle aggregation is quite significant and similar to the one obtained with POPC/POPG (i.e., anionic vesicles).

Pep-1 Induced Vesicle Fusion. Vesicle fusion implies that (1) the inner content of two or more vesicles is mixed and (2) lipids from previously separated bilayers coexist in the same bilayer after fusion (*27*). Fusion may result from a variety of stimuli (*27*). Pep-1 induced lipidic vesicle fusion seems plausible because vesicle aggregation (see previous section) creates propitious conditions (*28*). Moreover, pep-1 is amphipathic, which is a common characteristic among fusiogenic peptides (*18*).

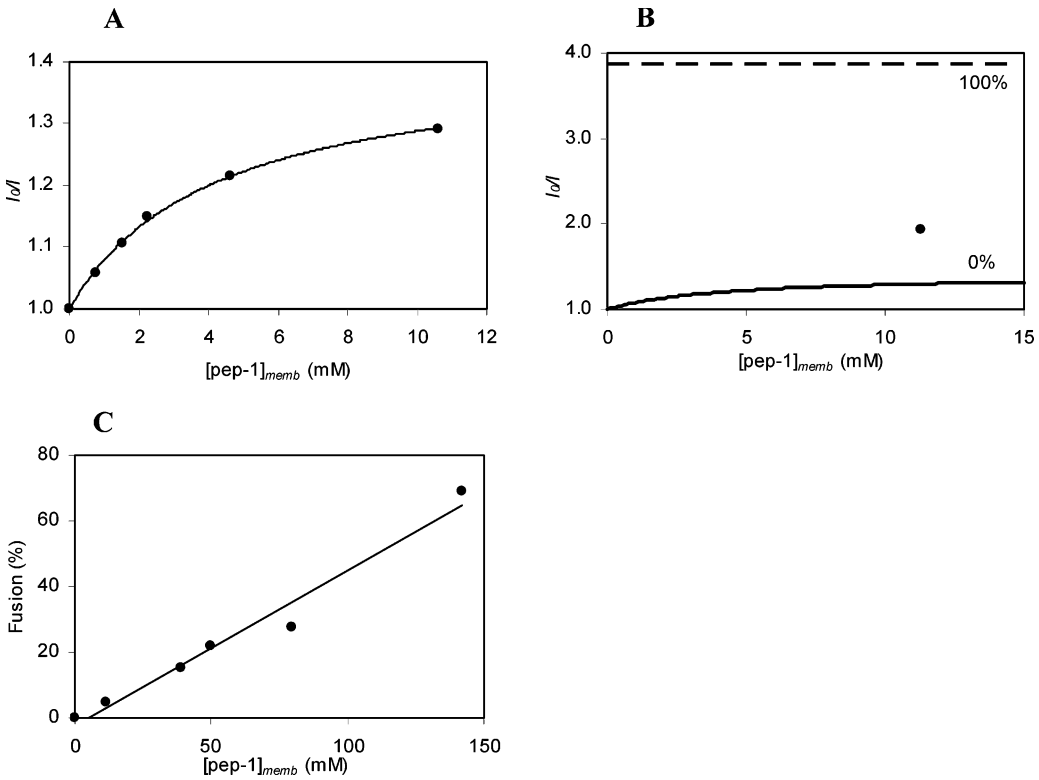

FIGURE 2: Vesicle fusion induced by pep-1. Fusion assays were monitored by FRET between NBD (donor) and rhodamine B (acceptor) (λ_{ex} = 463 nm; λ_{em} = 590 nm; sensitized emission of acceptor). Vesicle suspensions doped with 1% N-NBD-PE and 1% N-Rh-PE were prepared in 10 mM HEPES, pH 7.4, buffer containing 150 mM NaCl. Panel A shows a Stern−Volmer plot of the fluorescence emission quenching of 100 μM POPC LUVs doped with 1% N-Rh-PE (λ_{em} = 570 nm; λ_{ex} = 590 nm) by pep-1 (the effective pep-1 concentration in membrane is considered; eq 10 in ref *26*). The Lehrer equation (see eq 11 in ref *26*) was fitted to the data (solid line). Panel B shows the relative fusion scale of 50 μM POPC/POPG (4:1) LUVs; 0% fusion (full line) is obtained by the Stern−Volmer plot of the Rh B quenching by pep-1 (Figure 2A), and 100% fusion (dashed line) is the fluorescence emission of vesicle suspensions in excess TX-100. Effective peptide membrane concentration in the membrane is used for the sake of comparison with other LUV compositions since the extent of peptide partition is dependent on the anionic lipid composition. The filled circle refers to the fluorescence intensity obtained by addition of 6.88 μM total concentration of pep-1. Fusion percentage (22.1%) was calculated from linear interpolation. Panel C shows the fusion percentage in POPC and POPC/POPG LUVs. All data were obtained in the presence of 6.88 μM pep-1 total concentration; however, effective concentration in membranes vary (see Table 2). Fusion extension and effective concentration in membranes are linearly correlated.

Table 2: Vesicle Fusion Induced by Addition of Pep-1

lipid	[lipid] (mM)	[pep-1]$_T$[a] (μM)	[pep-1]$_{memb}$[b] (mM)	I_0/I[c] (0% fusion)	I_0/I[d] (100% fusion)	I_0/I (assay)	fusion (%)[e]
POPC	0.05	6.88	11.3 ± 3.9	1.30 ± 0.61	4.35 ± 0.07	1.45 ± 0.02	4.9 ± 0.07
POPC/POPG (4:1)	0.05	6.88	49.8 ± 39.8	1.38 ± 1.27	3.87 ± 0.09	1.93 ± 0.004	22.1 ± 0.05
	0.1	6.88	39.0 ± 31.2	1.37 ± 1.27	3.15 ± 0.05	1.64 ± 0.02	15.2 ± 0.18
POPC/POPG (1:1)	0.05	0.54	9.3 ± 6.7	1.28 ± 1.08	3.98 ± 0.09	1.21 ± 0.02	0
		1.45	24.9 ± 17.9	1.35 ± 1.13	3.98 ± 0.09	1.38 ± 0.02	1.1 ± 0.02
		6.88	141.7 ± 85.6	1.40 ± 1.02	3.98 ± 0.09	3.18 ± 0.07	69.0 ± 1.5
	0.1	6.88	79.3 ± 47.9	1.38 ± 1.00	3.28 ± 0.05	1.90 ± 0.03	27.4 ± 0.43

[a] Refers to total pep-1 concentration in bulk solution. [b] Refers to effective peptide in lipidic matrix. [c] Refers to pep-1 quenching fluorescence of rhodamine B. [d] Refers to the addition of Triton X-100. [e] The vesicle fusion percentage of different lipidic mixtures (POPC, POPC/POPG (4:1) and POPC/POPG (1:1)) in 10 mM HEPES, pH 7.4, buffer containing 150 mM NaCl was determined as illustrated in Figure 2B. Results are presented along with standard errors.

The FRET-based methodology described elsewhere (*16*−*18*) to study vesicle fusion was adapted to account for the N-Rh-PE fluorescence quenching by pep-1 (Figure 2A). The Rh fluorescence intensity depends on the exact effective pep-1 concentration in the membrane environment, [pep-1]$_{memb}$ (see eq 10 in ref *26*, reported as [Q]$_L$), even in the absence of fusion because N-Rh-PE fluorescence is quenched by pep-1. This fluorescence emission intensity corresponding to 0% fusion is calculated from the Stern−Volmer formalism (Figure 2A,B). In excess TX-100, donor/acceptor mean interdistance becomes much bigger than the Förster radius, R_0, minimizing the fluorescence intensity (100% of the fusion scale). Figure 2B illustrates the data analysis procedure. NBD quenching by TX-100 (*18*) is not relevant for our purpose.

The results obtained using different lipid concentrations, lipidic charge densities, and pep-1 concentration are presented in Table 2. Fusion is only significant when [pep-1] = 6.88 μM, which is also true for aggregation. Anionic lipids may not have a direct role in fusion. POPG interference with fusion may result from enhanced partition into the membrane (*11*). When fusion percentage is plotted as a function of [pep-1]$_{memb}$ for systems having different anionic charge densities and lipid concentrations (Figure 2C), one single homogeneous data set is obtained. Thus, [pep-1]$_{memb}$ seems to be

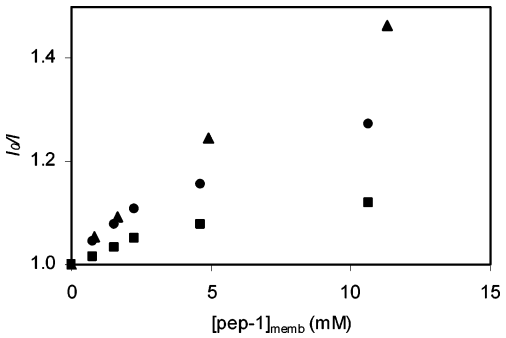

FIGURE 3: Anionic lipid segregation induced by pep-1. The assays were followed by FRET between NBD (donor) and rhodamine (acceptor) (λ_{ex} = 463 nm; λ_{em} = 590 nm; sensitized emission of acceptor). The POPC vesicle suspension was prepared with 1% N-Rh-PE and 1% C6-NBD-PG (or C6-NBD-PC in the control assay, ■) in 10 mM HEPES, pH 7.4, buffer containing 150 mM NaCl. The total lipidic concentrations used were 50 (▲) and 100 μM (●). A more pronounced decrease of Rh B fluorescence intensity relative to the control assay means a greater distance between donor and acceptor, that is, segregation of anionic lipids near the partition local of pep-1 in vesicles.

the key regulator issue in vesicle fusion. Pep-1 organization in the aqueous environment is another important factor (no fusion detected in 1.45 μM pep-1 solution). Fusiogenic activity is usually associated with α-helix conformation in membranes (*18*). This suggests that pep-1 may adopt α-helix conformation at 6.88 μM in the presence of lipidic bilayers. However, direct evidence from CD spectroscopy, for instance, is prevented due to the typical low sensitivity of these techniques.

Pep-1 Induced Anionic Lipid Segregation. Some cell-penetrating peptides such as penetratin are believed to have their biochemical mode of action dependent on the interaction with anionic lipids (*29*). Electrostatic interaction is essential for lipidic bilayer structure perturbation afterward. To test the hypothesis that perturbation results from peptide-induced anionic lipid lateral redistribution in the membranes, we used NBD-labeled PG (anionic) and Rh-labeled PE (zwitterionic) in POPC vesicles and carried out FRET experiments. Anionic lipid segregation results in a decrease in FRET efficiency in the presence of peptide. Control experiments were carried out using NBD-labeled PC instead of PG (the quenching of Rh B by the peptide is accounted for in the control). Figure 3 shows that pep-1-induced anionic lipid segregation occurs to an extent that depends both on the lipidic and on the peptide concentrations. Variations in FRET efficiency are not detected when 20% (molar) POPG is present in the vesicles (results not shown), as expected due to the "dilution" of anionic lipidic probes in excess anionic lipids.

Pore Formation in the Absence of Transmembrane Potential. Some membrane-interacting peptides, such as mellitin, possess unspecific lytic ability (*30*, *31*). Mellitin resembles pep-1 for the presence of a proline residue in its sequence (*27*) among other reasons. These similarities prompted us to test pep-1-induced pore formation across lipidic membranes. Co^{2+} is an aqueous quencher of NBD fluorophores (*19*, *20*) and was used to quench N-NBD-PE inserted in LUVs in the presence and absence of pep-1 (a method based on previously published ones (*19*)). In the absence of pep-1, Co^{2+} is expected to leave 50% of the N-NBD-PE fluorophores accessible if added to a LUV suspension after vesicles are formed and all the fluorophores

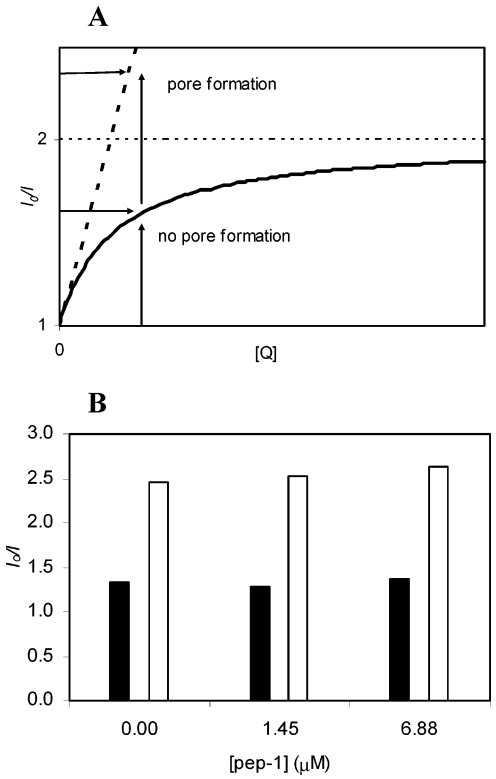

FIGURE 4: Vesicle pore formation induced by pep-1. Co^{2+} quenching of fluorescence emission of LUVs doped with 1% N-NBD-PE (λ_{em} = 460 nm; λ_{ex} =531 nm) was performed to test for pep-1-induced pore formation in vesicles. Vesicles with 20 mM Co^{2+} accessible to both layers and vesicles with 20 mM quencher accessible just to external layer have been produced in a 10 mM HEPES, pH 7.4, buffer containing 150 mM NaCl. In panel A, the hyperbole-like curve (full line) simulated with the Lehrer equation with f_B = 50% (see eq 11 in ref *26*) indicates the NBD fluorescence quenching of the latter vesicles in the case of no pore formation. If the addition of pep-1 leads to a more pronounced quenching (dashed line), near linearity (the limit where the quencher is accessible to all NBD fluorophores) pores are formed. At a given quencher concentration, I_0/I, can be used to account for pore formation. Panel B shows the ratio of NBD intensity of 100 μM POPC LUVs in the absence of quencher and in the presence of 20 mM Co^{2+} for the vesicles with Co^{2+} accessible to both layer (white columns) and accessible only to the outer layer (black columns). Comparing the results with control, it is possible to conclude that there is no pore formation in the presence of 1.45 or 6.88 μM pep-1.

if it is added before vesicles are formed. In the case that pores or other lytic perturbations are formed by the peptide, Co^{2+} first present only outside lipidic vesicles is able to penetrate vesicles and reach all the fluorophores, that is, the quenching extent is dependent on lytic perturbations of the membrane induced by pep-1 (Figure 4A). Results presented in Figure 4B show that no lytic action occurs in POPC vesicles because peptide presence does not change NBD quenching by Co^{2+}. Similar results were obtained with POPC/POPG (4:1) vesicles (results not shown). These results were confirmed in LUVs with encapsulated Rh B (dissolved in buffer). The addition of pep-1 does not induce a significant quenching of Rh B fluorescence emission (data not shown), revealing that peptide is inaccessible to vesicle lumen and that there is no ion leakage.

Asymmetric Lipidic Flip-Flop in the Absence of Transmembrane Potential. Flip-flop refers to the lipidic exchange between outer and inner layers (*23*) and may be promoted by peptide insertion in membranes (*23*, *24*). Peptides perturb

membranes causing defects at the interfacial packing that allow passage of the polar lipidic heads through the aliphatic region of membranes (*24*). The same methodology used before for pore formation assays was used to test for asymmetric lipidic flip-flop, except that C6-NBD-PC and C6-NBD-PG were used instead of N-NBD-PE. The latter probe does not translocate across membranes due to the bulky NBD residue at its polar head (*17*). Results (not shown) do not present evidence of asymmetric flip-flop of lipids in any of the lipidic systems tested (POPC and DPPC with and without anionic lipids). In case that flip-flop occurs at all, it is bidirectional and occurs at the same rate in the inner/outer and opposite direction.

Peptide Translocation across Lipidic Bilayers. The biochemical activity of pep-1 is related to its ability to translocate across lipidic membranes. Translocation assay methodologies were based on the peptide quencher properties relative to Rh B (Figure 2A). We prepared MLVs with peptide solutions from the start (samples A) or buffer without peptide. In the latter samples, peptide was added after vesicle formation (samples B) to the final peptide concentration used in samples A. In the case that translocation occurs, fluorescence intensity in samples B decreases with time until the fluorescence intensity of samples A is reached. No translocation was detected in POPC and POPC/POPG (4:1) vesicles both in the absence (Figure 5A) and presence of phosphine (results not shown).

Previous studies have shown that translocation of peptidic sequences across a synthetic bilayer is largely stimulated in the presence of a transmembrane potential (*14*, *32*, *33*). In a recently published work, Terrone et al. (*32*) showed that penetratin translocation in LUVs is mediated by transbilayer potential in a manner dependent on vesicle composition. The effect of transbilayer potential in pep-1 translocation was evaluated in POPC, POPC/POPG (4:1), and POPC/POPG (1:1) doped with N-Rh-PE. After peptide addition to LUVs, a significant fluorescence quenching of Rh B emission fluorescence was recorded in studied lipidic systems ($I_0/I \approx 2$, which is an expected value because in these conditions pep-1 is accessible only to Rh B in the external layer). If translocation occurs in the presence of a transbilayer potential, an increase of Rh emission fluorescence quenching is expected (pep-1 is accessible to Rh in the internal layer). The presence of valinomycin-induced negative transbilayer potential (maximum transbilayer potential about 120 mV (*32*, *33*), stable for 10 min (*14*)) in K^+-loaded vesicles in Na^+-buffer causes a significant translocation of pep-1 in POPC/POPG (4:1) and POPC/POPG (1:1) (Figure 5B) on the second time scale. In POPC, the translocation occurs to a minor extent. The rapid translocation is in agreement with in vivo studies (*8*) that show translocation of the peptide across cell membranes on the minute time scale. The effect of a positive transbilayer potential was tested in POPC/POPG (4:1) vesicles. The addition of valinomycin to Na^+-loaded vesicles in K^+-buffer does not alter the fluorescence emission quenching of Rh B by pep-1. This result shows that a positive transbilayer potential does not lead to translocation. Similar results were obtained with vesicles dispersed in buffer containing 150 mM KCl (K^+ in and out) and with vesicles prepared in buffer with 150 mM NaCl (Na^+ in and out).

Figure 5C, which represents a Stern−Volmer-like plot, shows that translocation is dependent on the effective

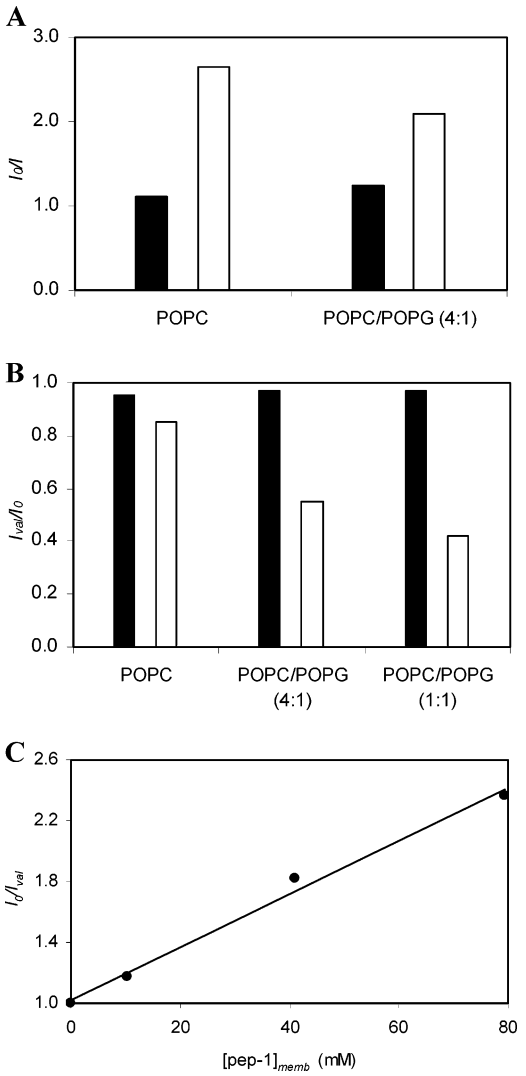

FIGURE 5: Pep-1 translocation across lipidic bilayer. Translocation assays were followed by fluorescence quenching of rhodamine B ($\lambda_{ex} = 570$ nm; $\lambda_{em} = 590$ nm) by pep-1 in 100 μM vesicles doped with 1% N-Rh-PE. In panel A, POPC and POPC/POPG (4:1) MLVs (10 mM HEPES, pH 7.4, buffer containing 150 mM NaCl) were used. The results are presented in terms of intensity ratio without and with 6.88 μM pep-1 added at the moment of the vesicle preparation (white columns) and after the vesicle preparation (black columns). In case translocation exists, the same fluorescence intensity is expected for both columns. No peptide translocation was detected. Panel B shows translocation of pep-1 in the presence of transmembrane potential in POPC, POPC/POPG (4:1), and POPC/POPG (1:1) LUVs (loaded with 10 mM HEPES pH 7.4 buffer containing 150 mM KCl and dispersed in buffer containing 150 mM NaCl). Rhodamine B fluorescence emission was recorded, and a decrease to approximately half of the initial value was detected after 6.88 μM pep-1 addition (pep-1 accessible to N-Rh-PE in external layer). The Rh B fluorescence intensity ratio after (I_{val}) and before (I_0) addition of valinomycin ($1{:}10^4$ mol/mol lipid) is represented for the three lipidic systems in the presence (white columns) and absence (black columns) of 6.88 μM pep-1. A decrease in I_{val}/I_0 upon valinomycin addition (negative transmembrane potential) indicates that pep-1 is accessible to N-Rh-PE in the inner layer and translocation across bilayer occurs. An enhanced effect is visible with an increase in anionic lipid. Panel C shows a Stern−Volmer-like plot, which represents I_0/I_{val} (see panel B) dependence on effective pep-1 concentration in membrane (see eq 10 in ref *26*). Translocation extension is dependent on effective pep-1 concentration in membrane (increases with peptide concentration in membrane).

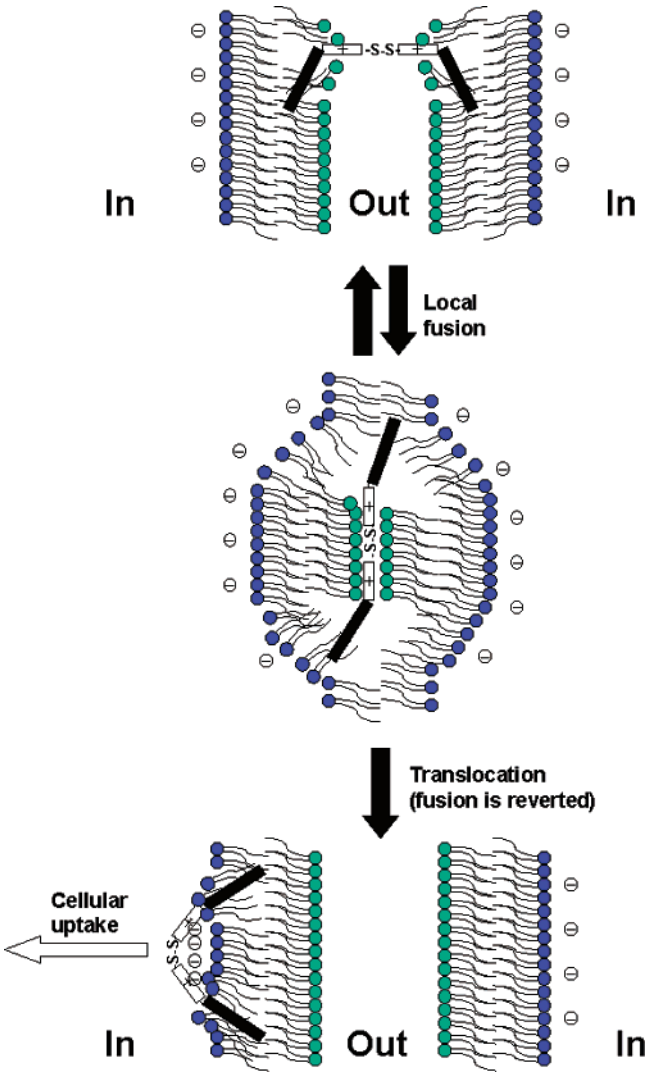

FIGURE 6: Putative pep-1 translocation mechanism across lipidic bilayer. This scheme outlines a possible mechanism for pep-1 translocation. The peptide has the ability of inserting in the bilayer outer interface and causes local and transient fusion of membranes (experimental results show clustering of vesicles without collapse and no lytic lesions). Transiently fused biological membranes (negatively charged inner face) bring the cationic sequences of the peptide closer to the anionic inner leaflet of the membranes. In this situation, electrostatic attraction is strong enough to move pep-1 to one of the inner leaflets of the membranes and segregate anionic lipids. The inverted micelle-like structure originated from fusion is then reverted. The partition equilibrium in the cell inner lipidic hemilayer is shifted toward the nonlipidic environment due to the reduction of pep-1 dimers (*11*) and cellular uptake. The role of partition equilibria in the regulation of pep-1 action across lipidic bilayers is addressed in ref *11*.

concentration of peptide in membrane ($[\text{pep-1}]_{\text{memb}}$). The results show that the translocation driving force is the negative membrane potential across bilayer and affinity of peptide to membrane determines the extent of translocation.

In the presence of negative transmembrane potential, no significant drop in NBD fluorescence was detected, when valinomycin was added (after 6.88 μM pep-1 addition) to POPC/POPG (4:1) LUVs doped with N-NBD-PE or to POPC vesicles doped with C6-NBD-PC or C6-NBD-PG (Co^{2+} accessible to the external layer of the vesicles in both cases). Fluorescence intensities with the quencher accessible to internal and external layers were used as a positive control. No pore formation or significant phospholipid flip-flop occurs during peptide translocation (data not shown).

CONCLUSION

Pep-1 is effective in inducing vesicle aggregation and lipidic fusion. Aggregation takes place by vesicle clustering, but lipidic exchange among vesicles is possible. The process is dependent both on anionic lipid content and on peptide concentration. Segregation of anionic lipids in the presence of peptide is detected. Despite all these effects, no evidence was found for lytic action or ion leakage. Translocation occurs only in vesicles with a negative membrane potential and is enhanced by the presence of anionic lipids, probably by electrostatic attraction of the peptide to anionic bilayers.

Taking our work as a whole, one concludes that the main driving force for peptide translocation is a charge gradient across membrane (negative inside). In biological membranes, the transmembrane potential caused by charge asymmetry between outer and inner leaflets created by anionic lipids in the inner layer is probably responsible for translocation. Moreover, pep-1 is a strong perturber of lipid membrane organization (Figure 6), which is probably a key role of its action because the energetic cost of solvation layer removal (mandatory for crossing an unperturbed membrane) would be prohibitive. Bilayer perturbation renders electrostatic attraction dominant over solvation effects. As proposed schematically in Figure 6, fusion is probably the main cause of close range electrostatic attraction between positively charged peptide and negatively charged lipids in the cell membrane inner leaflets. Transient inverted micelle-like structures may be formed, leading to translocation. An active role of membrane aggregation in translocation was very recently proposed for the cell-penetrating peptide penetratin (*32*).

ACKNOWLEDGMENT

We thank Dr. Fernando Antunes and Nuno M. V. Pedroso for helping with fluorescence microscopy and Dr. M. Prieto and Dr. Cláudio Soares for valuable critical discussions.

REFERENCES

1. Wadia, J. S., Becker-Hapak, M., and Dowdy, S. F. (2002) Protein transport, in *Cell-penetrating peptides, processes and applications* (Langel, Ü., ed) pp 365−375, CRC Press Pharmacology & Toxicology Series, CRC Press, New York.
2. Bogoyevitch, M. A., Kendrick, T. S., Dominic, C. H., and Barr, R. K. (2002) Taking the cell by stealth or storm? Protein transduction domain (PTDs) as versatile vectors for delivey, *DNA Cell Biol. 21*, 879−894.
3. Bonetta, P. (2002) Getting protein into cells, *Scientist 17*, 38−40.
4. Eguchi, A., Akuta, T., Okuyama, H., Senda, T., Yokoi, H., Inokuchi, H., Fujita, S., Hayakama, T., Takeda, K., Hasegawa, M., and Nakanisshi, M. (2001) Protein transduction domain of HIV-1 Tat protein promotes efficient delivery of DNA into mammalian cells, *J. Biol. Chem. 247*, 27205−27210.
5. Richard, J. P., Melikov, K., Vives, E., Ramos, C., Verbeure, B., Gait, M. J., Chernomordik, L. V., and Lebleu, B. (2003) Cell-penetrating peptides, a reevaluation of the mechanism of cellular uptake, *J. Biol. Chem. 278*, 585−590.
6. Schwarze, S. R., Hruska, K. A., and Dowdy, S. F. (2000) Protein transduction: unrestricted delivery into all cells? *Trends Cell Biol. 10*, 290−295.
7. Chaloin, L., Mau, N. V., Divita, G., and Heitz, F. (2002) Interactions of cell-penetrating peptides with membranes, in *Cell-penetrating peptides, processes and applications* (Langel, Ü., ed)

pp 23−51, CRC Press Pharmacology & Toxicology Series, CRC Press, New York.
8. Morris, M. C., Depollier, J., Mery, J., Heitz, F., and Divita, G. (2001) A peptide carrier for the delivery of bilogically active proteins into mammalian cells, *Nat. Biotechnol. 19*, 1143−1147.
9. Chariot, simple efficient protein delivery system. http://www.activemotif.com/products/cell/chariot (accessed July 2003).
10. Morris, C. M., Chalion, L., Heitz, F., and Divita, G. (2002) Signal sequence-based cell-penetrating peptides and their application for gene delivery, in *Cell-penetrating peptides, processes and applications* (Langel, Ü., ed) pp 93−113, CRC Press Pharmacology & Toxicology Series, CRC Press, New York.
11. Henriques, S., and Castanho, M. (2004) Environmental factors that affect the cell penetrating peptide pep-1 action across lipidic membranes, *Chem.Phys.Chem.* submitted for publication.
12. Wieprecht, T., Beyermann, M., and Seeling, J. (2002) Thermodynamics of the coil-α-helix transition of amphipathic peptides in membrane in a membrane environment; the role of vesicle curvature, *Biophys. Chem. 96*, 191−201.
13. Mayer, L. D., Hope, M. J., and Cullis, P. R. (1986) Vesicles of variable sizes produced by a rapid extrusion procedure, *Biochim. Biophys. Acta 858*, 161−168.
14. van Dalen, A., Killian, A., and de Kruijff, B. (1999) $\Delta\psi$ stimulates membrane translocation of the C-terminal part of a signal sequence, *J. Biol. Chem. 274*, 19913−19918.
15. Persson, D., Thorén, P. E. G., and Nordén, B. (2001) Penetratin-induced aggregation and subsequent dissociation of negatively charged phospholipid vesicles, *FEBS Lett. 505*, 307−312.
16. Haugland, R. P. (2002) *Handbook of Fluorescent Probes and Research Products*, 9th ed., Molecular Probes, New York.
17. Maier, O., Oberle, V., and Hoekstra, D. (2002) Fluorescent lipid probes: some properties and applications (a review), *Chem. Phys. Lipids 116*, 3−18.
18. Pécheur, E.-I., Martin, I., Ruysschaert, J.-M., Bienvenüe, A., and Hoekstra, D. (1998) Membrane fusion induced by 11-mer anionic and cationic peptides: a structure−function study, *Biochemistry 37*, 2361−2371.
19. Caputo, G. A., and London, E. (2003) Using a novel dual fluorescence quenching assay for measurement of tryptophan depth within lipid bilayes to determine hydrophobic α-helx location within membranes, *Biochemistry 42*, 3265−3274.
20. Chattopadhyay, A., and London, E. (1988) Spectroscopic and ionization of N-(7-nitrobenz-2-oxa-1,3-diazol-4-yl)-labeled lipid in model membranes, *Biochim. Biophys. Acta 938*, 24−34.
21. Pencer, J., White, G. F., and Hallet, F. R. (2001) Osmotically induced shape changes of large unilamellar vesicles measured by dynamic light scattering, *Biophys. J. 81*, 2716−2728.
22. Wimley, W. C., and White, S. H. (2000) Determining the membrane topology of peptides by fluorescence quenching, *Biochemistry 39*, 161−170.
23. Kol, M. A., Laak A. N. C. van, Rijkers, D. T. S., Killian, J. A., Kroon, A. I. P. M. de, and Kruijff, B. de (2003) Phospholipid flop induced by transmembrane peptides in model membranes is modulated by lipid composition, *Biochemistry 42*, 231−237.
24. John, K., Schreiber, S., Kubelt, J., Herrmann, A., and Müller, P. (2002) Transbilayer movement of phospholipids at the main phase transition of lipid membranes: implications for rapid flip-flop in biological membranes, *Biophys. J. 83*, 3315−3323.
25. Marx, U., Lassmann, G., Holzhütter, H.-G., Wüstner, D., Müller, P., Höhlig, A., Kubelt J., and Herrmann A. (2000) Rapid flip-flop of phospholipids in endoplasmic reticulum membranes studied by a stopped-flow approach, *Biophys. J. 78*, 2628−2640.
26. Santos, N. C., Prieto, M., and Castanho, M. A R. B. (1998) Interaction of the major epitope region of HIV protein gp41 with membrane model systems. A fluorescence study, *Biochemistry 37*, 8674−8682.
27. Basañez, G. (2002) Membrane fusion: the process and its energy suppliers, *Cell. Mol. Life Sci. 59*, 1478−1490.
28. Nieva, J. L., and Nir, S. (2000) Interactions of peptides with liposomes: pore formation and fusion, *Prog. Lipid Res. 39*, 181−206.
29. Dupont, E., Joliot, A., and Prochiantz, A., (2002) Penetratins, in *Cell-penetrating peptides, processes and applications*, (Langel, Ü., ed) pp 23−51, CRC Press Pharmacology & Toxicology Series, CRC Press, New York.
30. Matsuzaki, K., Yoneyama, S., and Miyajima, K. (1997) Pore formation and translocation of melitin, *Biophys. J. 73*, 831−838.
31. Papo, N., and Shai, Y. (2003) Exploring peptide membrane interaction using surface plasmon resonance: differentiation between pore formation versus membrane disruption by lytic peptides, *Biochemistry 42*, 458−466.
32. Terrone, D., Sang, S. L. W., Roudaia, L., and Silvius, J. R. (2003) Penetratin and related cell-penetrating cationic peptides can translocate across lipid bilayers in the presence of a transbilayer potential, *Biochemistry 42*, 13787−13799.
33. Maduke, M., and Roise, D. (1993) Import of a mitochondrial presenquence into protein-free phospholipid vesicles, *Science 260*, 364−367.
34. Santos, N. C., Prieto, M., and Castanho, M. A R. B. (2003) Quantifying molecular partition into model systems of biomembranes: an emphasis on optical spectroscopic methods, *Biochim. Biophys. Acta 1612*, 123−135.

BI036325K

Chapter 3

Does pep-1 form pores?

Chapter 3.

Does pep-1 form pores?

3.1. Introduction

A translocation mechanism for peptides involving direct interaction with membrane lipids was proposed shortly after the identification of these basic sequences with capacity to pass through the membrane [15, 16]. This was further supported by the strong correlation of uptake with lipid-binding affinity [168]. A passive diffusion by charged molecules is not likely to occur due to the membrane properties including the low dielectricity in the core of the bilayer. Nevertheless, different mechanisms have been proposed to explain a possible internalization mechanism independent on endocytosis (Figure 3.1).

One of the earliest energy-independent mechanism proposed for transmembrane translocation is the "inverted micelle" model [53]. The proposed mechanism was based on Nuclear Magnetic Resonance (NMR) studies in which the penetratin and an analogue were compared. The first peptide was demonstrated to induce formation of hexagonal phase/inverted micelles and to have the capacity to translocate, whereas the analogue does not form these structures, or translocates across the lipidic membranes. In this model the interaction of the peptide with membrane in promoted by electrostatic interactions between the cationic peptide and the negative charges in the lipidic

membranes. A recruitment of negatively-charged phospholipids and induction of formation of an inverted micelle occurs upon interaction of the peptide with the lipidic membrane. The hydrophilic cavity of the micelle would accommodate putatively the cargo (Figure 3.1.A) [53]. However, this mechanism cannot account for the uptake of highly basic peptides such as oligoarginines (which do not contain hydrophobic amino acids required to induce hexagonal phase formation) [34], either for the uptake of high cargoes.

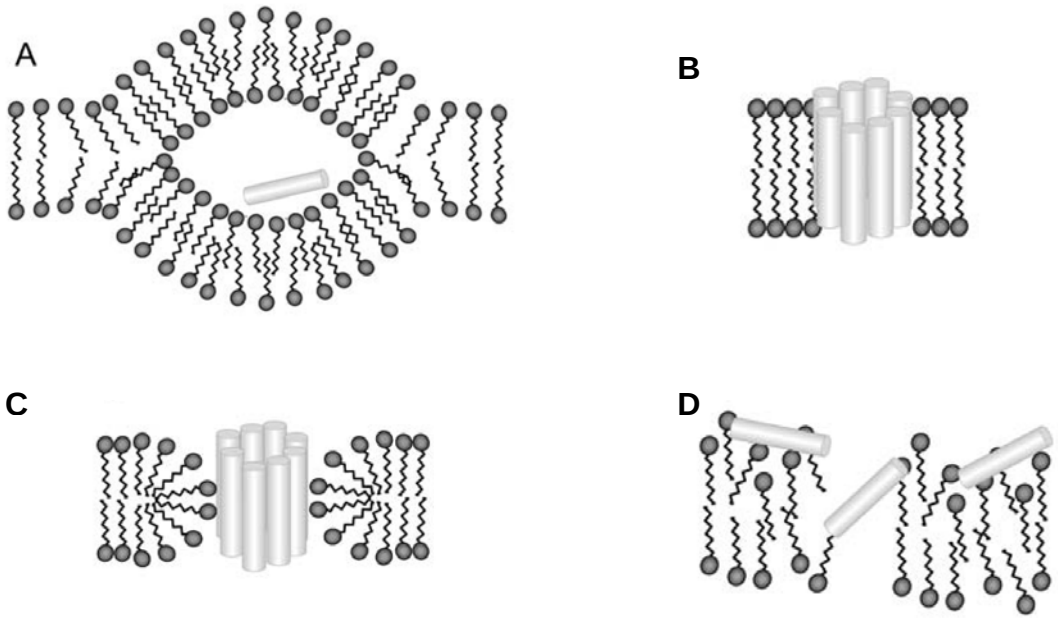

Figure 3.1. Schematic representation of permeation mechanisms independent on endocytosis. These models are dependent on the mode of peptide interaction with phospholipid bilayers: **A)** peptide passes through the membrane enclosed in "inverted micelle", which originates from membrane bilayer disruption upon peptide insertion; **B)** barrel-stave pore formed by a cluster of peptide molecules which span across the lipidic membrane; in this model hydrophobic interactions are relevant for pore formation and stability; **C)** toroidal pore across lipidic membrane, in which the phospholipids headgroups are always in contact with the peptidic chain to screen the net positives charge of peptide molecules; and **D)** Carpet model, peptide molecules bind to the membrane surface "carpeting" the membrane surface; above a threshold concentration the peptide disrupt the lipid packing leading to the peptide internalization. Image adapted from reference [169].

A mechanism involving pore formation has been suggested for MPG, an amphiphatic peptide that can be an efficient carrier for nucleic acids [170]. This is a typical feature of several toxins and antimicrobial peptides that have an action at

membrane level. In this mechanism the interaction of the peptide with the membrane is followed by alteration of membrane structure and in some cases entry of peptide into the interior of the target cell [171]. It is clear that peptide-lipid interactions govern the function of most membrane-lytic peptides, rather than a receptor-mediated process [172]. Three alternative mechanisms were proposed to account for the membrane permeability of amphipathic lytic peptides: "barrel-stave" pore (Figure 3.1.B), "toroidal" pore (Figure 3.1.C) and "carpet" model (Figure 3.1.D). In all models there is an initial adsorption of the peptide with the membrane surface. Adsorption in the lipid headgroup surface leads to a lateral expansion of the membrane and a thinning of the hydrophobic core [173, 174]. The lipidic membrane can respond in different ways to reduce the strain imposed on the lipidic bilayers by the adsorption of peptide, depending on different physicochemical characteristics of the peptide and membrane [175].

The "barrel-stave"-type pore (Figure 3.1.B) was first proposed for alamethicin, an amphipathic peptide with helical conformation [176]. This model is dominated by hydrophobic interactions between peptide and membrane, with the peptide chain inserted perpendicular to the lipidic bilayer surfaces and recruiting more peptide molecules to form a transmembrane pore that resembles a "barrel-stave" [177, 178]. In this arrangement hydrophobic amino acid residues interact with the lipid membrane while the hydrophilic residues face inwards to the lumen of the pore [177, 178]. Such organization requires peptides that span the lipid bilayer with an amphipathic α-helix conformation [172], forming contacts with other peptide molecules. Therefore, their length should match the bilayer thickness [175]. Weakly-charged peptides are compatible with this model to avoid intermolecular electrostatic repulsion within the pore [179]. Noteworthy, in this model peptide-membrane interactions are predominantly driven by hydrophobic interactions and they should bind to phospholipid membranes irrespective of their charge [172].

In the toroidal model (Figure 3.1.C), which has been proposed for magainins, melittin and protegrins [180], pores are also formed, but headgroups are always in contact with inserted peptides, even when they adopt a transmembrane orientation. In this model, to relieve the curvature strain caused by peptide binding, phospholipids bend continuously from the top to the bottom. Peptide pack together with lipid

headgroups to form a pore [34, 175, 180]. This model is usually associated with highly-charged peptides that do not self-associate at low peptide concentration [179]. The lipid headgroups play an important role in screening the peptide charges, whereas in the barrel-stave such screening is absent [180]. A cooperative assembly of pores only occurs when the concentration of peptides on the membrane surface exceeds a certain limiting value [179].

Another translocation mechanism involving membrane permeation is based on the "carpet" model (Figure 3.1.D) which was proposed for the first time to describe the mode of action of dermaseptin S [181]. In this model, reorientation of peptide chains can be hampered by strong electrostatic interactions between positively-charged residues and lipid headgroups [175], as a result peptides bind onto the surface of membrane and cover it in a carpet-like manner [172]. Membrane permeation occurs only if there is a high local concentration of membrane-bound peptide, where peptide molecules accumulation on the membrane surface causes tension between the two leaflets of the bilayer, which above a threshold concentration leads to disintegration of the membrane [175] due to disruption of the bilayer curvature [172]. In this mechanism the peptide does not necessarily adopt a specific structure upon its binding to the membrane, neither span across lipidic bilayer or assemble with their hydrophilic surfaces facing each other [172]. The carpet model seems to be a more general permeabilization mechanism than barrel-stave pore [175].

The formation of transient holes can occur as an intermediate step before the collapse of the membrane [172, 175], enabling the passage of low molecular weight molecules prior to membrane disruption [172]. In this transient pores peptide molecules remains in contact with the lipid headgroups during all the process and a peptide match with the bilayer thickness is not required; such features are similar to the toroidal pore model [175]. The similarities between carpet model and toroidal model suggest that torus-type pores may be part of a transient step before the membrane collapse [182].

In all models described an initial association of the peptide with the surface of the bilayer constitutes the first step, which is generally assumed to be governed by electrostatic interaction with negatively charged membrane lipids. However entropy-driven events in partition can also take part on the next steps [169]. Electrostatic

interaction are long range [183], so the structure of the peptide is less important in interactions governed by electrostatic interaction than when hydrophobic interactions are dominating. Actually many peptides are unstructured in solution but acquire a secondary structure upon interaction with lipidic membranes [184]. However it is worth mentioning that the nature of membrane perturbation depends on the orientation of the peptides. Interfacially-adsorbed peptides with an horizontal orientation with respect to the membrane plane perturb the lipid bilayer significantly more severely than transmembrane peptides that form barrel-stave pores [179]. It is suggested by Zemel *et al*. that the membrane perturbations induced by peptide can provides unspecific driving force that facilitates the pore formation, depending on the peptide orientation [179].

The above referred models that involve pore formation mechanisms may be relevant to CPPs with pronounced toxic effects, or ultimately can explain its toxic effect for high peptide/lipid ratios. This is relevant because peptide translocation resulting in membrane permeabilization conferring cytotoxic effects hampers it use in drug delivery applications [169].

3.2. *Energy-independent translocation of cell-penetrating peptides occurs without formation of pores. A biophysical study with pep-1*

3.2.1. Motivation and methodologies

It has been previously suggested by Deshayes *et al.* [185] that pep-1 is able to pass trough the membrane by a mechanism mediated by pore formation. In this hypothesis the pore is formed with the hydrophobic domain, which upon interaction with membrane becomes helical and inserts in the membrane with a perpendicular orientation to the membrane surface [185]. The pore model proposed is not clear and the possible perpendicular orientation is putative. No experimental evidences are presented.

Our previous results on permeability of LUVs to Co^{2+} in the presence of pep-1 suggests that this peptide in unable to form pores or induce leakage [186], however the hypothesis of pore suggested by Deshayes *et al*. [185] prompt us to make a more detailed study and to consider more carefully this possibility. In that way several questions regarding the differences between different permeation models need to be addressed, for instance: Is the binding of the peptide to the lipidic membranes electrostaticaly driven only or is dependent on hydrophobic interactions? Does pep-1 lie on the membrane surface or inserts in the hydrophobic core? Are there alterations in peptide conformation upon interaction with membrane?

Different methodologies were used to answer these questions. A characterization of the secondary structure of pep-1 and the study of the effect of membranes on peptide conformations were carried out by circular dichroism (CD) spectroscopy and also by Attenuated total reflection Fourier transform infrared (ATR-FTIR) spectroscopy techniques. The possible orientation of peptide when in the presence of lipidic bilayers was also studied by ATR-FTIR. The prospect of pore formation was tested with electrophysiological measurements by the use of planar lipid membranes (PLM) and also by confocal fluorescence microscopy using GUVs.

CD is a technique that has been widely used for determination of the secondary structure of proteins/peptides. CD refers to differential absorption of the left and right-handed circularly polarized light that occurs when a chromophore is chiral (optically

active) [187]. In practice, when two circularly polarized light components are absorbed by the sample in different extension, the resultant radiation would trace out an ellipse. The CD instrument detects the two components independently and then displays the dichroism at a given wavelength of radiation, which can be expresses as the ellipticity in degrees.

CD ellipticity is highly sensitive to the different secondary structures which have ellipticity bands with characteristic wavelengths and magnitudes [188], mainly in the far-UV (in the wavelength range 170-250nm). There are three major secondary structures identifiable by CD: a random coil structure that is coincident with the well defined poli(Pro)II (P2) CD spectral form with a strong negative band around 195nm; a α-helix conformation with minima bands at 208 and 222nm and a positive band at 192nm; and β-sheet with a positive band below 200nm but with a single negative band at ~ 220nm [187, 189-191]. (Figure 3.2). The CD signal of β-sheet conformation is weaker that the others.

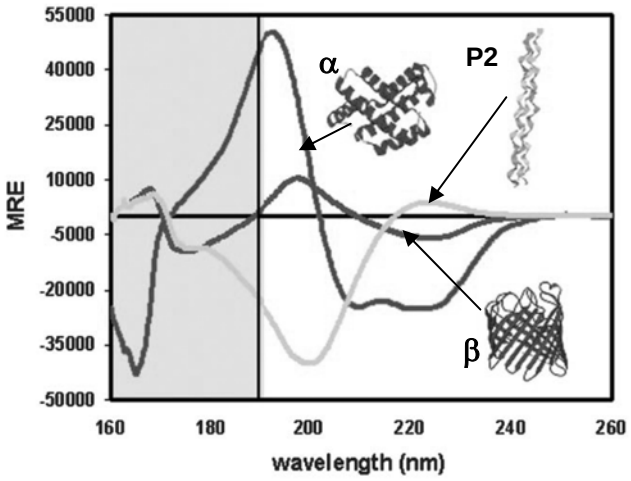

Figure 3.2. CD spectra of α-helix, β-sheet and poliproline II deconvoluted from a reference protein set. MRE is the mean residue ellipticity. Figure adapted from [192].

Protein/peptide structure is determined by comparison of the obtained spectra with CD data in literature. A number of algorithms can be used to provide an estimation of the secondary structure composition of proteins/peptides. Most procedures use data bases which comprise sets of CD spectra of different proteins whose structures have been solved by x-ray crystallography [191]. For a CD analysis is necessary to know precisely the peptide concentration to calculate the mean residue ellipticity (MRE) for

comparison with the data base spectra. Generally all the methods assume that the spectrum of a protein/peptide can be represented by a linear combination of the spectra of the secondary structure elements [188].

ATR-FTIR is a powerful tool to study the structure of peptides and their interaction with lipids without introducing a perturbing probe and requires small quantities of sample [193]. Because of the long IR wavelength, light scattering does not affect such measurements, in contrast to most other spectroscopic techniques. In ATR-FTIR experimental setup a drop of the sample (liposomes containing the peptides) is spread on the internal reflection plate (IRE) (e.g. trapezoidal Ge plate, see Figure 3.3) by slowly evaporation of the solvent, which results in several thousands macroscopically aligned multibilayers [194].

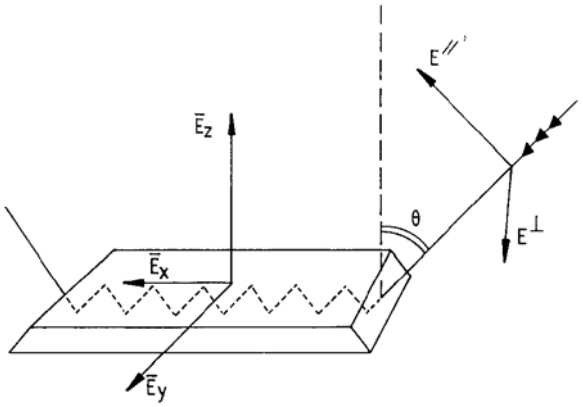

Figure 3.3. Total internal reflection at the interface of an internal reflection element (trapezoidal plate design). The components of electric field along the X, Y and Z axis are shown. The incident light can be polarized with a parallel orientation with the respect to plane of incidence ($E_{//}$) or perpendicular to plane of incidence ($E_{\perp}$). The angle θ is the light beam incident angle with respect to the IRE surface. Figure adapted from the reference [194].

The light travels inside the plate by means of a series of internal reflections from one surface of the plate to the other (see Figure 3.3), creating an exponentially decaying evanescent radiation outside the plate. Absorption of the energy of the evanescent field by the supported membranes and the peptide, provides ATR-FTIR spectra which contain information about the structure of the sample [195]. The spectra of peptide-lipid systems possess well-resolved absorbance bands not only on the lipidic membranes but also on the different structural groups within peptides. The amide I mode, among various "amid vibrational modes", is the most sensitive to the protein secondary structure and is found between 1700 and 1600cm^{-1} [193, 195, 196]. Amide I frequencies are essentially determined by the properties of the peptide backbone structure and so

practically independent on the amino acid sequence, its hydrophilic or hydrophobic character, its size, and its charge [196]. Determination of the peptide/protein secondary structure relies on the fact that the amide I vibrations of different conformations occurs at different frequencies as specified in the Table 3.1.

Table 3.1. Amide I frequencies of typical secondary structures elements in proteins in non-deutered (H_2O) and deutered (D_2O) environments. Table adapted from [195]. (↑↓ antiparallel)

Secondary structure	Frequency (cm^{-1})	
	H_2O	**D_2O**
α_I - helix	1658-1650	1655-1646
α_{II} - helix	1666-1658	1658-1652
3_{10} - helix	1670-1660	1670-1660
↑↓β- sheet	1638-1632	1636-1630
↑↓β- sheet	1695-1675	1680-1670
Intermolecular β- sheet	1625-1615	1625-1615
β- turns	1685-1655	1675-1640
γ- turns	1690-1650	1690-1650
irregular	1660-1652	1648-1640
amide or aromatic side chains	1618-1605	1615-1600

For secondary structure determination, the spectra of deutered and non-deutered samples can be intercompared to gain insight. This procedure relies on the possible interference of the solvent due to the strong HOH bending mode around $1643cm^{-1}$ [197] and also on the fact that in non-deutered form the random coil and α-helix conformation absorb IR radiation at the same frequency range (see Table 3.1). In the deutered form the random coil is shifted to lower wavenumbers, which facilitate the distinction and quantification of these two types of structure. Moreover, non-deutered amino acid chains can also contribute to the spectra in the amide I vibration range (see Table 3.1) [196].

For determination of the secondary structure of a peptide a curve-fitting of the amide I band that includes the decomposition of the amid I band into its constituent bands and their assignment (see Table 3.1), is necessary (for further information on curve-fitting and band assignment see references [193, 196, 197]). The component

bands are calculated and assigned to secondary structures comparing the results with previous reports, for instance [195-199].

For secondary structure determination is broadly accepted that CD measurements provide more accurate estimations of α-helix content whereas IR is more sensitive to the presence of β-sheets [200], so both techniques complement each other.

With polarized light in ATR-FTIR measurements is possible to have information about the orientation of the peptide with respect to lipidic membranes [195]. The method is based on the fact that the IR light absorption is maximal if the dipole transition moment is parallel to the electric field component of the incident light. In an ordered membrane deposited on the IRE surface all the lipid molecules have the same orientation with respect to a normal to the IRE surface. By measuring the spectral intensity with polarized light is therefore possible to detect changes in the orientation of dipoles of both peptides and phospholipids [194]. In practice, spectra with parallel and perpendicular polarization of the infrared light (relative to the incident plane) are collected, which enable the calculation of the dichroic spectrum (i.e. the difference between the spectra recorded with parallel and perpendicular polarization) and of the ATR dichroic ratio (R^{ATR}; which is the ratio between the integrated absorbance of a band measured with a parallel polarization of the incident light ($A_{//}$) and the absorbance measured with a perpendicular polarization of the incident light ($A_{\perp}$) [194]:

$$R^{ATR} = \frac{A_{//}}{A_{\perp}} \qquad \text{(eq. 3.1)}$$

This parameter provides information on the orientation of the peptide inserted in the lipidic bilayer. A larger absorbance for the parallel polarization (upward deviation on the dichroism spectrum) indicates a dipole oriented preferentially closer to the normal of the ATR plate, whereas a larger absorbance for the perpendicular polarization (downward deviation in the dichroism spectrum) indicates a dipole oriented approximately parallel to the ATR plate [201].

To determine the orientation of a specific peptide with respect to the membrane is necessary to first assign the contribution of each band in the IR spectrum and then to quantify the possible contribution of α-helix conformation within the peptide (this is the secondary structure that is commonly associated with linear peptides inserted in lipidic

membranes [172, 184]). By determination of R^{ATR} relative to the α-helical band is possible to calculate the orientation of the α-helix long axis with respect to the IRE surface normal and therefore the orientation of the peptide within the membrane [194]. Briefly, the R^{ATR} is related to an orientational order parameter *S* by the equation:

$$R^{ATR} = \frac{E_x^2}{E_y^2} + \frac{E_z^2}{E_y^2}\left(1 + \frac{3S}{1-S}\right) \qquad \text{(eq. 3.2)}$$

where E_x^2, E_y^2 and E_z^2 are the time averaged square electric field amplitudes of the evanescent wave in the lipidic film at the IRE/film interface. The $S_{experimental}$ is related with the helix axis by the relation:

$$S_{experimental} = S_{membrane} \times S_{helix} \times S_{dipole} \qquad \text{(eq. 3.3)}$$

where $S_{membrane}$ describes the distribution function of the lipid membrane with respect to the IRE, S_{helix} describes the orientation of the helix with respect to the membrane plane, and S_{dipole} describes the dipole orientation of amide I with respect to the helix axis (see Figure 3.4 for a better understanding). S_{dipole} is correlated with the angle α (angle between the amide I transition dipole moment and the helix angle; see Figure 3.4) by the equation:

$$S_{dipole} = \frac{3\cos^2\alpha - 1}{2} \qquad \text{(eq. 3.4)}$$

It is normally assumed that $S_{membrane}$ = 1 and S_{dipole} is a characteristic of the secondary structure (for helix conformation the angle α is considered to be 33.3º [201]; this value permits the calculation of the S_{dipole} by the eq. 3.4). With the $S_{experimental}$ and S_{dipole}, S_{helix} can be determined and therefore the tilt β (see Figure 3.4) of the helix axis with respect to the membrane normal by the following equation [194]:

$$\beta = \arccos\frac{2S_{helix} + 1}{3} \qquad \text{(eq. 3.5)}$$

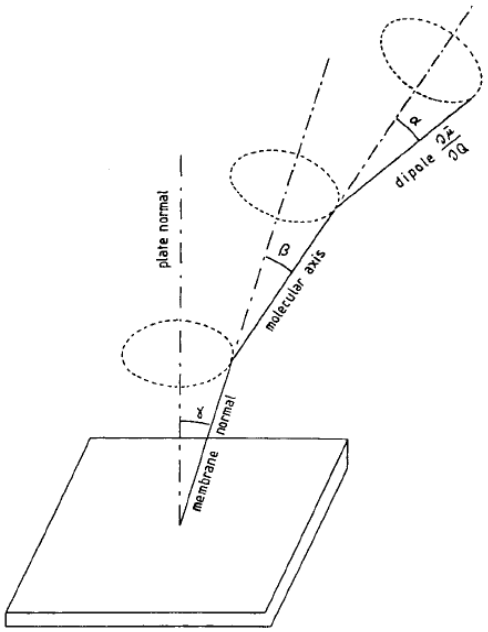

Figure 3.4. Axially symmetric distributions for the calculation of the angle of a dipole in relation with the IRE normal. The angle between the plate normal and the lipidic membrane is angle γ (assumed to be 0), the angle between the molecular axis (helix axis) and the membrane normal is angle β and the transition dipole moment in relation with the helix angle is α (assumed to be ~33.3º). By experimental determination of the order parameter S (see text) it is possible to determine the peptide tilt (angle β) in respect with the membrane normal. Figure adapted from the reference [194].

Previous reports on pep-1 secondary structure suggest that the hydrophobic domain of pep-1 has tendency to adopt an α-helical conformation when in contact with the membrane environment [185]. Taking into account the possible helical conformation of the peptides, ATR-FTIR can be used to determine the orientation of the hydrophobic domain when the pep-1 is interacting with lipidic membranes.

Different strategies can be used to detect pore formation in lipidic bilayers. The most important evidence for the possibility of barrel-stave model is the single-channel conductance induced by peptides when in lipidic bilayers, can be detected by ion conductance and are characterized by reproducible multiple discrete states [180]. Ion conductance can be studied with electrophysiological measurements using planar lipid membranes (PLMs) [202], also known as black lipid membranes (BLMs). With macroscopically assembled PLMs is possible to have access to both sides of the lipidic bilayers; the measurement of current flow across the lipidic bilayer gives information on the possible pore formation or membrane perturbation induced by the presence of peptides.

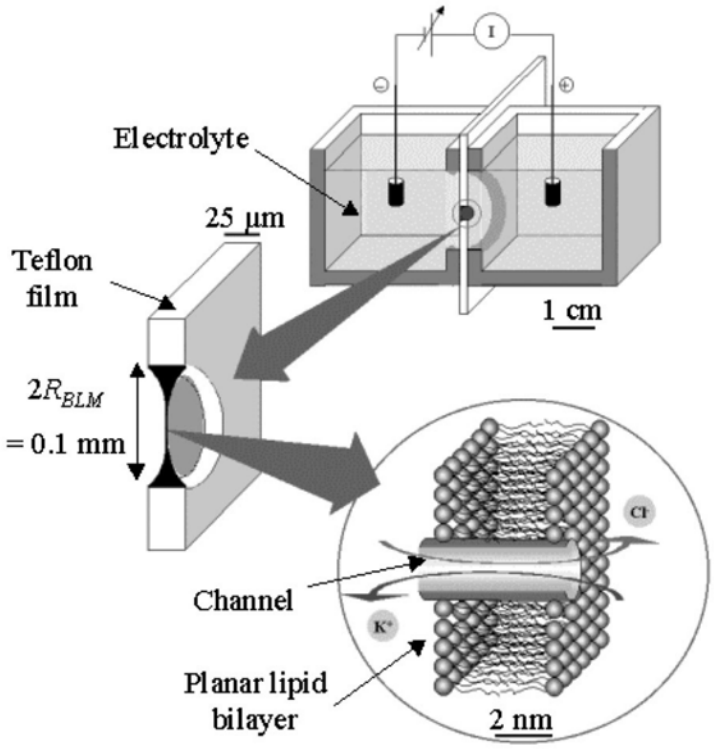

Figure 3.5. Experimental setup for planar lipid bilayers electrophysiology. Two chambers (*cis* and *trans*) are separated by a Teflon film which contains a small hole, ~50 to 200 µm in diameter. The chamber is filled with electrolyte-containing buffer and a lipid bilayer is formed across the hole. Electrodes are connected to each chamber (via salt bridges). The membrane potential is controlled (clamped) and the current is amplified using a voltage-clamp amplifier. Channel formation is monitored by step-wise increases in the current due to channels into the membrane. Figure adapted from [203].

PLMs can be prepared by the method originally developed by Montal and Mueller [202], where the experimental setup is prepared with the two chambers, *cis* and *trans*, separated by a thin Teflon film (25µm) containing a hole where lipidic membrane is formed (Figure 3.5). The chambers should be filled with an electrolyte-containing solution where the level of solution should be initially below the aperture. Lipid solution should be spread over the surface on two chambers to form a lipid monolayer at water-air interface. To form a planar lipid bilayer the two monolayers are folded together by raising the solution level of each compartment above the hole [202]. Both compartments have an electrode and are connected through a salt bridge. The formation and stability of bilayer membrane can be checked by continuously following membrane capacitance [204, 205]. This method has the possibility to form asymmetric bilayers by spreading lipid solutions with different lipid compositions in *cis* and *trans* chamber [202].

A planar lipid bilayer can be regarded as an insulator, therefore the presence of a conducting channel will lead to an electric field perturbation [203] which can be recorded with time. A pattern with reproducible multiple discrete states upon voltage potential application is indicative of pore formation by a barrel-stave mechanism (Figure 3.6)

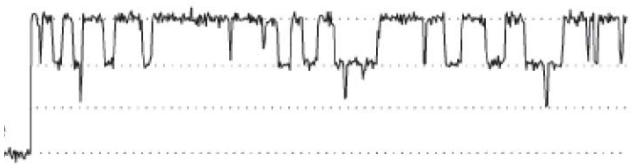

Figure 3.6. Current fluctuations with discrete conducting states, (step-wise increase) typical for proteins/peptides able to induce a channel formation across lipidic bilayers.

GUVs vesicles are suitable membrane models systems due to their size (diameter >10μm), which is similar to the size of the plasma membrane of the cells and can be directly visualized using microscopy techniques [206]. GUVs can be obtained by electroformation based on the protocol originally developed by Angelova and Dimitrov [207] among other techniques. In this protocol GUVs are formed by lipid swelling on platinum electrodes, under an electrical field. In a chamber (Figure 3.7), containing two parallel platinum wire electrodes, connected to an alternating current field generator, the lipid solution is spread onto each of the two wires and dried. An aqueous solution is added until wires cover. Upon attenuate electric field application osmotic forces and electrostatic forces drive the formation of liposomes [207].

To gain more information on the lytic action of peptides a strategy developed by Ambroggio *et al.* was used [208]. In this methodology, GUVs filled with fluorescent dyes with different sizes are followed by confocal microscopy. With this approach, visual information is obtained and related to the possible leakage mechanism. The capacity of this peptide to induce leakage is imaged and, in the case of pore formation, the pore size can be estimated [208, 209] (Figure 3.8). Briefly, to evaluate whether pores are formed, GUVs were prepared in a sucrose solution containing three dyes emitting at different wavelengths and with different sizes (Alexa Fluor^{633} C5-maleimide (Mr ~1330), Alexa Fluor^{488}-Dextran (Mr~10000) and Alex Fluor^{488} Dextran Mr ~3000). To remove the fluorescence dye from outside the vesicles GUVs solution was passed

through a sephadex G-100 column equilibrated with a glucose iso-osmolar solution. Vesicles loaded with sucrose and dispersed in a glucose solution led the GUVs to precipitate, making imaging in the inverted confocal fluorescence microscope easier.

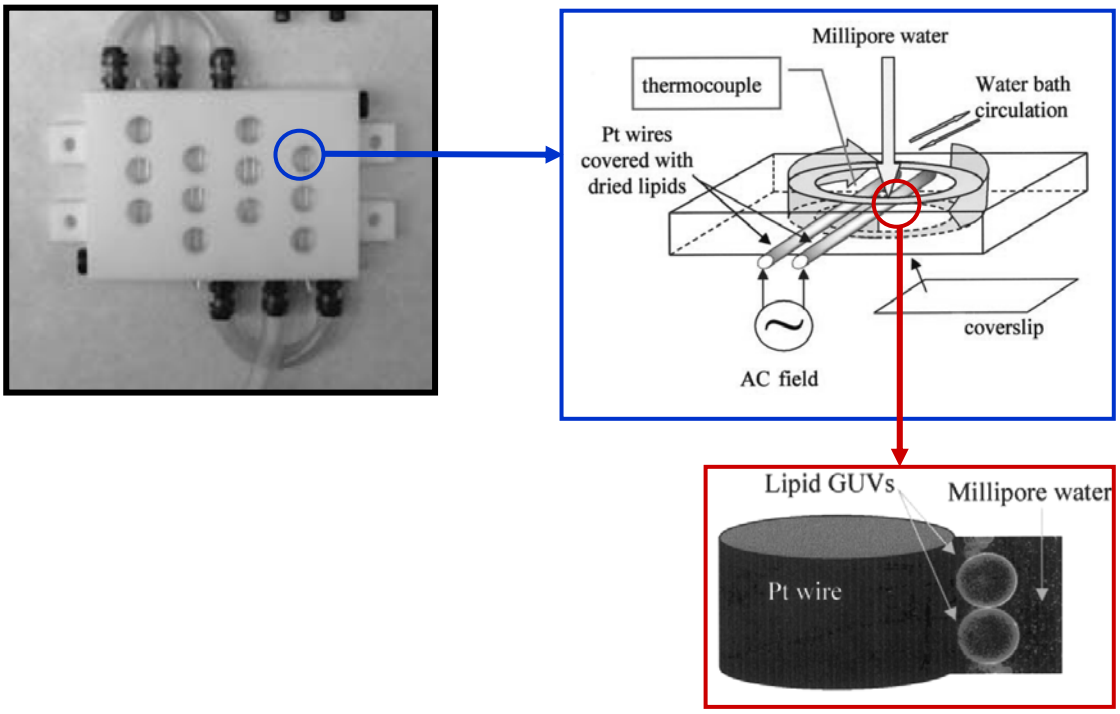

Figure 3.7. Array of individual chambers (12) to prepare GUVs by the electroformation method. The array is prepared with Teflon and Pt wires (with a diameter of 0.5mm) and the water flux from the circulating bath in a plastic tube surrounding the module. Lipid is dried on the pt wires and GUVs are formed upon Alternating current application. Figure adapted from [206] and [210].

In the case of pore formation, after peptide addition, a sequential escape of the three dyes (from the smaller to the large one), or the leak of just one or two dyes will give information about pore size (see Figure 3.8). Membrane integrity can be evaluated by a membrane dye [208, 209].

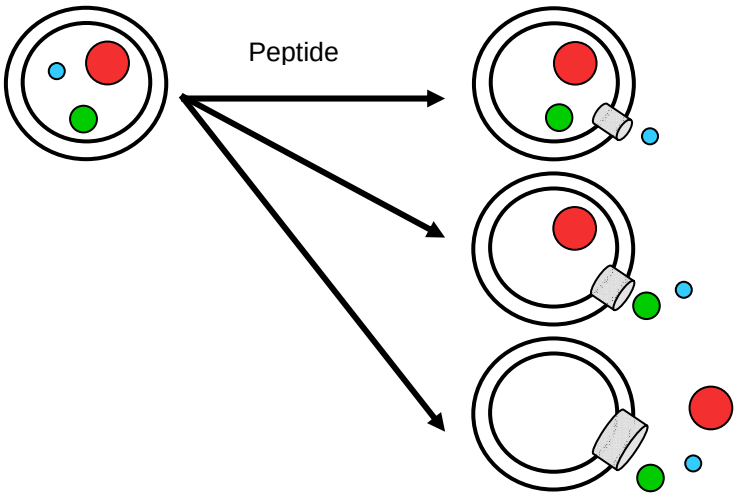

Figure 3.8. Approach for direct visualization of the lytic activity of peptides. By the use of GUVs loaded with fluorescent dyes with different size and by screening these fluorescent markers with confocal microscopy is possible to evaluate the leakage caused by the peptide. If the membrane becomes leaky to one, two or the three dyes one has information on the pore size. In this schematic representation the dyes with different sizes are represented by blue, green and red.

The methodologies above referred were used to evaluate pore formation induced by the pep-1. The following manuscript presents the most relevant results achieved with these studies.

3.2.2. Declaration on authorship of published manuscript: *Energy-independent translocation of cell-penetrating peptides occurs without formation of pores. A biophysical study with pep-1*

I, Sónia Troeira Henriques declare that the experimental design was carried on by me under advice of Dr. Miguel ARB Castanho. All the laboratory work, data analysis, discussion were carried on by me under supervision of Dr. Luis A. Bagatolli, Dr. Fabrice Homblé and Dr. Alexandre Quintas. CD measurements were carried on at *Instituto Superior de Ciências da Saúde Egas Moniz* (Costa da Caparica, Portugal) and supervised by Dr. Alexandre Quintas. ATF-FTIR and electrophysiological measurements were carried out with guidance of Dr. Fabrice Homblé at *Université libre de Bruxelles* (Brussels, Belgium) and the studies with GUVs were carried out at Southern Denmark University (Odense, Denmark) with Dr. Luis Bagatolli.

Manuscript preparation was carried on by me with contribution from the other co-authors.

I, Miguel ARB Castanho, as Sónia T Henriques supervisor, hereby acknowledge and confirm the information above is correct.

_____ _____

Sónia Troeira Henriques Miguel ARB Castanho

Molecular Membrane Biology
2007, 1–14, iFirst article

informa
healthcare

Energy-independent translocation of cell-penetrating peptides occurs without formation of pores. A biophysical study with pep-1

SÓNIA TROEIRA HENRIQUES[1], ALEXANDRE QUINTAS[2], LUIS A. BAGATOLLI[3], FABRICE HOMBLÉ[4], & MIGUEL A.R.B. CASTANHO[1]

[1]*Centro de Química e Bioquímica, Faculdade de Ciências da Universidade de Lisboa, Campo Grande, Lisboa, Portugal,* [2]*Instituto Superior de Ciências da Saúde Egas Moniz, Campus Universitário, Monte da Caparica, Portugal,* [3]*MEMPHYS, Center for Biomembrane Physics, Department of Biochemistry and Molecular Biology, SDU, Odense M, Denmark, and* [4]*Structure et fonction des Membranes Biologiques, Université Libre de Bruxelles, Brussels, Belgium*

(Received 21 June 2006; and in revised form 19 October 2006)

Abstract
Pep-1 is a cell-penetrating peptide (CPP) with the ability to translocate across biological membranes and introduce active proteins inside cells. The uptake mechanism used by this CPP is, as yet, unknown in detail. Previous results show that such a mechanism is endocytosis-independent and suggests that physical-chemical interactions between the peptide and lipid bilayers govern the translocation mechanism. Formation of a transmembrane pore has been proposed but this issue has always remained controversial. In this work the secondary structure of pep-1 in the absence/presence of lipidic bilayers was determined by CD and ATR-FTIR spectroscopies and the occurrence of pore formation was evaluated through electrophysiological measurements with planar lipid membranes and by confocal microscopy using giant unilamellar vesicles. Despite pep-1 hydrophobic domain tendency for amphipathic α-helix conformation in the presence of lipidic bilayers, there was no evidence for membrane pores in the presence of pep-1. Furthermore, alterations in membrane permeability only occurred for high peptide/lipid ratios, which induced the complete membrane disintegration. Such observations indicate that electrostatic interactions are of first importance in the pep-1-membrane interactions and show that pores are not formed. A peptide-lipid structure is probably formed during peptide partition, which favours peptide translocation.

Keywords: *Peptide carrier, peptide-membrane interaction, translocation mechanism, membrane pore, peptide secondary structure, model membranes*

Introduction

Whilst the introduction of hydrophilic molecules into mammalian cells is controlled by the lipid membrane barrier, the use of cell-penetrating-peptides (CPPs) has become a good strategy to overcome the membrane impermeability. A CPP is a short, basic and water-soluble, peptide able to translocate through cell membranes, with high efficiency and low toxicity, in a way independent on receptors [1,2].

Despite their potential for drug delivery, the mechanism used by CPPs to translocate across the cell membrane, without damaging it, is still a mystery. A single general mechanism for all does not seem reasonable and more than one mechanism for each individual peptide is a possibility [2–4]. Nonetheless, the existence of the basic amino acid residues in all the peptides suggests that the electrostatic interaction with phospholipid bilayers is a common step in the mechanism of action of CPPs.

Many CPPs including penetratin, TAT and oligoarginines are internalized by an endocytotic pathway (so-called 'energy-dependent' mechanism) [2–4]. However, the strong correlation of uptake with lipid-binding affinity, the direct observation of translocation in model membranes, and the importance of electrostatic interactions, suggests that a translocation mechanism involving only direct physical interactions with lipids can operate for some peptides [1].

Pep-1 (Ac-KETWWETWWTEWSQPKKKRKV-cysteamine) is a chimeric CPP with a primary amphipathicity, which can be divided into three domains: (i) a so-called hydrophobic domain

Correspondence: Miguel A. R. B. Castanho, Centro de Química e Bioquímica, Faculdade de Ciências da Universidade de Lisboa, Ed. C8, Campo Grande, 1749-016 Lisboa, Portugal Tel: +351 217500931. Fax: +351 217500088. E-mail: castanho@fc.ul.pt

ISSN 0968-7688 print/ISSN 1464-5203 online
DOI: 10.1080/09687860601142936

(KETWWETWWTEW), responsible for hydrophobic interactions with proteins and for an interaction with the cell membrane; (ii) a hydrophilic Lys-rich domain derived from the nuclear localization signal (NLS) of simian virus 40 (SV-40) large T antigen (KKKRKV), required to improve solubility and intracellular distribution of the peptide, and (iii) a spacer domain (SQP) which improves the flexibility and the integrity of the other two domains. This CPP has advantages relative to the others because it does not need covalent link with the cargo [5]; physical assemblies between peptide and macromolecules, stabilized by hydrophobic and electrostatic interactions, are formed [6].

Our previous works demonstrated that pep-1 is able to translocate *in vitro* or *in vivo* by a physical-mediated mechanism promoted by transmembrane potential [6,7], with no evidences for any alternative 'energy-dependent' process [6]. The high efficiency of the peptide to be translocated by an 'energy-independent' process seems to be related to its primary amphipathicity, which is responsible for the high affinity for lipidic membranes [8]. Furthermore, it has been shown that the C-terminal cysteamine group is relevant for membrane affinity and translocation efficiency [8–10].

A variety of models have been suggested to describe an 'energy-independent' pathway for the translocation of CPPs (recently reviewed in references [1,11]) and a possible mechanism is pore formation. In our previous studies, with model membranes, no evidence for pore formation was detected in the presence of pep-1 [7] and this result was confirmed by Weller et al. [10]. However, this issue remains very controversial as electrophysiological studies using oocyte membrane [12] suggest that a transmembrane pore-like structure could be formed, mediated by pep-1 conformational changes.

The main aim of the present work is to find out if pore formation occurs and is a relevant mechanism for pep-1 translocation. Attenuated total reflection-Fourier transform infrared (ATR-FTIR) spectroscopy was performed in order to identify the peptide conformation and its orientation when inserted in the membrane [13]. The pore formation hypothesis was tested by electrophysiological measurement in Planar Lipid Membranes (PLMs) [14] and by confocal microscopy using Giant Unilamellar Vesicles GUVs [15].

Material and methods

Reagents

Pep-1 with purity >95% was produced by custom synthesis by GenScript Corporation (Piscataway, New Jersey). Synthetic lipids 1-Palmitoyl-2-Oleoyl-sn-Glycero-3-Phosphocholine (POPC), 1-Palmitoyl-2-Oleoyl-sn-Glycero-3-(Phospho-rac-(1-glycerol)) (POPG), 1,2-Dipalmitoyl-sn-Glycero-3-phosphocholine (DPPC), 1,2-Diphytanoyl-sn-Glycero-3-phosphocholine (DPhPC) and 1,2-Dipalmitoyl-sn-Glycero-3-Phosphoethalonamine-N-(Lissamine Rhodamine B Sulfonyl) (N-Rh-PE), were obtained from Avanti polar lipids (Alabaster, Alabama). Cholesterol (Chol) and Thioflavin T (ThT) were from Sigma-Aldrich (St. Louis, Missouri). Alexa Fluor^{633} C5-maleimide (Mr ~1300), Alexa Fluor^{546}- Dextran (Mr ~10000) Alexa Fluor^{488}-Dextran (Mr ~3000) and 1,1′-dioctadecyl-3,3,3′,3-tetramethylindocerbocyanine perchlorate ($DiIC_{18}$) were purchased from Molecular Probes (Eugene, Oregon).

The samples were prepared in 10 mM HEPES buffer with 150mM NaCl and pH 7.4, unless stated otherwise.

Circular Dichroism (CD) measurements

CD spectra were recorded for 68.8 μM pep-1 in aqueous solution or in the presence of lipid. 1 mM of POPC or POPC:Chol (2:1 molar) large unilamellar vesicles (LUVs), prepared by the extrusion method [16], were used for these studies (peptide/lipid molar ratio = 0.069). Samples with negatively-charged lipids (e.g., POPG down to 20%) were not possible to prepare due to aggregation of vesicles induced by pep-1 at these peptide/lipid ratios (see [8]), which are mandatory to perform spectra with good S/N ratios. Samples were prepared in 10 mM phosphate buffer with 75 mM NaF, pH 7.5. The CD measurements were made on a Jasco J-810 Circular Dichroism Spectropolarimeter equipped with a Julabo F25-HE Temperature Unit Control in a quartz cell with an optical path of 0.1 cm at 20°C. Wavelengths from 260 to 185 nm were recorded with a 0.1 nm step and a 20 nm/min speed. Spectra were collected and averaged over 3 scans and corrected for background contributions. Molar absorptivity was calculated considering $\varepsilon = 1.8 \times 10^4$ $M^{-1}cm^{-1}$ (data not shown). Computer fittings using the Jasco software package JWSSE-480 with the CD reference dataset of Yang [17] were performed to estimate the contributions of spectral components from different secondary structures.

ATR-FTIR spectroscopy

Attenuated total reflection infrared (ATR-FTIR) spectra were obtained on a Bruker Equinox 55 FTIR spectrophotometer (Ettlingen, Germany) equipped with a MCT detector (broad band

12000–420 cm^{-1}, liquid N_2 cooled, 24 h hold time) at a resolution of 2 cm^{-1}. The spectrometer was continuously purged with dry air (Whatman 75–62, Haverhill, MA, USA). The internal reflection element was a 52 × 20 × 2 mm trapezoidal germanium ATR plate (ACM, Villiers St Frédéric, France) with an aperture angle of 45° yielding 25 internal reflections. A total of 128 scans (800–4000 cm^{-1}) were averaged for each spectrum with a resolution of 2 cm^{-1}. The spectrophotometer was continuously purged. Background of the internal reflection element was collected and subtracted to the samples. Peptide samples in the absence/presence of lipid were prepared with 10 mM HEPES buffer pH 7.4 and spread on the Ge plate under a stream of N_2 to evaporate the solvent (see [18] for further information).

Secondary structure of the pep-1, in absence and in the presence of membranes with various lipidic compositions: POPC, POPC:Chol (2:1 molar) and DPPC, was evaluated (negatively-charged phospholipids could not be used due to precipitation caused by pep-1, as stated above). After liposome formation, pep-1 was added to the solution to obtain a final peptide concentration of 20% (w/w) and mixed in vortex; the lipidic concentration was maintained at 2 mg/mL (~2.6 mM, depending on the exact lipid molar mass) and the peptide concentration at 0.4 mg/mL (0.138 mM, peptide/lipid molar ratio = 0.053). A film with 8 μg peptide + 40 μg lipid was prepared by spreading the peptide/lipid solution on the Ge plate. The kinetic of peptide deuteration was evaluated; non-deutered and deutered samples were compared.

The determination of protein secondary structures was performed using a curve-fitting procedure, where the amide I band was decomposed into the various component bands which can be assigned to the different types of secondary structure. First the band positions were determined by deconvolution using a Lorentzian deconvolution function (FWHH = 30), a Gaussian apodization function (FWHH = 15) and a 2 cm^{-1} resolution enhancement. The amide I was fitted with bands placed at the positions found and the integrated absorbance of the component bands was calculated. The components bands were assigned to secondary structures comparing the results with data presented in different references [19–23].

Orientation of the secondary structure

ATR-FTIR Spectroscopy provides information on the orientation of peptides inserted in lipid bilayers [18,23]. Peptide spectra were recorded with parallel and perpendicular polarized incident light at the same conditions as non-polarized spectra (see above). With polarized light it is possible to determine the dichroic spectra (see Supplementary Figure S.2 in the Online version for results obtained with pep-1) and the dichroic ratio (R^{ATR}) which provides information about the orientation of the peptide inserted in lipidic bilayers.

The integrated areas corresponding to the α-helix components from the two polarized spectra were determined and the ratio of the integrated areas is the dichroic ratio of α-helix, R_α^{ATR}. Dichroic ratios were used to determine the tilt angle with the membrane normal (see [13] for further information). The angle between helix axis and the amide I transition dipole moment is 33.3° [24]. R^{iso} was used to compute the film thickness and the values of the electric field components at 1650cm^{-1} as described previously [18]. For these calculations refractive indexes of 4.0 and 1.44 were used for the Ge plate and the sample film, respectively.

Electrophysiological studies

PLMs were formed according to the Montal and Mueller method [25]. Briefly, a thin teflon film (25 μm) with a hole (130–160 μm) was clamped between two compartments (referred as *cis* and *trans* chambers) filled with HEPES buffer (the level of solution was kept below the hole) 5 μl of a lipid solution (20 mg/ml in n-hexane) were spread in each compartment and the solvent was left to evaporate (10 min). Raising the level of the buffer solution above the aperture, first in one side and then in the other, induced the formation of the bilayer in the teflon hole. The two chambers were connected (through Ag/AgCl electrodes and a 1 M KCl agar bridge) to a BLM-120 amplifier (biologic). The *cis* chamber was connected to the active input of the BLM-120 amplifier and *trans* chamber was held at ground. The electrical potential was defined as *cis* with respect to *trans*. The formation of bilayer was followed by membrane capacitance, see [26]. Only membranes with a resistance > 100GΩ were used to perform the measurements. Pep-1 was added to the *cis* side of the chamber and the ion current was recorded for increasing potential differences (alternating from negative to positive potential). The electric signal was low pass filtered at 100 Hz, sampled at 44.1 kHz and stored on CD using a DRA 200 analog to digital converted (biologic). DPhPC was used to perform PLMs because it is known to form stable bilayers [27], this lipid exhibits no detectable phase transition over a large temperature range (−120°C to +120°C) [28] and the presence of methyl groups along acyl chains results in considerable disorder chain [29], so a fluid-like

phase is expected at room temperature. DPhPC was preferred over POPC because POPC did not form bilayers. Both lipids form fluid phase bilayers at room temperature. The charge effect was tested by the presence of 10% and 20% (mol/mol) of POPG in the bilayers. Different peptide concentrations were added at *cis* chamber. Asymmetrical membranes were also tested with 20% POPG in the *trans* side and pure DPhPC in the *cis* side. Titrations with peptide were realized in the *trans* side or in the *cis* side or alternating (one addition in the *trans* side and other in the *cis* side). Controls without peptide were carried on.

Leakage experiments with GUVs

Membrane leakage induced by pep-1 was evaluated in GUVs using the method previously described by Ambroggio et al. [15,30]. Briefly, for GUVs production 4 μl of lipid stock solution (0.2 mg/ml) in chloroform were spread on each Pt wire under a stream of N_2, residual organic solvent was removed in a vacuum chamber overnight. Sucrose solution with three dyes, (2 μM Alexa Fluor^{633} C5-maleimide (Mr ~1300), 2 μM Alexa Fluor^{546}-Dextran (Mr ~10000) and 2 μM Alexa Fluor^{488}-Dextran (Mr ~3000)) with an overall osmolarity of 150 mOsM, was equilibrated at a temperature above lipid phase transition and added to the chamber (500 μl final volume) covering the Pt electrodes. The Pt wires were connected to a function generator and a low frequency AC field (sinusoidal wave function with a frequency of 10 Hz and amplitude of 1.5V) was applied for 120 min to form GUVs. Vesicle solutions were carefully removed from the chamber and placed into a sephadex G-100 column equilibrated with a gluocose isoosmolar solution [15]. With this procedure the fluorescent dyes located out of the vesicles are removed and vesicles with homogeneous size (about 10–15 μm) are obtained. GUVs solution suspended in glucose (250 μL) were added to an eight well plastic chamber (Lab-tek Brand Products) and left to precipitate overnight. The density difference between glucose and sucrose causes the precipitation of the vesicles, which facilitates observation in the inverted confocal fluorescence microscope. An isoosmolar solution of pep-1 was added to the chamber and the fluorescence intensity of the different dyes was followed for a period of time of up to 30 min; different peptide concentrations were studied in the presence of GUVs prepared with POPC or POPC:-POPG (4:1 molar). The membrane integrity was evaluated repeating these experiments with GUVs labelled with a membrane dye (0.5% DiIC$_{18}$/lipid mol/mol) and with 2 μM Alexa Fluor^{633} C5-maleimide internalized. An inverted scanning confocal fluorescence microscope (Zeiss -LSM 510 META, Carl Zeiss, Jena, Germany) was used to perform the experiments. The excitation wavelengths were 543 nm (HeNe laser, 1 mW; for DiIC$_{18}$ or Alexa Fluor^{546}- Dextran), 488 nm (Ar laser, 30 mW; for Alexa Fluor^{488}-Dextran) and 633 nm (HeNe laser, 5 mW; for Alexa Fluor^{633} C5-maleimide). The objective used for the experiments was a Zeiss C-Apochromat 40×1.20 W corr (water immersion, NA = 1,2). The fluorescent images were simultaneously collected using the fluorescence microscope's META detection device (Polychromatic 32-channel detector) by selecting the proper emission wavelength range for the different fluorescent probes. The time-dependence of the fluorescent intensities of the different dyes during the course of the experiment were quantitatively recorded and treated by the standard Zeiss LSM 510 META software package (with the inclusion of the multiple time series software option).

Lipid quantification in GUVs solution was carried out to enable the determination of the peptide/lipid ratio. POPC GUVs doped with 5% N-Rh-PE were prepared using the same procedure above described and the Rh fluorescence emission intensity ($\lambda_{excitation} = 570$ nm and $\lambda_{emission} = 590$ nm) was followed before and after the washing step in the Sephadex G100 column. The calibration curve was set with multilamellar vesicles dispersions in sucrose or glucose with a well-known lipidic concentration. Blanks were discounted. Considering the total lipid added to the Pt wire, the final lipid concentration in the chamber is ~4 μM; after GUV formation the average lipid concentration determined was 1.03 ± 0.49 μM (8 samples) before washing step and 0.71 ± 0.22 μM (4 samples) after vesicle washing.

Results and discussion

Pep-1 has a high affinity for zwiterionic membranes, which is enhanced in the presence of negatively-charged phospholipids [8]. The peptide has an amphipathic nature, the hydrophobic domain, containing five Trp residues, inserts in the membrane with a shallow position [8,10], but not accessible to the aqueous environment [8]. The hydrophilic domain, with five basic residues, does not insert in the hydrophobic core of the membrane [9]. This highly charged domain is probably responsible for the first contact of the peptide with the membrane due to electrostatic attraction between the polar phospholipids headgroup and the positive charges of pep-1 [9]. The dehydration induced by the hydrophilic domain at membrane surface and the insertion of hydrophobic domain promote mem-

brane destabilization. As a consequence of membrane destabilization induced by pep-1, aggregation and fusion events with LUVs were detected [7]. These perturbations in the membrane occurred without evidence for pore formation. [7,10]. Fusion events without leakage were also observed for other CPPs such as R_7W, TATP59W and TATLysP59W [31]. Moreover, membrane integrity in HeLa cells is only disrupted in the presence of high peptide concentration (concentration much higher than the one required for the translocation to occur) [10].

At variance, Deshayes et al. proposed a barrel-stave-like mechanism of pore formation [12]. Such a hypothesis is based on the observation that pep-1 undergoes conformational changes after insertion in the lipidic bilayer (hydrophobic domain change from unordered to α-helix structure) and due to changes in the membrane conductance in voltage-clamped oocytes, when a transmembrane potential is applied. Moreover, it is suggested that the helical axis of pep-1 is inserted with a perpendicular orientation to the membrane plane; this proposal was putative.

Secondary structure determination

In the present work a study of the peptide secondary structure was carried out in the absence and presence of lipidic membranes at physiological pH. To evaluate the conformational state of pep-1, its secondary structure was studied by both CD spectroscopy and ATR-FTIR spectroscopy in the presence and absence of lipidic bilayers. It is normally accepted that CD spectroscopy is a powerful technique to identify the presence of random coil and α-helix contributions [17,32,33] where IR is more sensitive to β-sheets structures [34].

In CD measurements a good computer fitting with concomitant quantification of different spectral components contributions was obtained in the spectra carried out on aqueous solution with 68.8 μM pep-1 (Figure 1A). Contributions of α-helix and random coil were identified.

LUVs are an adequate model of biological membranes with no significant curvature effects as the ones present in SUVs (small unilamellar vesicles) [35]. The secondary structure of 68.8 μM pep-1 in the presence of 1mM POPC or POPC:Chol (2:1 molar) vesicles (Figure 1B and C) has a higher contribution of α-helix than in aqueous environment.

ATR-FTIR spectroscopy enables to further extend the information on peptide secondary structure because this technique is more robust than CD spectroscopy to identify the presence of β-structures. Amide I mode ($\sim$1700–1600 cm^{-1}) is the most sensitive to the protein secondary structure [23].

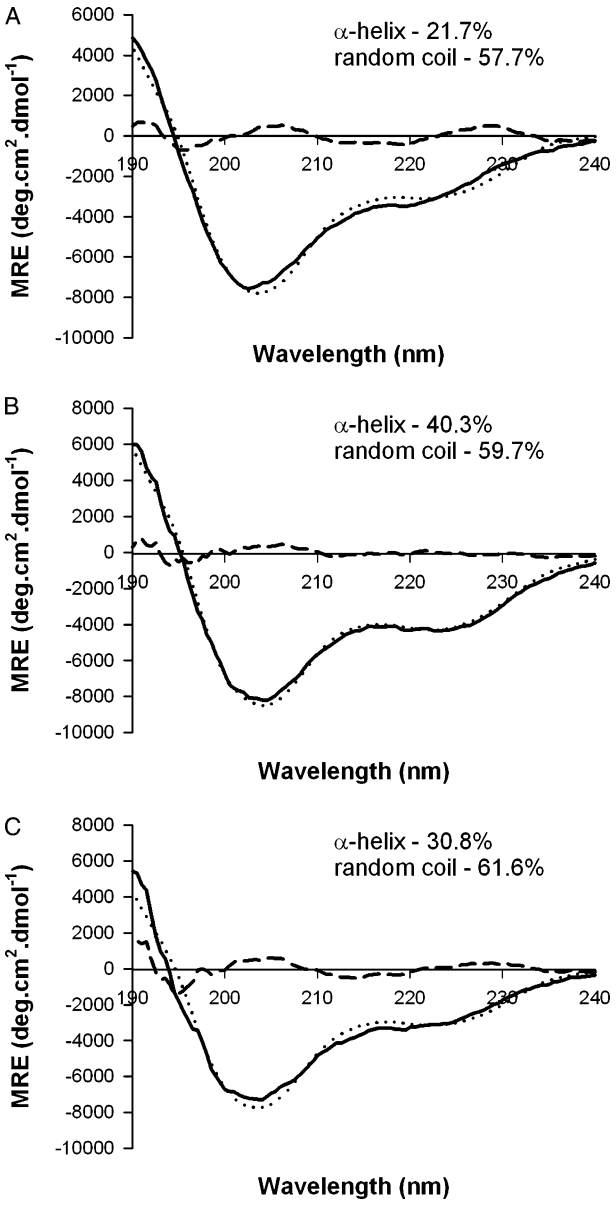

Figure 1. The 68.8 μM pep-1 Far-UV CD spectra obtained, Mean Residue Elipticity (MRE) is presented, (A) in aqueous solution, (B) in the presence of 1 mM POPC LUVs or (C) in the presence of 1 mM POPC:Chol (2:1 molar). Solid lines represent original spectra; dotted lines fitted spectra and dashed lines the residual. The samples were prepared in 10 mM phosphate buffer (pH 7.5) containing 75 mM NaF.

The membrane phase effect was evaluated with different lipids at room temperature, instead of heating/cooling one lipidic system, to avoid artefacts/denaturation in the pep-1. At room temperature POPC forms fluid phase bilayers, POPC:Chol (2:1 molar) forms liquid-ordered phases and DPPC forms gel phase bilayers.

A broad band was obtained in the absence and presence of the lipidic systems (Figure 2A), suggesting that there are contributions of different conformations. Comparison of deconvoluted spectra

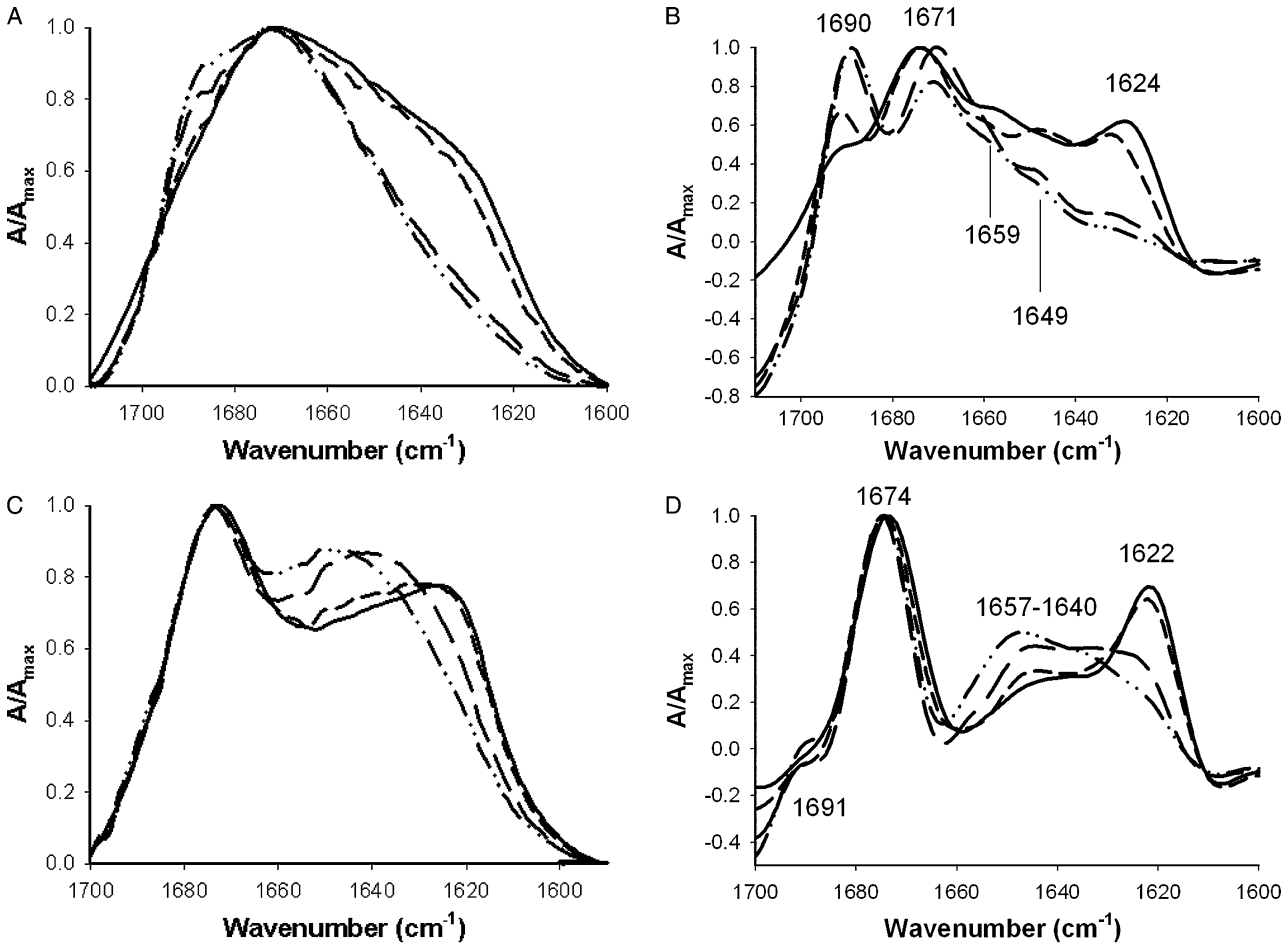

Figure 2. ATR-FTIR amide I band of 8 μg of pep-1 in aqueous solution (solid line) or in the presence of 40 μg of lipid in multilayers with different compositions: POPC (alternated dashes and dots), POPC:Chol (2:1 molar) (long dashes) and DPPC (short dashes). (A) Non-deutered form, (B) Deconvoluted spectra of the non-deutered form. (C) Recorded after 1 h of deuteration. (D) Deconvoluted spectra of deutered form. All the spectra were normalized. The samples were prepared in 10 mM HEPES with 150 mM NaCl (pH 7.4).

(Figure 2B) reveals that the same secondary structures but with different percentages are present in the different conditions tested.

Spectra of deutered samples (1 h of deuteration; see $^{1}H/^{2}H$ exchange kinetic in Supplementary material Online, Figure S.1) were used to improve the assignment of band components and for a better quantification of secondary structure. In the non-deutered form the random coil and α-helix conformation absorb at the same wave number range. At variance, the band of the deutered form of the random coil is usually shifted to lower wave numbers. Therefore, the deutered form facilitates the identification and quantification of the two classes of structures. Moreover, the amide I in non-deutered form can also have contribution of the water hydration [23] and of amino acid side chains [20], which further hampers detailed data analysis.

The spectra of pep-1 or pep-1-lipid mixtures dried on the Ge plate were compared after 1 h of deuteration (Figure 2C). Deconvolution (Figure 2D) shows 3 peaks (1691, 1674 and 1622 cm^{-1}), and a large shoulder between 1657–1640 cm^{-1}.

By comparison with deconvoluted spectra obtained in non-deutered and deutered forms (Figure 2B,D) it is possible to say that there is a contribution of intermolecular β-structure (1692 and 1625 cm^{-1} in ^{1}H, which are shifted to 1674 and 1622 cm^{-1} in ^{2}H) [21,23]. The existence of intermolecular β-structure instead of intramolecular β-sheet is identified by the low frequency signal at 1625 cm^{-1} in ^{1}H, and 1622 cm^{-1} in ^{2}H; in the case of intramolecular β-sheet a longer wave number was expected for the low frequency component (1636–1630 cm^{-1} instead of 1625 cm^{-1}) [23]. The existence of a contribution at ~1674 cm^{-1} in ^{1}H suggests the existence of β-turns [23]. In ^{2}H a peak with this wavenumber has a contribution of β-turn [19] and also with the high frequency component of intermolecular β-sheet. Absorbances between 1657 cm^{-1} and 1640 cm^{-1} in ^{2}H are characteristic for α-helix and random coil [23]. Results obtained with

CD spectroscopy confirm the existence of these two contributions.

For the quantification of each contribution a five-band fitting was preformed in deutered spectra, as follows: (i) 1705–1685cm^{-1}, (ii) 1680–1669cm^{-1}, (iii) 1660–1648cm^{-1}, (iv) 1648–1640cm^{-1}, (v) 1630–1620cm^{-1}. Band assignment and relative weights are present in Table I.

In the presence of lipids, the contribution of β-sheet (bands with maximum at 1674 cm^{-1} and 1621 cm^{-1}) decreases, while α-helix (1657 cm^{-1}) and random coil contributions (1640 cm^{-1}) increase. The contribution at ~1690 cm^{-1} is weak for all the conditions and may result from a small fraction of peptide quantity in non-deutered form in β-sheet conformation (see Figure 2 and Table I).

In ATR-FTIR measurements, an increase in intermolecular β-sheet signal, with the peptide quantity spread in the Ge plate, was verified (data not shown). It was previously published that pep-1 has a tendency to aggregate in aqueous solution [8]; in order to verify that the β-structure signal is due to intermolecular interactions resulting from peptide aggregation with β-sheet conformation, a titration of the ThT dye with a pep-1 stock solution was realized (see Supplementary material online). An increase in ThT fluorescence intensity emission (with excitation at 450 nm) with peptide concentration (see Figure S.3 in Supplementary material online) confirms that pep-1 has a tendency to aggregate with β-sheet conformation.

While analysing ATR-FTIR results one should bear in mind that samples are semi-dehydrated. When the sample is semi-dehydrated for multi-bilayer deposition, the fraction of pep-1 not inserted in the membranes precipitates in the aggregated form and contributes in this form to the ATR-FTIR spectrum. Comparison of spectra in Figure 2 shows that the signal at 1621 cm^{-1} (intermolecular β-structure component) decreases in the order H_2O = DPPC > POPC:Chol > POPC. The percentage of peptide precipitated decreases when the membrane becomes more fluid (membrane fluidity follows the order: DPPC < POPC:Chol < POPC) which is related to the ability of the peptide to insert in the membrane [8]. Therefore, the relative percentage for the contribution of the different secondary structures is affected by the contribution of aggregates in solution. To evaluate if there is alteration in the α-helix content of the fraction of peptides inserted in the lipidic matrix it is a better approach to compare the contribution of α-helix components in relation to random coil component. For instance in the absence of lipid α-helix/random coil contribution = 3.8%/32.7% = 0.12. When DPPC is present, 7.7%/35.4% = 0.22, and for POPC = 14.6%/44.2% = 0.33 (see Table I). These results show that in the presence of lipidic bilayers there is an increase in α-helix contribution relative to random coil, and this contribution is enhanced by membrane fluidity (see Figure 2 and Table I).

CD and ATR-FTIR measurements were carried out with different peptide and lipidic concentrations but the peptide/lipid ratios were nearly the same (0.069 and 0.054, respectively). With CD measurements it was possible to identify the presence of random coil and α-helix contributions; this facilitated the band assignment in amide I ATR-FTIR spectra. A fraction of peptide, either in the absence or in the presence of vesicles, is aggregated when the peptide/lipid suspensions is spread over the Ge Plate (identified by the presence of intermolecular β-sheet). An α-helix conformation of the other fractions is favoured when the pep-1 is inserted in the membrane (see Figure 1, Figure 2 and Table I). Considering the primary structure of pep-1, the hydrophobic domain has a bigger tendency to acquire an amphipathic α-helix conformation, in agreement with NMR results proposed by others [10,12], while the hydrophilic domain is expected to be in the random coil conformation. The presence of Pro residue in the spacer domain, between hydrophilic and hydrophobic domains, is responsible for the separation of α-helix and random coil conformations, inducing the flexibility necessary for the integrity of these two domains.

Table I. Pep-1 secondary structure evaluated by ATR-FTIR spectroscopy in the absence/presence of different lipidic multibilayers at 20°C and pH7.4*.

Frequencies (cm^{-1})	Assignment	POPC	POPC:Chol (2:1)	DPPC	Aqueous solution
1690	↑↓ β-Sheet	2.8±0.1	1.9±0.0	1.3±0.3	1.3±0.5
1674	Turn and ↑↓ β-Sheet	31.2±1.1	28.8±1.7	34.5±2.6	39.5±2.1
1657	α-helix	14.6±0.6	11.2±0.4	7.7±1.5	3.8±1.1
1640	Random coil	44.2±0.1	47.2±2.3	35.4±1.2	32.7±1.4
1621	Intermolecular β-Sheet	7.2±0.4	10.9±0.1	21.1±2.1	22.7±0.8

*Samples were spread on Ge plate from solutions with 138 μM pep-1 and ~2.6 mM lipid (8 μg of pep-1 and 40 μg lipid); spectra were recorded after 1 h of deuteration. Five bands were used to fit amide I spectra as follows: (i) 1705–1685 cm^{-1}, (ii) 1680–1669 cm^{-1}, (iii) 1660–1648 cm^{-1}, (iv) 1648–1640 cm^{-1}, and (v) 1630–1620 cm^{-1}. The frequency (cm^{-1}) of Amide I components and the respective percentage for each condition are presented in the form.

Orientation of the pep-1 when partitioned in lipidic membranes

Polarized ATR-FTIR is a powerful technique to obtain information about peptide orientation in a lipid bilayer [18]. Calculation of the α-helix mean tilt angle, with membrane normal, was performed. This required the evaluation of R_{α}^{ATR} (see Material and methods section). Barrel-stave-like pore formation, such as the one proposed for antimicrobial peptides [36] and pep-1 [12], demand the α-helix domain of peptide to span across lipid membrane with an amphipathic helix and acquire an orientation parallel to the membrane normal (0°) [36]. In POPC vesicles and POPC:Chol (2:1 molar) the mean tilt angle of helix contribution with respect to the normal to the membrane is 46.5° and 44.5°, respectively. These values are close to the average value expected for a randomly oriented structure (54.7°) [37]. So, peptide populations with no preferred orientation cannot be discarded. A perpendicular orientation relative to the bilayer surface for peptide hydrophobic domain was not expected from the previous quenching experiments [8]. These findings are not consistent with a barrel-stave-like organization.

In DPPC an angle closer to membrane normal (20°) was found for the α-helix domain. This result supports the idea that peptide is constricted to gel line defects in these rigid membranes [8].

Membrane disruption caused by pep-1

When planar bilayers, PLMs, are used it is possible to have access to both sides of the membrane and the ion flux can be determined by electrical measurements. The electrical capacity of bilayers prepared by the Montal and Mueller method matches that of biological membranes [25].

DPhPC, which form stable and neutral bilayers at room temperature, was used. Pep-1 was added to the *cis* chamber and the ionic current was recorded for increasing potential differences alternating from negative to positive potential (from 0 to $\pm$100mV). Different peptide concentrations were added (0–3 μM). For low peptide concentration (0.5 μM) there was no effect; increasing peptide concentration ($\sim$2 μM), ion current fluctuations were detected in the presence of transmembrane potential (Figure 3A). The current-voltage relationship (Figure 3B) shows that these current fluctuations are amplified with the transmembrane potential; however, the shape of fluctuations is completely disordered. When the transmembrane potential was increased to values higher than $\pm$100 mV, or the peptide concentration was increased ($\sim$3 μM), the membrane was destroyed.

In the presence of a transmembrane potential, an increase in peptide concentration in the membrane due to electrostatic attraction is expected. Therefore, the membrane becomes more loosely packed, which results in transient membrane permeability instabilities in the presence of the electric field (Figure 3B). In the presence of a barrel-stave pore a single-channel conductance was expected, which is characterized by reproducible multiple discrete conducting states [36]. A barrel-stave model cannot account for the results performed with DPhPC PLMs because the conductance induced by the pep-1 is continuously variable rather than discrete [36] (Figure 3A).

The charge effect in the membrane was tested in DPhPC bilayers with 10% or 20% of POPG and also with asymmetrical membranes. These membranes were less stable. By the addition of peptide to bilayers an intermediary step with current fluctuations did not occur. The membrane became leaky at low pep-1 concentration ($\sim$1 μM) (data not shown). This is probably due to high electrostatic attraction of pep-1 to negatively-charged membranes [8].

The hypothesis of pore formation whether barrel-stave-like or not was further tested by fluorescence microscopy with GUVs loaded with three fluorescent dyes differing in their molecular sizes (Alexa Fluor^{633} C5-maleimide (Mr $\sim$1300), Alexa Fluor^{488}-Dextran (Mr $\sim$3000) and Alexa Fluor^{546} -Dextran (Mr $\sim$10000)). This experimental setup enables direct observation of any change in the membrane permeability during time course observations [15,30]. Moreover, in the case of pore formation it is also possible to have information on pore size due to sequential escape of the dyes from the GUVs. The membrane integrity was evaluated with $DiIC_{18}$ to probe the membrane bilayer structure [30]; this dye was incorporated in GUVs loaded with Alexa Fluor^{633} C5-maleimide (Mr $\sim$1300)

GUVs prepared with POPC or POPC:POPG (4:1 molar) with a final lipid concentration of $\sim$0.7 μM were studied in the presence of different peptide concentrations. POPC:POPG vesicles in the presence of peptide concentrations bellow $\sim$0.7 μM did not undergo noticeable effect in the membrane shape, permeability or integrity; none of the probes escape from the GUVs, during the time window of the experiment ($\sim$30 min). With higher peptide concentration ($>$0.7 μM) GUVs were completely destroyed with the simultaneous leakage of the three dyes (Figure 4), which resulted in deformed lipid aggregates (see also Movies 1 and 2 in the Supplementary material Online).

Figure 5 confirms membrane destruction caused by pep-1 in these conditions, where the leakage of

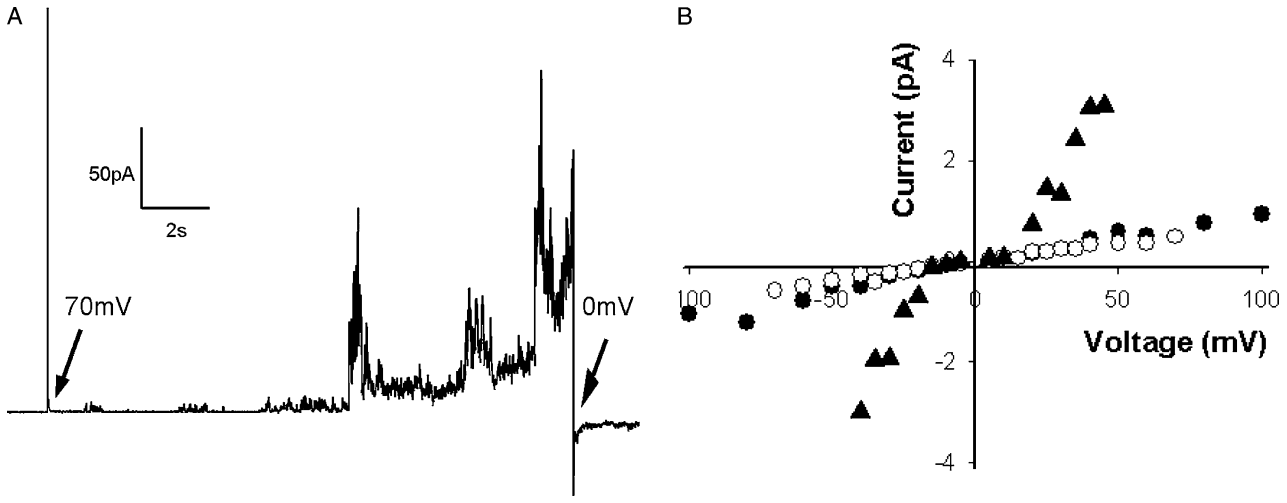

Figure 3. Electrical measurements in the DPhPC planar bilayers prepared in buffer with 10 mM HEPES (pH 7.4) and 150 mM NaCl. Pep-1 was added to the *cis* compartment. (A) Current fluctuations in the presence of 2 μM pep-1 at the membrane voltage was clamped at +70 mV. (B) Current-voltage relationship in the absence (filled circle) or in the presence of 0.86 μM pep-1 (open circle) or 2.58 μM pep-1 (filled triangle). Current signals were averaged over 10 s.

Alexa Fluor^{633} C5-maleimide (Mr ~1300) and the membrane disintegration (followed with $DiIC_{18}$) occurred concomitantly. These results prove that the peptide does not induce pore formation. Instead, it induces disintegration of the vesicles with a detergent-like mechanism (see Movies 1 and 2 in the Supplementary material Online). It is worth stressing that the approximate lipid concentration in GUVs solution is ~0.7 μM which is approximately the peptide concentration required for the membrane disruption. With lower peptide concentrations there was no effect on the membrane permeability.

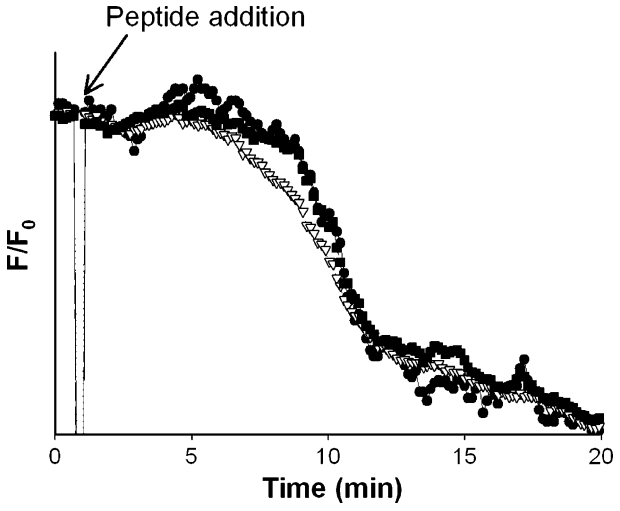

Figure 4. Pep-1 (0.9 μM) interaction with POPC:POPG (4:1) GUVs (0.7 μM) by confocal microscopy. Time course of the normalized fluorescence intensity, of the three internalized vesicles: Alexa Fluor^{546}- Dextran (Mr ~10000) (open triangle), Alexa Fluor^{488}-Dextran (Mr ~3000) (filled circle) and Alexa Fluor^{633} C5-maleimide (Mr ~1300) (filled square). Fluorescence intensity was determined in each micrograph using the standard Zeiss LSM 510 META software package (with the inclusion of the multiple time series software option) to quantify the average fluorescence intensity over time. Background was corrected and fluorescence intensities were normalized to zero time.

Similar results were obtained with POPC vesicles, but a higher peptide concentration was required for vesicle destruction, about 2–4 μM. This is expected because pep-1 has higher affinity for negatively-charged vesicles [8].

The lag time between peptide addition and vesicles destruction is dependent not only on peptide affinity for membranes but also on the peptide concentration and its diffusion in the chamber (continuous stirring was not possible in these conditions) [15].

Taken together, the results obtained in GUVs and in PLMs suggest that pep-1 at low peptide/lipid (P/L) ratios does not cause significant alterations in membrane properties and does not induced serious perturbations in permeability. For high bulk P/L ratio the membrane is disrupted with a detergent-like mechanism. The P/L ratio required to cause this effect is dependent on the membrane composition, which governs the local peptide concentration in the membrane.

'Carpet'-model disintegration vs. barrel-stave pore formation

Aurein and Citropin, antibiotic peptides, disrupt membranes in a similar way to pep-1 and a 'carpet' model mechanism was proposed [15]. In this model, electrostatic interactions drive the peptide binding onto the surface of the membrane and cover it in a 'carpet'-like manner. Membrane permeation only occurs above a certain critical local peptide concentration, resulting in disintegration of the membrane.

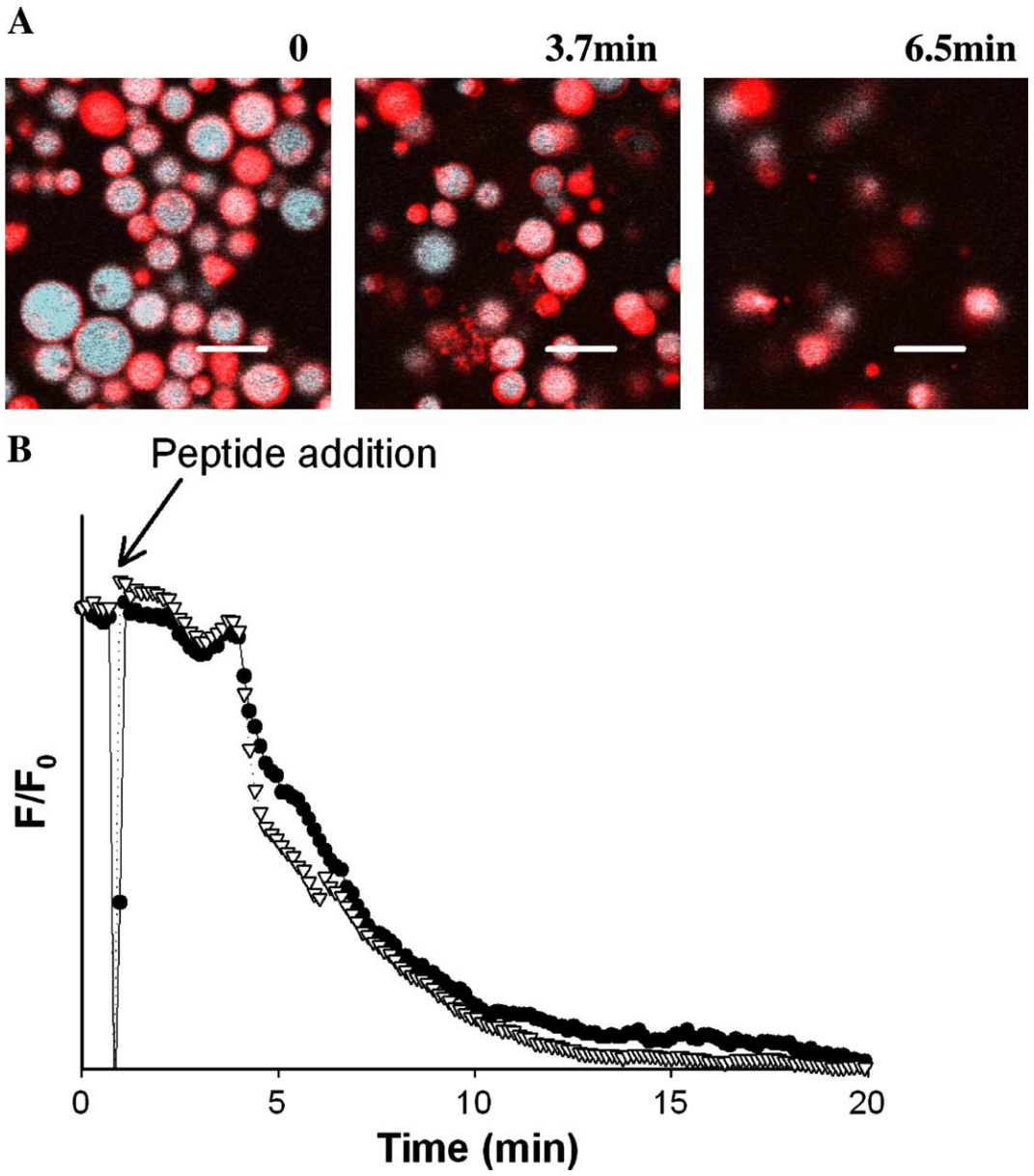

Figure 5. Direct visualization of membrane integrity, of POPC:POPG (4:1 molar) GUVs (0.7 μM) in the presence of pep-1 (0.9 μM), by confocal microscopy. (A) GUVs before and after peptide addition (3.7 and 6.5 min). Pictures show the merge fluorescence of the DiIC18 and Alexa Fluor^{633} C5-maleimide (Mr ~1300) (red and blue, respectively in online version). Scale bar, 15 μm. (B) Time course of the normalized fluorescence intensity of the two dyes during the experiment: $DiIC_{18}$ (open triangle), and Alexa Fluor^{633} C5-maleimide (Mr ~ 1300) (filled circle). Fluorescence intensity was determined as stated in Figure 4. Part A of this Figure is reproduced in colour in *Molecular Membrane Biology* online.

A previous step before the collapse of the membrane packing may include the formation of transient holes in the bilayer [38]. The formation of such holes enables the passage of low molecular weight molecules prior to complete lyses [38]. These small transient holes explain the ion current fluctuations detected in DPhPC PLMs and also the results obtained by Deshayes et al. [12]. Nevertheless, such holes do not make the membrane permeable for molecules with a molecular weight $\geq$ 1300 Da (See Figures 4 and 5 and also Movies 1 and 2 in the Supplementary material online), so this mechanism cannot explain the translocation of proteins as big as β-Galactosidase (116 KDa), which, as verified previously, can be translocated by pep-1 in HeLa cells [6,9].

The adequacy of a 'carpet' model-like mechanism to explain membrane disruption and absence of the pore formation (barrel-stave or other) are further supported by the fact that the hydrophobic domain length in α-helix conformation mismatches the membrane depth. Considering 1.5 Å per residue

for an ideal α-helical structure [15], 19.5 Å length is expected for the peptide domain inserted in the membrane while 40 Å is the thickness for fluid lipid bilayers [39]. In barrel-stave pore the peptide interaction with the target membrane is driven predominantly by hydrophobic interactions and the peptides should bind to phospholipid membranes irrespective of their charge [38], with a transmembrane domain that spans across the membrane [36]. These events are favoured in the absence of Trp residues in the peptide [40]. Pep-1 however does not fulfil any of such requirements for pore formation.

Membrane destruction is an extreme event that only occurs at very high pep-1 concentration. Therefore 'carpet'-like mechanism may explain the cytotoxicity of pep-1, but does not explain its translocating activity at lower concentrations [5,6,10].

Conclusions

Pep-1 translocates and transports proteins across membranes even with relatively low peptide concentrations [5,6,10]. With concentrations required for peptide translocation pep-1 shows a high affinity for membranes [8] and is able to induce membrane destabilization [7] without evidence of pore formation [7,10]. Translocation occurs both *in vitro* [7] and *in vivo* [6] by a mechanism mediated by the transmembrane potential. Such a mechanism is governed by electrostatic interaction between the peptide and the membrane and the peptide ability to destabilize membranes seems to play an important role.

For high peptide concentration more pronounced membrane damage occurs, which induces toxicity in cells [5,10]. Membrane disintegration occurs for high P/L ratios and is dependent on the peptide affinity for membranes. A 'carpet'-model mechanism is suggested by all sets of data but only in extreme conditions, far from typical physiological conditions.

It should be stressed that in the presence of a transmembrane potential, translocation occurs and peptide accumulation in the membrane is not favoured, i.e., the membrane saturation/disintegration point is only reached at very high peptide concentration, which explains the low cytotoxicity of pep-1.

In spite of the α-helix contribution increase when pep-1 inserts in the membrane, there was no direct evidence for a transmembrane pore. Pep-1 first interaction with membrane is driven by electrostatic interaction [9] followed by membrane carpeting, which occurs with lateral rearrangement of the acidic lipids [7]. Similar phenomena were observed with other peptides and a 'membrane-thinning' effect was proposed [41]. In this model, the peptide aggregates on the surface and the reduced local surface tension allow the peptide to intercalate the membrane. Flexible sealing between peptide side-groups and lipid head-groups minimize leakage during the CPP passage through the membrane [1].

Supplementary material available online

(1) Pep-1 deuteration in the presence of lipidic bilayers monitorized by ATR-FTIR; (2) Pep-1 dichroic spectrum obtained by ATR-FTIR spectroscopy; (3) Evaluation of existence of pep-1 β-sheet aggregates by Thioflavin T fluorescence, and (4) Movies showing the interaction of the pep-1 with GUVs.

Acknowledgements

Fundação para a Ciência e Tecnologia (Portugal) is acknowledged for the grant SFRH/BD/14337/2003 to S. T. Henriques. FEBS is acknowledged for financial support to S. T. Henriques for a short-term visit to Dr Luis Bagatolli laboratory at MEMPHYS/BMB, Syddansk University, Odense, Denmark. Research in the laboratory of Dr Luis Bagatolli is funded by a grant from SNF, Denmark (21-03-0569) and the Danish National Research Foundation (which supports MEMPHYS-Centre for Biomembrane Physics). F. Homblé is a Research Director from the National Fund for Scientific Research, Belgium.

References

[1] Magzoub M, Graslund A. 2004. Cell-penetrating peptides: from inception to application. Q Rev Biophys 37:147–195.
[2] Thoren PE, Persson D, Isakson P, Goksor M, Onfelt A, Norden B. 2003. Uptake of analogs of penetratin, Tat(48-60) and oligoarginine in live cells. Biochem Biophys Res Commun 307:100–107.
[3] Richard JP, Melikov K, Vives E, Ramos C, Verbeure B, Gait MJ, Chernomordik LV, Lebleu B. 2003. Cell-penetrating peptides. A reevaluation of the mechanism of cellular uptake. J Biol Chem 278:585–590.
[4] Drin G, Cottin S, Blanc E, Rees AR, Temsamani J. 2003. Studies on the internalization mechanism of cationic cell-penetrating peptides. J Biol Chem 278:31192–31201.
[5] Morris MC, Depollier J, Mery J, Heitz F, Divita G. 2001. A peptide carrier for the delivery of biologically active proteins into mammalian cells. Nat Biotechnol 19:1173–1176.
[6] Henriques ST, Costa J, Castanho MA. 2005. Translocation of beta-galactosidase mediated by the cell-penetrating peptide pep-1 into lipid vesicles and human HeLa cells is driven by membrane electrostatic potential. Biochemistry 44:10189–10198.
[7] Henriques ST, Castanho MA. 2004. Consequences of nonlytic membrane perturbation to the translocation of the cell penetrating peptide pep-1 in lipidic vesicles. Biochemistry 43:9716–9724.

[8] Henriques ST, Castanho MA. 2005. Environmental factors that enhance the action of the cell penetrating peptide pep-1 A spectroscopic study using lipidic vesicles. Biochim Biophys Acta 1669:75–86.

[9] Henriques ST, Costa J, Castanho MA. 2005. Re-evaluating the role of strongly charged sequences in amphipathic cell-penetrating peptides: a fluorescence study using Pep-1. FEBS Lett 579:4498–4502.

[10] Weller K, Lauber S, Lerch M, Renaud A, Merkle HP, Zerbe O. 2005. Biophysical and biological studies of end-group-modified derivatives of Pep-1. Biochemistry 44: 15799–15811.

[11] Fischer R, Fotin-Mleczek M, Hufnagel H, Brock R. 2005. Break on through to the other side –biophysics and cell biology shed light on cell-penetrating peptides. Chembiochem 6:2126–2142.

[12] Deshayes S, Heitz A, Morris MC, Charnet P, Divita G, Heitz F. 2004. Insight into the mechanism of internalization of the cell-penetrating carrier peptide Pep-1 through conformational analysis. Biochemistry 43:1449–1457.

[13] Vigano C, Manciu L, Buyse F, Goormaghtigh E, Ruysschaert JM. 2000. Attenuated total reflection IR spectroscopy as a tool to investigate the structure, orientation and tertiary structure changes in peptides and membrane proteins. Biopolymers 55:373–380.

[14] Zhang S, Udho E, Wu Z, Collier RJ, Finkelstein A. 2004. Protein translocation through anthrax toxin channels formed in planar lipid bilayers. Biophys J 87:3842–3849.

[15] Ambroggio EE, Separovic F, Bowie JH, Fidelio GD, Bagatolli LA. 2005. Direct visualization of membrane leakage induced by the antibiotic peptides: maculatin, citropin, and aurein. Biophys J 89:1874–1881.

[16] Mayer LD, Hope MJ, Cullis PR. 1986. Vesicles of variable sizes produced by a rapid extrusion procedure. Biochim Biophys Acta 858:161–168.

[17] Yang JT, Wu CS, Martinez HM. 1986. Calculation of protein conformation from circular dichroism. Methods Enzymol 130:208–269.

[18] Goormaghtigh E, Raussens V, Ruysschaert JM. 1999. Attenuated total reflection infrared spectroscopy of proteins and lipids in biological membranes. Biochim Biophys Acta 1422:105–185.

[19] Torrecillas A, Martinez-Senac MM, Goormaghtigh E, de Godos A, Corbalan-Garcia S, Gomez-Fernandez JC. 2005. Modulation of the membrane orientation and secondary structure of the C-terminal domains of Bak and Bcl-2 by lipids. Biochemistry 44:10796–10809.

[20] Goormaghtigh E, Cabiaux V, Ruysschaert JM. 1994. Determination of soluble and membrane protein structure by Fourier transform infrared spectroscopy. I. Assignments and model compounds. Subcell Biochem 23:329–362.

[21] Arrondo JL, Goni FM. 1999. Structure and dynamics of membrane proteins as studied by infrared spectroscopy. Prog Biophys Mol Biol 72:367–405.

[22] Barth A, Zscherp C. 2002. What vibrations tell us about proteins. Q Rev Biophys 35:369–430.

[23] Tatulian SA. 2003. Attenuated total reflection Fourier transform infrared spectroscopy: a method of choice for studying membrane proteins and lipids. Biochemistry 42:11898–11907.

[24] Bechinger B, Ruysschaert JM, Goormaghtigh E. 1999. Membrane helix orientation from linear dichroism of infrared attenuated total reflection spectra. Biophys J 76: 552–563.

[25] Montal M, Mueller P. 1972. Formation of bimolecular membranes from lipid monolayers and a study of their electrical properties. Proc Natl Acad Sci USA 69: 3561–3566.

[26] Fuks B, Homble F. 1994. Permeability and electrical properties of planar lipid membranes from thylakoid lipids. Biophys J 66:1404–1414.

[27] Redwood WR, Pfeiffer FR, Weisbach JA, Thompson TE. 1971. Physical properties of bilayer membranes formed from a synthetic saturated phospholipid in n-decane. Biochim Biophys Acta 233:1–6.

[28] Lindsey H, Petersen NO, Chan SI. 1979. Physicochemical characterization of 1,2-diphytanoyl-sn-glycero-3-phosphocholine in model membrane systems. Biochim Biophys Acta 555:147–167.

[29] Hung WC, Chen FY, Huang HW. 2000. Order-disorder transition in bilayers of diphytanoyl phosphatidylcholine. Biochim Biophys Acta 1467:198–206.

[30] Ambroggio EE, Kim DH, Separovic F, Barrow CJ, Barnham KJ, Bagatolli LA, Fidelio GD. 2005. Surface behavior and lipid interaction of Alzheimer beta-amyloid peptide 1-42: a membrane-disrupting peptide. Biophys J 88:2706–2713.

[31] Thoren PE, Persson D, Lincoln P, Norden B. 2005. Membrane destabilizing properties of cell-penetrating peptides. Biophys Chem 114:169–179.

[32] Sreerama N, Venyaminov SY, Woody RW. 1999. Estimation of the number of alpha-helical and beta-strand segments in proteins using circular dichroism spectroscopy. Protein Sci 8:370–380.

[33] Woody RW. 1995. Circular dichroism. Methods Enzymol 246:34–71.

[34] Oberg KA, Ruysschaert JM, Goormaghtigh E. 2004. The optimization of protein secondary structure determination with infrared and circular dichroism spectra. Eur J Biochem 271:2937–2948.

[35] Wieprecht T, Beyermann M, Seelig J. 2002. Thermodynamics of the coil-alpha-helix transition of amphipathic peptides in a membrane environment: the role of vesicle curvature. Biophys Chem 96:191–201.

[36] Yang L, Harroun TA, Weiss TM, Ding L, Huang HW. 2001. Barrel-stave model or toroidal model? A case study on melittin pores. Biophys J 81:1475–1485.

[37] Thulstrup EW, Michl J. 1989. Elementary polarization spectroscopy. New York: VCH Publishers; 52 pp.

[38] Shai Y. 1999. Mechanism of the binding, insertion and destabilization of phospholipid bilayer membranes by alpha-helical antimicrobial and cell non-selective membrane-lytic peptides. Biochim Biophys Acta 1462:55–70.

[39] Wiener MC, White SH. 1992. Structure of a fluid dioleoylphosphatidylcholine bilayer determined by joint refinement of x-ray and neutron diffraction data. III. Complete structure. Biophys J 61:434–447.

[40] Herbig ME, Weller K, Krauss U, Beck-Sickinger AG, Merkle HP, Zerbe O. 2005. Membrane surface-associated helices promote lipid interactions and cellular uptake of human calcitonin-derived cell penetrating peptides. Biophys J 89:4056–4066.

[41] Ludtke S, He K, Huang H. 1995. Membrane thinning caused by magainin 2. Biochemistry 34:16764–16769.

Online supplementary material

(1) Pep-1 deuteration in the presence of lipidic bilayers monitorized by ATR-FTIR

The $^{1}H/^{2}H$ exchange kinetics was studied to establish an appropriate duration for peptide deuteration to evaluate secondary structure by ATR-FTIR spectroscopy. The kinetics of pep-1 deuteration in the presence of POPC bilayers is fast (Figure S.1). There are no significant differences in amide I band after 1 min of deuteration. A decrease in the area of the amide II band (1590–1505 cm^{-1}) is also noticed. The shape change in amide I and the area decrease in amide II bands suggest that the pep-1 is easily accessible to the solvent [1]. A fast kinetics of pep-1 deuteration was observed for all the lipidic systems tested (POPC, POPC:Chol (2:1) and DPPC).

(2) Pep-1 dichroic spectrum obtained by ATR-FTIR spectroscopy

The dichroic spectrum is the difference between the spectra recorded with parallel and perpendicular polarizations; the perpendicular spectrum was multiplied by the dichroic ratio of the lipid ν (C=O) determined at 1738cm^{-1} (R^{iso}) to take into account the difference in the relative power of the evanescent fields (see [2] for further information). The dichroic spectrum provides information on the peptide orientation relative to the normal of membrane plane [2].

The dichroic spectrum, //-$R^{iso}\perp$, for pep-1 in the presence of different lipids shows a positive dichroism signal, for amide I region, indicating that the peptide has a preferential orientation in the lipid membrane (see Figure S.2). This band, however, is relatively broad (FWHH > 50cm^{-1}) with a maximum at 1674cm^{-1} and a shoulder at 1650cm^{-1}.

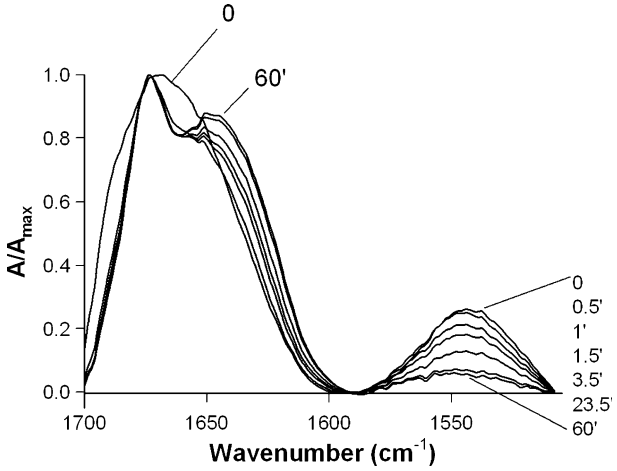

Figure S.1. $^{1}H/^{2}H$ exchange kinetic of pep-1 in the presence of POPC bilayers (20% w/w). Spectra of 8 μg of pep-1 in the presence of 40μg of POPC were recorded as a function of the deuteration time (from 0 to 60 min of deuteration). All the spectra were normalized.

(3) Evaluation of existence of pep-1 β-sheet aggregates by Thioflavin T fluorescence

ThT dye was used to evaluate if pep-1 forms β-sheet aggregates in aqueous solution. In the absence of β-sheet aggregates the dye has an excitation and emission maxima at 350 and 438nm, respectively. In the presence of amyloid fibrils the ThT excitation spectrum shifts with a new peak at 450nm and emission at 482nm [3]. Titration of 15μM ThT with a pep-1 stock solution (688 μM) was followed by fluorescence intensity at $\lambda_{emission}$ = 490nm with $\lambda_{excitation}$ = 450nm.

(4) Movies showing the interaction of the pep-1 with GUVs

Movie 1. Leakage of the probes entrapped in GUVs. 0.9μM pep-1 was added to the vesicles composed by POPC:POPG (4:1 molar) with a lipid concentration ~ 0.7μM. Fluorescence merge of the three dyes (Alexa $Fluor^{546}$- Dextran (Mr ~ 10000) (red), Alexa $Fluor^{488}$-Dextran (Mr ~ 3000) (green) and Alexa $Fluor^{633}$ C5-maleimide (Mr ~ 1300) (blue)) is presented. The three dyes escape from the vesicles at the same time. In the film the velocity was increased 40 times.

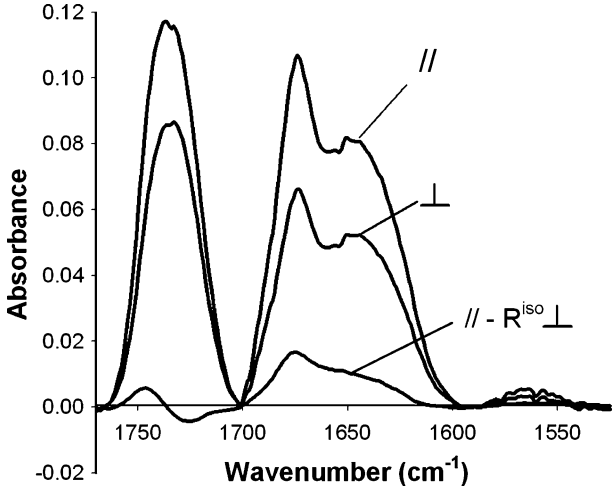

Figure S.2. ATR-FTIR spectra of pep-1 (20% w/w) partitioned in POPC bilayers obtained using parallel or perpendicular polarization. The dichroic spectrum was obtained by the difference between the spectra recorded with parallel and perpendicular polarizations; the perpendicular spectrum was multiplied by R^{iso}. All the spectra are in the same scale, but dichroic spectrum intensity has been multiplied by 2.

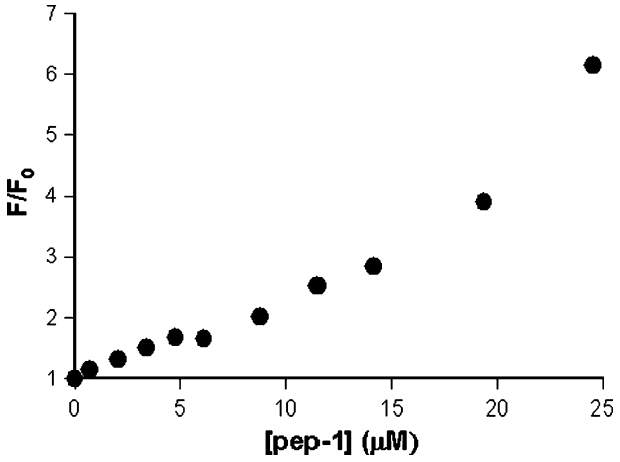

Figure S.3. Peptide concentration effect in the ThT (15μM) fluorescence emission intensity, with excitation at 450nm and emission at 490nm. Experiments were carried out in 10mM HEPES buffer, pH 7.4, with 150mM NaCl.

Movie 2. Leakage of $DiIC_{18}$-labelled GUVs filled with Alexa Fluor^{633} C5-maleimide (Mr ~1300). 0.9μM pep-1 was added to the vesicles composed by POPC:POPG (4:1 molar) with a lipid concentration ~ 0.7μM. Fluorescence merge of the $DiIC_{18}$ (red) and Alexa Fluor^{633} (blue) is presented. Membrane disruption and Maleimide escape occurred at once, which demonstrates that membrane is disrupted in these conditions. In the film the velocity was increased 30 times.

Supplementary material references:

[1] Manciu L, Chang XB, Buyse F, Hou YX, Gustot A, Riordan JR, Ruysschaert JM. 2003. Intermediate structural states involved in MRP1-mediated drug transport. Role of glutathione. J Biol Chem 278:3347–3356.

[2] Bechinger B, Ruysschaert JM, Goormaghtigh E. 1999. Membrane helix orientation from linear dichroism of infrared attenuated total reflection spectra. Biophys J 76:552–563.

[3] LeVine H 3rd. 1993. Thioflavine T interaction with synthetic Alzheimer's disease beta-amyloid peptides: detection of amyloid aggregation in solution. Protein Sci 2: 404–410.

Chapter 4

Pep-1 and mammalian cells

Chapter 4.

Pep-1 and mammalian cells

4.1. Introduction

It is accepted that Tat peptide and penetratin are internalized by an endosomal-dependent mechanism; however there is no consensus in the specific endocytic pathway used for the import of these peptides [62, 68, 70]. A description of these endocytic pathways, how can they be used, what is the physiological significance of these routes and how can be used for the uptake of extracellular material is presented next.

4.1.1. Endocytic routes for cell entry

Endocytosis is a hallmark of all eukaryotic cells and is responsible for the uptake of membrane proteins and lipids, extracellular ligands and soluble molecules from the cell surface [211]. It modulates the delivery of essential metabolites to cells (e.g. nutrients uptake) and also the responses to many protein hormones and growth factors. Proteins targeted for destruction are taken up by endosomes and delivered to lysosomes for digestion [212]. In addition, endocytosis is also involved in synaptic vesicle

recycling and regulation of cell-surface expression of signalling receptors, remodelling of the plasma membrane and the generation of cell polarity [211]. To meet these different functions endocytic pathways have different regulation processes, specificity for different cargoes and destination within cells [211]. Endocytosis can be divided into two broad categories: phagocytosis, responsible for the uptake of large particles, and pinocytosis for the uptake of fluid and solutes [213-215] (see Figure 4.1).

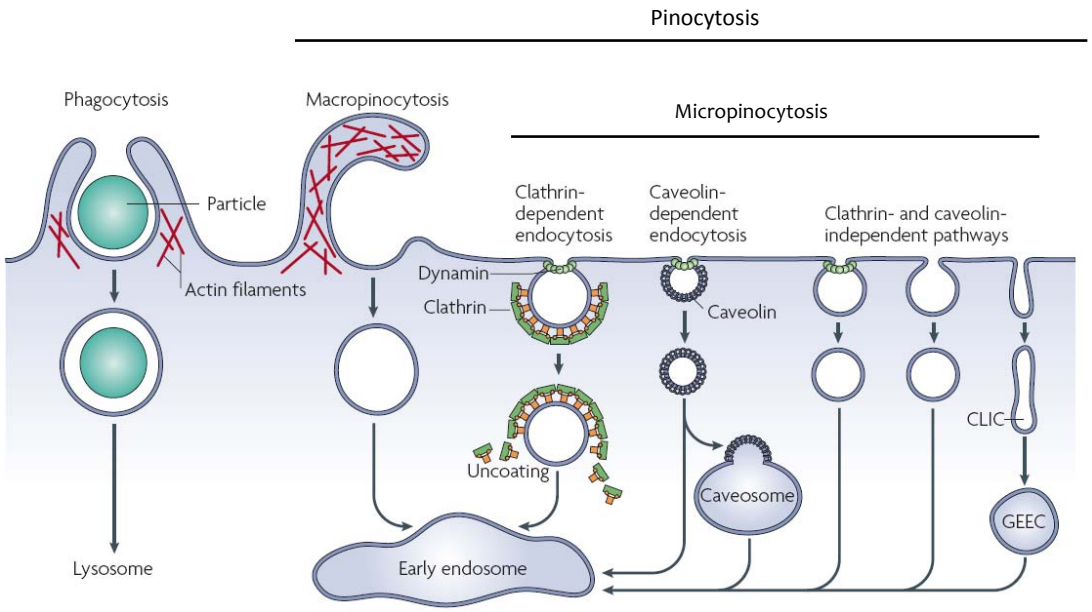

Figure 4.1. Different endocytosis routes for cell entry. Endocytic pathways can be classified according to the size of the endocytic vesicle, the nature of the cargo and the mechanism of vesicle formation. Large particles can be engulfed by phagocytosis, while solutes are internalized by pinocytosis. Phagosomes are responsible for internalization and afterwards degradation in lysosomal compartment. In macropinocitosis, large uncoated vesicles are formed, while in clathrin- and caveolin- mediated uptake vesicles are coated and present a smaller and uniform size. Clathrin- and caveolin- independent pathways are uncoated but present a small size when compared with macropinosomes or phagosomes. These vesicles are here designated as clathrin and dynamin-independent carriers (CLIC) and are derived from the plasma membrane. Virtually all the pinocytosis routes reach early endosomes but may first traffic to intermediate compartments such as the caveosome or glycosyl phosphatidylinositol-anchored protein enriched early endosomal compartment (GEEC). The fate of cargos macromolecules internalized by these different endocytic pathways is dependent on the cargo nature and possible target signal. By default, macromolecules without signal sequence end in lysosomal compartment where enzymatic degradation takes place. Image adapted from reference [216].

Phagocytosis is conducted primarily by specialized cells like neutrophils, macrophages and dendritic cells, that function to clear pathogens such as bacteria or

yeast and other particles such as remnants of dead cells or fat particles [214] higher than > 0.5μm in diameter [213]. It is an active and highly regulated process that involves interaction with specific cell-surface receptors, that trigger the formation of phagocytic compartments and subsequent internalization of the particles [213]. There are multiple modes of phagocytosis, which are determined by the particle to be ingested and the receptor that recognizes that particle; however in all the phagosomes actin drives its formation [214].

Pinocytosis, also known as fluid-phase uptake, can be followed by the intracellular accumulation of tracer molecules (e.g. enzymes, proteins, or labelled compounds known to be internalized by a specific pinocytosis route) present in the medium. Endocytosis can be initiated with non-specific binding of solutes to the cell membrane or captured by specific high-affinity receptors. Such receptors are concentrated into specialized endocytic transport vesicles where the molecule and its receptor determine the pathway through which the solute enters into the cell [214]. Fluid-phase uptake can be divided into macropinocytosis and micropinocytosis [213].

Macropinocytosis is related to phagocytosis but is less specific [215, 217]. They are alike in morphology but differ in the biochemical mechanisms employed in their regulation [213]. Typically, macropinocytosis is triggered by growth factor stimulation or downstream-activated signalling molecules [217] and refers to the formation of large irregular primary endocytic vesicles by the closure of lamellipodia at ruffling membrane domains [213, 217], which can be transiently induced in most cells [214]. Macropinosomes are uncoated dynamic structures and can reach several μm in diameter [217]. Macropinocytosis fulfils diverse functions such as endocytic removal of large membrane domains, alter the adhesive and communicative properties of the cell and it is involved in cell contraction and migration [217]. The formation of large macropinosomes is also driven by actin as occurs for phagosomes [214].

Micropinocytosis refers to endocytic processes and differs mechanistically from the previous ones. It involves more selective plasma-membrane domains [214] that originate small pinocytic vesicles that appear somewhat uniformly over the cell surface [218]. Micropinocytosis can be divided in three mechanistically distinct pathways of uptake: clathrin-mediated endocytosis; caveolin-mediated endocytosis and clathrin- and

caveolin- independent endocytosis, which probably encompasses more than one pathway [214].

Clathrin-mediated endocytosis occurs in all mammalian cells and is responsible for the continuous uptake of essential nutrients. It is also involved in cell and serum homeostasis and is required for efficient recycling of synaptic vesicle membrane proteins after neurotransmission [214]. Clathrin-mediated endocytosis is involved in concentrating of transmembrane receptors together with their bound ligands into "coated pits" [214]. This receptor-mediated endocytosis starts with the invagination of a coated pit that is encapsulated by clathrin-induced excision from the plasma membrane to form a "coated vesicle", which rapidly loses it clathrin coat and fuses with an endosome [212].

Caveolae-mediated endocytosis is a dynamin-dependent endocytic route. Caveolae are 50-80nm flask-shaped, plasma-membrane invaginations enriched in caveolins, sphingolipids and cholesterol that are present in many cells [216]. Different signalling molecules and membrane transporters are concentrated in these caveolae domains pointing to a role in the regulation of specific signalling cascades [214]. Caveolar cargoes are diverse, including lipids, proteins, lipid-anchored proteins and pathogen [216]. A cargo molecule can be internalized by different mechanisms under different conditions, the molecular basis for the correlation between caveolae-localized receptors and triggered endocytosis remains to be elucidated [214, 216].

The mechanisms responsible for caveolae- and clathrin- independent endocytosis seem to be dependent on rafts, which can presumably be captured by, and internalized within any endocytic vesicles. The unique lipid composition of these domains, where specific glycolipids and membrane proteins are associated, may be responsible for their specific sort [214]. In contrast to clathrin-dependent endocytosis, in which a ligand-receptor binding is required, no such well defined finding for clathrin-independent endocytosis has been identified. A possible mechanism is the association of cargo with plasma membrane domains. However association of the cargo with such domains does not assume subsequent internalization by endocytosis [216]. The potential mechanisms for the selection o cargo for endocytosis can be divide into lipid- and protein-based mechanisms and were reviewed in reference [216]. An example is cholera toxin B (CTxB) which seems to be internalized by a non-clathrin, non-caveolar

mechanism. CTxB is observed in parts of the membrane where its receptor, the monosialoganglioside GM1, is located [216]

Overall, it seems that endocytosis is regulated by the cargo nature and its hypothetical receptor, thus cargo molecules internalized by endocytosis are not passive passengers [214]. A variety of destinations can be followed after entry into the endocytic route. The fate of internalized solutes is also dependent on the cargo molecules. Virtually all routes of pinocytosis merge at early endosomes (see Figure 3.1); cargo molecules are then organized to be delivered to different intracellular targets or to be recycled back to the plasma membrane (e.g. some endocytic receptors such as LDL receptors) [216]. Lysosome is the default destination of any material that does not possess a signal sequence with target information. In the lysosome, macromolecules degradation takes place due to hydrolytic enzymes within the compartment [219]. It is worth mentioning that when two cargo molecules are internalized by the same mechanism they may have different intracellular destinations [216]. A particular amino acid sequence for instance may target proteins to the endoplasmic reticulum or a protein modification may target proteins to lysosomes [219].

4.2. Pep-1 internalization into mammalian cells

Uptake of pep-1 into mammalian cells is of first importance for peptide functionality and applications *in vivo*. The elucidation of the mechanism for cell entry is compulsory in order to fully take advantage of its properties. In this chapter two articles with studies carried on with pep-1 and HeLa cells are presented.

In the article titled: *Translocation of β-Galactosidase mediated by the cell-penetrating peptide pep-1 into lipid vesicles and Human HeLa cells is driven by membrane electrostatic potential*, the principles that govern the mechanisms of internalization of pep-1 associated with the protein β-Galactosidase are unravelled.

In the short communication titled: *Re-evaluating the role of strongly charged sequences in amphipathic cell-penetrating peptides. A fluorescence study using pep-1*, the effect of an attached fluorescent dye and the importance of the hydrophilic domain to translocation efficiency are revealed. A comparison between labelled and non-labelled peptide is presented.

4.2.1. Translocation of β-Galactosidase mediated by the cell-penetrating peptide pep-1 into lipid vesicles and Human HeLa cells is driven by membrane electrostatic potential.

4.2.1.1. Motivation and methodologies

The functionality of pep-1 as CPP is related to its capacity to internalize macromolecules inside cells. Results presented in chapter 2 reveal its high affinity for lipidic membranes and ability to pass through model membranes by a mechanism mediated by electrostatic interactions and promoted by transmembrane potential [153, 186]. Previous reports on CPP translocation suggest endocytosis as the main mechanism [59, 61]. In this chapter a comprehensive study on the pep-1 capacity to pass through cell membrane and to introduce a macromolecule inside mammalian cells is presented. The possibility of a physical mechanism mediated by transmembrane potential was tested against an alternative mechanism mediated by endocytosis using HeLa cells (Adherent human negroid cervix epitheloid carcinoma cells). The result and conclusions are presented in the published article titled: *Translocation of β-Galactosidase mediated by the cell-penetrating peptide pep-1 into lipid vesicles and Human HeLa cells is driven by membrane electrostatic potential*.

Most of published studies on CPP translocation with cellular lines were carried out with fluorescently-labelled peptides and in the absence of a cargo. Such procedures can create artefacts and bias CPP activity; moreover the significance of these peptides as CPP is not achieved unless its capacity to internalize cargoes inside cells is proven. In addition, recent observations show that fixation conditions can mask the peptide internalization mechanism [55, 58]. In order to avoid such artefacts, a protein cargo was followed through the studies, instead of the peptide.

β-Galactosidase (β-Gal) from *E. Coli* was chosen to study the capacity of pep-1 to internalize a protein and to evaluate the translocation efficiency. This protein does not have a valid signal sequence inside human cells and consequently is unable to address a specific organelle inside the cell. This protein is a homotetramere (116kDa each subunit) with an enzymatic activity dependent on it quaternary structure. The usage of a protein with these characteristics is useful because its cellular location, upon internalization mediated by pep-1, can give valuable information about the possible entry route.

Moreover, accessing its enzymatic activity one can conclude on the stability/functionality of the protein upon interaction with pep-1 and after cellular uptake. A disruptive aggressive process leave the protein unable to work as a catalytic. One should also emphasise the protein size; if pep-1 is able to mediate the uptake of this large protein one can consider that proteins can be internalized by a mechanism where size restriction is not operative (not likely a pore, for instance).

A photophysical characterization of the protein and of the complex pep-1/β-Gal was performed by means of Trp fluorescence (each subunit of β-Gal has 38 Trp residues) using the methodologies referred in chapter 2. β-Gal enzymatic activity was followed upon pep-1/β-Gal complex formation for different pep-1/β-Gal ratios. Internalization of β-Gal mediated by pep-1 into HeLa cells was accessed by immunofluorescence using epifluorescence microscopy and confocal microscopy. Enzymatic activity after cellular internalization was also studied.

For immunofluorescence detection, cell fixation and permeabilization procedures were performed prior to primary antibody anti-β-Gal addition. Primary antibody can be recognized by a secondary antibody with a fluorescent marker (e.g. Fluorescein isothiocyanate (FITC) or tetramethylrhodamine (TRITC)) (Figure 4.2).

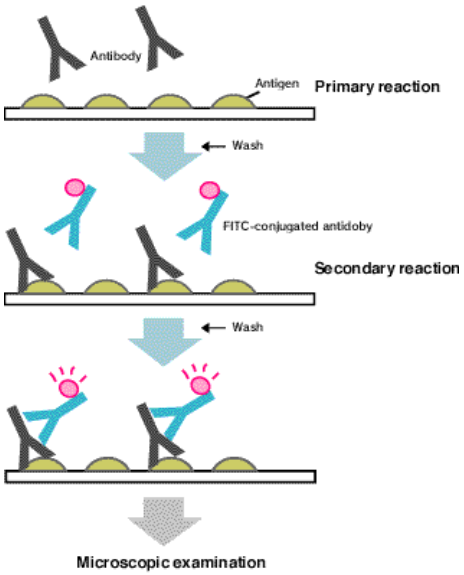

Figure 4.2. β-Gal internalization mediated by pep-1 can be detected by indirect immunofluorescence method. In the primary reaction binding of antibody anti-β-Gal with the antigen occurs. Followed by the secondary reaction where FITC-conjugated secondary antibody binds to anti-β-Gal to obtain complexes of β-Gal-antibody-FITC-conjugated antibody. FITC fluorescence is observed by fluorescence microscopy after washing. Source: http://www.mbl.co.jp/e/diagnostics/product/method.html.

The entry by a mechanism dependent on endocytosis was tested by co-localization of β-Gal with different endocytic markers: Dextran-TRITC was used to

follow macropinocytosis; antibody anti-early endosome antigen 1 to localize early endosomes; antibody anti-caveolin-1 to target caveosomes in caveolae endocytosis and antibody anti-cathepsin D to localize lysosomes. The two fluorescent markers (one to identify β-Gal location and the other to mark the specific endosomal compartment) were imaged in the same cells and each fluorophore was excited and detected independently by confocal microscopy to avoid any signal crossover. Quantification of co-localization of β-Gal with each endosomal marker was performed by comparison of a z-series of 14 images in 6-10 cells [220-222]. Briefly, using the open source Image J software (http://rsb.info.nih.gov/ij/), the pixels of interest were first identified by generating a mask for each channel (in this particular case, red and green signals) to eliminate background signal resulting from the non-specific binding signal. Shared pixels between the red and green masks were identified and quantified; the overlap was defined as the percentage of total pixel intensity for the shared pixels.

β-galactosidase is an enzyme responsible by the hydrolysis of β-galactosides into monosaccharide's, releasing β-(1-4) linked galactose from the non-reducing end of oligosaccharides. This enzyme's substrate specificity can be used to evaluate it activity by the use of synthesizing compounds which when hydrolyzed by β-gal result in a measurable product. The most commonly used chromogenic subtract is o-nitrophenyl-β-galactopyranoside (ONPG); when β-gal cleaves ONPG, o-nitrophenol is released, which has a yellow colour and its formation can be accessed by absorbance at 420nm [223]. Alternatively, a fluorescence based assay can be used because it is more sensitive than the colorimetric ones. An example is 4-methylumbelliferone-β-D-galacto-pyranoside (MUG) which becomes fluorescent upon hydrolysis, producing 4-methylumbelliferone (4-MU) along with galactose (Figure 4.3). 4-MU emits fluorescence at 440nm (excitation at 360nm), whereas the precursor molecule MUG does not. A basic pH is necessary for the development of the fluorescence signal (i.e. higher quantum yield) from 4-MU. Addition of NaOH stops the enzymatic reaction and enables the development of the fluorescent signal [224].

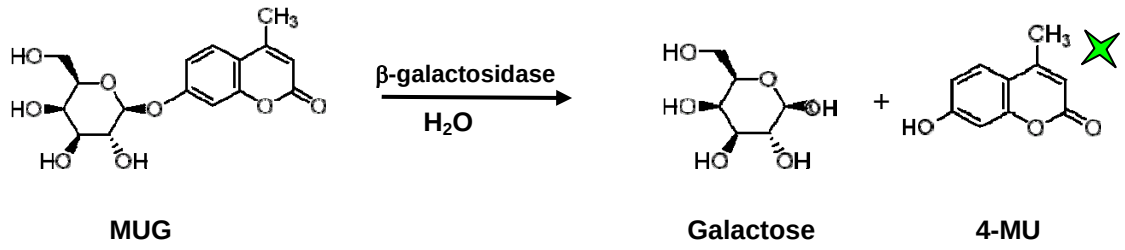

Figure 4.3. Reaction catalysed by β-galactosidase using a non-fluorescent substrate (4-MUG; 4-methylumbelliferone-β-D-galacto-pyranoside) which can be converted into a fluorescent product (4-MU; 4-methylumbelliferone) along with galactose.

The enzymatic activity of β-Gal was followed by progression curves of MUG hydrolysis and the initial velocity of the enzymatic reaction. Considering that the substrate is at non-limiting concentrations, MUG conversion into 4-MU is limited to enzyme concentration and functionality. For further information on enzymatic parameters see reference [212].

Oligoarginine is able to translocate lipid membranes; a passive diffusion across the non-polar interior of plasma membrane seems unrealistic to describe the internalization of a peptidic sequence with such polarity. An association of oligoarginines with cell surface groups with complementary charge was proposed by Rothbard *et al.* to attenuate the polarity of the basic amino acids [81]. The previous chapter, shows that the presence of anionic phospholipids facilitates the association of pep-1 with the cell membrane but is not sufficient to promote the passage of this positively charged peptide through the lipidic membrane [153]. Translocation, *in vitro* was only achieved when negative transmembrane potential across the lipidic membrane exists [186].

The transmembrane potential is related to the concentration gradient and permeabilities of K^+, Na^+ and Cl^- ions [225]. Channels that enable the potassium flow in and out of the cell are much more abundant than channels that enable the passage of the other ions, therefore, the changes in membrane potential are intimately dependent on K^+ permeability [225-227]. Intracellular K^+ is mainly regulated by active inflow of K^+ trough the Na^+/K^+ pump and passive influx and efflux of K^+ depending on the concentration gradient through K^+ leak channels in the cell membrane [225]. Depolarization of the resting membrane potential can be achieved by an increase in

extracellular K^+ which induces a decrease of the electrochemical gradient of these ions across the cell membrane [228]. In practice this can be obtained by substitution of extracellular Na^+ by K^+ [110, 228, 229].

The possible effect of electrochemical gradient on pep-1 translocation in cultured cells was tested by incubating cells with an isotonic buffer with K^+ concentrations ranging between 5mM and 115mM. The intracellular concentration of potassium is about 140mM whereas the extracellular concentration is believed to be around 5mM [81]. With the partial of the sodium salt in PBS with equimolar amounts of the equivalent potassium salt, it was possible to obtain different degrees of membrane depolarization (the total ionic strength was kept constant ($[K^+]$ + $[Na^+]$ =150mM)). Therefore it was possible to evaluate the effect of membrane polarization.

Membrane polarization can be related to a certain extent with the potassium Nernst potential, which is dependent on K^+ concentration in extracellular medium (the intracellular concentration was considered to be constant and 140mM). Negative transmembrane potential was calculated by potassium Nernst potential, E_K, by the use of the equation:

$$E_K = \left(\frac{RT}{F}\right)\ln\left(\frac{K_0}{K_i}\right) \qquad \text{(eq. 3.1)}$$

R is the gas constant, *T* is the absolute temperature, *F* is the Faraday constant and K_0 and K_i are the extracellular and intracellular potassium concentrations respectively. With increasing extracellular K^+ concentration a decrease in the negative potential is noticed. It should be stresses that the contributions of other ions is also important for the total membrane potential and make the membrane potential more positive than the potassium Nernst potential prediction at low extracellular concentration of K^+. Nevertheless Potassium Nernst is a good approximation [81].

The methodologies above referred were used to evaluate the internalization of pep-1/β-Gal inside cultured cells; the following manuscript presents the most relevant results achieved on the studies with pep-1 and mammalian cells.

4.2.1.2. Declaration on authorship of published manuscript: *Translocation of β-Galactosidase mediated by the cell-penetrating peptide pep-1 into lipid vesicles and Human HeLa cells is driven by membrane electrostatic potential*.

I, Sónia Troeira Henriques declare that the experimental design, the laboratory work, the data analysis, discussion and manuscript preparation were carried out by me under supervision of Dr. Miguel ARB Castanho and Dr. Julia Costa. *In vitro* studies were carried on Faculdade de Ciências and supervised by Dr. Miguel ARB Castanho while studies with mammalian cells were carried on ITQB under supervision of Dr. Julia Costa.

I, Miguel ARB Castanho, as Sónia T Henriques supervisor, hereby acknowledge and confirm the information above is correct.

.

_____ _____

Sónia Troeira Henriques Miguel ARB Castanho

Translocation of β-Galactosidase Mediated by the Cell-Penetrating Peptide Pep-1 into Lipid Vesicles and Human HeLa Cells Is Driven by Membrane Electrostatic Potential†

Sónia Troeira Henriques,‡ Júlia Costa,§ and Miguel A. R. B. Castanho*,‡

Centro de Química e Bioquímica, Faculdade de Ciências da Universidade de Lisboa, Ed. C8, Campo Grande, 1749-016 Lisboa, Portugal, and Instituto de Tecnologia Química e Biológica, Apartado 127, 2780 Oeiras, Portugal

Received February 14, 2005; Revised Manuscript Received May 25, 2005

ABSTRACT: The cell-penetrating peptide (CPP) pep-1 is capable of introducing large proteins into different cell lines, maintaining their biological activity. Two possible mechanisms have been proposed to explain the entrance of other CPPs in cells, endosomal-dependent and independent types. In this work, we evaluated the molecular mechanisms of pep-1-mediated cellular uptake of β-galactosidase (β-Gal) from *Escherichia coli* in large unilamellar vesicles (LUV) and HeLa cells. Fluorescence spectroscopy was used to evaluate the translocation process in model systems (LUV). Immunofluorescence microscopy was used to study the translocation in HeLa cells. Enzymatic activity detection enabled us to monitor the internalization of β-Gal into LUV and the functionality of the protein in the interior of HeLa cells. β-Gal translocated into LUV in a transmembrane potential-dependent manner. Likewise, the extent of β-Gal incorporation was extensively decreased in depolarized cells. Furthermore, β-Gal uptake efficiency and kinetics were temperature-independent, and β-Gal did not colocalize with endosomes, lysosomes, or caveosomes. Therefore, β-Gal translocation was not associated with the endosomal pathway. Although an excess of pep-1 was mandatory for β-Gal translocation in vivo, transmembrane pores were not formed as concluded from the trypan blue exclusion method. These results altogether indicated that protein uptake both in vitro with LUV and in vivo with HeLa cells was mainly, if not solely, dependent on negative transmembrane potential across the bilayer, which suggests a physical mechanism governed by electrostatic interactions between pep-1 (positively charged) and membranes (negatively charged).

The introduction of hydrophilic molecules into mammalian cells has become a key strategy for the investigation of intracellular processes and drug therapy. CPPs[1] are very attractive for these purposes because of their ability to mediate cellular uptake of proteins and nucleic acids, which is otherwise impossible because of membrane selective permeability (*1*−*7*). These peptides are small (9−33 amino acid residues), and their only common feature is the presence of basic amino acid residues (*2*).

The most widely used CPPs are derived from HIV-1 tat (TAT) and *Drosophila* Antennapedia homoprotein (*1*, *4*, *6*). Covalent linkage of CPP with cargo molecules leads to their nontoxic import into cells, both rapidly and efficiently, while maintaining functional activity inside the cell (*2*). The process, however, is dependent on CPP, cargo, and cell type (*8*). The translocation of these cationic peptides is not well understood. A single general mechanism for all does not seem reasonable, and there are examples of CPPs (e.g., TAT) that are able to use both endosomal and nonendosomal pathways (*5*, *9*).

Pep-1 (Ac-KETWWETWWTEWSQPKKKRKV-cysteamine) is an artificial CPP that has the ability to establish hydrophobic interactions with the cargo molecule, which may render covalent links unnecessary and favor the native structure (*10*). This sequence contains a Trp-rich hydrophobic domain, KETWWETWWTEW, a hydrophilic sequence, KKKRKV, that is the nuclear localization sequence of simian virus 40 large T antigen, and a spacer, SQP, linking the two previous ones (*10*). This peptide has been successfully used to translocate different biomolecules into distinct cell lines, for instance, proteins into protoplasts (*11*), antibodies into

† This work was funded by Grant POCTI/BCI/38631 from FCT, Portugal, and Grant LSHG-CT-2004-503228 from the European Commission. We thank FCT, Portugal, for Grant SFRH/BD/14337/2003 under the program POCTI to S.T.H.

* To whom correspondence should be addressed. Telephone: +351217500931. Fax: +351217500088. E-mail: castanho@fc.ul.pt.

‡ Faculdade de Ciências da Universidade de Lisboa.

§ Instituto de Tecnologia Química e Biológica.

[1] Abbreviations: CPP, cell-penetrating peptide; NLS, nuclear localization sequence; SV-40, simian virus 40; TAT, CPP derived from HIV-1 tat; β-Gal, β-galactosidase; LUV, large unilamellar vesicles; MUG, 4-methylumbelliferyl galactoside; 4-MU, 4-methylumbelliferone; PMSF, phenylmethanesulfonyl fluoride; phosphine, tris(2-cyanoethyl)-phosphine; POPC, 1-palmitoyl-2-oleoyl-*sn*-glycero-3-phosphocholine; POPG, 1-palmitoyl-2-oleoyl-*sn*-glycero-3-[phospho-*rac*-(1-glycerol)]; DPPC, 1,2-dipalmitoyl-*sn*-glycero-3-phosphocholine; DPPS, 1,2-dipalmitoyl-*sn*-glycero-3-(phospho-L-serine); MEME, Minimum Essential Medium Eagle; NEAA, nonessential amino acids; FBS, fetal bovine serum; BSA, bovine serum albumin; PBS, phosphate-buffered saline solution; TRITC, tetramethylrhodamine β-isothiocyanate; FITC, fluorescein isothiocyanate; MTT, 3-(4,5-dimethylthiazol-2-yl)-2,5-diphenyltetrazolium bromide; TX-100, Triton X-100; DMSO, dimethyl sulfoxide; DAPI, 4′,6-diaminidino-2-phenylindole.

10.1021/bi0502644 CCC: $30.25
Published on Web 07/07/2005

porcine renal epithelial cells (LLC-PK1) (*12*), and peptides into rat pheochromocytoma cells (PC-12) (*13*). The unspecificity of this peptide is a potential advantage for ubiquitous applications.

It has been shown that pep-1 translocates across lipidic vesicles only when a negative transmembrane potential exists (*14*). However, it is not known if endocytosis is also involved in pep-1 translocation in vivo as described for CPPs Tat 48−60 and $(Arg)_9$ (*5*, *9*). Furthermore, it is necessary to determine if the translocation of cargo proteins via pep-1 follows a mechanism identical to that of the free peptide.

In this work, we used β-galactosidase (β-Gal) from *Escherichia coli* as the cargo protein. β-Gal is a homotetramere with an enzymatic activity (EC 3.2.1.23) that is easy to assess and dependent on its quaternary structure (*15*). Each subunit contains 1023 amino acid residues (116 kDa), with 38 Trp residues that enable a characterization by fluorescence spectroscopy. The formal global charge at pH 7.4 is approximately −38 (the estimated charged is based on the pK_a's for the isolated amino acids and was determined using the software available at www.scripps.edu/~cdputnam/protcalc.html).

In this work, we have studied formation of the pep-1−β-Gal complex and its translocation across membranes. We have found that β-Gal translocation into LUV and human HeLa cells depends on the negative transmembrane potential. Alternative pathways, such as classical and caveolin-mediated endosomal pathways, or possible pore formation induced by pep-1, did not account for translocation of β-Gal into the HeLa cells.

EXPERIMENTAL PROCEDURES

Reagents. Pep-1 (Ac-KETWWETWWTEWSQPKKKRKV-cysteamine) that was >95% pure was obtained from GenScript Corp. (Piscataway, NJ). β-Gal from *E. coli*, 4-methylumbelliferyl galactoside (MUG), porcine pancreatic lyophilized trypsin, phenylmethanesulfonyl fluoride (PMSF), cholesterol (chol), Triton X-100 (TX-100), and dextran (M_r = 10 000) were obtained from Sigma-Aldrich (St. Louis, MO). Tris(2-cyanoethyl)phosphine (phosphine) and dextran tetramethylrhodamine β-isothiocyanate (TRITC) conjugate (M_r = 10 000) were from Molecular Probes (Eugene, OR). 1-Palmitoyl-2-oleoyl-*sn*-glycero-3-phosphocholine (POPC), 1-palmitoyl-2-oleoyl-*sn*-glycero-3-[phospho-*rac*-(1-glycerol)] (POPG), 1,2-dipalmitoyl-*sn*-glycero-3-phosphocholine (DPPC), and 1,2-dipalmitoyl-*sn*-glycero-3-(phospho-L-serine) (DPPS) were from Avanti Polar-Lipids (Alabaster, AL); Minimum essential medium Eagles with Earle's salts (MEME), L-glutamine, nonessential amino acids (NEAA), fetal bovine serum (FBS), streptomycin and penicillin, and trypsin-EDTA solution (0.05% trypsin and 0.53 mM EDTA·4Na) were obtained from Gibco Invitrogen Corp. (Carlsbad, CA). 4′,6-Diaminidino-2-phenylindole (DAPI) was from Sigma. The primary antibodies used were as follows: mouse monoclonal anti-β-Gal (AB1; 1/500 dilution) from Promega (Madison, WI), rabbit polyclonal anti-β-Gal (AB2; 1/500) from 5Prime (Boulder, CO), mouse monoclonal anti-EEA1 (1/100) from BD Biosciences (Palo Alto, CA), mouse monoclonal anti-cathepsin D (1/20) from Sigma-Aldrich (St. Louis, MO), and rabbit polyclonal anti-caveolin-1 (1/50) from Santa Cruz Biotechnology (Santa Cruz, CA). The secondary antibodies were goat polyclonal anti-mouse IgG TRITC conjugate (1/60) and goat polyclonal anti-rabbit IgG fluorescein isothiocyanate (FITC) conjugate (1/100) obtained from Sigma-Aldrich.

Photophysics of β-Gal in Aqueous Solution. The experiments in aqueous solution and with LUV were performed at room temperature with a UV−vis Jasco V-530 spectrophotometer and a SLM Aminco 8100 spectrofluorometer (equipped with a 450 W Xe lamp and double monochromators). The solutions were prepared in 10 mM HEPES buffer (pH 7.4) containing 150 mM NaCl, at physiologic ionic strength. Fluorescence intensities were corrected for the inner filter effect with the equation $I_c = I \times 10^{0.5A}$, where I_c is the corrected intensity, I the measured intensity, and A the absorbance at the excitation wavelength.

Protein photophysical characterization was carried out by means of Trp fluorescence emission ($\lambda_{excitation}$ = 280 nm). Fluorescence emission characterization and determination of quantum yield (*16*) were performed. Variation of fluorescence emission intensity with concentration (0−269 nM) and fluorescence quenching by acrylamide (aqueous soluble Trp quencher) were carried out in the absence and presence of a reducing agent, 1 mM phosphine. The quenching assay was performed by titration of β-Gal with acrylamide (0−60 mM) and followed by fluorescence emission with a $\lambda_{excitation}$ of 290 nm (to minimize the relative quencher/fluorophore light absorption ratio). The Stern−Volmer equation ($I_0/I = 1 + K_{SV}[Q]$, where I and I_0 are the fluorescence intensity in the presence and absence of quencher, respectively, K_{SV} is the Stern−Volmer constant, and [Q] is the concentration of quencher; for a revision, see ref *17*) was applied to the data. Data were corrected for simultaneous absorption of the fluorophore and quencher (see eq *5* in ref *18*).

Enzymatic Assay of β-Gal. Enzyme activity of β-Gal was determined by hydrolysis of 4-methylumbelliferone β-D-galactopyranoside (MUG), a nonfluorescent substrate, to 4-methylumbelliferone (4-MU), a fluorescent product ($\lambda_{excitation}$ = 360 nm, $\lambda_{emission}$ = 440 nm) (*19*). Time progression curves were performed (0−60 min); briefly, enzyme was added to 2.5 mM MUG (substrate at nonlimiting concentrations), in 10 mM HEPES buffer (pH 7.4), containing 150 mM NaCl, to start the reaction. The reaction was stopped by the addition of 0.2 M NaOH-containing buffer (to a final substrate dilution of 1/40, pH 13.2). The assay was followed by 4-MU fluorescence intensity. The concentration was determined by A_{360} [$\epsilon_{360} = 1.9 \times 10^4$ M^{-1} cm^{-1} (*20*)].

Formation of the Pep-1−β-Galactosidase Complex. The titration of 72 nM protein with peptide was performed up to a pep-1/β-Gal molar ratio of 100. Trp fluorescence emission spectra were monitored to follow complex formation. The maximum of the fluorescence emission spectrum of β-Gal occurs at a wavelength significantly different from that of pep-1 (329 nm vs 346 nm). The fluorescence emission spectra of pep-1 in the absence of β-Gal and vice versa were followed simultaneously, under the same conditions. Enzymatic activity of β-Gal and quenching of Trp fluorescence by acrylamide at different pep-1/β-Gal ratios was followed as mentioned above.

Interaction of β-Gal and the Pep-1−β-Gal Complex with Large Unilamellar Vesicles. LUV were prepared, in 10 mM HEPES buffer (pH 7.4) containing 150 mM NaCl, by the

extrusion method (*21*). To evaluate the interaction of 72 nM β-Gal (free or complexed with pep-1 at different concentrations) with LUV, Trp fluorescence spectral shifts were followed ($\lambda_{excitation} = 280$ nm) by titration of samples with lipidic suspensions (0−3.75 mM). POPC and POPC/POPG (4/1) bilayers in vesicles are in liquid crystalline phases; POPC/chol (2/1) bilayers in vesicles are in the liquid-ordered phase, and DPPC and DPPC/DPPS (4/1) bilayers are in the gel phase.

Uptake of the Pep-1−β-Gal Complex in LUV with Negative Transmembrane Potential. The pep-1−β-Gal complex (molar ratio of 320) was incubated (30 min) with POPC/POPG (4/1) (final lipid concentration of 0.5 mM) LUV in the absence or presence of negative transmembrane potential (see ref *14* for a description of production of LUV with a negative transbilayer potential). Briefly, valinomycin was added, at a $1/10^4$ molar ratio (moles per mole of lipid), to K^+-loaded LUV dispersed in Na^+ buffer. Afterward, a trypsin solution (final concentration of 1.3 mM) was added, and the mixture was allowed to digest the nonincorporated pep-1 and β-Gal, incubated for 30 min at 37 °C. After that, incubation with 4 mM PMSF (final concentration) was carried out for 15 min to inhibit trypsin. To induce LUV permeabilization and leakage of the incorporated β-Gal, 0.2% (w/v) TX-100 was added. Released β-Gal was detected by means of its enzymatic activity, namely, by MUG hydrolysis during 20 min at 37 °C followed by fluorescence spectroscopy, as described above. Controls without pep-1 were performed, and the slight contribution from nonincorporated β-Gal resistant to trypsin hydrolysis was discounted.

Cell Culture and Cell Viability Assays. Adherent human negroid cervix epitheloid carcinoma cells (HeLa) were grown in MEME supplemented with 2 mM Glu, 2 mM NEAA, 10% (v/v) FBS, and 1% (v/v) streptomycin and penicillin, in a 5% CO_2 humidified atmosphere at 37 °C. Cells were split in a 1/4 dilution every 3−4 days, after they reached confluency, which was monitored using an inverted microscope (Olympus CK30). Cell viability was determined by the colorimetric assay with 3-(4,5-dimethylthiazol-2-yl)-2,5-diphenyltetrazolium bromide (MTT). MTT is reduced by mitochondrial dehydrogenases of viable cells (*22*). Briefly, cells were grown in 96-well plates and washed with serum-free medium; 10 μL of MTT (5 mg/mL) was added to each well, and a 3 h incubation at 37 °C was performed. The purple product was solubilized in dimethyl sulfoxide (DMSO), and the absorbance at 540 nm was determined. Alternatively, cell viability was determined by the trypan blue exclusion assay. Briefly, after being detached, the cell suspension was added to a trypan blue solution (1/10 dilution) and counted in hemacytometer. Viable cells exclude trypan blue; nonviable cells absorb the dye and appear blue.

Cellular Uptake of Proteins and Dextran Monitored by Immunofluorescence Microscopy. For immunofluorescence microscopy, cells were grown on 12 mm diameter glass coverslips in 24-well plates to approximately 70% confluence. Prior to the uptake assays, the pep-1−β-Gal complex was formed in serum-free medium (*23*) during 30 min at room temperature following the instructions of the supplier (*Active Motif*; Rixensart) (*24*). Translocation efficiency was evaluated with different pep-1/β-Gal ratios (4, 32, 100, 200, 320, 600, and 1000) at 10.8 nM β-Gal. Coverslips were inverted and placed over a drop of a macromolecular complex solution (*25*) and incubated for 60 min at 37 °C. Cells were washed three times in PBS containing 0.5 mM $MgCl_2$, fixed in 4% (w/v) paraformaldehyde for 20 min, permeabilized with 0.1% (w/v) TX-100 for 15 min, and then incubated in a blocking solution that consisted of PBS containing 1% bovine serum albumin (BSA) for 1 h (*26*). After that, incubations with primary and secondary antibodies in blocking solution, for 2 and 1 h, respectively, were performed. Washings were carried out in PBS. Coverslips were mounted in Airvol and observed in the Leica DMRB fluorescence microscope and/or in the Bio-Rad MRC1024 confocal microscope. The nucleus was visualized with DAPI that was added to the secondary antibody mixture at a dilution of 1/1000. The kinetics of the β-Gal translocation process was evaluated by incubation at a pep-1/β-Gal ratio of 320 for 10, 20, 30, 40, 50, 60, and 120 min at 4 or 37 °C. Enzymatic activity of internalized β-Gal by HeLa cells was monitored by the use of MUG (see Enzymatic Assay of β-Gal). After incubation of the complex for 60 min at 4 or 37 °C, trypsin was added to the cells to hydrolyze nonincorporated peptide and protein. Cells were centrifuged at 500*g* for 5 min, washed twice in PBS, and resuspended in 0.1% (w/v) TX-100 for 15 min for permeabilization. Then 2 mM substrate was added to cells, and product progression curves were followed for 120 min at 37 °C. NaOH was added, and product formation was monitored as described above. A control without pep-1 was carried out.

The uptake of the anti-mouse IgG−TRITC conjugate mediated by pep-1 was monitored by immunofluorescence microscopy under live conditions, without the paraformaldehyde fixation step, in a 60 min incubation at 4 or 37 °C, at a 1/320 protein/pep-1 ratio.

Cells were also incubated with the endocytic tracer dextran−TRITC at 2 mg/mL associated with pep-1, at 37 and 4 °C for 60 min, in the presence or absence of 20 mg/mL nonlabeled dextran.

Confocal Microscopy and Colocalization Analysis. For each picture, laser intensities and amplifier gains were adjusted to prevent pixel saturation. This was done using GLOW LUT in the Leica Confocal software. Each fluorophore that was used was excited and detected separately to avoid any signal crossover. Each picture consisted of a z-series of 14 images of 1024 × 1024 pixel resolution with a pinhole Airy unit. Colocalization analysis was performed using open source Image J version 1.30 (http://rsb.info.nih.gov/ij/). The procedure was applied for a population of 6−10 cells. Quantification of colocalization of β-Gal (AB1 or AB2) with endosomes (anti-EEA1), lysosomes (anti-cathepsin D), and caveosomes (anti-caveolin-1) was based on that previously described (*27*).

Effect of Transmembrane Potential on the Uptake of the Pep-1/β-Gal Complex by HeLa Cells. To decrease the transmembrane potential, cells were incubated, for 30 min at 37 °C, with the pep-1−β-Gal complex preformed in PBS buffer, containing different K^+ concentrations, with Na^+ replaced by K^+, at increasing concentrations (*28*). Quantification of internalized β-Gal was carried out by using enzymatic activity. Cell viability in the presence of different K^+ concentrations was determined by the trypan blue exclusion method. Absolute fluorescence intensity data were divided by the number of viable cells.

RESULTS

Formation of the Pep-1−β-Gal Complex in Aqueous Solution. To investigate the suitability of β-Gal for cellular uptake studies mediated by pep-1, characterization of the protein and the complex formed in aqueous solution has been performed. Each subunit of β-Gal contains 38 Trp, 35 Phe, and 25 Tyr residues. Fluorescence emission with a $\lambda_{excitation}$ of 280 nm is largely dominated by the Trp residues. Most hydrophobic residues are not accessible to the aqueous environment as concluded from the β-Gal crystallographic structure. In aqueous solution, fluorescence emission has a quantum yield (Φ) of 0.099 ± 0.005 (constant up to 269 nM) with a band maximum at 329 nm which was significantly different from the maximum of free Trp. This blue-shifted emission is in agreement with most of the Trp residues being inaccessible to the aqueous environment. The low accessibility of Trp residues to the aqueous environment was confirmed by acrylamide quenching; K_{SV} was significantly lower from that obtained for free Trp (5.6 ± 0.3 and 18.9 ± 0.3 M^{-1}, respectively). The initial velocity of MUG hydrolysis, catalyzed by β-Gal, was 17.5 μM min^{-1}, and linearity was maintained for 30 min.

Since the cytoplasm is a reducing environment, we have tested the effect of the reducing agent phosphine (1 mM) on β-Gal conformation and activity. The quantum yield was slightly decreased (Φ = 0.067 ± 0.007), but the accessibility of Trp to aqueous solution (K_{SV} by acrylamide is 5.4 ± 0.2 M^{-1}) was not altered. A concomitant slight decrease in the initial velocity of enzymatic activity occurred (12.0 μM min^{-1}).

The initial velocity of the enzymatic reaction catalyzed by β-Gal was maintained up to a peptide/protein molar ratio of 16. In this range, the peptide strongly interacts with the protein (see the Supporting Information for experimental results and discussion). The initial velocity decreased to 78% (v_0 = 13.4 μM min^{-1}) and 54% (v_0 = 9.4 μM min^{-1}) of the starting value at pep-1/β-Gal ratios of 40 and 400, respectively. In a reducing environment, a more pronounced decrease was observed: for the 400 complex, v_0 = 5.8 μM min^{-1}, which corresponded to a reduction of 52% of the enzymatic activity in the absence of pep-1 (12.0 μM min^{-1}).

Transmembrane Potential Is Required for Translocation of the Pep-1−β-Gal Complex into LUV. No spectral alterations occurred when β-Gal was in the presence of neutral or negatively charged LUV [POPC, POPC/POPG (4/1), POPC/chol (2/1), DPPC, and DPPC/DPPS (4/1)] (Table 1). A slight blue shift in emission spectra was detected for pep-1−β-Gal complexes (molar ratios of 4, 16, 38, 60, and 400) in POPC, POPC/POPG (4/1), and POPC/chol (2/1) lipidic systems (Table 1).

We investigated the uptake of β-Gal mediated by pep-1 into LUV after the induction of an electrostatic gradient across the membrane by valinomycin. Briefly, after a 30 min incubation with the complex, hydrolysis of the pep-1−β-Gal complex outside LUV was achieved with trypsin; then the activity of β-Gal enclosed in the LUV lumen was determined after release with TX-100. Product formation concentration was enhanced by a factor of 5 in the presence of the negative transmembrane potential (when compared with the situation without a potential). The fraction of translocated protein is low, which is expected considering the total volume of the vesicles in the total bulk solution (~0.016%).

Table 1: Partition of the Pep-1−β-Gal Complex into LUV[a]

lipid	sample	aqueous solution (nm)	3.75 mM lipid (nm)	shift (nm)[b]
POPC	β-Gal	329	329	0
	pep-1−β-Gal (4/1)	330	325	5
	pep-1−β-Gal (16/1)	331	327	4
	pep-1−β-Gal (38/1)	336	332	4
	pep-1−β-Gal (60/1)	337	332	5
	pep-1−β-Gal (400/1)	343	336	7
	pep-1	346	338	8
POPC/POPG (4/1)	β-Gal	329	329	0
	pep-1−β-Gal (4/1)	330	327	3
	pep-1−β-Gal (16/1)	332	330	2
	pep-1−β-Gal (38/1)	337	333	4
	pep-1−β-Gal (60/1)	335	331	4
	pep-1	346	338	8
POPC/chol (2/1)	β-Gal	329	329	0
	pep-1−β-Gal (4/1)	330	325	5
	pep-1−β-Gal (16/1)	331	325	3
	pep-1−β-Gal (38/1)	335	330	5
	pep-1−β-Gal (60/1)	341	336	5
	pep-1	346	337	9

[a] Maximum fluorescence emission of the pep-1−β-Gal complex, at different ratios, in aqueous solution [10 mM HEPES buffer containing 150 mM NaCl (pH 7.4)] and in the presence of a 3.75 mM lipidic suspension. [b] The shift is the difference between the two conditions.

Therefore, these results indicate not only that pep-1 improves the affinity of the protein for the membrane but also that the presence of a transmembrane potential induces its translocation across a bilayer.

Pep-1 Does Not Induce Pore Formation in HeLa Cells. It has been suggested that protein uptake mediated by pep-1 involves pore formation (*29*), but this is controversial in light of biophysical studies with lipidic vesicles (*14*). To test this hypothesis, we have determined the cell viability by the trypan blue exclusion method. This method relies on the inclusion of the dye trypan blue by dead cells once their plasma membrane is permeable or damaged. If pep-1 would induce pores on the plasma membrane of cells, a larger amount of intracellular trypan blue would be observed. However, this was not the case since viabilities were similar for control cells (96.4 ± 0.6%) or cells incubated with pep-1 and the pep-1−β-Gal complex (95.5 ± 1.6 and 95.6 ± 0.1%, respectively). These results indicated that pep-1 did not induce permeability changes and hence pore formation in the plasma membrane of HeLa cells.

To evaluate the possible toxic effect of pep-1 on the cells, we have used an independent cell viability test, the MTT assay. MTT is a very sensitive way of determining cytotoxicity. In living cells, mitochondrial dehydrogenase enzymes oxidize the yellow MTT and convert it into purple formazan crystals (*22*). It was observed that the peptide induced a reduction in cell viability of approximately 22%. Since viability calculated by the trypan blue assay was not decreased after addition of pep-1, these results suggested that pep-1 might inhibit mitochondrial dehydrogenases.

Electrostatic Transmembrane Potential Is a Sine-Quanon Requirement for Translocation of the Pep-1−β-Gal Complex into HeLa cells. To monitor the uptake of the pep-1−β-Gal complex by HeLa cells, increasing pep-1 concentrations and

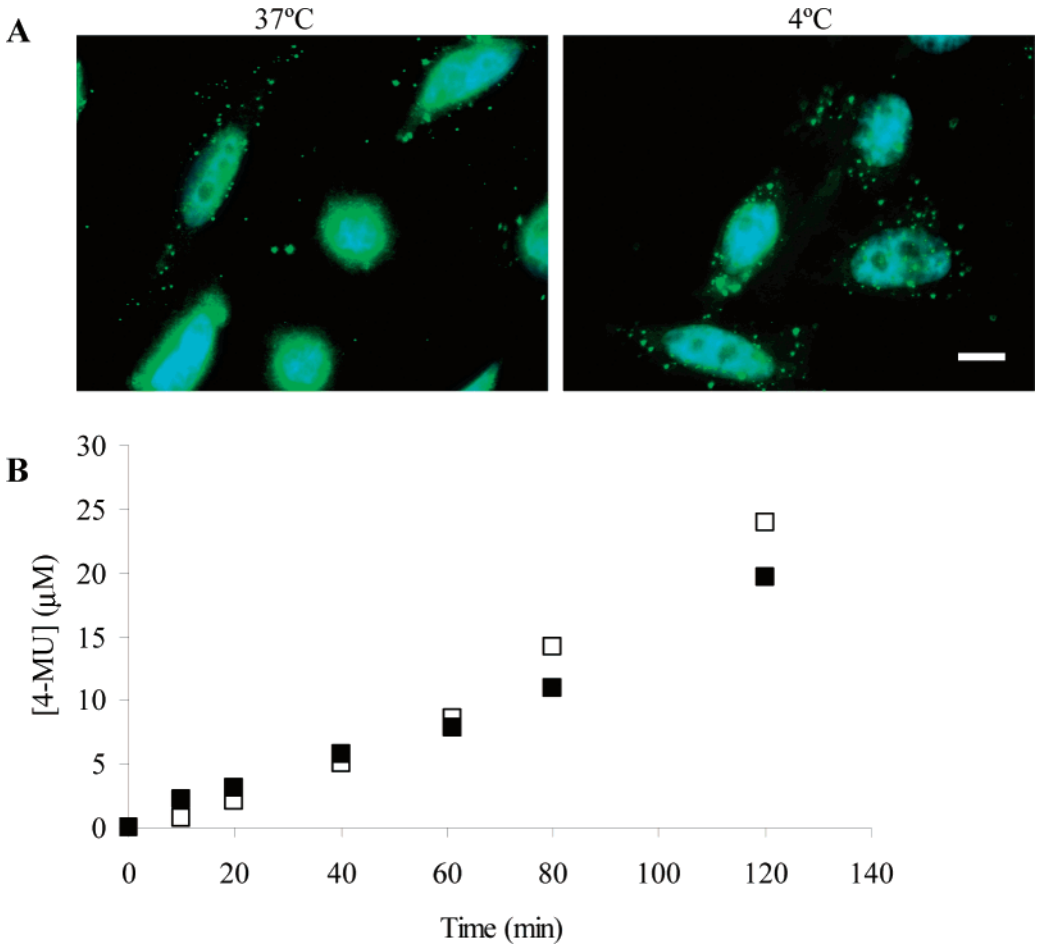

FIGURE 1: Translocation of β-Gal, mediated by pep-1, into HeLa cells. Panel A shows immunofluorescence microscopy detection of β-Gal. The pep-1−β-Gal complex (molar ratio of 320) was incubated with HeLa cells, at 37 or 4 °C, for 60 min. Cells were fixed with 4% paraformaldehyde and permeabilized with 0.1% (w/v) TX-100. β-Gal was detected with rabbit polyclonal anti-β-Gal and the secondary anti-rabbit antibody coupled to FITC. DAPI was used to identify the nucleus. Internalized β-Gal is in the cytosol. The scale bar is 10 μm. Panel B shows enzymatic activity of β-Gal internalized in a HeLa cell suspension. β-Gal uptake, after incubation with the pep-1−β-Gal complex (molar ratio of 320) for 60 min at 4 (■) or 37 °C (□), was followed by the progression curve of enzymatic MUG hydrolysis, at 37 °C. The control without pep-1 was subtracted. The formation of 4-MU monitored by fluorescence intensity at 440 nm with excitation at 360 nm indicates that β-Gal was efficiently translocated, at both temperatures, in an active form.

different incubation times have been tested. After a 60 min incubation at a pep-1/β-Gal ratio of 320, a significant uptake of β-Gal has been observed (Figure 1A). β-Gal was found dispersed in aggregates within the cytosol. The presence of protein inside the cell and not adsorbed on the cell surface was confirmed by confocal microscopy. Apparently, the translocation efficiency did not increase for complex ratios between 320 and 1000. For lower ratios, between 4 and 200, uptake of β-Gal did not occur. Therefore, the chosen pep-1/β-Gal ratio for all the experiments was 320. At this ratio, there was an excess of soluble pep-1 in solution (see Figure S1 of the Supporting Information).

Transfection was relatively fast; after 10 min, it was already possible to identify a small quantity of protein in some cells. The level of transfection increased until approximately 40 min; after this time, it seemed to stabilize (data not shown). Translocation occurred with a similar efficiency at 4 °C (Figure 1A). To test if β-Gal was active after translocation, MUG hydrolysis was monitored in cells incubated at 37 and 4 °C with the complex. It was observed that β-Gal was indeed active after translocation at both temperatures (Figure 1B).

For a typical animal cell characterized by dominant potassium permeability, increasing the external potassium concentration necessarily reduces the transmembrane potential due to the decrease in the electrochemical gradient of K^+ across the cell membrane (*28*, *30*). Negative transmembrane potential is dominated by potassium potential equilibrium, which can be estimated by the potassium Nernst potential (E_K): $E_K = (RT/F) \ln(K_0/K_i)$, where R is the gas constant, T is the absolute temperature, F is Faraday's constant, and K_0 and K_i are the extracellular and intracellular potassium concentrations, respectively. So, increasing the extracellular K^+ concentration leads to less negative Nernst potentials (Figure 2).

To test if the electrostatic membrane potential would be required for translocation of the pep-1−β-Gal complex, HeLa cells have been incubated with the complex at increasing external K^+ concentrations. The total ionic strength ($[K^+] + [Na^+] = 150$ mM) was kept constant. The internalized β-Gal concentration was estimated from enzymatic MUG hydrolysis. This assay was performed for 30 min to guarantee that the initial velocity of the reaction was maintained, and that the concentration of β-Gal uptake was directly related

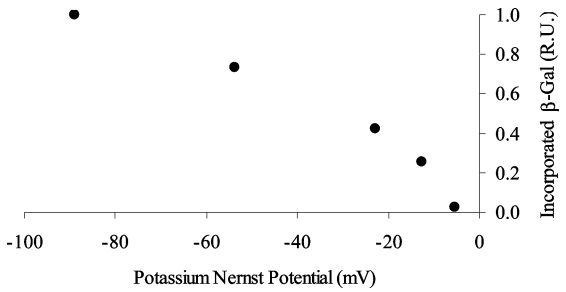

FIGURE 2: Variation of uptake of β-Gal into a HeLa cell suspension, mediated by pep-1, with potassium Nernst potential. The pep-1−β-Gal complex (molar ratio of 320) was incubated with HeLa cells, for 30 min at 37 °C, in the presence of increasing external K^+ concentrations, and a constant ionic strength ($[K^+] + [Na^+] = 150$ mM). The relative level of β-Gal uptake was determined from β-Gal enzymatic hydrolysis of MUG for 20 min at 37 °C. The potassium Nernst potential was determined considering an internal K^+ concentration of 140 mM; the external K^+ concentration ranged from 5 to 114.6 mM, which corresponded to a range from −89 to −5.4 mV, respectively (see the equation in the text). An increasing external K^+ concentration severely reduces the level of β-Gal uptake.

with 4-MU production. A decrease in the absolute value of the electrochemical K^+ gradient (calculated considering K_i = 140 mM) led to a severe drop in the level of β-Gal uptake (Figure 2). When K_0 = 114.6 mM, uptake was almost completely inhibited.

Although for low extracellular K^+ concentrations the contribution of other conductors makes the membrane potential less negative than that predicted by K^+ Nernst potential (*28*), the dependence of β-Gal uptake on transmembrane K^+ Nernst potential was clear.

The Pep-1−β-Gal Complex Is Not Internalized by HeLa Cells via the Endosomal Pathways. Other CPPs such as the one derived from TAT and $(Arg)_9$ (*5*) seem to translocate proteins across cells by two different mechanisms: one is fast and physical in nature and the other is mediated by endocytosis. In the case of an endosomal-dependent pathway of β-Gal uptake mediated by pep-1, colocalization with endosomes or lysosomes at some extension would be expected. To evaluate this possibility, colocalization of pep-1-translocated β-Gal with EEA1 (early endosomal marker), caveolin-1 (caveosomes marker), and cathepsin D (lysosomal marker) was performed. Monitoring localization of the protein, instead of a fluorescence-labeled pep-1, is a better choice. It prevents problems associated with the apparent uptake of cationic peptides bound to negatively charged membranes, causing an artifactual localization in cells (*5*) and the possible influence of the fluorescent label in the uptake and intracellular localization of the peptide (*31*). The percentages of colocalization with each of the organelles from the endocytic pathway determined after immunofluorescence confocal microscopy were very low (shown on the right in Figure 3), after incubation for 60 or 120 min. Similar results were obtained at 4 °C. These results indicate that the uptake of β-Gal did not involve the endocytic pathway.

It has been suggested that fixation conditions could lead to an artifactual uptake of cationic peptides associated with the cell membrane at 4 °C (*5*, *9*, *32*). The uptake of a protein

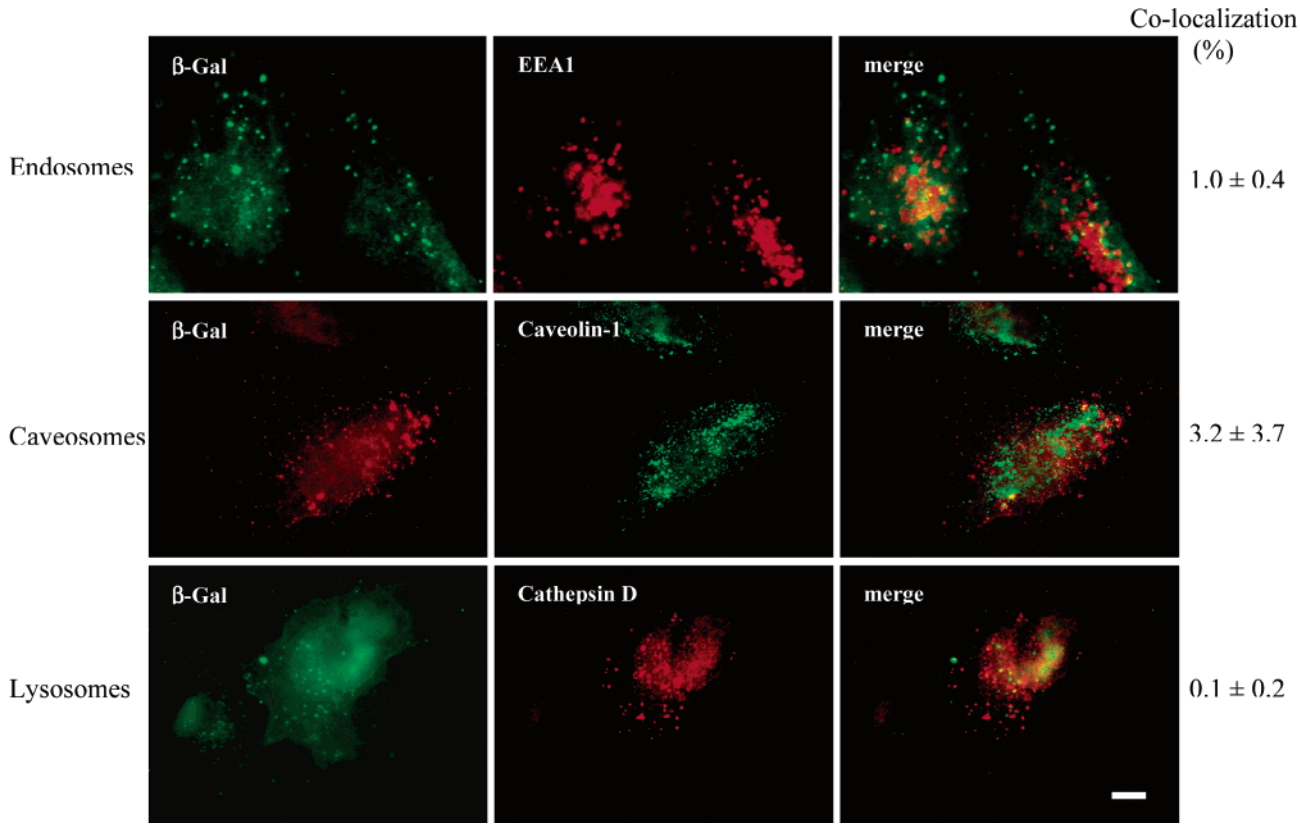

FIGURE 3: Immunofluorescence microscopy localization of pep-1-translocated β-Gal, EEA1, caveolin-1, and cathepsin D from HeLa cells. Cells were incubated with the pep-1−β-Gal complex (molar ratio of 320) for 60 min. Cells were fixed with 4% paraformaldehyde and permeabilized with 0.1% (w/v) TX-100. β-Gal, detected with rabbit polyclonal or mouse monoclonal antibodies, was colocalized with early endosomal EEA1, caviosomal caveolin-1, and lysosomal cathepsin D. Secondary antibodies were the anti-rabbit antibody coupled to FITC and the anti-mouse antibody coupled to TRITC. Pictures of a *z*-series of 14 images from the confocal microscope were analyzed with Image J version 1.3 to perform colocalization analysis. Six to 10 cells were observed. The scale bar is 10 μm.

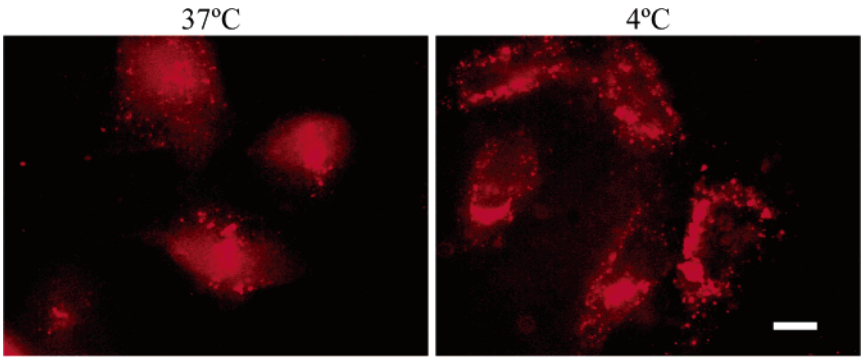

FIGURE 4: Uptake into HeLa cells of anti-mouse antibody conjugated with TRITC, mediated by pep-1. Incubation of cells with a pep-1−anti-mouse−TRITC complex was performed for 60 min at 4 or 37 °C. Cells were visualized under live conditions in a fluorescence microscope. The scale bar is 10 μm.

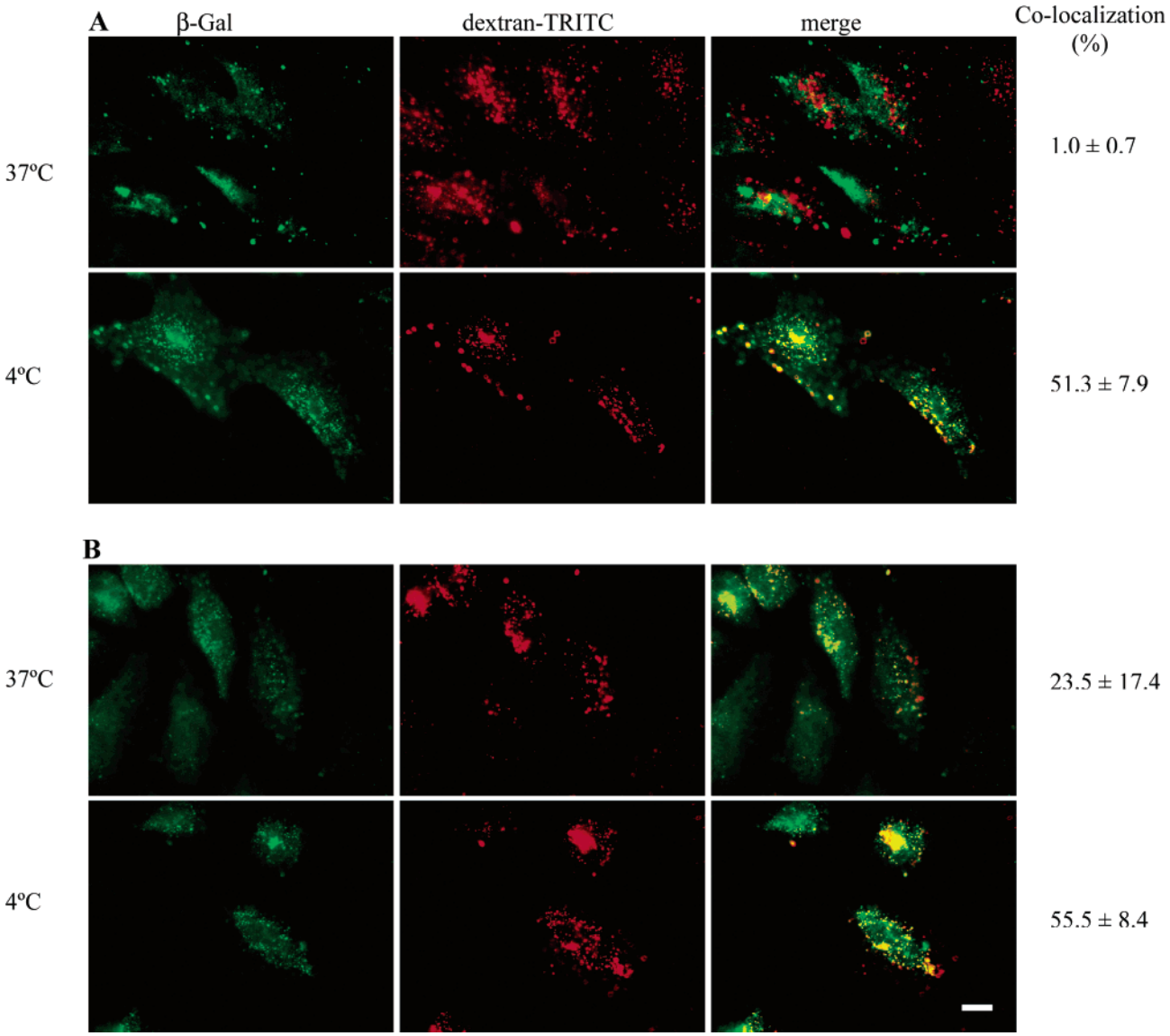

FIGURE 5: Immunofluorescence microscopy localization of translocated β-Gal and the dextran−TRITC marker in HeLa cells (incubation for 60 min at 37 or 4 °C). Panel A shows incubation with the pep-1−β-Gal complex (molar ratio of 320) where the endocytic dextran−TRITC marker (2 mg/mL) was added to the complex at the time of cell incubation. Panel B shows incubation with the preformed pep-1−β-Gal−dextran−TRITC complex. Cells were fixed with 4% paraformaldehyde and permeabilized with 0.1% (w/v) TX-100. β-Gal was detected with rabbit polyclonal anti-β-Gal and anti-rabbit antibodies coupled to FITC. Pictures of a z-series of 14 images from the confocal microscope were analyzed with Image J version 1.3 and were used to perform colocalization analysis. Six to 10 cells were used. The scale bar is 10 μm.

covalently marked with a fluorescent probe can be visualized by fluorescence microscopy without the need to fixate or permeabilize the cells. The uptake of anti-mouse TRITC at 4 and 37 °C was performed and visualized by immunofluorescence microscopy without fixation (Figure 4). It was possible to identify the presence of protein inside the cell at

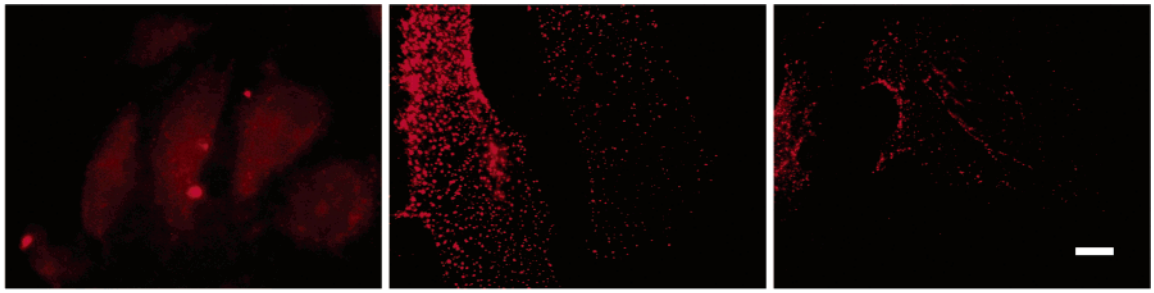

pep-1	-	+	+
dextran-TRITC (2mg/mL)	+	+	+
dextran (20mg/mL)	-	-	+

FIGURE 6: Uptake of the dextran−TRITC marker, mediated by pep-1, into HeLa cells. Comparison of dextran−TRITC (2 mg/mL) uptake, mediated by pep-1, at 4 °C for 60 min when the dextran−TRITC−pep-1 complex was preformed in the presence or absence of dextran (20 mg/mL). Cells were fixed with 4% paraformaldehyde and permeabilized with 0.1% (w/v) TX-100. The dextran−TRITC marker at 4 °C was detected only when pep-1 was present. In the presence of dextran (nonconjugated), the rate of uptake of the dextran−TRITC marker is decreased, indicating a competition of pep-1 for nonconjugated dextran. The scale bar is 10 μm.

both temperatures. This indicated that internalized protein was not an artifact associated with fixation.

The Polysaccharide Dextran Is Translocated into HeLa Cells by Pep-1. Uptake of the dextran−TRITC complex by HeLa cells occurs by a classical endosomal pathway. At 37 °C, β-Gal did not colocalize with the dextran−TRITC marker (1.0%) (Figure 5A), supporting the idea that β-Gal would be translocated into the cells by a mechanism independent of the endocytic pathway. However, at 4 °C, there was an extensive colocalization between β-Gal and the dextran−TRITC marker (51.3%) (Figure 5A). At 4 °C, the classical endosomal pathway is inhibited, so the endocytic dextran−TRITC marker did not enter the cells via this pathway (see control in Figure 6, left image). The internalization of the dextran−TRITC marker at 4 °C and its colocalization with β-Gal suggested that the uptake of translocation of the polysaccharide was mediated by pep-1. However, if the dextran−TRITC marker was preincubated together with pep-1 and β-Gal, a ternary complex seems to be formed and β-Gal−dextran−TRITC colocalization occurred, even at 37 °C (Figure 5B).

To confirm that pep-1 was translocating the dextran−TRITC marker via the polysaccharide without interference of artifacts from the fluorophore moiety, the HeLa cells were incubated with pep-1−dextran−TRITC complex, at 4 °C, in the presence of nonlabeled dextran (Figure 6). It was observed that the presence of nonlabeled dextran dramatically reduced the amount of dextran−TRITC marker translocated into the cells, showing competition between nonlabeled dextran and the dextran−TRITC marker. This confirmed that pep-1 mediated the transport of the polysaccharide into HeLa cells without any artifactual interference of TRITC.

DISCUSSION

β-Gal from *E. coli* was chosen for the study of the interaction of pep-1 with a protein and evaluation of the translocation efficiency inside human tumoral cells. Its enzymatic activity is easy to access. Trp residues enable fluorescence spectroscopy techniques to be used as analytical tools. The absence of a signal sequence makes the protein unable to address any specific organelle inside the cell; therefore, this molecule is very useful in evaluating if the pep-1-mediated translocation leads protein to a specific organelle in human cells. HeLa cells are derived from a human cervix epitheloid carcinoma; they are relatively large (approximately 20 μm) and particularly suitable for organelle visualization by immunofluorescence studies. Therefore, they were chosen as the cellular model system.

β-Gal characterization in aqueous solution and in the presence of LUV revealed that Trp residues are protected from interaction with aqueous solution and no significant interaction with membranes was observed. Enzymatic assays revealed that β-Gal maintains its quaternary structure, which is required for enzymatic activity (*15*) in aqueous solution, under reducing and nonreducing conditions. These results showed that the reducing environment did not modify the β-Gal conformation, so maintenance of enzyme activity inside the cell was expected.

Fluorescence quenching upon the titration of the protein with pep-1 suggests the existence of an excess of pep-1 in solution not interacting with the protein above peptide/protein molar ratios of 60 (data and detailed discussion in the Supporting Information). Enzymatic activity is still detected in the pep-1−β-Gal complex (a molar ratio of up to 400), which eliminates the severe perturbation of β-Gal structure due to pep-1.

The wavelength of maximal fluorescence emission intensity of pep-1 in lipidic membranes systems is higher than that observed for the complex (see Table 1). The blue shift observed for pep-1−β-Gal complexes relative to that of pep-1 alone together with its dependence on the peptide/protein molar ratio showed that pep-1 is mediating the partitioning of β-Gal into lipidic membranes.

Pep-1 translocation in LUV was previously found to be dependent on the transmembrane potential across bilayers (*14*). In fact, in this work, the same was concluded for the translocation of β-Gal mediated by pep-1 in LUV. These results suggested a common translocation mechanism for free and complexed pep-1. This property has been shown previously for other free peptides (*28*, *33*) but is here presented for the first time for a CPP−cargo protein complex, to the best of our knowledge.

β-Gal from *E. coli* was efficiently transported by pep-1 into HeLa cells, maintaining its enzymatic activity. The translocation of protein is dependent on peptide concentration; at a pep-1/β-Gal molar ratio of up to 200, translocation was not detected. With a pep-1/β-Gal ratio of 320, the process is very efficient. At this ratio, there is free pep-1 in solution (see Figure S1 of the Supporting Information), which seems to play a role in the translocation process. An excess of pep-1 is probably necessary for membrane destabilization (*14*), facilitating the uptake of the protein. If the translocation was mediated by pore formation, a very large pore (≈104 Å × 140 Å, estimated from the β-Gal crystallographic structure) would be necessary for a protein as large as β-Gal (116 kDa) to pass across the bilayer. A pore with such a diameter would probably induce leakage of the cellular contents at some extension, compromising cellular viability. Cell viability was maintained in the presence of pep-1 and the complex, and pore formation was not detected. This is in agreement with the study of interaction of pep-1 with LUV (see ref *14*), where pep-1 translocation occurred without pore formation.

The high velocity of the translocation mechanism (10 min was enough to detect protein inside the cell) and the independence of temperature (see Figure 1A,B) suggested a physical mechanism not dependent on complex cellular biochemical processes. This hypothesis was confirmed by the correlation found between cell depolarization and β-Gal translocation. Destroying the potassium electrochemical gradient drastically reduced the level of β-Gal uptake in HeLa cells (see Figure 2). These results are in agreement with those obtained with LUV. Therefore, in vivo the membrane charge asymmetry (*34*, *35*) and the combined effect of membrane potentials (*36*) seemed to be the driving forces responsible for the translocation process.

Inside the cell, the protein was found in the cytosol and did not colocalize with endosomes, lysosomes, or caveosomes (see Figure 3). These results were consistent with a translocation process independent of the classical endosomal pathways or caveolin-mediated endosomal pathways. In the case of endocytosis being a secondary mechanism for uptake, at least a small colocalization with one of these organelles would be expected. Monitoring localization of the protein, instead of pep-1, prevents problems associated with the apparent uptake of cationic peptides bound to negatively charged membranes, causing an artifactual localization in cells (*5*). Lebleu and co-workers found that TAT and oligoarginine uptake was dependent on endocytosis (*5*), but Nordén and co-workers (*9*) have proven that for arginine-rich peptides both nonendocytic and endocytic uptake pathways were involved in their cellular internalization. This nonendocytic mechanism was fast and biologically relevant (*9*). An endocytic pathway was not detected for pep-1, but a physical transmembrane crossing mechanism was.

A translocation mechanism independent of endocytosis was further confirmed under nonfixation conditions with anti-mouse TRITC where protein uptake at 4 °C has been observed (see Figure 4).

The transport of the dextran−TRITC marker mediated by pep-1 under conditions where the endocytosis was inhibited was also demonstrated (see Figures 5 and 6). It has been suggested by Morris et al. (*10*) that pep-1 interacts with macromolecules via hydrophobic interactions. Given the hydrophilic nature of the molecule, the capacity of pep-1 to translocate dextran demonstrated that hydrophobic pockets are not essential for complex formation and uptake. Complex formation of pep-1 and dextran is probably due to polar interactions and hydrogen bonding.

In conclusion, the interaction of pep-1 with β-Gal from *E. coli* was extensively studied to gain insight into the translocation mechanism at the molecular level. It has been demonstrated that pep-1 can establish a variety of electrostatic and/or hydrophobic and/or hydrophilic interactions with the cargo. The existence of a negative transmembrane potential promotes uptake of β-Gal, mediated by pep-1, in vitro and in vivo, and the absence of a transmembrane potential inhibits it. The charge asymmetry (negative inside) seems to be the driving force for translocation to occur. There was no evidence found for the involvement of the endocytic pathway in the uptake of cargo mediated by pep-1. Furthermore, pep-1 did not induce the formation of pores in the membrane. These results together suggested that the peptide and the cargo translocate only by a physical process.

ACKNOWLEDGMENT

We thank Dr. Adriano Henriques (Instituto de Tecnologia Química e Biológica) for the anti-β-galactosidase antibodies. We thank the Cell Imaging Service (IGC, Oeiras, Portugal) for the use of the confocal microscope.

SUPPORTING INFORMATION AVAILABLE

Further experimental results and discussion. This material is available free of charge via the Internet at http://pubs.acs.org.

REFERENCES

1. Wadia, J. S., Becker-Hapak, M., and Dowdy, S. F. (2002) Interactions of cell-penetrating peptides with membranes, in *Cell-penetrating peptides, processes and applications* (Langel, Ü., Ed.) pp 365−375, CRC Press Pharmacology and Toxicology Series, CRC Press, New York.
2. Bogoyevitch, M. A., Kendrick, T. S., Dominic, C. H., and Barr, R. K. (2002) Taking the cell by stealth or storm? Protein transduction domain (PTDs) as versatile vectors for delivey, *DNA Cell Biol. 21*, 879−894.
3. Bonetta, P. (2002) Getting protein into cells, *Scientist 17*, 38−40.
4. Eguchi, A., Akuta, T., Okuyama, H., Senda, T., Yokoi, H., Inokuchi, H., Fujita, S., Hayakama, T., Takeda, K., Hasegawa, M., and Nakanisshi, M. (2001) Protein transduction domain of HIV-1 Tat protein promotes efficient delivery of DNA into mammalian cells, *J. Biol. Chem. 247*, 27205−27210.

5. Richard, J. P., Melikov, K., Vives, E., Ramos, C., Verbeure, B., Gait, M. J., Chernomordik, L. V., and Lebleu, B. (2003) Cell-penetrating peptides, a reevaluation of the mechanism of cellular uptake, *J. Biol. Chem. 278*, 585−590.
6. Schwarze, S. R., Hruska, K. A., and Dowdy, S. F. (2000) Protein transduction: Unrestricted delivery into all cells? *Trends Cell Biol. 10*, 290−295.
7. Chaloin, L., Mau, N. V., Divita, G., and Heitz, F. (2002) Interactions of cell-penetrating peptides with membranes, in *Cell-penetrating peptides, processes and applications* (Langel, Ü., Ed.) pp 23−51, CRC Press Pharmacology and Toxicology Series, CRC Press, New York.
8. Joliot, A., and Prochiantz, A. (2004) Transduction peptides: From technology to physiology, *Nat. Cell Biol. 6*, 189−196.
9. Thorén, P. E. G., Persson, D., Isakson, P., Goksör, M., Önfelt, A., and Nordén, B. (2003) Uptake of analogs of penetratin, Tat(48−60) and oligoarginine in live cells, *Biochem. Biophys. Res. Commun. 307*, 100−107.
10. Morris, M. C., Depollier, J., Mery, J., Heitz, F., and Divita, G. (2001) A peptide carrier for the delivery of biologically active proteins into mammalian cells, *Nat. Biotechnol. 19*, 1143−1147.
11. Wu, Y., Wood, M. D., and Katagiri, F. (2003) Direct delivery of bacterial avirulance proteins intro resistant *Arabidopsis* protoplasts lead to hypersensitive cell death, *Plant J. 33*, 131−137.
12. Ikari, A., Nakaro, M., Kawano, K., and Suketa, Y. (2002) Up-regulation of sodium-dependent glucose transporter by interaction with heat shock protein 70, *J. Biol. Chem. 277*, 33338−33343.
13. Zhou, J., and Hsieh, J.-T. (2001) The inhibitory role of DOC-2/DAB2 in growth factor receptor-mediated signal cascade, *J. Biol. Chem. 276*, 27793−27798.
14. Henriques, S. T., and Castanho, M. A. R. B. (2004) Consequences of nonlytic membrane perturbation to the translocation of the cell penetrating peptide pep-1 in lipidic vesicles, *Biochemistry 43*, 9716−9724.
15. Nichtl, A., Buchner, J., Jaenicke, R., Rudolph, R., and Scheibel, T. (1998) Folding and association of β-galactosidase, *J. Mol. Biol. 282*, 1083−1091.
16. Fery-Forgues, S., and Lavabre, D. (1999) Are fluorescence quantum yields so tricky to measure? A demonstration using familiar stationery products, *J. Chem. Educ. 76*, 1260−1264.
17. Lakowics, J. R. (1999**)** *Principles of fluorescence spectroscopy*, 2nd ed., Kluwer Academic/Plenum, New York.
18. Coutinho, A., and Prieto, M. (1993) Ribonuclease T1 and alcohol dehydrogenase fluorescence quenching by acrylamide. A laboratory experiment for undergraduate students, *J. Chem. Educ. 70*, 425−428.
19. McGuire, J. B. J., James, T. J., Imber, C. J., St. Peter, S. D., Friend, P. J., and Taylor, R. P. (2002) Optimisation of an enzymatic method for β-galactosidase, *Clin. Chim. Acta 326*, 123−129.
20. Haugland, R. P. (2002) *Handbook of fluorescent probes and research products*, 9th ed., Molecular Probes, Eugene, OR.
21. Mayer, L. D., Hope, M. J., and Cullis, P. R. (1986)Vesicles of variable sizes produced by a rapid extrusion method, *Biochim. Biophys. Acta 858*, 161−168.
22. Mosmann, T. (1983) Rapid colorimetric assay for cellular growth and survival: Application to proliferation and citotoxicity assays, *J. Immunol. Methods 65*, 55−63.
23. Coulpier, M., Anders, J., and Ibáñez, C. F. (2002) Coordinated activation of autophosphorylation sites in the RET receptor tyrosine kinase. Importance of tyrosine 1062 for GDNF mediated neuronal differentiation and survival, *J. Biol. Chem. 277*, 1991−1999.
24. Chariot, simple efficient protein delivery system. http://www.activemotif.com/products/cell/chariot.php (accessed May 2005).
25. Tisdale, E. J. (2002) Glyceraldehyde-3-phosphate dehydrogenase is phosphorylated by pyotein kinase C and plays a role in microtubule dynamics in the early secretory pathway, *J. Biol. Chem. 277*, 3334−3341.
26. Sousa, V. L., Brito, C., Costa, T., Lanoix, J., Nilsson, T., and Costa, J. (2003) Importance of Cys, Gln, and Tyr from the transmembrane domain of Human β3/4 fucosyltransferase III for its localization and sorting in the Golgi of baby hamster kidney cells, *J. Biol. Chem. 278*, 7624−7629.
27. Sousa, V. L., Brito, C., and Costa, J. (2004) Delection of the cytoplasmic domain of human α3/4 fucosyltransferase III causes the shift of the enzyme to early golgi compartments, *Biochim. Biophys. Acta 1675*, 95−104.
28. Rothbard, J. B., Jessop, T. C., Lewis, R. S., Murray, B. A., and Wender, P. A. (2004) Role of membrane potential and hydrogen bonding in the mechanism of translocation of guanidium-rich peptides into cells, *J. Am. Chem. Soc. 126*, 9506−9507.
29. Deshayes, S., Heitz, A., Morris, M. C., Charnet, P., Divita, G., and Heitz, F. (2004) Insight into the mechanism of internalization of the cell-penetrating carrier peptide pep-1 through conformational analysis, *Biochemistry 43*, 1449−1457.
30. Chifflet, S., Hernández, J. A., Grasso, S., and Cirillo, A. (2003) Nonspecific depolarization of the plasma membrane potential induces cytoskeletal modifications of bovine corneal endothelial cells in culture, *Exp. Cell Res. 282*, 1−13.
31. Szeto, H. H., Schiller, P. W., Zhao, K., and Luo, G. (2005) Fluorescent dyes alter intracellular targeting and function of cell-penetrating tetrapeptides, *FASEB J.* (in press).
32. Lundberg, M., and Johansson, M. (2002) Positively charged DNA-binding proteins cause apparent cell membrane translocation, *Biochem. Biophys. Res. Commun. 291*, 367−371.
33. Terrone, D., Sang, S. L. W., Roudaia, L., and Silvius, J. R. (2003) Penetratin and related cell-penetrating cationic peptides can translocate across lipid bilayers in the presence of a transbilayer potential, *Biochemistry 42*, 13787−13799.
34. Gennis, R. B. (1989) *Molecular structure and functions*, Springer-Verlag, New York.
35. Manno, S., Takakuwa, Y., and Mohandas, N. (2002) Identification of a functional role for lipid asymmetry in biological membranes: Phosphatidylserine-skeletal protein interactions modulate membrane stability, *Proc. Natl. Acad. Sci. U.S.A. 99*, 1943−1948.
36. O'Shea, P. (2003) Intermolecular interactions with/within cell membranes and the trinity of membrane potentials: Kinetics and imaging, *Biochem. Soc. Trans. 31*, 990−996.

BI0502644

SUPPORTING INFORMATION

As expected titration of β-Gal with pep-1 led to a progressive red-shift in the emission spectra (Figure S1A) until the pep-1 maximum emission wavelength (346 nm) was achieved. Fluorescence spectrum for each pep-1:β-Gal ratio has the contribution of β-Gal and pep-1 in free and complexed form. The occurrence of the fluorescence emission spectral peak at 346 nm for the 100 pep-1:β-Gal ratio suggests an excess of free pep-1 in this condition. The result of integrated fluorescence intensity of the complex at different pep-1:β-Gal ratios are presented in Figure S1B. Curve 1 represents the fluorescence intensity variation of the complex, where three regimes were detected: I) up to 14 molar ratio there was a slight decrease in intensity; II) from 14 to 60 ratio there was a small increase in intensity and III) from 60 up, the slope increased. This curve was compared with the summed fluorescence intensities from free peptide and free protein (curve 2 in Figure S1B). Fluorescence quenching occurs in the first regime; in the second regime the fluorescence quenching was less pronounced, and in the third regime quenching was barely noticeable. This last regime corresponds to peptide-saturated protein. From peptide:protein molar ratios of 60 and up peptide added to solution will remain free (unbound to the protein). In reducing environment the results were similar but the second regime did not vanish in the pep-1:β-Gal ratio experimental range (<100).

A hypothesis to explain the results at molecular level is that in the first regime electrostatic interaction between pep-1 and β-Gal take place for charge neutralization (β-Gal has -38 charge and pep-1 +3; a peptide/protein ratio of 13 is required for neutralization). These interactions are strong enough to induce a decrease in fluorescence intensity relative to the summed individual contributions pep-1 and β-Gal. In the second regime weaker interactions are occurring (quenching is diminished); considering the amphipathic-like nature of pep-1, hydrophobic interactions between pep-1 and β-Gal can be speculated. Pep-1 in free form appears to be dominant after a 60 ratio. Inexistence of a third slope in reducing environment up to a ratio of 100 suggests an increase of peptide affinity to β-Gal.

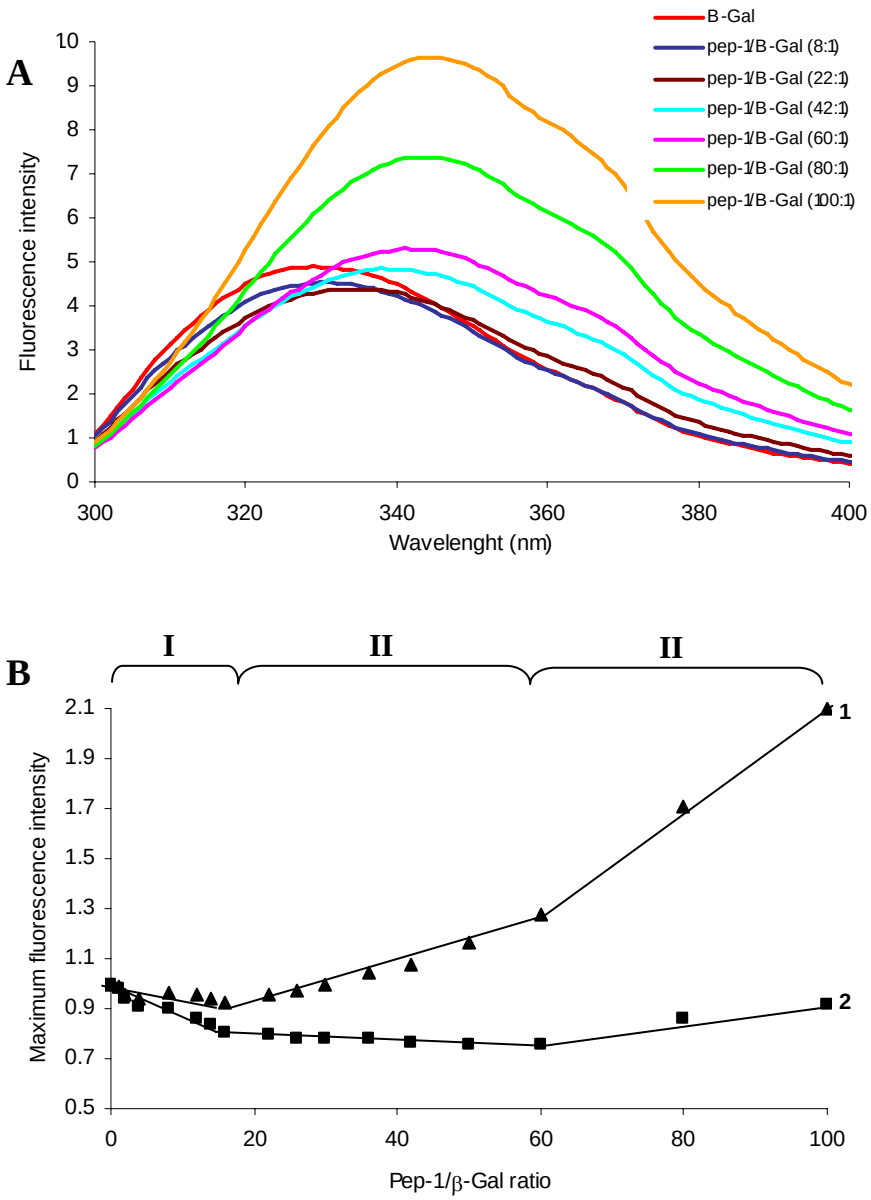

FIGURE S1: Pep-1/β-Gal complex formation by β-Gal titration with pep-1. Panel A shows some of the fluorescence emission spectra obtained at constant protein concentration (72 nM) with excitation at 280 nm. There is a change in the integrated intensity besides spectral shifting. Panel B shows the dependence of the integrated emission intensity on Pep-1:β-Gal molar ratio (curve 1). When the complex integrated intensity is divided by the sum of the isolated contributions of free β-Gal and free pep-1 (curve 2), it is possible to identify three different regimes having different slopes. I) up to 14 molar ratio quenching of fluorescence exists (direct or indirect consequence of electrostatic interaction between pep-1 and protein); II) from 14 to 60 molar ratio quenching of protein by pep-1 still exists but is less pronounced (hydrophobic interactions between pep-1 and β-Gal are probably dominant in this regime); III) β-Gal fluorescence intensity has a slightly increase (suggesting that there are no more pep-1-protein interactions).

4.2.2. Re-evaluating the role of strongly charged sequences in amphipathic cell-penetrating peptides. A fluorescence study using pep-1.

4.2.2.1. Motivation and methodologies

In the previous paper [230] we have tracked the internalization of the cargo (β-Gal) mediated by pep-1. The cargo was followed instead of the CPP to avoid possible artefacts associated with high affinity of peptides for membranes which may remain attached to cells and an apparent localization in the cell could result therefrom [55, 56]. The experimental work presented in the previous paper [230] was important to confirm the ability of pep-1 to introduce large proteins inside the cell and to gain information about the translocation mechanism. Besides the translocation mechanism, we decided to gain insight on the pep-1 route after internalization. A modified pep-1 with a fluorescent probe attached to the hydrophilic domain was used.

CPPs internalization into cellular lines has been followed by means of several methodologies through the literature. Fluorescent labels are commonly used to investigate the mechanisms of cellular uptake and intracellular distribution of CPPs [15, 27, 31, 32, 54, 58-61, 65-67, 70, 73, 75, 78, 79, 105, 168, 231-255]. Fluorescein is the most frequent probe attached to CPPs [15, 27, 31, 58, 60, 61, 65, 73, 75, 79, 231, 232, 234, 235, 237, 238, 241, 243-245, 250], however Lucifer yellow [105], Rhodamine [32, 54, 59, 66, 242], Texas red [67, 233], NBD [59, 78, 239] or Alexa fluor [63, 251] are other possibilities. Alternatively CPPs can be biotynilated and detected by avidin or streptavidine [63, 252] or detected by a specific antibody [256]. Microscopy [32, 61, 65-67, 241, 242, 254, 257], flow cytometry [67, 237, 245, 257, 258] or spectrofluorimetry [59, 78] are techniques that can be employed for CPP internalization detection.

To follow the pep-1 uptake into cultured cells the probe carboxyfluorescein (CF) was used. CF was linked to the hydrophilic domain by an extra Lys residue and the C terminal was blocked with a Ser instead of Cysteamine to avoid steric constraints. The final hydrophobic domain sequence was: KKRKVK(CF)-S.

Fluorescein, as other labels are relatively large and lipophilic, and may significantly modify physicochemical properties of CPPs [259]. A careful evaluation of the possible effect of this fluorescent label attached to pep-1 was carried on.

The characterization of the interaction of pep-1-CF with model membranes was followed by Trp fluorescence, as previously explained (see chapter 2 and reference

[153]), and by CF fluorescence. Partition and in-depth location of peptide in lipidic membranes was studied and compared with results obtained for unlabelled pep-1.

Alterations on membrane polarization were evaluated by the use of lipophilic probes $DiSBAC_2(3)$. This dye belongs to the family of bis-barbituric acid oxonols, also referred to as DiBAC dyes, or as "bis-oxonol", which have an excitation maximum close to 490nm [260]. When it moves from a polar environment to a non-polar environment, like lipidic membranes, its fluorescence quantum-yield is markedly increased. Upon membrane depolarization the uptake the dye by the membrane increases and the overall fluorescence intensity also increases. When the membrane is hyperpolarized, partition to the membrane decreases and also does fluorescence intensity [261]. $DiSBAC_2(3)$ has affinity for liposomes, in the presence of peptide one can evaluate if the membrane is becoming more or less polarized.

The possibility of peptide translocation across mammalian cells was evaluated in the presence/absence of β-Gal by fluorescence microscopy using the same methodology previously referred (see section 4.2.1.3 and reference [230]), however it was verified that pep-1-CF fluorescence intensity was not strong enough to be followed by microscopy. To overcome this limitation a fluorescence plate reader was used instead, taking advantages on trypan blue (TB) quencher properties [262-265]. TB diffuses rapidly into non-viable cells [266], however is unable to enter into viable cells [267], consequently TB will quench non-specific background fluorescence and also the fraction of peptide adsorbed at cell surface and non-internalized pep-1CF [262]. With this approach it is possible to follow internalization at several incubation times in non-fixation conditions; briefly, TB is added after cell incubation and CF fluorescence is followed in the plate reader.

Methodologies and results obtained are explained in more details in the short communication: *Re-evaluating the role of strongly charged sequences in amphipathic cell-penetrating peptides. A fluorescence study using pep-1*.

4.2.2.2. Declaration on authorship of published manuscript: *Re-evaluating the role of strongly charged sequences in amphipathic cell-penetrating peptides. A fluorescence study using pep-1*.

I, Sónia Troeira Henriques declare that the experimental design, the laboratory work, the data analysis, discussion and manuscript preparation were carried out by me under guidance of Dr. Miguel ARB Castanho and Dr. Julia Costa. *In vitro* studies were carried on Faculdade de Ciências (University of Lisbon) and supervised by Dr. Miguel ARB Castanho while studies with mammalian cells were carried out in ITQB under supervision of Dr. Julia Costa.

I, Miguel ARB Castanho, as Sónia T Henriques supervisor, hereby acknowledge and confirm the information above is correct.

_____ _____

Sónia Troeira Henriques Miguel ARB Castanho

FEBS Letters 579 (2005) 4498–4502 FEBS 29811

Re-evaluating the role of strongly charged sequences in amphipathic cell-penetrating peptides
A fluorescence study using Pep-1

Sónia T. Henriques[a], Júlia Costa[b], Miguel A.R.B. Castanho[a,*]

[a] *Centro de Química e Bioquímica, Faculdade de Ciências da Universidade de Lisboa, Ed. C8, Campo Grande, 1749-016 Lisboa, Portugal*
[b] *Instituto de Tecnologia Química e Biológica, Apartado 127, 2780 Oeiras, Portugal*

Received 13 June 2005; accepted 30 June 2005

Available online 26 July 2005

Edited by Peter Brzezinski

Abstract Cell-penetrating peptides (CPPs) are able to translocate across biological membranes and deliver bioactive proteins. Cellular uptake and intracellular distribution of CPPs is commonly evaluated with fluorescent labels, which can alter peptide properties. The effect of carboxyfluorescein label in the Lys-rich domain of the amphipathic CPP pep-1, was evaluated and compared with non-labelled pep-1 in vitro and in vivo. A reduced membrane affinity and an endosomal-dependent translocation mechanism, at variance with non-labelled pep-1, were detected. Therefore, the charged domain is not a mere enabler of peptide adsorption but has a crucial role in the translocation pathway of non-labelled pep-1.

Keywords: Cell-penetrating peptide; Drug delivery; Translocation mechanism; Transmembrane potential

1. Introduction

The discovery of various basic peptides (9–33 amino acid residues) with ability to translocate across cell membranes has attracted much interest in biomedical research [1]. These peptides, known as cell-penetrating peptides (CPPs), have been successfully used to deliver biopharmaceutical macromolecules in vivo. The use of such delivery systems is of great interest to evade the poor cellular access and bioavailability of drugs [2].

The translocation mechanism used by this group of carriers has been extensively studied in the last 10 years, but the results are frequently contradictory and disperse. A single general mechanism for all does not seem reasonable and more than one mechanism for a unique peptide is a possibility [3,4]. To evaluate the cellular uptake and intracellular distribution of CPP, fluorescent labels are commonly used. However, when these labels are large and lipophilic they may alter physicochemical properties and the cellular distribution of the peptide [5].

Pep-1 (Ac-KETWWETWWTEWSQPKKKRKV-cysteamine) is a synthetic peptide carrier forming physical assemblies with a great variety of proteins and other macromolecules, which have been successfully translocated in different cell lines [6–10]. It has been shown that pep-1 translocates across membranes by a physical process mediated by transmembrane potential, both in vitro and in vivo, in free form [11] or when complexed with a protein, with no evidence for an alternative mechanism [7]. Because the translocation is solely physically mediated, the hydrophobicity and charge distribution of the peptide and its interaction with membranes is of first importance. The amphipathicity of the carrier is probably responsible by the strong interaction with the lipidic membranes [12]. Unlike other cationic CPPs (e.g., penetratin) [13] pep-1 has a high affinity for neutral vesicles and for membranes in gel-like phase. The presence of cysteamine group in C terminal seems to play a crucial role in the delivery efficiency of cargoes into cells [12].

In the present paper, the study of a modified peptide with a carboxyfluorescein probe (pep-1CF) is compared with pep-1. In this peptide, the hydrophilic domain (KKKRKV-cysteamine) has been customized to accommodate the label. An extra Lys was introduced to link the probe and C terminal is blocked with a Ser instead of cysteamine to avoid steric constraints (KKRKVK(CF)-S). The effect of the alteration introduced in this hydrophilic domain in the translocation mechanism is presented, using both the Trp residues and CF moiety as reporters of the so-called hydrophobic and hydrophilic domains, respectively.

2. Materials and methods

Pep-1 and Pep-1CF with purity >95% were obtained from *GenScript Corporation*, New Jersey. β-Galactosidase from *Escherichia coli* (β-Gal), 4-methylumbelliferyl-galactoside (MUG), Triton X-100 (TX-100) and trypan blue (TB) were obtained from Sigma–Aldrich, MO. 1-Palmitoyl-2-oleoyl-*sn*-glycero-3-phosphocholine (POPC), 1-palmitoyl-2-oleoyl-*sn*-glycero-3-(phospho-rac-(1-glycerol)) (POPG), were from Avanti Polar-Lipids, Alabama. 5-Doxyl-stearic acid (5DS) and 16-doxyl-stearic acid (16DS) from Aldrich Chem Co., WI. Minimum essential medium Eagles with Earle's salts (MEME) and supplements were obtained from Gibco Invitrogen Corporation, CA.

*Corresponding author. Fax: +351217500088.
E-mail address: castanho@fc.ul.pt (M.A.R.B. Castanho).

Abbreviations: CPP, cell-penetrating peptide; CF, carboxyfluorescein; β-Gal, β-galactosidase; MUG, 4-methylumbelliferyl-galactoside; TX-100, Triton X-100; TB, trypan blue; POPC, 1-palmitoyl-2-oleoyl-*sn*-glycero-3-phosphocholine; POPG, 1-palmitoyl-2-oleoyl-*sn*-glycero-3-(phospho-rac-(1-glycerol)); 5DS, 5-doxyl-stearic acid; 16DS, 16-doxyl-stearic acid; MEME, minimum essential medium Eagles; LUVs, large unilamellar vesicles; 4-MU, 4-methylumbelliferone

0014-5793/$30.00
doi:10.1016/j.febslet.2005.06.085

2.1. Characterization of pep-1CF in aqueous solution

Pep-1CF solutions were prepared in HEPES buffer (10 mM HEPES, pH 7.4 containing 10 mM (low ionic strength) or 150 mM NaCl (the so-called physiologic ionic strength)). The assays were performed at room temperature in a UV–Vis spectrophometer Jasco V-560 and in a spectrofluorometer SLM Aminco 8100. Fluorescence intensity values were corrected for inner filter effect [14].

The absorption and fluorescence emission characteristics of the hydrophobic domain (by means of Trp fluorescence; $\lambda_{exc} = 280$ nm, $\lambda_{em} = 350$ nm) and of the hydrophilic domain (by CF group; $\lambda_{exc} = 490$ nm, $\lambda_{em} = 520$ nm), were studied. Quantum yield-dependence on peptide concentration (0–18 μM) and ionic strength (by means of NaCl concentration variation) were also evaluated. Fluorescence quenching of Trp residues by acrylamide was carried out using $\lambda_{exc} = 290$ nm to minimize the relative quencher/fluorophore light absorption ratio. Quenching data were corrected as described in [12].

2.2. Interaction of pep-1CF with model membranes

Large unilamellar vesicles (LUVs), with typical 100 nm diameter were prepared by the extrusion method described elsewhere [15] and used as model of biological membranes. Liquid-crystal phase vesicles composed by POPC or POPC:POPG (4:1 molar) were used to model the outer leaflet (neutral) and the inner leaflet (negatively charged) of mammals' biological membranes [16]. The extent and kinetics of partition and the in-depth location of pep-1CF were evaluated using the same procedure as for pep-1 [12]. Both hydrophobic and hydrophilic domains were studied.

The $DiSBAC_2(3)$ dye is a probe with a higher affinity for depolarized than polarized membranes and its apparent quantum yield being dependent on the extent of interaction with membranes [17]. These fluorescence properties were used to evaluate alterations in transmembrane potential of model membranes upon addition of pep-1CF. Vesicles in the absence and presence of a negative transmembrane potential were prepared as described in [11]; $DiSBAC_2(3)$ was added to lipidic suspension to a final concentration of 0.25 mM and fluorescence emission intensity ($\lambda_{exc} = 540$ nm, $\lambda_{em} = 558$ nm) was followed during titration of lipidic suspension with pep-1CF (576 μM stock solution) or non-labelled pep-1 (688 μM stock solution).

2.3. Translocation studies of pep-1CF in HeLa cells

Adherent human negroid cervix epitheloid carcinoma cells (HeLa) were grown in MEME supplemented with 2 mM L-Glu, 2 mM non-essential aminoacids, 10% (v/v) fetal bovine serum and 1% (v/v) streptomycin and penicillin, in a 5% CO_2 humidified atmosphere at 37 °C. Cell viability was determined by the TB exclusion assay, see [7].

The translocation of pep-1CF and it capacity to mediate the uptake of β-Gal were followed in non-fixation conditions. Cells with 90% confluence, seeded in 96-well plates, were incubated with 40 μL of 3.5 μM pep-1CF, (in free or complexed form with β-Gal (peptide/protein ratio of 320), prepared in free-serum medium), in sixplicates, during 0, 30, 60, 90, 120, 150, 180, 210 and 240 min at 4 or 37 °C.

The quencher properties of TB and it inability to enter in viable cells [18] were used to evaluate the pep-1CF translocation. This hydrophilic molecule is able to quench non-internalized particles, including the fraction adsorbed to the cell membrane, but is inaccessible to internalized fraction [19], so removal of extracellular peptide is needless. The pep-1CF fluorescence was followed, before and after addition of TB (1.9 μL of stock solution, 0.4% w/v), with excitation and emission filters at 485/20 (centre/width) and 590/35 nm, respectively, in a FL500 microplate fluorescence reader. To evaluate the effect of protein in the extension of peptide internalization, the same procedure was followed with pep-1CF complexed.

Delivery efficiency of β-Gal mediated by pep-1CF was evaluated by it enzymatic activity using a non-fluorescent substrate (MUG) which is converted in a fluorescent product (4-methylumbelliferone, 4-MU), see [7] for a detailed description. Briefly, after incubation with pep-1CF/β-Gal complex (see above), cells were washed three times with phosphate buffer saline solution to eliminate non-incorporated protein and peptide. Internalized β-Gal was accessed after cell permeabilization with 0.1% (w/v) TX-100. Substrate (0.1 mM MUG) was added to the cells and incubated with the enzyme during 30 min at 37 °C. NaOH was added to stop the reaction (pH ≈ 12) and product formation (4-MU) was monitored with excitation and emission filters at 360/40 and 460/40 nm, respectively. The same procedure was performed with non-labelled peptide. Controls without pep-1 or pep-1CF were carried out.

The effect of peptide in the protein was determined by comparing it enzymatic activity in free and complexed forms (with non-labelled pep-1 or pep-1CF) in vitro (see [7]).

3. Results and discussion

3.1. Pep-1CF aggregates in aqueous solution

Similarly to non-labelled pep-1 [12], Trp residues in the hydrophobic domain of pep-1CF, have a red-edge excitation shift and an efficient fluorescence quenching by acrylamide (51.8 ± 12 and 42.1 ± 9.1 M^{-1} for low and physiologic ionic strength, respectively) with a negative deviation from linearity. These results indicate that the peptide aggregates in solution (see [12]). Nevertheless, the quantum yield and steady-state anisotropy of the CF group in hydrophilic domain is not dependent on concentration, for both ionic strengths (10 and 150 mM), which suggests that internal organization of the peptide is not affected by these factors.

3.2. Partition and in-depth location of pep-1CF in model membranes

Affinity of hydrophobic and hydrophilic domains for lipidic membranes was evaluated by titration of an aqueous suspension of the pep-1CF (5.76 μM) with lipidic vesicles; both Trp and CF fluorescence emission were monitored. Spectral alterations on fluorescence emission and anisotropy ($r = 0.05$) were not detected, either for POPC or POPC:POPG (4:1) LUVs. These results suggest that the hydrophilic domain does not strongly interact with model membranes. When Trp residues were followed, the addition of lipidic suspension led to both blue-shifted emission spectra (Fig. 1A) and an increase in the fluorophore quantum yield (Fig. 1B). The partition coefficients (determined by fluorescence emission intensity as in [12]) are $(4.2 \pm 0.8) \times 10^2$ for POPC and $(1.7 \pm 0.2) \times 10^3$ for POPC:POPG (4:1) at physiologic ionic strength. These values are significantly smaller than the ones obtained for non-labelled pep-1 ($(3.4 \pm 0.6) \times 10^3$ and $(2.8 \pm 0.4) \times 10^4$ [12]), which indicates a decrease in membrane affinity even for the hydrophobic domain. Concomitantly, partition rates decrease ($t_{1/2} = 197$ ms in POPC and 147 ms in POPC:POPG (4:1) for pep-1CF in comparison with 120 and 34 ms, respectively, for unlabelled pep-1).

An extensive fluorescence emission quenching of Trp residues by acrylamide, in the presence of lipidic membranes, is indicative of significant amounts of peptide non-inserted in the membrane, at discrepancy with pep-1 in the same conditions where no significant acrylamide quenching was detected [12].

In-depth location of the hydrophobic domain of pep-1CF was carried out by means of fluorescence quenching of Trp residues with doxyl-derivatized stearic acids. The quenching is more efficient when the quencher is closer to the Trp residues. Therefore, 5DS probes the bilayer interface while 16DS probes its core [20]. Quenching by 5DS is more efficient than by 16DS, this is true for POPC ($K_{SV,5DS} = 16.1 \pm 3.8$ M^{-1}, $K_{SV,16DS} = 5.2 \pm 0.9$ M^{-1}) and POPC:POPG (4:1) ($K_{SV,5DS} = 15.3 \pm 3.5$ M^{-1}, $K_{SV,16DS} = 4.9 \pm 1.0$ M^{-1}). This is evidence for a position of the hydrophobic region at the membrane interface in both lipidic systems studied. The same conclusion was obtained in the study of non-labelled pep-1 [12].

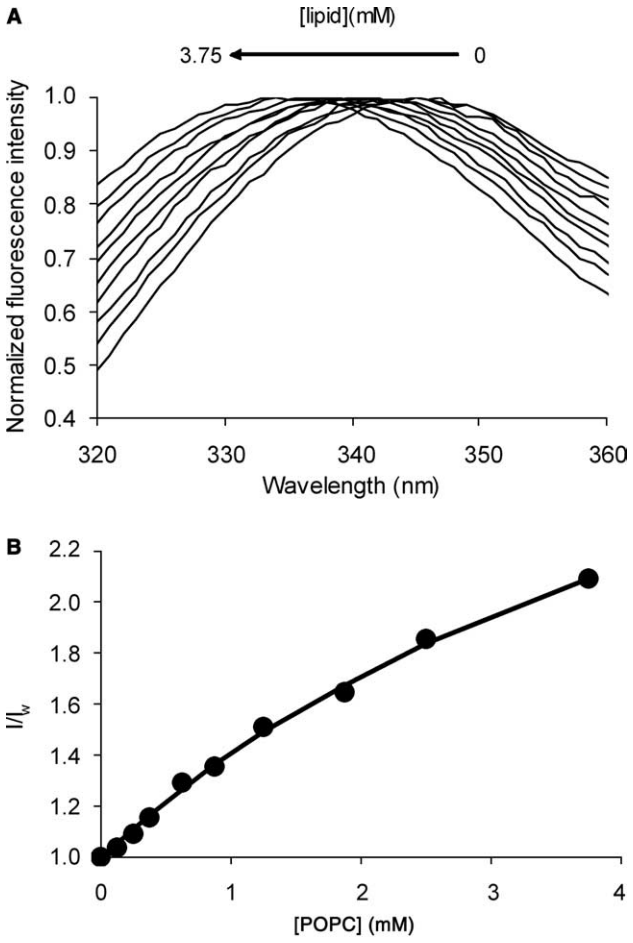

Fig. 1. Partition of Pep-1CF-hydrophobic domain in POPC LUVs (λ_{exc} = 280 nm). (A) shifting of pep-1CF fluorescence emission spectra with lipidic concentration (0–3.75 mM). (B) Fluorescence intensity emission maximum dependence on lipidic concentration.

Quenching of CF group by 5DS and 16DS was negligible, supporting the hypothesis that the hydrophilic domain does not insert in the membrane.

3.3. Translocation of pep-1 and pep-1CF in LUVs is dependent on transmembrane potential

To evaluate pep-1CF translocation in model membranes, the fluorescence of $DiSBAC_2(3)$ was followed. The quantum yield of the probe increases with depolarization of membranes.

Titration of POPC LUVs (in absence (1) or presence (2) of transmembrane potential) with pep-1CF is presented in Fig. 2. The variation of probe fluorescence emission differs for the two situations (with/without potential). When transmembrane potential exists the addition of pep-1CF induces an increase in fluorescence intensity, so membrane is depolarized. In the absence of a transmembrane potential a decrease quantum yield was detected, which indicates a polarization of membrane.

These results suggest that in the absence of transmembrane potential the peptide accumulates in the outer leaflet of membrane, without translocation. The positive global charge of pep-1CF is responsible by membrane polarization.

In the presence of a transmembrane potential (negative inside) pep-1CF is able to translocate across membrane, reducing the negative transmembrane potential, with an increase in quantum yield of $DiSBAC_2(3)$.

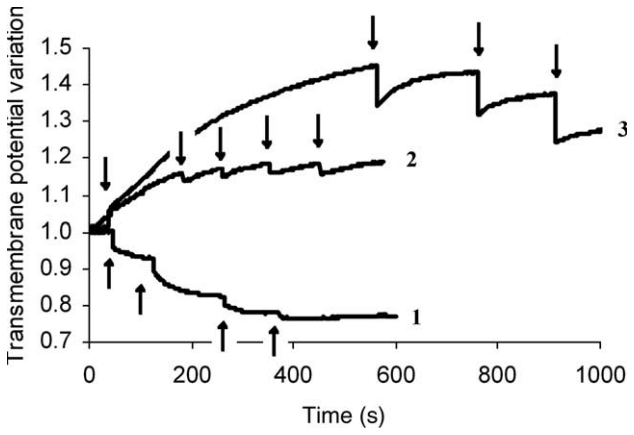

Fig. 2. Variation of transmembrane potential in POPC LUVs by titration with pep-1CF in absence (1) or presence of transmembrane potential (2) or with non-labelled pep-1 in presence of transmembrane potential (3). Monitored with $DiSBAC_2(3)$ fluorescence emission (λ_{exc} = 540 nm, λ_{em} = 558 nm) (inserts indicate addition of 5μL from pep-1CF or pep-1 stock solution).

Similar results were obtained with non-labelled pep-1 using this (Fig. 2, curve (3)) and other methodologies [11], but the effect of a negative transmembrane potential is more pronounced, which suggest that pep-1 has a more efficient translocation than pep-1CF. This is expected considering the lower affinity of pep-1CF for phospholipids membranes.

3.4. Translocation kinetic of pep-1CF and pep-1CF/β-Gal in HeLa cells

Translocation of pep-1CF in HeLa cells was evaluated at 4 and 37 °C (Fig. 3) by the use of TB quenching properties. Its capacity to interact with the CF dye and to quench its fluorescence emission was used to distinguish internalized from surface-bound pep-1CF [18]. The quenching extent is decreased when the peptide translocates across cell membranes and become inaccessible to the quencher.

At 37 °C, we observed fluorescence recovery up to 240 min incubation at variance with results at 4 °C where the fluorescence intensity remained unchanged during the same time (Fig. 3A). This suggest that translocation of pep-1CF occurs via endocytosis. Recently, it has been found that two N-terminally CF-labelled CPPs are internalized by HeLa cells via raft-mediated endocytosis [21].

Significant differences in the kinetics of translocation, for free (Fig. 3A) or complexed (Fig. 3B) forms, of Pep-1CF were not detected.

The uptake of the β-Gal cargo itself, at 4 and 37 °C, was evaluated by following the enzymatic hydrolysis, of a non-fluorescent substrate (MUG) to a fluorescent product (4-MU). The hydrolysis step is carried out at 37 °C after the translocation incubation step. We observed that the translocated protein was active and that the uptake of protein was much more efficient at 37 °C than at 4 °C (180 min after incubation the fluorescence emission intensity of 4-MU was found to be 14.5 times higher at 37 °C relative to 4 °C).

In order to investigate the effect of CF-derivatization in peptide translocation, we compared the efficiency of β-Gal internalization mediated by pep-1 vs. pep-1CF (Fig. 4). When the

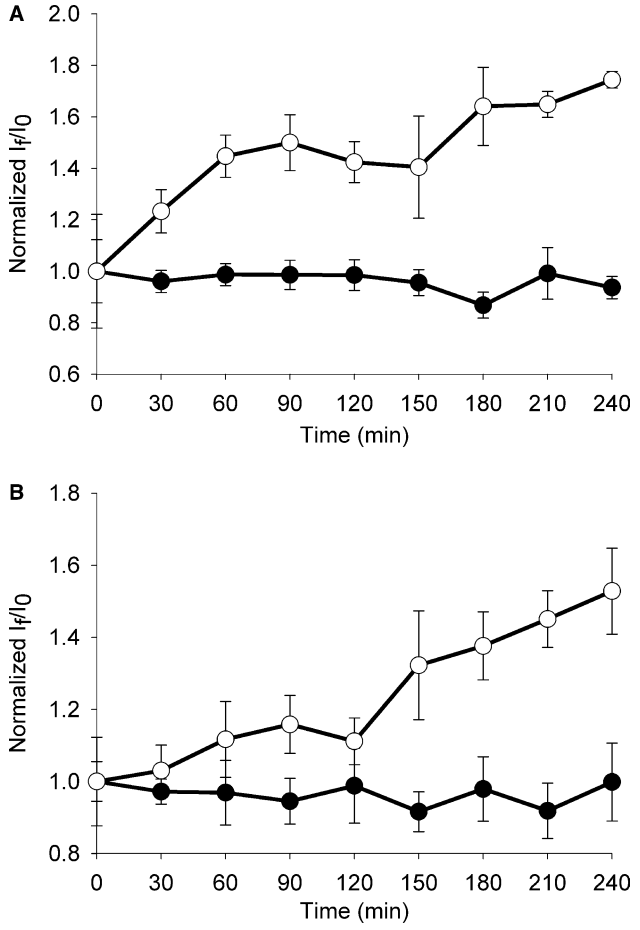

Fig. 3. Kinetics of Pep-1CF uptake in HeLa cells: (A) in free form or (B) complexed with β-Gal at 37 °C (white circles) or 4 °C (black circles). Internalization was followed by means of fluorescence emission (I_f) dequenching of CF. Peptide internalization into cells leads to fluorescence recovery due to inaccessibility to TB (quencher). The relative fluorescence intensity, I_f/I_0 (I_0 is the fluorescence intensity in the absence of TB) was normalized at $t = 0$.

β-Gal uptake was mediated by pep-1 there were no significant differences between 4 and 37 °C [7]. However, efficiency was different for the labelled and unlabelled peptides (Fig. 4),

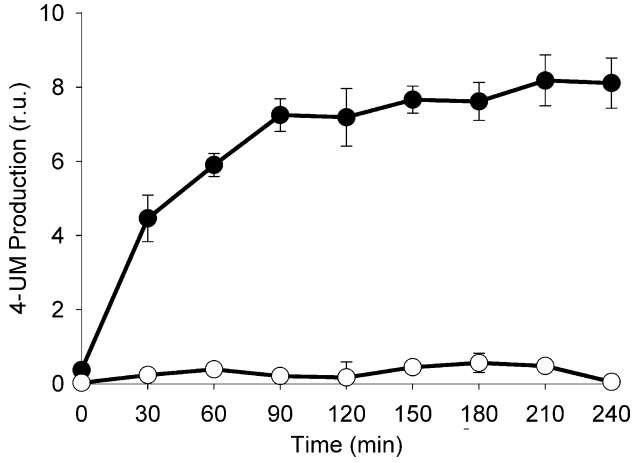

Fig. 4. Delivery of β-Gal into HeLa cells at 37 °C, followed by enzymatic production of 4-UM, mediated by pep-1CF (white circles) or by pep-1 (black circles).

revealing that the hydrophilic domain of the peptide is of critical importance for translocation.

We analysed the enzyme activity, in vitro, in free and in complexed forms. The determined v_0 of β-Gal are: 19.18 ± 0.24 μM/min for free form; 11.60 ± 0.53 μM/min when complexed with unlabelled-pep-1 and 19.61 ± 0.38 μM/min in the complex with pep-1CF. The presence of pep-1 reduces the activity of the enzyme (in agreement with [7]), but this does not hold for pep-1CF. This suggests that the pep-1CF does not interact as strongly with the protein, which is an additional effect induced by the presence of CF in the Lys-rich domain. This supports the hypothesis that pep-1 interacts with the cargo both by means of hydrophobic and electrostatic interactions [7].

The mechanism of translocation of pep-1CF is different from the one identified previously for pep-1. A simple physical mechanism mediated by electrostatic interaction between pep-1 and membrane is supported by different sets of experimental data [7,11]. However, Pep-1CF follows a different pathway, dependent on temperature, i.e., endocytic.

It should be stressed that pep-1CF has translocation ability via physical (non-endocytic) processes (Fig. 2), however, such ability is clearly decreased compared to unlabelled pep-1 (Fig. 2), in agreement with its smaller partition into membranes. At 4 °C, the low cell membrane fluidity also contributes to inhibit physical translocation of pep-1CF. It is only at 37 °C that the endocytic pathway becomes an alternative to the physical process and translocation occurs. A small contribution of the endocytic pathway for translocation of unlabelled pep-1 at 37° cannot be discarded, although a physical process is clearly dominant [7,11].

A reduced protein-uptake mediated by pep-1CF is due, not only, to a decrease in translocation efficiency but also to a diminished interaction of the pep-1CF with β-Gal.

3.5. Conclusion

Translocation of pep-1 is mediated by a physical process governed by electrostatic interactions [7,11]. Modification of the hydrophilic domain, with a CF group, extensively decreases the affinity of pep-1 for phospholipid membranes and for the cargo macromolecule, which affects the translocation of the peptide alone as well as its capacity as delivery agent. It was recently proposed that labelling CPPs influence the final location inside the cell [5]. We now generalize this difference to a decrease in the extension of internalization and to a change in the main mechanism of translocation. A small chemical modification of these sequences may modify the translocation efficiency and even its pathway. It is worth mention that oligo-Arg peptides have translocation ability on their own [22] with no need for "hydrophobic" sequences.

Acknowledgments: We thank FCT, Portugal for the grant SFRH/BD/14337/2003 under the program POCTI to S.T. Henriques. This work was funded by grants POCTI/BCI/38631 from FCT, Portugal, and LSHG-CT-2004-503228 from the European Commission.

References

[1] Bogoyevitch, M.A., Kendrick, T.S., Dominic, C.H. and Barr, R.K. (2002) Taking the cell by stealth or storm? Protein transduction domain (PTDs) as versatile vectors for delivery. DNA Cell Biol. 21, 879–894.

[2] Wadia, J.S., Becker-Hapak, M. and Dowdy, S.F. (2002) Interactions of cell-penetrating peptides with membranes in: Cell-penetrating Peptides, Processes and Applications (Langel, Ü., Ed.), CRC Press Pharmacology & Toxicology Series, pp. 365–375, CRC Press, NY.
[3] Richard, J.P., Melikov, K., Vives, E., Ramos, C., Verbeure, B., Gait, M.J., Chernomordik, L.V. and Lebleu, B. (2003) Cell-penetrating peptides, a reevaluation of the mechanism of cellular uptake. J. Biol. Chem. 278, 585–590.
[4] Thoren, P.E.G., Persson, D., Isakson, P., Goksör, M., Önfelt, A. and Nordén, B. (2003) Uptake of analogs of penetratin, Tat(48–60) and oligoarginine in live cells. Biochem. Biophys. Res. Commun. 307, 100–107.
[5] Szeto, H.H., Schiller, P.W., Zhao, K. and Luo, G. (2005) Fluorescent dyes alter intracellular targeting and function of cell-penetrating tetrapeptides. FASEB J. 19, 118–120.
[6] Morris, M.C., Depollier, J., Mery, J., Heitz, F. and Divita, G. (2001) A peptide carrier for the delivery of biologically active proteins into mammalian cells. Nat. Biotechnol. 19, 1143–1147.
[7] Henriques, S.T., Costa, J. and Castanho, M.A.R.B. (2005) Translocation of β-galactosidase mediated by the cell-penetrating peptide pep-1 into lipid vesicles and human HeLa cells is driven by membrane electrostatic potential. Biochemistry 44, 10189–10198.
[8] Wu, Y., Wood, M.D. and Katagiri, F. (2003) Direct delivery of bacterial avirulance proteins intro resistant *Arabidopsis* protoplasts lead to hypersensitive cell death. Plant J. 33, 131–137.
[9] Ikari, A., Nakaro, M., Kawano, K. and Suketa, Y. (2002) Up-regulation of sodium-dependent glucose transporter by interaction with heat shock protein 70. J. Biol. Chem. 277, 33338–33343.
[10] Zhou, J. and Hsieh, J.-T. (2001) The inhibitory role of DOC-2/DAB2 in growth factor receptor-mediated signal cascade. J. Biol. Chem. 276, 27793–27798.
[11] Henriques, S.T. and Castanho, M.A.R.B. (2004) Consequences of nonlytic membrane perturbation to the translocation of the cell penetrating peptide pep-1 in lipidic vesicles. Biochemistry 43, 9716–9724.
[12] Henriques, S.T. and Castanho, M.A.R.B. (2005) Environmental factors that enhance the action of the cell penetrating peptide pep-1. A spectroscopic study using lipidic vesicles. Biochem. Biophys. Acta 1669, 75–86.
[13] Christiaens, B., Symoens, S., Vanerheyden, S., Engelborghs, Y., Joliot, A., Prochiantz, A., Vandekerckhove, J., Rosseneu, M. and Vanloo, B. (2002) Tryptophan fluorescence study of the interaction of penetratin peptides with model membranes. Eur. J. Biochem. 269, 2918–2926.
[14] Caputo, G.A. and London, E. (2003) Using a novel dual fluorescence quenching assay for measurement of tryptophan depth within lipid bilayers to determine hydrophobic α-helix location within membranes. Biochemistry 42, 3265–3274.
[15] Mayer, L.D., Hope, M.J. and Cullis, P.R. (1986) Vesicles of variable sizes produced by a rapid extrusion procedure. Biochim. Biophys. Acta 858, 161–168.
[16] Gennis, R.B. (1989) Biomembranes, Molecular Structure and Function, Springer-Verlag, NY.
[17] Haugland, R.P. (2002) Handbook of Fluorescent Probes and Research Products, 9th edn, Molecular Probes, Eugene.
[18] Wan, C.P., Park, C.S. and Lau, B.H. (1993) A rapid and simple microfluorometric phagocytosis assay. J. Immunol. Meth. 4, 1–7.
[19] Hed, J., Hallden, G., Johansson, S.G. and Larsson, P. (1987) The use of fluorescence quenching in flow cytofluorometry to measure the attachment and ingestion phases in phagocytosis in peripheral blood without prior cell separation. J. Immunol. Meth. 101, 119–125.
[20] Fernandes, M.X., Torres, J.G. and Castanho, M.A.R.B. (2002) Joint determination by brownian dynamics and fluorescence quenching of the in-depth location profile of biomolecules in membranes. Anal. Biochem. 307, 1–12.
[21] Foerg, C., Ziegler, U., Fernandez-Carnedo, J., Giralt, E., Rennert, R., Beck-Sickinger, A.G. and Merkle, H.P. (2005) Decoding the entry of the two novel cell-penetrating peptides in HeLa cells: lipid raft-mediated endocytosis and endosomal escape. Biochemistry 44, 72–81.
[22] Sarai, N. and Matile, S. (2003) Anion-mediated transfer of polyarginine across liquid and bilayer membranes. J. Am. Chem. Soc. 125, 14348–14356.

Chapter 5

Conclusion

Chapter 5.

Conclusion

5.1. The overall mechanism – the importance of the lipidic membrane and electrostatic interaction on pep-1 uptake.

The results presented through the thesis, along with some other published work related to pep-1 properties and its ability to internalize will be interpreted and gathered with other information available in the literature. Pep-1 translocation across plasma membrane has also been the subject of a recent review [268], which is presented in Chapter 6.

Interaction of peptides with lipidic membranes comprises three thermodynamic steps governed by electrostatic forces, hydrogen bond formation and hydrophobic interactions. The first step is initiated by the electrostatic attraction between peptide and membranes; the second step involves a transition of the peptide into the plane of binding, which depends on the hydrophobic/hydrophilic balance of the molecules

groups and forces involved; and the third step involves a conformation modification of the bound peptide, normally from a random coil conformation into a α-helix structure upon interaction with lipidic bilayer [183]. Insertion in the lipid matrix may follow.

The interaction of pep-1 can be described by these three steps as follow: in the first step, mainly governed by electrostatic interaction between peptide and membrane, there is an increase of peptide concentration at membrane surface due to large electrostatic interactions between basic amino acid residues and the phosphate groups in lipid molecule [183]; in the second step, pep-1 in close proximity to the membrane removes the hydration shell at membrane surface and promotes membrane destabilization by hydrophobic domain insertion [186]; in the third step, hydrophobic domain upon interaction with membrane acquires an α-helical conformation, as verified by us [269] and also by others [185, 270]. Such secondary structure modification is understood with respect to a reduction on the free energy at membrane surface and is thus an important driving force for membrane binding [183].

The hydrophobic domain inserts in the membrane with a shallow position [153, 269]. This location was also confirmed by others [270]. Upon peptide insertion, liposome aggregation and fusion were detected [186], which indicates that pep-1 is able to destabilize the lipidic membrane. It is worth mentioning that the absence of membrane leakage as detected by us [186, 269] and by others [270, 271] conflicts with the pore formation hypothesis suggested by Deshayes *et al.* [185, 272]. The peptide orientation in the membrane further rule out such hypothesis [153, 269]. A pore formation implies that the peptide spans across lipidic membrane with a perpendicular orientation to the membrane plane [172, 175]. Such orientation is thermodynamically unfavourable for pep-1 due to peptide length and structure: the hydrophilic domain with a large charge density and random coil conformation does not insert in the bilayer and the hydrophobic domain length with an α-helical conformation (~19.5Å) does not match the bilayer membrane thickness (~40Å), which is further hampered by the presence of five Trp residues in this domain, which work as anchors at membrane interface [273, 274].

A membrane disintegration for high peptide/lipid ratios, as observed by us [269], and also by others [270, 271] suggests that the hydrophilic part binds onto the surface of the membrane and cover it in a “carpet”-like manner, whereas the hydrophobic domain, in the interface region, induces membranes destabilization, which above a critical local

peptide concentration (dependent on the lipidic composition and peptide affinity for these bilayers) induces membrane disintegration. This is an extreme event and cannot explain the capacity of peptide to translocate. Together, our results demonstrate that the pep-1 has a high affinity for membranes and is able to destabilize the lipidic bilayer without leakage of the aqueous contents of the vesicles. Membrane disintegration occurs in extreme conditions (peptide/lipid ≥1), which also explain the pep-1 cytotoxicity in cultured cells with peptide concentrations much above the concentrations used for transfection purposes [84, 270].

The plasma membrane is characterized by a negative transmembrane potential, due to electrochemical gradient and also by membrane composition asymmetry (inner leaflet is enriched on negatively-charged phospholipids, while the outer leaflet is mainly composed by zwitterionic phospholipids). *In vitro* studies show pep-1 capacity to disturb membranes without forming pores and to translocate by a mechanism dependent on transmembrane potential; moreover it also shows that pep-1 has a higher affinity for membranes with negatively-charged phospholipids. In cultured cells it was possible to confirm the capacity of pep-1 to translocate by a mechanism dependent on membrane potential gradient and no evidences for an endosomal pathway, were detected [230] in agreement with a previous report by Morris *et al*. [84].

The importance of the peptide affinity for the membrane on the translocation process was confirmed with pep-1CF, where both a loss in membrane affinity and a decrease in uptake were identified. This suggests that translocation efficiency and partition of pep-1 in lipidic membranes are strongly correlated. However, comparing results at 4ºC and 37ºC it was possible to identify a slight internalization of pep-1CF by an endocytosis-dependent uptake (at 4ºC internalization was inhibited). This small uptake by endocytosis seems to operate only when the membrane affinity is severely decreased or lost, suggesting that membrane partition and the capacity to perturb it, dictate the extent to which the peptide enters the cell by a physical mechanism in detriment of endocytosis.

Briefly, it is possible to conclude that the high affinity of pep-1 for lipidic bilayers leads to a high local concentration in the membrane, disturbing the cell surface. This effect associated with the transmembrane potential (negative inside) facilitates pep-1 passage through the plasma membrane [153, 186]. Electrostatic attractions, which are

long range and are dominate when compared with hydrophobic ones [183], reallocate the peptide from the outer layer to the inner layer (more negatively-charged than the outer layer). The reduced local surface tension allows the peptide to intercalate the membrane and a flexible sealing between peptide side-groups and lipid head-groups minimize leakage during the peptide passage through the membrane and no leakage occurs [186, 269]. Once in contact with cytoplasm, pep-1 decreases the affinity for the lipidic membrane due to disulfide bond cleavage in the reducing environment [153], and is transferred into cytoplasm where is then available for uptake by cellular compartments. When a cargo molecule is associated with the peptide, an excess of pep-1 molecules in free form is required for an efficient translocation. This suggests that part of the pep-1 molecules take part on pep-1/cargo complex formation whereas the pep-1 molecules in free form are responsible for interaction with plasma membrane [230]. The overall mechanism is outlined in the Figure 5.2:

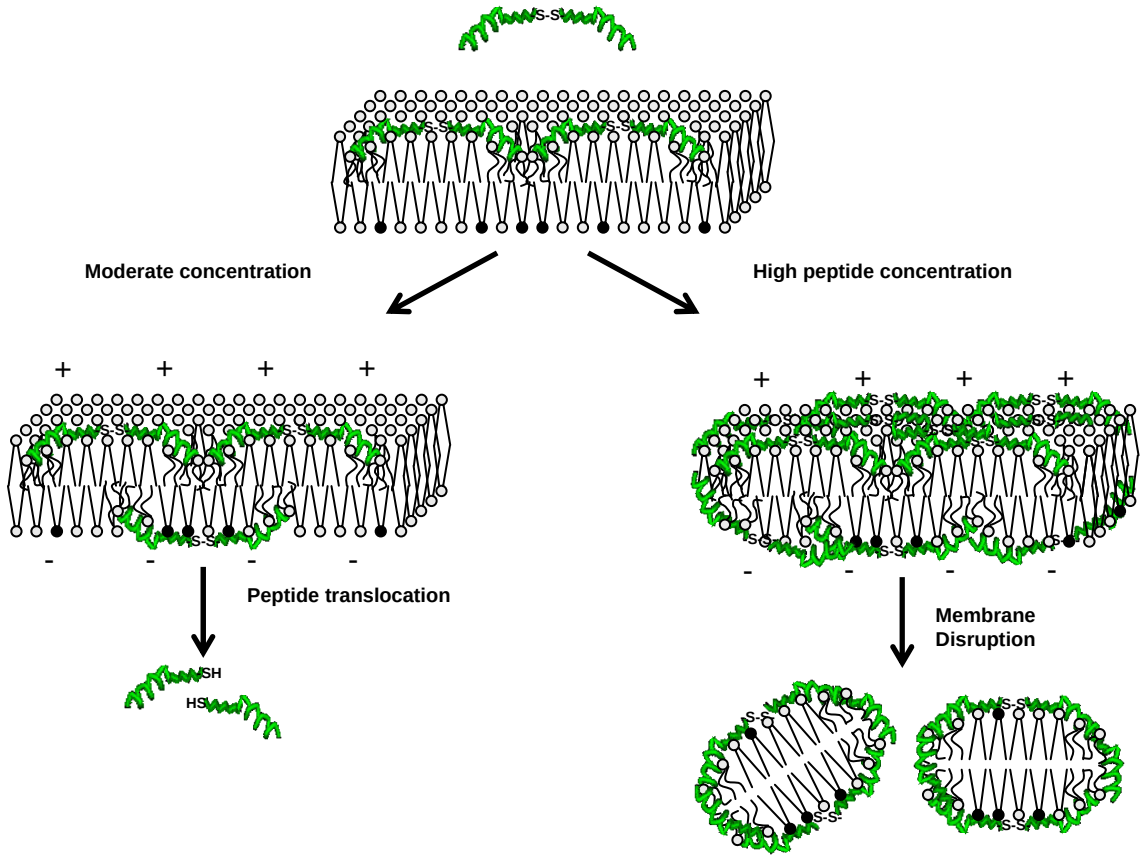

Figure 5.2. Pep-1 translocation mechanism across biological membranes is initiated by pep-1 partition into lipidic membrane. The peptide-lipid interaction is first governed by electrostatic interaction between hydrophilic domain and lipid headgroups, and subsequently in close proximity to the membrane hydrophobic domain inserts in the membrane, acquires an α-helical conformation and perturbs membrane. In extreme conditions where peptide concentration is higher than lipid concentration, peptide becomes cytotoxic due to membrane disintegration by a "carpet" model-like mechanism. In physiological conditions due to negative transmembrane potential and membrane asymmetry pep-1 passes from the outer layer to the inner layer by a electrostatic-mediated process where the peptide intercalates the membrane during the peptide passage through the membrane and no leakage occurs. When pep-1 faces the cytoplasm, loses the affinity for lipidic membrane. Therefore the equilibrium is shifted to intracellular environment, which facilitates peptide and cargo uptake.

5.2. Towards a new phase regarding CPP mechanisms: the coexistence of translocation mechanisms

The plasma membrane is a barrier to the passage of a number of therapeutic agents. The efficient delivery of macromolecules into living cells is a challenge. In spite of all the approaches that have been used in the last decade to overcome membrane impermeability, they all present serious drawbacks. The recent strategy that employs the use of cationic peptides as carriers to introduce macromolecules has attracted much attention during the past few years and is a new hope on drug delivery for therapeutic purposes [1]. The use of CPPs for a general application implies the knowledge of the mechanism used to pass through the membrane and this has been the main goal in CPP research. In the last 20 years the studies on CPPs mechanism can be divided into three phases.

First it was observed that internalization of CPPs and their cargoes was not inhibited by incubation at low temperature, by depletion of cellular ATP or by inhibitors of endocytosis. Furthermore structure-activity studies and the use of D-isomers indicated that the internalization of CPPs was not dependent on receptor recognition. Based on these observations the internalization of CPPs was commonly accepted to be both endocytosis- and receptor-independent and a translocation mechanism involving direct interaction with membranes and lipids was proposed [15, 16, 27, 53]. This hypothesis was supported by the strong correlation between lipid-binding affinity and cell uptake [168] and also by the observation of translocation in model membrane systems [78, 79, 147].

More recently it was verified that the fixation procedures used for immunochemistry and cell visualization may lead to artifactual cell localization [55, 56]. These observations led to a re-evaluation of the internalization mechanism by Richard *et al.* [60] followed by Thorén *et al.* [58] in 2002 and 2003. The confirmation of the involvement of endosomal pathway for internalization of, penetratin, TAT and oligoarginine [58, 60] led to a drastic turn on the CPP research and subsequent reports have shown that many CPPs are internalized by endocytosis [59, 61-66, 275]. From that period until now it was generally assumed that all the CPPs were internalized by an endocytic pathway and this can be regarded as the second phase on the CPP research. However, a consensus in the specific route was never reached and contradictory results

have been published [60, 62, 68]. In a picture where endosomal pathway is the physiological route used by CPP uptake, the escape from endosomes for an efficient delivery of a functional cargo must involve membrane interaction and a physically driven mechanism. Moreover the direct observation of the uptake of some CPPs in model membranes [77-79, 147] reinforces this mechanism. CPPs are an heterogeneous family with peptides from different sources (see reference [34]) and the mechanism of their action cannot be only black or white. A thorough and open-minded evaluation of the mechanism should be done.

Our results with pep-1 [153, 186, 230, 269, 276] together with recently published reports [242, 248, 251, 252, 258] suggest a third phase in the CPP research, where the main physiological mechanism used by CPPs is dependent on the peptide and experimental conditions. A greater contribution of physically-mediated process in detriment of endocytosis is dependent on the bulk peptide concentration, the cargo molecule, the peptide affinity for cell membrane and the quantity of cells, which modulate the peptide concentration in membrane vicinity. For a further comprehension of this statement I will compare the uptake mechanism of different CPPs: Penetratin, TAT and analogues, maurocalcine, $S4_{13}$-PV and pep-1. This has also been object of a recent review by us ([277] presented in Annex I).

Penetratin does not show a strong affinity for zwitterionic membranes [74, 278, 279] and does not induce significant membrane destabilization [234, 280]. Interaction with model membranes is only evident when negatively-charged phospholipids are present [74, 278]. A large consensus on internalization of penetration by endocytosis as the physiological uptake route is evident through the literature [58, 59, 65] with no evidences for an alternative pathway [58].

For TAT, oligoarginine and other TAT analogues a more pronounced affinity for the membrane, together with capacity to induce more severe membrane destabilization when compared with penentratin, was oberved [234, 280]. For these peptides a contribution of the endocytosis and energy-independent mechanism was reported [58, 281, 282] while other authors claim that endocytosis is the only physiological mechanism for TAT internalization [60, 61, 65, 70]. This apparent contradiction was recently elucidated by Duchardt *et al.* [248]. In this report the uptake of penetratin, TAT and oligoarginine was compared and evaluated at different peptide concentrations. Penetratin uptake mechanism was found to be endocytosis-dependent even at high

concentrations (20 μM) while for TAT and oligoarginine the endocytosis is particularly operative at low concentrations (2μM). At higher concentrations (20 μM) these later peptides were insensitive to endosomal inhibitors and a rapid release into the cytoplasm by a membrane mediated mechanism was detected. It was proposed that a critical concentration of peptide associated with the plasma membrane is required to trigger this physically-driven mechanism [248]. Similar conclusions were obtained by Fretz *et al.* [251] where the uptake mechanism followed by oligoarginine was dependent on the existence of a threshold concentration which when exceeded promotes direct translocation across the plasma membrane [251]. Moreover, Nakase *et al.* identified that higher quantities of oligoarginine were obtained in the cytoplasm when cells were incubated at 4ºC than at 37ºC. They proposed that when endosomal pathways are inhibited, and an alternative pathway can operate, the peptide is more efficiently translocated into the cytosol. When incubation is held at 37ºC, oligoarginine release in the cytoplasm is difficult due to endosome entrapment [67]. At variance, for penetratin a physically-driven mechanism was not operative and a strong contribution of the endocytic mechanism was always evident [248].

Results obtained with the chimaeric peptide $S4_{13}$-PV (a combination of a 13 aminoacid sequence derived from the dermaseptin S4 ($S4_{13}$ domain) with the NLS from SV-40 large T antigen and also with CPP properties [32]) also support the finding that the peptide affinity for cell membrane and the cell concentration close to the cell surface dictates the main uptake mechanism. The uptake efficiency of this peptide was not reduced in the presence of endocytic inhibitors [257]. However, at low peptide concentration a contribution of endocytosis was verified [242]. A transient membrane destabilization due to electrostatic interactions between the $S4_{13}$-PV peptide and negatively-charged components at cell surface is considered to be responsible for the translocation [257, 283]. Endosomal internalization with low peptide concentration suggests that higher peptide concentrations are mandatory to induce membrane destabilization.

The hypothesis of the coexistence of endosomal and physically-mediated mechanisms was also proposed by Boisseau *et al.* [258] in a study with maurocalcine, a CPP isolated from the scorpion *Scorpio maurus palmatus* [236]. A contribution of both mechanisms was identified where the physically-driven mechanism results from a transmembrane potential [258]. In a recent study with maurocalcine analogues, where

peptides with different point mutations were compared, it was verified that the analogues with a stronger interaction with membrane lipids have a better penetration into cells [252]. Conversely, analogues with less cellular uptake presented a diminished ability to interact with negatively-charged lipids [252].

In all the above referred peptides no interaction with zwiterionic membranes or significant destabilizations were verified through the studies and it was evident that the interaction with model membranes only occurs in the presence of anionic lipids or proteoglycans [66, 252, 278, 280, 283]. In contrast, pep-1 has a high affinity for lipidic membranes, even in the absence of negatively-charged phospholipids or proteoglycans [153] and induces a significant membrane destabilization [186, 269] which seems to favour internalization [230]. At physiological concentrations, endocytosis was not detected even at 37ºC [230, 276], and so it is possible to conclude that the physically-driven uptake is the only mechanism with physiological relevance for the pep-1. The observation that the pep1-CF, with a lower affinity for lipidic membrane when compared with pep-1, is not internalized at 4ºC but has a slight internalization at 37ºC, indicating an endosomal internalization, supports the hypothesis that membrane-affinity and the local concentration of the peptide partitionated in the membrane dictates the preferred uptake mechanism.

Overall, is possible to conclude that the strategy used by a specific CPP to internalize inside the cell is dependent on the bulk peptide concentration [242, 248, 251], on the cargo molecule attached [241, 282], on the cellular line and the number of cells [284]. Altogether these factors modulate the peptide affinity for lipidic membrane and the peptide concentration on the membrane. Penetratin and pep-1 can be regarded as two extremes in the CPPs family. In one hand the penetratin with a low affinity for lipidic membrane and low ability to disturb it [234, 280] is mainly (if not solely) internalized by endocytosis [58, 248]. Pep-1, in the other extreme, with a high affinity for lipidic membranes [153] and able to disturb the membrane stability [186, 269] translocates across biological membranes without evidence for endocytosis mechanism.

There are two requisites for an efficient cargo delivery by a CPP: a specific location inside the cell and an escape from endosomes into the cytoplasm. This implies membrane interaction and permeation. pH gradient in/out the lisosomes (pH5 in endosomal lumen and pH7 in cytosol) was suggested as a possible driving force to

promote the release of CPPs into cytosol [65], as supported by Magzoub *et al.* studies [77] where translocation into model membranes driven by a pH gradient was shown for penetratin. Another possibility is a transmembrane potential-driven mechanism [78, 81]. Once inside the endosomes the transmembrane potential (luminal side is positive) drives translocation from the endosomal lumen to the cytoplasm environment. The ability to pass through a pure lipid membrane mediated by the transmembrane potential was verified for TAT [282], oligoarginine and penetratin [78].

The energy-independent mechanism has physiological relevance if the uptake occurs in non-toxic conditions. The importance of electrostatic interactions between the peptide and the cell membrane is consensual trough the literature (see for instance [168, 230, 234, 252, 255, 276, 283, 285]). The transmembrane potential between extracellular and intracellular medium (negative inside) was implicated in the uptake of different CPPs as oligoarginine [81], TAT [282], maurocalcine [258], and pep-1 [186, 230].

The biological application of CPPs as carriers is a compromise between efficacy and non-toxicity. Like CPPs, AMPs are short and cationic sequences with a high affinity for membranes, and in extreme conditions CPPs show antimicrobial effects [253] and can also be toxic for mammalian cells [270] (see also the review paper [277] in Annex I).

Our contribution in the CPP field was important to exclude the general acceptance of an endosomal pathway to explain the uptake of all the CPPs. Pep-1, being clearly related to a physical mechanism was significant to reach this third stage where the particular peptide and the experimental conditions dictate the mechanism. This project has also contributed with new methodologies to study the translocation across model membranes, which has been the topic of a review [286] presented in Annex I.

Chapter 6

Annex I

Chapter 6.

Annex I

6.1. *Translocation or membrane disintegration? Implication of peptide-membrane interactions in pep-1 activity.*

The review titled: *Translocation or membrane disintegration? Implication of peptide-membrane interactions in pep-1 activity,* presents the most significant results obtained on pep-1 translocation studies. Our results together with other published reports are reviewed. In this review the pep-1 ability for cell penetration and/or antimicrobial activity is highlighted. The threshold between these two properties relies in the peptide concentration; the composition of the membrane and the final peptide/lipid ratio. In mammalian cells and at pep-1 physiological conditions the pep-1 works as a CPP. With some bacteria strains pep-1 may work as AMP.

6.1.1. Declaration on authorship of published manuscript: *Translocation or membrane disintegration? Implication of peptide-membrane interactions in pep-1 activity.*

I, Sónia Troeira Henriques declare that the manuscript preparation was carried on by me under advice of Dr. Miguel ARB Castanho.

I, Miguel ARB Castanho, as Sónia T Henriques supervisor, hereby acknowledge and confirm the information above is correct.

_____	_____
Sónia Troeira Henriques	Miguel ARB Castanho

Journal of Peptide Science
J. Pept. Sci. 2007; **13**: 000–000
Published online in Wiley InterScience (www.interscience.wiley.com). DOI: 10.1002/psc.1003

JOURNAL OF PEPTIDE SCIENCE

Review

Translocation or membrane disintegration? Implication of peptide–membrane interactions in pep-1 activity‡

SÓNIA TROEIRA HENRIQUES* and MIGUEL A. R. B. CASTANHO

Centro de Química e Bioquímica, Faculdade de Ciências da Universidade de Lisboa, Ed. C8, Campo Grande, 1749-016 Lisboa, Portugal

Received 29 June 2007; *Revised 1 October 2007*; *Accepted 8 September 2007*

Abstract: The Cell membrane is impermeable for most peptides, proteins, and oligonucleotides. Moreover, some cationic peptides, the so-called cell-penetrating peptides (CPPs), are able to translocate across the membrane. This observation has attracted much attention because these peptides can be covalently coupled to different macromolecules, which are efficiently delivered inside the cell. The mechanism used by these peptides to pass across the membrane is a controversial matter of debate. It has been suggested that endocytosis is the main mechanism of internalization and this was confirmed by several studies for different peptides. Pep-1 is an exception worthy of attention for its ability to translocate cargo macromolecules without the need to be covalently attached to them. A preferential internalization by an endocytosis-independent mechanism was demonstrated both *in vitro* and *in vivo*. Pep-1 has a high affinity to lipidic membranes, it is able to insert and induce local destabilization in the lipidic bilayer, although without pore formation. No cytotoxic effects were found for pep-1 concentrations where translocation is fully operative. At much higher concentrations, membrane disintegration takes place by a detergent-like mechanism that resembles anti-microbial peptide activity. In this review, the ability of pep-1 to transverse the membrane by an endocytosis-independent mechanism, not mediated by pores as well as an ability to induce membrane disintegration at high peptide concentration, is demonstrated. Copyright © 2007 European Peptide Society and John Wiley & Sons, Ltd.

Keywords: cell-penetrating peptides; peptide-membrane interactions; translocation mechanism; drug delivery; anti-microbial peptides

INTRODUCTION

The hydrophobic nature of the cell membrane is responsible for cellular integrity and is one of the limitations for the introduction of hydrophilic macromolecules in the cytoplasm. Microinjection, electroporation, liposomes and viral vectors have been used as delivery strategies to overcome membrane permeability. All these methods have drawbacks such as toxicity, poor specificity and being time consuming [1]. The observation that some cytoplasmic proteins are able to cross the membrane when added to extracellular medium, (e.g. HIV-1 transcriptional activator Tat protein [2] and the *Drosophila* antennapedia transcription protein (pAntp) [3]) originated an alternative strategy based on the basic amino acid sequences within these proteins which are translocating-enabling sequences. The observation that these basic peptides allow cellular delivery of conjugated molecules such as peptides or proteins made these molecules attractive and a new class of vectors, known as cell-penetrating peptides (CPPs), emerged [4]. This family now includes all the peptides with the ability to translocate across membranes, whether natural peptides, synthetic, or chimaeric peptides.So far, these vectors have been used to translocate a wide range of macromolecules into living cells such as proteins [5–7], peptides [8,9], oligonucleotides [10,11], peptide nucleic acids [12], and polysaccharides [13]. Nanoparticles [14] and liposomes [15] have also been internalized in cells by means of CPP.

The mechanism used by these peptides to translocate across biologic membranes has been a subject of debate and controversy in the literature (Ref. 16 and references therein). The CPP derived from pAntp (penetratin) and the one from Tat protein (TAT) are the two most intensively studied CPPs. Both peptides use endocytic pathways to reach the cytoplasm [17–23]. Moreover, even in a scenario where the endocytosis is the physiological means of CPP uptake, the escape of the CPP/cargo from endosomes into the cytoplasm is mandatory for a successful delivery of the cargo molecule. An escape from endosomes due to acidification was proposed for penetratin and TAT and confirmed [24]. A translocation dependent on a transmembrane potential was also identified *in vitro* for TAT and penetratin [25].

PEP-1 A CHIMAERIC PEPTIDE

Pep-1 (acetyl-KETWWETWWTEWSQPKKKRKV-cysteamine) is a CPP with primary amphipathicity (i.e

*Correspondence to: Sónia Troeira Henriques, Centro de Química e Bioquímica, Faculdade de Ciências da Universidade de Lisboa, Ed. C8, Campo Grande, 1749-016 Lisboa, Portugal;
e-mail: sthenriques@fc.ul.pt

‡ This article is part of Special Issue of the Journal of the Peptide Science entitled "2nd workshop on biophysics of membrance-active peptides".

BIOGRAPHY

Sónia Troeira Henriques obtained her degree in Biochemistry in 2003 and has recently finished her Ph.D. programme at the Faculty of Science, University of Lisbon, Portugal. Her research focuses on the study of the interaction of peptides, mainly cell-penetrating peptides, with model membranes and with mammalian cellular lines, using fluorescence and IR spectroscopy methodologies, surface plasmon resonance and fluorescence microscopy.

Miguel Castanho graduated in Biochemistry (University of Lisbon, Portugal, 1990), has a Ph.D. degree in Molecular Biophysics (Technical University of Lisbon, Portugal, 1993) and habilitation in Physical Biochemistry (University of Lisbon, Portugal, 1999). He became a group leader in the Faculty of Sciences (University of Lisbon, Portugal), where he started working on the mechanism of action of membrane active peptides at the molecular level. His work includes the development of methodologies aiming at specific functional and structural information, related to cell-penetrating, antimicrobial, viral fusion inhibitor and neuropeptides. Both *in-vitro* and *in-vivo* work is carried out, using mainly optical spectroscopic techniques. Miguel Castanho has recently been appointed full professor (Biochemistry) at the Faculty of Medicine (University of Lisbon, Portugal).

amphipathicity resulting from the aminoacid sequence itself, not from the folding structure) composed by: (i) a Trp-rich domain (KETWWETWWTEW), responsible for hydrophobic interactions with both proteins and cell membranes, (ii) a hydrophilic domain (KKKRKV) derived from a nuclear localization signal (NLS) of Simian Virus 40 (SV-40) large T-antigen, required to improve solubility, and (iii) a spacer domain (SPQ), which improves the flexibility and the integrity of the other two domains [26]. A cysteamine group is present in the *C*-terminal and an acetyl group caps the *N*-terminus. In oxidizing conditions dimmers may form due to a disulfide linking of cysteamine groups.

Pep-1 has been efficiently used to introduce several large proteins inside different cellular lines such as mammalian cells [26–29] or plant cells converted into protoplasts [30]. The efficiency of translocation, however, can vary depending on the cell type and the cargo molecule.

PEP-1 INTERACTION WITH MEMBRANES

Pep-1 is intrinsically fluorescent, which overcomes the necessity to couple a fluorescent dye in fluorescence spectroscopy studies. Trp fluorescence emission is environmental-sensitive: when Trp residues are totally exposed to aqueous environment its fluorescence emission has a spectral maximum at ~350 nm; at variance, in a more hydrophobic environment there is a blue shift in fluorescence emission spectrum with a concomitant increase in quantum yield (Figure 1(A)). The pep-1 extent of interaction with lipid membranes was quantified by means of molar ratio partition coefficient, K_P ($K_P = [Pep-1]_{Lipid}/[Pep-1]_{Aqueous}$). The increase in the fluorescence intensity (I) with lipid concentration was used to determine K_P ($I = (I_W + K_p\gamma_L[L]I_L)/(1 + K_P\gamma_L[L])$; where I_W and I_L are the fluorescence intensities in the absence of lipid and limit value for increasing lipid concentrations, respectively, γ_L is the molar volume of lipid and [L] is the lipid concentration – for more details see Ref. 31). Pep-1 has high affinity for neutral membranes vesicles. The peptide insertion kinetics is fast and the interaction is highly enhanced in the presence of negatively-charged phospholipids (Figure 1(B)) [32]. This suggests that the highly charged hydrophilic domain, should be responsible for the first contact with the membrane owing to the electrostatic interactions between the polar headgroup of phospholipids and the positive charges of pep-1. This was further confirmed by the effect of ionic strength on peptide–membrane interaction [33]. The hydrophobic domain, containing five Trp residues, inserts in the membrane with a shallow positioning [32]. Together, the dehydration at membrane surface by the hydrophilic domain and the insertion of the hydrophobic domain promote membrane destabilization. Membrane destabilization was confirmed by aggregation (Figure 2(A)) and fusion (Figure 2(B)) of vesicles in the presence of pep-1 [33,34]. Moreover, segregation of anionic phospholipids induced by the presence of pep-1 was also detected [34]. However, pore formation was not detected [34–37]. At variance, other study [38] proposed a pore formation by a barrel-stave-like mechanism. This conclusion was based on changes in the membrane conductance in voltage-clamped oocytes, when a transmembrane potential was applied [38].

In reducing conditions the peptide decreases its affinity for the membrane [32]. Under these conditions the disulfide link in between two peptide molecules is reduced. Therefore, the loss in affinity can result from an alteration in peptide conformation due to the cleavage of the disulfide bond. The importance of the cysteamine group was confirmed with peptide molecules without this group (non-capped peptide [35] or peptide with an amide group [35] or a fluorophore [39]) at *C*-terminal). The modified peptides have a decreased capacity to translocate into cells.

DOI: 10.1002/psc

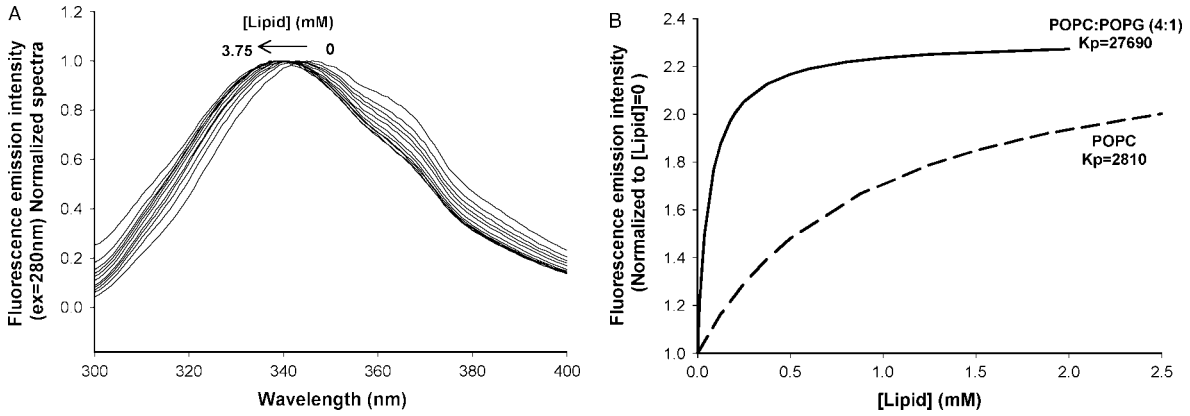

Figure 1 Pep-1 interaction with phospholipid bilayers, reported by Trp fluorescence emission (excitation at 280 nm). Titration of 6.88 μM pep-1 with large unilamellar vesicles (LUVs) of POPC, followed by normalized Trp fluorescence emission spectra (**A**) and total Trp fluorescence emission (**B**). With lipid addition there is a blue shift in the emission spectra and an increase in fluorescence intensity. The pep-1 affinity for lipidic membranes can be quantified by means of partition coefficient, K_P, which was calculated by fluorescence emission intensity and obtained by non-linear regression fit (data points omitted for the sake of clarity) – see text and Refs. 31,32 for further information. Neutral bilayers (POPC) and negatively-charged membranes [POPC : POPG (4 : 1)] are compared. A more extensive partition is obtained with negatively-charged vesicles (for further details see Ref. 32).

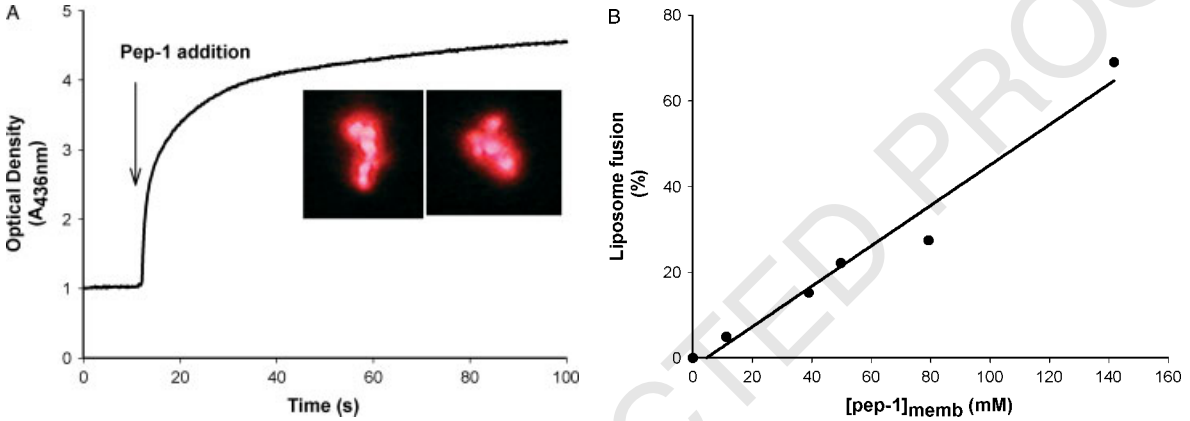

Figure 2 Vesicle aggregation and fusion induced by pep-1. (**A**) Aggregation of LUVs [25 μM POPC : POPG (4 : 1)] induced by 6.88 μM pep-1, followed by optical density and confirmed by fluorescence microscopy (inserts). (**B**) Fusion percentage in POPC and POPC/POPG LUVs. All data were obtained in the presence of 6.88 μM pep-1 total concentration; however, effective concentration in membranes vary (Ref. 34). Fusion extension and effective concentration in membranes are linearly correlated.

Pep-1 interaction with membranes is associated with a conformational alteration [35,36,38]. In aqueous environment the peptide is mainly unstructured but with a tendency to aggregate forming inter-molecular β-sheet aggregates [36]. In the presence of lipidic membranes, a structural alteration from random coil to α-helix conformation, was detected. NMR studies show that the part of the molecule that undergoes structural alteration is the hydrophobic domain [35,38]. This domain is known to easily insert in the membrane [32].

PEP-1 TRANSLOCATION ACROSS CELL MEMBRANES

Pep-1 has been efficiently used in different cellular lines, with several proteins and cargoes. Although, *in vitro* studies with model membranes revealed a high affinity for lipidic bilayers and capacity to perturb the membrane mainly in the presence of anionic phospholipids [34], peptide translocation *in vitro* was only detected in the presence of a negative transmembrane potential (negative inside) [34]. In the absence of transmembrane potential, the peptide inserts only in the outer layer [32]. An excess of negative charges inside the liposome promotes the passage of the peptide from the outer layer to the inner layer (Figure 3(A)) [34].

The pep-1 uptake by endocytosis was tested by means of different methodologies. Delivery efficiency of a cargo molecule attached to pep-1 was compared at 4 and 37 °C [13,26] and no differences in delivery efficiency were observed (Figure 4). These results were confirmed not only by imaging methods following the protein by immunofluorescence [13,26] but

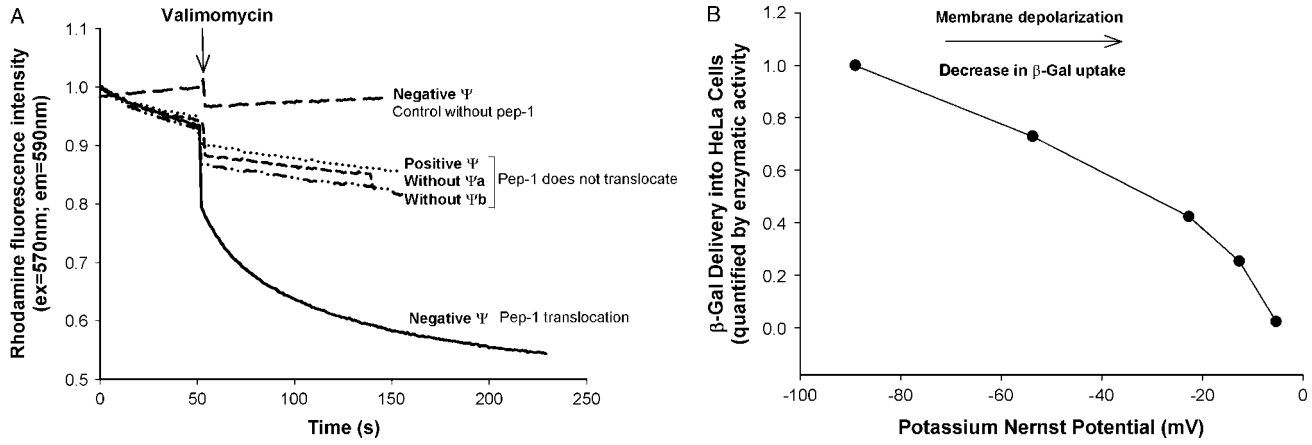

Figure 3 Pep-1 passes through membranes by a mechanism dependent on negative transmembrane potential, Ψ, (inside). (**A**) Pep-1 translocation *in vitro* followed by rhodamine (Rh) quenching [POPC : POPG (4 : 1) LUVs doped with 1% of Rh-labelled phospholipid] induced by the pep-1. In the absence of a Ψ pep-1 is able to quench Rh fluorophores in the outer layer. In the presence of a negative Ψ (created by the addition of valinomycin to liposomes loaded with K^+ and dispersed in Na^+) pep-1 translocates and a drop in Rh fluorescence is clear. With a positive Ψ (liposomes loaded with Na^+ and dispersed in K^+) pep-1 does not translocate. Controls without pep-1 and where a Ψ is not established in the presence of valinomycin (**a** – liposomes loaded with Na^+ and dispersed in Na^+; **b** – liposomes loaded with K^+ and dispersed in K^+) (Ref. 34 for further details) are also represented. (**B**) β-Gal delivery into HeLa cells, mediated by pep-1. Pep-1/β-Gal complex was incubated with HeLa cells, for 30 min at 37 °C. Cell polarization was decreased by increasing external K^+ concentrations, and maintaining the ionic strength constant ($[K^+] + [Na^+] = 150$ mM). The relative level of β-Gal uptake was determined by its enzymatic activity (Ref. 13). Depolarization of cells severely reduces the level of β-Gal uptake.

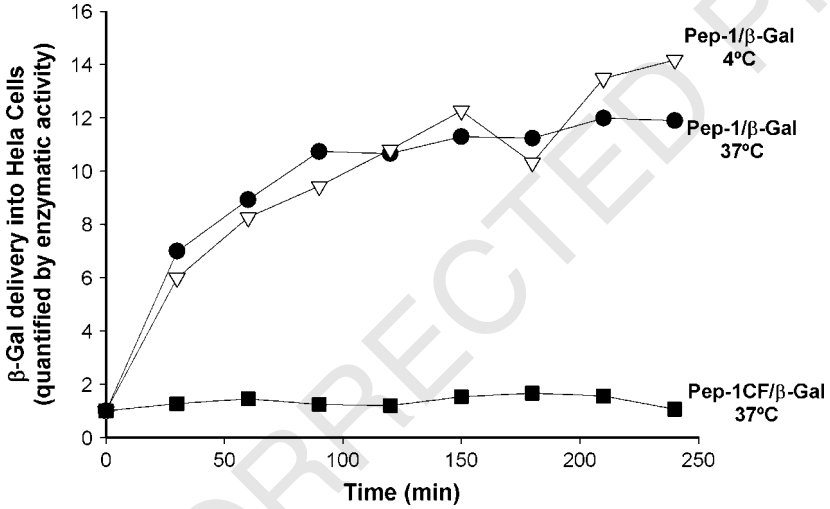

Figure 4 β-Gal delivery into HeLa cells mediated by pep-1 or pep-1 CF, followed by β-Gal enzymatic activity. HeLa cells were incubated during different intervals [16] with Pep-1/β–Gal complex or pep-1CF/β-Gal (molar ratio 320) at 37 or 4 °C. No fixation procedures were used in this protocol. Pep-1 is able to internalize β-Gal in HeLa cells maintaining its enzymatic activity. No differences were detected for incubations at 4 or 37 °C, which suggests an endocytosis-independent internalization. β-Gal internalization is decreased when pep-1CF is used instead of pep-1 (Ref. 39 for further details).

also by protein activity (measurement of β-Gal enzymatic activity) (Figure 4) [13,26,39]. Procedures used to quantify the protein activity inside the cells exclude the possibility of artefacts associated with fixation procedures. Moreover co-localization of β-Gal internalized by the pep-1 with different endocytotic markers (Dextran, EEA1, Caveolin-1, and cathepsin D) followed by confocal microscopy revealed that this protein is inside cells and does not co-localize with any of these endocytic markers [13] (in the case of translocation by an endocytic pathway a co-localization with at least one of these endocytic markers would be expected when the incubation of cells with the complex pep-1/protein is performed at 37 °C).

At variance, Weller *et al.* proposed an endocytosis-mediated entrance based on the internalization of pep-1/Thioredoxin (TRX) in the presence/absence of endocytic inhibitors. In these experiments 0.1% NaN_3

DOI: 10.1002/psc

and 50 mM deoxy-D-glucose were added to the cells to inhibit ATP production. When pep-1/TRX was incubated with cells (still in the presence of NaN_3 and 50 mM deoxy-D-glucose) the TRX uptake was reduced [35]. As has been previously verified, pep-1 is able to interact with dextran molecules with 10 kDa (i.e. about 55 glucose monomers per dextran molecule) and introduce these molecules inside cells [13]. A decrease in the TRX uptake mediated by the pep-1 could thus result from the interference of glucose (which was present in a high concentration, 50 mM), decreasing pep-1/TRX complex formation and/or pep-1 capacity to deliver TRX inside cells.

Under *in vitro* conditions, pep-1 translocates through a mechanism mediated by the transmembrane potential. This hypothesis was also tested *in vivo*. Cellular depolarization inhibited β-Gal uptake mediated by pep-1 (Figure 3(B)) [13]. Considering the overall results we conclude that the endocytic pathway is not the main internalization pathway used by this peptide to introduce proteins inside cells.

A modified pep-1, in which a carboxyfluorescein (CF) probe was added at the *C*-terminus, lost the ability to internalize β-Gal (Figure 4) [39]. This was emcompassed by a decrease in the affinity for lipidic bilayers [39]. The loss in membrane affinity with a decrease in uptake suggests that translocation efficiency and partition of pep-1 in lipidic membranes are strongly correlated. However, comparing incubations at 4 and 37 °C it was possible to identify a slight internalization of pep-1 CF by an endocytosis-dependent uptake (at 4 °C internalization was inhibited) [39]. This small uptake by endocytosis seems to operate only when the membrane affinity is lost, suggesting that membrane affinity and the capacity to destabilize it, dictate the extent to which the peptide enters the cell by a physical mechanism (a process faster than the endocytosis) to the detriment of the endocytosis itself.

CAN PEP-1 WORK AS ANTI-MICROBIAL PEPTIDES?

Like CPPs, anti-microbial peptides (AMPs) are short and cationic peptides with high affinity for membranes. These peptides are characterized by an efficient killing of several species of bacteria with the ability to preserve host-cell integrity. The main target of these peptides is the bacterial membrane, provoking membrane lysis, membrane permeabilization or other forms of bilayers disruption [40].

A pep-1 translocation by pore formation was recently suggested [38] but this suggestion was not confirmed by experiments where the capacity of pep-1 to induce leakage was tested [34–37]. For high peptide/lipid ratios, pronounced membrane damage takes place in lipidic vesicles. Pore formation is not the course of the damage. A detergent-like mechanism seems to operate [36]. This explains the toxicity when pep-1 is present at high concentration [26,35].

Pep-1 anti-microbial activity was tested for different bacterial strains. The minimal inhibitory concentration (MIC) is dependent on the strain [37]. Although pep-1 is not as efficient as mellitin to kill bacteria, it is able to efficiently kill *bacillus subtilus* at a low concentration, and to kill other strains at higher concentrations. The capacity to kill bacteria was truly improved and comparable to the one observed for mellitin when Glu residues were replaced by Lys. The capacity of Lys-modified-pep-1 to kill bacteria is not related with the capacity to induce leakage [37], this further implying that pep-1 translocation and vector activity cannot be explained by a pore formation mechanism.

Considering these results we can conclude that pep-1 has the capacity to work as a CPP or as an AMP. The threshold between these two properties relies on the peptide concentration, the composition of the membrane, and the final peptide/lipid ratio.

CONCLUSION

Pep-1 translocates and is able to work as a vector to introduce proteins or other cargo molecules inside cells. This peptide is able to strongly interact with the lipid bilayer causing local pertubation, and is also able to cross the membrane by a physical mediated mechanism promoted by the transmembrane potential and not involving pore formation. For many CPPs endocytosis uptake may be the main mechanism of uptake but sound evidence show that pep-1 translocates by a mechanism mediated by physical peptide–membrane interactions when a favourable transmembrane potential is present. This does not exclude a possible internalization by an endocytic route in all situations. Nevertheless, the time required for the physical mechanism to be completed is lesser than that for the endocytic uptake. Therefore, if both mechanisms are operative the non-endocytic route is dominant. Differences between pep-1 and other CPPs can be related to the affinity for membrane lipids. Peptides with higher affinity have a greater propensity to be internalized by a non-endocytic mechanism. Lower affinity for membranes can favour endocytic uptake.

REFERENCES

1. Wadia JS, Becker-Hapak M, Dowdy SF. Protein transport. In *Cell-Penetrating Peptides, Processes and Applications*, Langel U (ed.). CRC Press: New York, 2002; 365–375.
2. Frankel AD, Pabo CO. Cellular uptake of the tat protein from human immunodeficiency virus. *Cell* 1988; **55**: 1189–1193.
3. Joliot A, Pernelle C, Deagostini-Bazin H, Prochiantz A. Antennapedia homeobox peptide regulates neural morphogenesis. *Proc. Natl. Acad. Sci. U.S.A.* 1991; **88**: 1864–1868.

4. Lindgren M, Hallbrink M, Prochiantz A, Langel U. Cell-penetrating peptides. *Trends Pharmacol. Sci.* 2000; **21**: 99–103.
5. Ezhevsky SA, Nagahara H, Vocero-Akbani AM, Gius DR, Wei MC, Dowdy SF. Hypo-phosphorylation of the retinoblastoma protein (pRb) by cyclin D : Cdk4/6 complexes results in active pRb. *Proc. Natl. Acad. Sci. U.S.A.* 1997; **94**: 10699–10704.
6. Fawell S, Seery J, Daikh Y, Moore C, Chen LL, Pepinsky B, Barsoum J. Tat-mediated delivery of heterologous proteins into cells. *Proc. Natl. Acad. Sci. U.S.A.* 1994; **91**: 664–668.
7. Rojas M, Donahue JP, Tan Z, Lin YZ. Genetic engineering of proteins with cell membrane permeability. *Nat. Biotechnol.* 1998; **16**: 370–375.
8. Rojas M, Yao S, Donahue JP, Lin YZ. An alternative to phosphotyrosine-containing motifs for binding to an SH2 domain. *Biochem. Biophys. Res. Commun.* 1997; **234**: 675–680.
9. Theodore L, Derossi D, Chassaing G, Llirbat B, Kubes M, Jordan P, Chneiweiss H, Godement P, Prochiantz A. Intraneuronal delivery of protein kinase C pseudosubstrate leads to growth cone collapse. *J. Neurosci.* 1995; **15**: 7158–7167.
10. Allinquant B, Hantraye P, Mailleux P, Moya K, Bouillot C, Prochiantz A. Downregulation of amyloid precursor protein inhibits neurite outgrowth in vitro. *J. Cell Biol.* 1995; **128**: 919–927.
11. Morris MC, Vidal P, Chaloin L, Heitz F, Divita G. A new peptide vector for efficient delivery of oligonucleotides into mammalian cells. *Nucleic Acids Res.* 1997; **25**: 2730–2736.
12. Pooga M, Soomets U, Hallbrink M, Valkna A, Saar K, Rezaei K, Kahl U, Hao JX, Xu XJ, Wiesenfeld-Hallin Z, Hokfelt T, Bartfai T, Langel U. Cell penetrating PNA constructs regulate galanin receptor levels and modify pain transmission in vivo. *Nat. Biotechnol.* 1998; **16**: 857–861.
13. Henriques ST, Costa J, Castanho MA. Translocation of beta-galactosidase mediated by the cell-penetrating peptide pep-1 into lipid vesicles and human HeLa cells is driven by membrane electrostatic potential. *Biochemistry* 2005; **44**: 10189–10198.
14. Lewin M, Carlesso N, Tung CH, Tang XW, Cory D, Scadden DT, Weissleder R. Tat peptide-derivatized magnetic nanoparticles allow in vivo tracking and recovery of progenitor cells. *Nat. Biotechnol.* 2000; **18**: 410–414.
15. Torchilin VP, Rammohan R, Weissig V, Levchenko TS. TAT peptide on the surface of liposomes affords their efficient intracellular delivery even at low temperature and in the presence of metabolic inhibitors. *Proc. Natl. Acad. Sci. U.S.A.* 2001; **98**: 8786–8791.
16. Magzoub M, Graslund A. Cell-penetrating peptides: from inception to application. *Q. Rev. Biophys.* 2004; **37**: 147–195.
17. Console S, Marty C, Garcia-Echeverria C, Schwendener R, Ballmer-Hofer K. Antennapedia and HIV transactivator of transcription (TAT) "protein transduction domains" promote endocytosis of high molecular weight cargo upon binding to cell surface glycosaminoglycans. *J. Biol. Chem.* 2003; **278**: 35109–35114.
18. Drin G, Cottin S, Blanc E, Rees AR, Temsamani J. Studies on the internalization mechanism of cationic cell-penetrating peptides. *J. Biol. Chem.* 2003; **278**: 31192–31201.
19. Fittipaldi A, Ferrari A, Zoppe M, Arcangeli C, Pellegrini V, Beltram F, Giacca M. Cell membrane lipid rafts mediate caveolar endocytosis of HIV-1 Tat fusion proteins. *J. Biol. Chem.* 2003; **278**: 34141–34149.
20. Lundberg M, Wikstrom S, Johansson M. Cell surface adherence and endocytosis of protein transduction domains. *Mol. Ther.* 2003; **8**: 143–150.
21. Potocky TB, Menon AK, Gellman SH. Cytoplasmic and nuclear delivery of a TAT-derived peptide and a beta-peptide after endocytic uptake into HeLa cells. *J. Biol. Chem.* 2003; **278**: 50188–50194.
22. Richard JP, Melikov K, Vives E, Ramos C, Verbeure B, Gait MJ, Chernomordik LV, Lebleu B. Cell-penetrating peptides. A reevaluation of the mechanism of cellular uptake. *J. Biol. Chem.* 2003; **278**: 585–590.
23. Thoren PE, Persson D, Isakson P, Goksor M, Onfelt A, Norden B. Uptake of analogs of penetratin, Tat(48–60) and oligoarginine in live cells. *Biochem. Biophys. Res. Commun.* 2003; **307**: 100–107.
24. Magzoub M, Pramanik A, Graslund A. Modeling the endosomal escape of cell-penetrating peptides: transmembrane pH gradient driven translocation across phospholipid bilayers. *Biochemistry* 2005; **44**: 14890–14897.
25. Terrone D, Sang SL, Roudaia L, Silvius JR. Penetratin and related cell-penetrating cationic peptides can translocate across lipid bilayers in the presence of a transbilayer potential. *Biochemistry* 2003; **42**: 13787–13799.
26. Morris MC, Depollier J, Mery J, Heitz F, Divita G. A peptide carrier for the delivery of biologically active proteins into mammalian cells. *Nat. Biotechnol.* 2001; **19**: 1173–1176.
27. Coulpier M, Anders J, Ibanez CF. Coordinated activation of autophosphorylation sites in the RET receptor tyrosine kinase: importance of tyrosine 1062 for GDNF mediated neuronal differentiation and survival. *J. Biol. Chem.* 2002; **277**: 1991–1999.
28. Ikari A, Nakano M, Kawano K, Suketa Y. Up-regulation of sodium-dependent glucose transporter by interaction with heat shock protein 70. *J. Biol. Chem.* 2002; **277**: 33338–33343.
29. Zhou J, Hsieh JT. The inhibitory role of DOC-2/DAB2 in growth factor receptor-mediated signal cascade. DOC-2/DAB2-mediated inhibition of ERK phosphorylation via binding to Grb2. *J. Biol. Chem.* 2001; **276**: 27793–27798.
30. Wu Y, Wood MD, Tao Y, Katagiri F. Direct delivery of bacterial avirulence proteins into resistant Arabidopsis protoplasts leads to hypersensitive cell death. *Plant J.* 2003; **33**: 131–137.
31. Santos NC, Prieto M, Castanho MA. Quantifying molecular partition into model systems of biomembranes: an emphasis on optical spectroscopic methods. *Biochim. Biophys. Acta* 2003; **1612**: 123–135.
32. Henriques ST, Castanho MA. Environmental factors that enhance the action of the cell penetrating peptide pep-1 A spectroscopic study using lipidic vesicles. *Biochim. Biophys. Acta* 2005; **1669**: 75–86.
33. Sharonov A, Hochstrasser RM. Single-molecule imaging of the association of the Cell-penetrating peptide Pep-1 to model membranes. •*Biochemistry* 2007.
34. Henriques ST, Castanho MA. Consequences of nonlytic membrane perturbation to the translocation of the cell penetrating peptide pep-1 in lipidic vesicles. *Biochemistry* 2004; **43**: 9716–9724.
35. Weller K, Lauber S, Lerch M, Renaud A, Merkle HP, Zerbe O. Biophysical and biological studies of end-group-modified derivatives of Pep-1. *Biochemistry* 2005; **44**: 15799–15811.
36. Henriques ST, Quintas A, Bagatolli LA, Homble F, Castanho MA. Energy-independent translocation of cell-penetrating peptides occurs without formation of pores. A biophysical study with pep-1. *Mol. Membr. Biol.* 2007; **24**: 282–293.
37. Zhu WL, Lan H, Park IS, Kim JI, Jin HZ, Hahm KS, Shin SY. Design and mechanism of action of a novel bacteria-selective antimicrobial peptide from the cell-penetrating peptide Pep-1. *Biochem. Biophys. Res. Commun.* 2006; **349**: 769–774.
38. Deshayes S, Heitz A, Morris MC, Charnet P, Divita G, Heitz F. Insight into the mechanism of internalization of the cell-penetrating carrier peptide Pep-1 through conformational analysis. *Biochemistry* 2004; **43**: 1449–1457.
39. Henriques ST, Costa J, Castanho MA. Re-evaluating the role of strongly charged sequences in amphipathic cell-penetrating peptides: a fluorescence study using Pep-1. *FEBS Lett.* 2005; **579**: 4498–4502.
40. Yeaman MR, Yount NY. Mechanisms of antimicrobial peptide action and resistance. *Pharmacol. Rev.* 2003; **55**: 27–55.

AQ1

6.2. *Cell-Penetrating Peptides and Antimicrobial Peptides: how different are they?*

The observation that some AMPs can translocate across the cell, without damaging cytoplamatic membrane, as well as kill pathogenic agents, has attracted much attention. Like CPPs, AMPs are short and cationic sequences with high affinity for membranes. Similarities between CPPs and AMPs prompted us to question if these two classes of peptides are really unrelated families. In the paper titled: *Cell-Penetrating Peptides and Antimicrobial Peptides: how different are they?*, a critical comparative consideration of the mechanisms underneath cellular uptake is reviewed. Various CPPs, presenting different membrane affinities and uptake mechanisms, are compared and related with antimicrobial activity of some peptides belonging to AMP family. A reflection and a new perspective about CPPs and AMPs are exposed.

6.2.1. Declaration on authorship of published manuscript: *Cell-Penetrating Peptides and Antimicrobial Peptides: how different are they?*

I, Sónia Troeira Henriques declare that the manuscript preparation was carried on by me, Manuel N. Melo and Dr. Miguel ARB Castanho. I was responsible for the part of the manuscript more focused on CPPs, while Manuel N. Melo had a significant contribution for the AMP part. The three of us were important for the critical view on antimicrobial and translocation activities presented.

I, Miguel ARB Castanho, as Sónia T Henriques supervisor, hereby acknowledge and confirm the information above is correct.

_____ _____

Sónia Troeira Henriques Miguel ARB Castanho

REVIEW ARTICLE

Cell-penetrating peptides and antimicrobial peptides: how different are they?

Sónia Troeira HENRIQUES, Manuel Nuno MELO and Miguel A. R. B. CASTANHO[1]

Centro de Química e Bioquímica, Faculdade de Ciências da Universidade de Lisboa, Ed. C8, Campo Grande, 1749-016 Lisbon, Portugal

Some cationic peptides, referred to as CPPs (cell-penetrating peptides), have the ability to translocate across biological membranes in a non-disruptive way and to overcome the impermeable nature of the cell membrane. They have been successfully used for drug delivery into mammalian cells; however, there is no consensus about the mechanism of cellular uptake. Both endocytic and non-endocytic pathways are supported by experimental evidence. The observation that some AMPs (antimicrobial peptides) can enter host cells without damaging their cytoplasmic membrane, as well as kill pathogenic agents, has also attracted attention. The capacity to translocate across the cell membrane has been reported for some of these AMPs. Like CPPs, AMPs are short and cationic sequences with a high affinity for membranes. Similarities between CPPs and AMPs prompted us to question if these two classes of peptides really belong to unrelated families. In this Review, a critical comparison of the mechanisms that underlie cellular uptake is undertaken. A reflection and a new perspective about CPPs and AMPs are presented.

Key words: antimicrobial peptide, cell-penetrating peptide, drug delivery, internalization, translocation mechanism.

INTRODUCTION

The hydrophobic nature of cellular membranes makes them impermeable for most peptides, proteins and oligonucleotides. Different strategies have been employed to penetrate the membrane barrier and deliver hydrophilic molecules inside the cell for either experimental or therapeutic purposes. So far, microinjection, electroporation, liposomes and viral vectors have been used. Most of these delivery strategies have serious drawbacks, such as low efficiency, poor specificity, poor bioavailability and extensive toxicity [1]. Moreover, they are time-consuming. The endocytic route has been used as an alternative for the import of hydrophilic macromolecules into living cells [2]. However, the proteins engaging in this mechanism stay enclosed within endosomes, and so fail to access the cytoplasm, thus missing their final target.

Peptides as vectors to introduce macromolecules into cells

An efficient strategy with which to penetrate the membrane barrier was identified by the observation that some intracellular proteins, when added to extracellular medium, were able to pass through the membrane. Tat (HIV-1 transcriptional activator protein) [3] and pAntp (*Drosophila* antennapedia transcription protein) [4] were the first proteins to be identified with this characteristic. The ability to translocate is attributed to basic amino acid sequences in these proteins, and the minimal peptide sequence necessary for the translocation to occur within Tat [5] and pAntp [6] have been elucidated. The observation that these basic peptides allow cellular delivery of conjugated molecules such as peptides [7] or proteins [8] made these molecules attractive, and a new class of vectors, initially known as PTDs (protein transduction domains) [9], but more recently re-baptized as CPPs (cell-penetrating peptides) [10], emerged. This family now includes all the peptides with the ability to translocate across membranes, regardless of whether they are natural, synthetic or chimaeric peptides.

So far, these vectors have been used to translocate a wide range of macromolecules into living cells, including proteins [8,9,11], peptides [7,12], oligonucleotides [13,14], peptide nucleic acids [15] and polysaccharides [16]. Nanoparticles [17] and liposomes [18] have also been internalized by means of CPPs.

Can AMPs (antimicrobial peptides) also work as vectors?

Most organisms produce gene-encoded AMPs as innate defences to prevent colonization and infection by several microbial pathogens [19–22]. Despite their ubiquity, AMPs can have very distinct sequences and modes of action [23,24]; nonetheless, they usually share several characteristics, such as their short length (a few tens of residues) and their cationicity, typically of charge 4+ or 5+ [25]. Other features of these peptides include their strong interaction with lipidic membranes, a usually broad killing spectrum and their ability to preserve host-cell integrity [23,24].

Clinically these peptides display antimicrobial activity at micromolar concentrations or less, and target bacteria do not seem to readily develop resistance. These properties make AMPs very promising candidates for new generations of drugs to fight antibiotic-resistant strains of pathogens [23,26].

Although most AMPs seem to act mainly at the membrane level [24,25], their translocation into the cytoplasm is not uncommon [27,28]; because of this property, membrane-crossing AMPs have also been used as templates for CPP development [29]. Thus AMPs can have clinical applications both as antibiotics and as precursors of drug transporters.

HOW DO CPPs TRANSLOCATE ACROSS THE CELL MEMBRANE?

There is no consensus regarding the mechanism of translocation of CPPs; the information available in the literature is controversial. First it was suggested that these peptides translocate by a

Abbreviations used: AMP, antimicrobial peptide; CF, carboxyfluorescein; CPP, cell-penetrating peptide; NLS, nuclear localization signal; pAntp, *Drosophila* antennapedia transcription protein; SV40, simian virus 40; Tat, HIV-1 transcriptional activator protein.

[1] To whom correspondence should be addressed (email castanho@fc.ul.pt).

Table 1 Source, amino acid sequences and possible internalization mechanism for some examples of peptides that work as CPPs or as AMPs

Name (sequence)	Source [reference] [internalization mechanism(s), reference(s)]
Penetratin (RQIKIWFQNRRMKWKK)	pAntp homeodomain (amino acids 43–58) [6] (mainly endocytosis [39], endosomal escape mediated by pH gradient or transmembrane potential [36,53])
Tat (GRKKRRQRRRPPQ)	HIV-1 transcriptional activator Tat protein (amino acids 48–60) [5] (mainly endocytosis [40], endosomal escape mediated by pH gradient or transmembrane potential [37])
Pep-1 (Ac-KETWWETWWTEWSQPKKKRKV-cysteamine)	Amphipathic chimaeric peptide with a tryptophan-rich domain and an NLS [57] (physical mechanism mediated by peptide–membrane interaction promoted by pore formation [60] or by transmembrane potential without pores [35])
$S4_{13}$-PV (ALWKTLLKKVLKAPKKKRKV-cysteamine)	Chimaeric peptide with AMP dermaseptin S4 and an NLS [61] (mainly physical mechanism promoted by a transient membrane destabilization [62])
Magainin 2 (GIGKFLHSAKKFGKAFVGEIMNS)	AMP from the skin of the South-African clawed frog *Xenopus laevis* [101] (translocation mediated by toroidal pore formation; peptide molecules translocate stochastically as the pore disintegrates [28])
Buforin 2 (TRSSRAGLQFPVGRVHRLLRK)	AMP from the stomach of the Korean common toad *Bufo bufo gargarizans* [102] (peptide molecules translocate stochastically after the formation and disintegration of a non-permeabilizing pore-like structure [84])
Apidaecins (RP - - - - - PRPPHPR (conserved sequence among class members)	AMP from the lymph fluid of several insects [103] (receptor-dependent membrane docking and translocation into target cell [104])

mechanism independent of receptors [30] and independent of the endosomal pathway [5,6]. A physically driven mechanism was suggested, because the cellular uptake at 4 °C and 37 °C was similar [5,6,30,31].

More recent observations led to controversial results, suggesting that the cell localization observed for CPPs is an artefact and results from cell fixation for immunochemistry and cell visualization [32]. The high peptide affinity for membranes may allow CPPs to remain attached to cells during washing. During the cell fixation process, CPPs are released, and the apparent localization inside the cell results therefrom. However, direct observation of translocation in model membrane systems for some CPPs [33–35] supports the existence of physically driven mechanisms governed by spontaneous peptide–membrane interactions. The translocation mechanism issue is thus complex and may differ for different classes of CPPs (Table 1).

CPPs derived from natural proteins

The CPP derived from pAntp has 16 amino acids and is the sequence necessary and sufficient for translocation to occur [6] (Table 1) and is commonly called 'penetratin'. The Tat fragment corresponding to residues 48–60 [5] (Table 1), and a shorter fragment (residues 47–57) [18,36,37], have frequently been used in CPP research.

An endosomal pathway for internalization was initially excluded by comparison of the uptake at 4 °C and 37 °C under fixation conditions [5,6,30]. After re-evaluation for the interference of artefacts during fixation, an internalization mediated by endocytosis was concluded for both penetratin [38,39] and Tat peptide [37,40–43]. The basic amino acids are essential for translocation to occur, and membrane binding seems to be the first step prior to endocytic uptake. Heparan sulfate proteoglycans at the cell membrane were proposed to act as receptor for penetratin [42,44–46] and Tat peptide [42,47].

Although it is accepted that these CPPs can enter the cells by endocytosis, there is no consensus in the specific endocytic pathway used for the import of these arginine-rich peptides. A raft-dependent pathway involving macropinocytosis [48] or caveolae [41,49,50], or a clathrin-dependent endocytosis [47,51,52], were proposed. The dissimilarities among these results can arise from the use of different cell lines, methodologies, labelled peptides, protein-conjugated peptides and different conditions, which can inhibit some pathways while favouring others.

Even in a picture where the endosomal pathway emerges as the physiological uptake of CPPs, the escape from endosomes into the cytoplasm through a physically driven mechanism persists. An escape from endosomes due to acidification was proposed for penetratin and Tat peptide [36,37]. This hypothesis is supported by the results obtained by Gräslund and co-workers [53] with penetratin encapsulated in large unilamellar vesicles. The escape of penetratin occurred only in the presence of a pH gradient. The role of intracellular pH in the internalization of CPPs was also investigated using neutralization agents [38].

A dependence of translocation on a negative transmembrane potential was identified *in vitro* for both penetratin and Tat peptide [34] and *in vivo* for Tat peptide [54]. Terrone et al. [34] suggested that a fraction of the peptide can transverse through the membrane by a transmembrane potential-driven mechanism, whereas the other fraction is internalized by an endosomal pathway. Once inside the endosomes, the transmembrane potential (luminal side positive) drives translocation from the endosomal lumen to the cytoplasm. By contrast, Drin et al. [38] did not find any internalization of penetratin in liposomes, even in the presence of a transmembrane potential. Recently Bárány-Wallje et al. [55], following electrophysiological measurements in planar bilayers, failed to detect translocation, even in the presence of applied voltages.

Chimaeric peptides

The usefulness of peptides as vehicles to introduce macromolecules into cells led to the development of many chimaeric peptides. Pep-1 (acetyl-KETWWETWWTEWSQPKKKRKV-cysteamine) is a CPP with primary amphipathicity (i.e amphipathicity resulting from the amino acid sequence itself, not from the folding structure [56]) that comprises a tryptophan-rich so-called 'hydrophobic' domain, a hydrophilic domain derived from an NLS (nuclear localization signal) of SV40 (simian virus 40) large T-antigen, and a

spacer between them [57]. A cysteamine group is present at the C-terminus [57] (Table 1).

Pep-1 has been used to introduce large proteins inside cell lines [57–59]. An endosomal pathway was rejected because (1) there was no difference in translocation efficiency at 37 °C and 4 °C [57] and (2) no co-localization of a delivered protein (β-galactosidase from *Escherichia coli*) with different cellular organelles (early endosomes, caveosomes and lysosomes) was detected [59]. By contrast, Weller et al. [58] proposed an endosome-mediated mechanism based on the internalization of Pep-1–protein complexes in the presence or absence of endocytic inhibitors.

Deshayes et al. [60] proposed a transient transmembrane-pore-like structure promoted by α-helix conformation of the hydrophobic domain when it interacts with membranes. This conclusion was not corroborated by other groups, because no membrane leakage was detected [35,58]. An alternative mechanism, mediated by electrostatic peptide–lipid interactions, was proposed after observation that Pep-1 translocation both *in vitro* [35] or *in vivo* [59] only occurs in the presence of a transmembrane potential.

When Pep-1 was modified at the C-terminus [lack of cysteamine group and grafting of a CF (carboxyfluorescein) group], the membrane affinity and the translocation efficiency was truly impaired, but a small uptake seems to occur by an endocytic mechanism [16].

The chimaeric peptide $S4_{13}$-PV, which results from the combination of a 13-amino-acid sequence derived from the dermaseptin S4 ($S4_{13}$ domain) with the NLS from SV40 large T-antigen (see Table 1), was proposed as a potential vehicle to introduce macromolecules into cells [61]. The uptake of this peptide under non-fixation conditions was not decreased in the presence of endocytic inhibitors [62]. An endocytic uptake was only evident at low peptide concentration [63]. The binding of the $S4_{13}$-PV peptide to the cell membrane is promoted by electrostatic interactions with negatively charged components at the cell surface, and a conformation change in the $S4_{13}$ domain upon insertion into the bilayers was detected [62]. The translocation of $S4_{13}$-PV across the cell membrane is considered to be a consequence of a transient membrane destabilization produced by peptide–membrane interactions [62]. Endosomal internalization at low peptide concentration suggests that higher peptide concentrations are necessary to induce membrane destabilization.

Translocation mechanism or mechanisms?

Considering the abovementioned examples, it is clear that the mechanism by which CPPs translocate across cell membrane and deliver their cargoes in the cytosol is far from being totally understood. Although some CPPs are able to translocate by an endocytic pathway, the escape from endosomes demands a physically driven mechanism.

The affinity of each CPP for lipid bilayers may be the key factor for their main mechanism of uptake. Penetratin, for instance, does not show a strong affinity for zwitterionic membranes [46,64,65] and does not induce significant membrane destabilization [66]. Interaction with model membranes only occurs in negatively charged lipid bilayers [46,65]. In studies of the interaction of this peptide with eukaryotic cells, negatively charged proteoglycans presented at the cell surface were regarded as essential for translocation to occur [42,44,45]. Cellular uptake of penetratin occurs via endocytosis, but requires the expression of proteoglycans [42], which demonstrates the importance of electrostatic interactions in increasing the affinity of the peptide for cell membranes [45].

By contrast, Pep-1 has a high affinity for lipidic membranes, even in the absence of negatively charged phospholipids or proteoglycans [67], and it induces significant membrane destabilization [35], which seems to favour internalization. Moreover, the introduction of a CF dye into the hydrophilic domain of Pep-1 and/or deletion of a cysteamine group decreased the peptide's affinity and, consequently, its uptake [16,58], and a slight internalization by endosomal pathway occurs [16]. This suggests that the membrane affinity and the capacity to destabilize it dictate the extent to which a peptide enters the cell by a physical mechanism (a fast process during which the endosomal pathway may be considered stationary) to the detriment of the endosomal pathway.

The hypothesis of the co-existence of endosomal and physically mediated mechanisms was also proposed by Boisseau et al. [68] in a study with maurocalcine, a CPP isolated from the Israeli gold scorpion (*Scorpio maurus palmatus*). A contribution of both mechanisms was identified where the physically driven mechanism results from a transmembrane potential. Moreover, Nakase et al. [69] showed that greater amounts of oligo-arginine were found in the cytoplasm when cells were incubated at 4 °C than at 37 °C. They proposed that, when endosomal pathways are inhibited and an alternative pathway can operate, the peptide is more efficiently translocated to the cytosol. When incubation is at 37 °C, oligo-arginine release in the cytoplasm is difficult, owing to endosome entrapment.

Translocation by a physical mechanism demands not only the existence of a high membrane affinity, but also a promoting force: pH gradients [53] and transmembrane potentials [34] are two possible driving forces. The existence of such driving forces is well understood in the cell context, where in/out media are characterized by the preservation of gradients.

HOW DO AMPs GET INSIDE CELLS?

The mechanisms by which AMPs gain access to a cell's interior can be classified as pore-dependent and pore-independent, the former being the most usual. In fact, there are relatively few AMPs that do not exert their main function via cell lysis, membrane permeabilization or other forms of bilayer disruption. Few AMPs attack internal targets, and, of those, only a small number can do so without membrane perturbation [70].

AMPs that induce membrane permeabilization

After the initial peptide–membrane interaction, mechanisms diverge; besides lysis, usually by a mechanism known as the 'carpet' model [71,72], two other models have been proposed for AMP pore formation: the barrel-stave pore and the toroidal pore (for further detailed information, see references [73,74]).

Independently of the pore type, diffusion of free peptide through the pore may not be the principal process of translocation; instead, it has been proposed that it is the peptide molecules that are involved in pore formation that stochastically translocate as the pore disintegrates [28]. Several factors support this statement, the most relevant being the fact that, for AMPs, the local concentration of membrane-bound peptide molecules is usually several orders of magnitude higher than in the aqueous phase (e.g. [75,76]); as such, there will be many more peptide molecules available for pore formation than for pore crossing. In addition, pore diameters are relatively narrow and usually not longer than the length of the peptides (alamethicin barrel stave pores have a diameter of 2–3 nm [77] and those of toroidal mellitin have a diameter of 3–4 nm [74]), preventing or hindering a free diffusion of the peptide; lastly, pore lifetimes are in the microsecond-to-millisecond range (between 40 μs for magainin and 200 ms for dermaseptins [28,78]), which is long compared with a single-molecule translocation time, but

probably not long enough to quickly equilibrate inner and outer peptide concentrations.

Given this hypothesis, pore formation can be regarded not only as a membrane perturbation process, but also as an important intermediate step towards cellular invasion by AMPs. This is in agreement with recent findings that indicate that a synergic effect of activity at both membrane and cytoplasm levels may be required to fully explain the mechanisms of some pore-forming AMPs [79–81].

Non-lytic AMPs

For AMPs that preferentially attack internal cellular targets, similar translocation mechanisms have been reported: for buforin 2, which translocates efficiently, but with little membrane activity [70,82,83], the structure and orientation in the bilayer have been observed to be very similar to those of magainin 2 (Table 1) [83,84]. From these results a model was proposed whereby buforin 2 molecules would form a toroidal pore, just as magainin 2 does, but less stable; this would result in shorter pore lifetimes – with a concomitant decrease in permeabilization – at the same time that the translocation rate would increase because pore disintegration, which is the actual translocation step, would become more frequent [83,84]. This model is supported by results that show that the presence of bilayer components that prevent the formation of toroidal pores (such as dioleyl phosphatidylethanolamine [28]) inhibit buforin 2 translocation, whereas anionic phospholipids, which decrease the charge repulsions between the cationic peptide molecules, stabilize the pore to a point that significant leakage and flip-flop is observed [84]. Buforin 2 translocation has also been shown to withstand cargo addition, as demonstrated by the attachment of green fluorescent protein [29,85], which makes this peptide a promising candidate for its development into a CPP.

Other mechanisms of translocation

Apidaecins, which are another class of non-lytic AMPs that are able to kill bacteria with undetectable membrane permeabilization, act by binding to a cytoplasmic target (Table 1) [86]. In this case, translocation has been proposed to occur by specific interaction with a putative membrane permease or transporter in the target bacterial cell; this was suggested by the fact that the all-D enantiomers of the peptides lose the ability to cross the membrane [86]. This characteristic confers a high selectivity on these peptides, which can even be modulated [87], but, on the other hand, the need for a membrane transporter makes apidaecins unappealing as templates for CPP design.

Despite their apparent simplicity, many AMPs have been shown to possess activity-specific regions: through sequence manipulation it has been possible to regulate translocating behaviour, target specificity or antimicrobial efficiency [87–89]. By means of these alterations, it has become possible to broaden the spectrum of CPP template candidates beyond non-cytotoxic translocating AMPs. This has been taken advantage of, for example, in the derivatives of the membrane-active Bac7 peptide [29,88,90], which, unlike their precursor, are not membrane-disruptive, but have retained translocation capabilities.

CPPs AND AMPs OR JUST MEMBRANE-ACTIVE PEPTIDES?

Membrane translocation is a corollary for membrane permeabilization. Although treated differently by people interested in CPPs and AMPs, the ability to reach the inner leaflet of lipid bilayers is of crucial importance to both. Potentially, all CPPs are AMPs and all AMPs are CPPs. At high enough concentration, peptides reported as CPP perturb membranes and become membrane permeabilizers (see reference [91], in which antimicrobial activity of different CPPs is evaluated), whereas AMPs may reach cytoplasmatic targets before membrane permeabilization. This is not surprising, because both CPPs and AMPs are very similar molecules: short cationic peptides. It should be stressed that both classes cannot be differentiated on account of their structure because there is a wide diversity of conformations within each class of peptides [25,92]. The attention devoted to both CPPs and AMPs is very application-oriented, which dictates why these very similar classes of molecules are considered in such a separate fashion. CPPs are mainly studied by people focusing on gene therapy and drug delivery. AMPs are mainly regarded as tools to fight bacterial infections. However, from the molecular mechanistic point of view, the separation of these peptides into two groups is really rather academic.

Cellular membranes of target cells where the activity of these two peptides are evaluated are quite different. CPPs are generally evaluated against mammalian cells, whereas the target of AMPs is the bacterial cell. The major differences rely on anionic-lipidic and cholesterol contents. The bacterial membrane has a higher percentage of negatively charged lipids and does not contain sterols [24]. Different effects reported with CPPs and AMPs can arise from the differences in membrane composition, factors which modulate peptide affinity and membrane destabilization.

Considering the overlap between the mode of action of CPPs and AMPs, it does not seem reasonable to obstinately seek an exclusive answer to the question whether CPPs enter cells through endocytic or physical processes. As indicated above in the present Review, depending on circumstances, the same peptide may potentially use both [16,63,68]. Moreover, endocytic entrapment has to be followed by physical membrane translocation if the peptide is to reach the cytoplasm. The physical pathway can be mechanistically described by the interaction equilibrium between the peptides in the medium and the outer leaflet of membranes, perturbation of bilayers, translocation among leaflets and a second equilibrium of the peptides between the inner leaflet of the membrane and the reducing conditions of the cell interior [67,93–95] (Figure 1). A more effective or faster formation of a membrane-disturbing structure, mediated by the AMP magainin, was identified when a transmembrane potential was present [96].

Certain chimaera peptides, such as Pep-1, may even be considered a ‘blend’ between AMPs and CPPs. Although reported as a CPP, Pep-1 is a strongly amphipathic cationic peptide, rich in basic amino acids and tryptophan, having a proline residue in its sequence. These are classical characteristics attributed to AMPs. The ability to cysteine-bridge monomers, which greatly improves translocation efficiency, further increases the similarities to AMPs. Not surprisingly, Pep-1 uses mainly physical routes to translocate membranes [35,57,59]. However, this route is not always operative [16], and endocytic pathways are alternatives. The results obtained with Pep-1 confirm the co-existence of endocytic and physically mediated pathways. Such co-existence was previously proposed by other authors [97] using other CPPs, but this proposal was largely overlooked. The kinetic factor is important, as progress through physically driven pathways is rapid compared with that through endocytic pathways: when both physical and endocytic pathways are operative, the physical pathway is dominant, owing to faster kinetics [67,93].

These peptides are able to destabilize the membrane (fusion and vesicle aggregation were detected) without evidence for pore formation or flip-flop [35,66]. A ‘membrane-thinning’ effect was proposed for the AMP magainin 2 [98], in which the peptide aggregates on the surface of the membrane and the decreased local surface tension allows the peptide to intercalate the membrane.

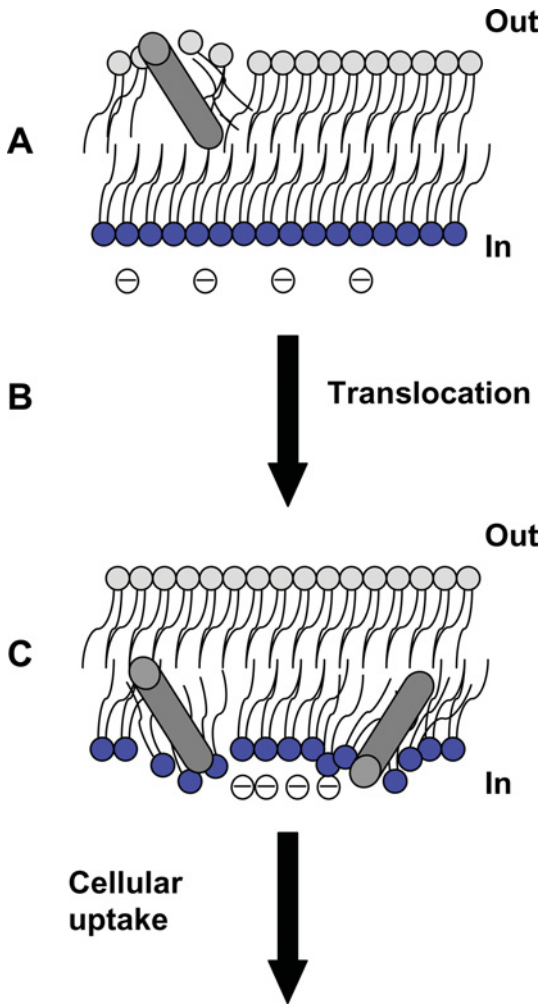

Figure 1 CPP translocation by a physically driven process can be regarded as a composite of three sequential steps

(**A**) The peptide (dark-grey cylinder) inserts in the bilayer outer interface (light-grey head-groups with fatty acid tails) and causes local membrane perturbation. (**B**) Owing to a membrane gradient (e.g. transmembrane potential, pH gradient) or concentration effects, the peptide overcomes the hydrophobic core of the bilayer by an unknown mechanism. (**C**) The peptide is released from the inner leaflet of the membrane (blue head-groups with fatty acid tails) to the cytoplasm. In a model artificial system (e.g. a vesicle) the system would tend to an equilibrium that can be accounted for by three different partition constants, one for each of the elementary steps (**A**, **B** and **C**).

Flexible sealing between peptide side groups and lipid head-groups minimize leakage during the peptide passage through the membrane [29].

A pore-formation mechanism was proposed for MPG (a 27-residue amphipathic peptide) and Pep-1 [60,99], which is also a common mechanism used by antimicrobial peptides. In the case of a transmembrane pore, a large pore would be necessary to allow the passage of attached macromolecules, a situation that compromises cell viability and all the significance of these peptides as vehicles. In some cases pore formation can explain the translocation of the peptides *per se*; however, these pores are not large enough to explain the translocation of proteins [28].

The history of CPP research can be summarized from two different periods, with a sudden change of paradigm in 2001 [32], later confirmed in 2003 [100]. First, the physical paradigm dominated. CPPs were considered to cross bilayers by a physical process. Since 2001–2003 there has been a tendency to think the opposite. Reality may not be so black-and-white, and this rather simplistic view of physically driven versus endocytic mechanisms seems inadequate. The CPP research community should go back to basics and redefine CPPs on the basis of their cargo translocation ability rather than their stand-alone peptide properties.

Most of the CPP research focuses on the peptides' membrane-translocation ability in the absence of cargoes. It is thus crucial to develop new methodologies to detect and quantify translocation of peptide-mediated cargo translocation in vesicles and cells.

As to the peptides themselves, and their interaction with lipid bilayers, it may be that the frontiers between fusogenic peptides, AMPs and CPPs become so undefined that, in the near future, only the unified broad-scope title of 'membrane-active peptides' will make sense.

REFERENCES

1 Wadia, J. S., Becker-Hapak, M. and Dowdy, S. F. (2002) Protein Transport, CRC Press, New York
2 Leamon, C. P. and Low, P. S. (1991) Delivery of macromolecules into living cells: a method that exploits folate receptor endocytosis. Proc. Natl. Acad. Sci. U.S.A. **88**, 5572–5576
3 Frankel, A. D. and Pabo, C. O. (1988) Cellular uptake of the tat protein from human immunodeficiency virus. Cell **55**, 1189–1193
4 Joliot, A., Pernelle, C., Deagostini-Bazin, H. and Prochiantz, A. (1991) Antennapedia homeobox peptide regulates neural morphogenesis. Proc. Natl. Acad. Sci. U.S.A. **88**, 1864–1868
5 Vives, E., Brodin, P. and Lebleu, B. (1997) A truncated HIV-1 Tat protein basic domain rapidly translocates through the plasma membrane and accumulates in the cell nucleus. J. Biol. Chem. **272**, 16010–16017
6 Derossi, D., Joliot, A. H., Chassaing, G. and Prochiantz, A. (1994) The third helix of the Antennapedia homeodomain translocates through biological membranes. J. Biol. Chem. **269**, 10444–10450
7 Theodore, L., Derossi, D., Chassaing, G., Llirbat, B., Kubes, M., Jordan, P., Chneiweiss, H., Godement, P. and Prochiantz, A. (1995) Intraneuronal delivery of protein kinase C pseudosubstrate leads to growth cone collapse. J. Neurosci. **15**, 7158–7167
8 Fawell, S., Seery, J., Daikh, Y., Moore, C., Chen, L. L., Pepinsky, B. and Barsoum, J. (1994) Tat-mediated delivery of heterologous proteins into cells. Proc. Natl. Acad. Sci. U.S.A. **91**, 664–668
9 Ezhevsky, S. A., Nagahara, H., Vocero-Akbani, A. M., Gius, D. R., Wei, M. C. and Dowdy, S. F. (1997) Hypo-phosphorylation of the retinoblastoma protein (pRb) by cyclin D:Cdk4/6 complexes results in active pRb. Proc. Natl. Acad. Sci. U.S.A. **94**, 10699–10704
10 Lindgren, M., Hallbrink, M., Prochiantz, A. and Langel, U. (2000) Cell-penetrating peptides. Trends Pharmacol. Sci. **21**, 99–103
11 Rojas, M., Donahue, J. P., Tan, Z. and Lin, Y. Z. (1998) Genetic engineering of proteins with cell membrane permeability. Nat. Biotechnol. **16**, 370–375
12 Rojas, M., Yao, S., Donahue, J. P. and Lin, Y. Z. (1997) An alternative to phosphotyrosine-containing motifs for binding to an SH2 domain. Biochem. Biophys. Res. Commun. **234**, 675–680
13 Allinquant, B., Hantraye, P., Mailleux, P., Moya, K., Bouillot, C. and Prochiantz, A. (1995) Downregulation of amyloid precursor protein inhibits neurite outgrowth *in vitro*. J. Cell Biol. **128**, 919–927
14 Morris, M. C., Vidal, P., Chaloin, L., Heitz, F. and Divita, G. (1997) A new peptide vector for efficient delivery of oligonucleotides into mammalian cells. Nucleic Acids Res. **25**, 2730–2736
15 Pooga, M., Soomets, U., Hallbrink, M., Valkna, A., Saar, K., Rezaei, K., Kahl, U., Hao, J. X., Xu, X. J., Wiesenfeld-Hallin, Z. et al. (1998) Cell penetrating PNA constructs regulate galanin receptor levels and modify pain transmission *in vivo*. Nat. Biotechnol. **16**, 857–861
16 Henriques, S. T., Costa, J. and Castanho, M. A. (2005) Re-evaluating the role of strongly charged sequences in amphipathic cell-penetrating peptides: a fluorescence study using Pep-1. FEBS Lett. **579**, 4498–4502
17 Lewin, M., Carlesso, N., Tung, C. H., Tang, X. W., Cory, D., Scadden, D. T. and Weissleder, R. (2000) Tat peptide-derivatized magnetic nanoparticles allow *in vivo* tracking and recovery of progenitor cells. Nat. Biotechnol. **18**, 410–414
18 Torchilin, V. P., Rammohan, R., Weissig, V. and Levchenko, T. S. (2001) TAT peptide on the surface of liposomes affords their efficient intracellular delivery even at low temperature and in the presence of metabolic inhibitors. Proc. Natl. Acad. Sci. U.S.A. **98**, 8786–8791

19 Koczulla, A. R. and Bals, R. (2003) Antimicrobial peptides: current status and therapeutic potential. Drugs **63**, 389–406
20 Tossi, A., Mitaritonna, N., Tarantino, C., Giangaspero, A., Sandri, L. and Winterstein, K. A. (2003) Antimicrobial Sequences Database (http://www.bbcm.units.it/~tossi/pag1. htm)
21 Powers, J. P. and Hancock, R. E. (2003) The relationship between peptide structure and antibacterial activity. Peptides **24**, 1681–1691
22 Hancock, R. E. (2001) Cationic peptides: effectors in innate immunity and novel antimicrobials. Lancet Infect. Dis. **1**, 156–164
23 Zasloff, M. (2002) Antimicrobial peptides of multicellular organisms. Nature (London) **415**, 389–395
24 Yeaman, M. R. and Yount, N. Y. (2003) Mechanisms of antimicrobial peptide action and resistance. Pharmacol. Rev. **55**, 27–55
25 Hancock, R. E. (1997) Peptide antibiotics. Lancet **349**, 418–422
26 Melo, M. N., Dugourd, D. and Castanho, M. A. R. B. (2006) Omiganan pentahydrochloride in the front line of clinical application of antimicrobial peptides. Recent Pat. Anti-Infect. Drug Discov. **1**, 201–207
27 Zhang, L., Rozek, A. and Hancock, R. E. (2001) Interaction of cationic antimicrobial peptides with model membranes. J. Biol. Chem. **276**, 35714–35722
28 Matsuzaki, K., Murase, O., Fujii, N. and Miyajima, K. (1995) Translocation of a channel-forming antimicrobial peptide, magainin 2, across lipid bilayers by forming a pore. Biochemistry **34**, 6521–6526
29 Magzoub, M. and Gräslund, A. (2004) Cell-penetrating peptides: from inception to application. Q. Rev. Biophys. **37**, 147–195
30 Derossi, D., Calvet, S., Trembleau, A., Brunissen, A., Chassaing, G. and Prochiantz, A. (1996) Cell internalization of the third helix of the Antennapedia homeodomain is receptor-independent. J. Biol. Chem. **271**, 18188–18193
31 Futaki, S., Suzuki, T., Ohashi, W., Yagami, T., Tanaka, S., Ueda, K. and Sugiura, Y. (2001) Arginine-rich peptides. An abundant source of membrane-permeable peptides having potential as carriers for intracellular protein delivery. J. Biol. Chem. **276**, 5836–5840
32 Lundberg, M. and Johansson, M. (2001) Is VP22 nuclear homing an artifact? Nat. Biotechnol. **19**, 713–714
33 Thoren, P. E., Persson, D., Karlsson, M. and Norden, B. (2000) The Antennapedia peptide penetratin translocates across lipid bilayers – the first direct observation. FEBS Lett. **482**, 265–268
34 Terrone, D., Sang, S. L., Roudaia, L. and Silvius, J. R. (2003) Penetratin and related cell-penetrating cationic peptides can translocate across lipid bilayers in the presence of a transbilayer potential. Biochemistry **42**, 13787–13799
35 Henriques, S. T. and Castanho, M. A. (2004) Consequences of nonlytic membrane perturbation to the translocation of the cell penetrating peptide pep-1 in lipidic vesicles. Biochemistry **43**, 9716–9724
36 Fischer, R., Kohler, K., Fotin-Mleczek, M. and Brock, R. (2004) A stepwise dissection of the intracellular fate of cationic cell-penetrating peptides. J. Biol. Chem. **279**, 12625–12635
37 Potocky, T. B., Menon, A. K. and Gellman, S. H. (2003) Cytoplasmic and nuclear delivery of a TAT-derived peptide and a β-peptide after endocytic uptake into HeLa cells. J. Biol. Chem. **278**, 50188–50194
38 Drin, G., Cottin, S., Blanc, E., Rees, A. R. and Temsamani, J. (2003) Studies on the internalization mechanism of cationic cell-penetrating peptides. J. Biol. Chem. **278**, 31192–31201
39 Thoren, P. E., Persson, D., Isakson, P., Goksor, M., Onfelt, A. and Norden, B. (2003) Uptake of analogs of penetratin, Tat(48–60) and oligoarginine in live cells. Biochem. Biophys. Res. Commun. **307**, 100–107
40 Richard, J. P., Melikov, K., Vives, E., Ramos, C., Verbeure, B., Gait, M. J., Chernomordik, L. V. and Lebleu, B. (2003) Cell-penetrating peptides. A reevaluation of the mechanism of cellular uptake. J. Biol. Chem. **278**, 585–590
41 Fittipaldi, A., Ferrari, A., Zoppe, M., Arcangeli, C., Pellegrini, V., Beltram, F. and Giacca, M. (2003) Cell membrane lipid rafts mediate caveolar endocytosis of HIV-1 Tat fusion proteins. J. Biol. Chem. **278**, 34141–34149
42 Console, S., Marty, C., Garcia-Echeverria, C., Schwendener, R. and Ballmer-Hofer, K. (2003) Antennapedia and HIV transactivator of transcription (TAT) "protein transduction domains" promote endocytosis of high molecular weight cargo upon binding to cell surface glycosaminoglycans. J. Biol. Chem. **278**, 35109–35114
43 Lundberg, M., Wikstrom, S. and Johansson, M. (2003) Cell surface adherence and endocytosis of protein transduction domains. Mol. Ther. **8**, 143–150
44 Letoha, T., Kusz, E., Papai, G., Szabolcs, A., Kaszaki, J., Varga, I., Takacs, T., Penke, B. and Duda, E. (2006) *In vitro* and *in vivo* NF-κB inhibitory effects of the cell-penetrating penetratin. Mol. Pharmacol. **69**, 2027–2036
45 Letoha, T., Gaal, S., Somlai, C., Venkei, Z., Glavinas, H., Kusz, E., Duda, E., Czajlik, A., Petak, F. and Penke, B. (2005) Investigation of penetratin peptides. Part 2. *In vitro* uptake of penetratin and two of its derivatives. J. Peptide Sci. **11**, 805–811
46 Ghibaudi, E., Boscolo, B., Inserra, G., Laurenti, E., Traversa, S., Barbero, L. and Ferrari, R. P. (2005) The interaction of the cell-penetrating peptide penetratin with heparin, heparan sulfates and phospholipid vesicles investigated by ESR spectroscopy. J. Peptide Sci. **11**, 401–409
47 Richard, J. P., Melikov, K., Brooks, H., Prevot, P., Lebleu, B. and Chernomordik, L. V. (2005) Cellular uptake of unconjugated TAT peptide involves clathrin-dependent endocytosis and heparan sulfate receptors. J. Biol. Chem. **280**, 15300–15306
48 Wadia, J. S., Stan, R. V. and Dowdy, S. F. (2004) Transducible TAT–HA fusogenic peptide enhances escape of TAT-fusion proteins after lipid raft macropinocytosis. Nat. Med. **10**, 310–315
49 Renigunta, A., Krasteva, G., Konig, P., Rose, F., Klepetko, W., Grimminger, F., Seeger, W. and Hanze, J. (2006) DNA transfer into human lung cells is improved with Tat-RGD peptide by caveoli-mediated endocytosis. Bioconjug. Chem. **17**, 327–334
50 Ferrari, A., Pellegrini, V., Arcangeli, C., Fittipaldi, A., Giacca, M. and Beltram, F. (2003) Caveolae-mediated internalization of extracellular HIV-1 tat fusion proteins visualized in real time. Mol. Ther. **8**, 284–294
51 Vendeville, A., Rayne, F., Bonhoure, A., Bettache, N., Montcourrier, P. and Beaumelle, B. (2004) HIV-1 Tat enters T cells using coated pits before translocating from acidified endosomes and eliciting biological responses. Mol. Biol. Cell **15**, 2347–2360
52 Saalik, P., Elmquist, A., Hansen, M., Padari, K., Saar, K., Viht, K., Langel, U. and Pooga, M. (2004) Protein cargo delivery properties of cell-penetrating peptides. A comparative study. Bioconjug. Chem. **15**, 1246–1253
53 Magzoub, M., Pramanik, A. and Gräslund, A. (2005) Modeling the endosomal escape of cell-penetrating peptides: transmembrane pH gradient driven translocation across phospholipid bilayers. Biochemistry **44**, 14890–14897
54 Rothbard, J. B., Jessop, T. C., Lewis, R. S., Murray, B. A. and Wender, P. A. (2004) Role of membrane potential and hydrogen bonding in the mechanism of translocation of guanidinium-rich peptides into cells. J. Am. Chem. Soc. **126**, 9506–9507
55 Bárány-Wallje, E., Keller, S., Serowy, S., Geibel, S., Pohl, P., Bienert, M. and Dathe, M. (2005) A critical reassessment of penetratin translocation across lipid membranes. Biophys. J. **89**, 2513–2521
56 Fernandez-Carneado, J., Kogan, M. J., Pujals, S. and Giralt, E. (2004) Amphipathic peptides and drug delivery. Biopolymers **76**, 196–203
57 Morris, M. C., Depollier, J., Mery, J., Heitz, F. and Divita, G. (2001) A peptide carrier for the delivery of biologically active proteins into mammalian cells. Nat. Biotechnol. **19**, 1173–1176
58 Weller, K., Lauber, S., Lerch, M., Renaud, A., Merkle, H. P. and Zerbe, O. (2005) Biophysical and biological studies of end-group-modified derivatives of Pep-1. Biochemistry **44**, 15799–15811
59 Henriques, S. T., Costa, J. and Castanho, M. A. (2005) Translocation of β-galactosidase mediated by the cell-penetrating peptide pep-1 into lipid vesicles and human HeLa cells is driven by membrane electrostatic potential. Biochemistry **44**, 10189–10198
60 Deshayes, S., Heitz, A., Morris, M. C., Charnet, P., Divita, G. and Heitz, F. (2004) Insight into the mechanism of internalization of the cell-penetrating carrier peptide Pep-1 through conformational analysis. Biochemistry **43**, 1449–1457
61 Hariton-Gazal, E., Feder, R., Mor, A., Graessmann, A., Brack-Werner, R., Jans, D., Gilon, C. and Loyter, A. (2002) Targeting of nonkaryophilic cell-permeable peptides into the nuclei of intact cells by covalently attached nuclear localization signals. Biochemistry **41**, 9208–9214
62 Mano, M., Henriques, A., Paiva, A., Prieto, M., Gavilanes, F., Simoes, S. and Pedroso de Lima, M. C. (2006) Cellular uptake of $S4_{13}$-PV peptide occurs upon conformational changes induced by peptide-membrane interactions. Biochim. Biophys. Acta **1758**, 336–346
63 Mano, M., Teodosio, C., Paiva, A., Simoes, S. and Pedroso de Lima, M. C. (2005) On the mechanisms of the internalization of $S4_{13}$-PV cell-penetrating peptide. Biochem. J. **390**, 603–612
64 Magzoub, M., Kilk, K., Eriksson, L. E., Langel, U. and Gräslund, A. (2001) Interaction and structure induction of cell-penetrating peptides in the presence of phospholipid vesicles. Biochim. Biophys. Acta **1512**, 77–89
65 Christiaens, B., Symoens, S., Verheyden, S., Engelborghs, Y., Joliot, A., Prochiantz, A., Vandekerckhove, J., Rosseneu, M. and Vanloo, B. (2002) Tryptophan fluorescence study of the interaction of penetratin peptides with model membranes. Eur. J. Biochem. **269**, 2918–2926
66 Thoren, P. E., Persson, D., Lincoln, P. and Norden, B. (2005) Membrane destabilizing properties of cell-penetrating peptides. Biophys. Chem. **114**, 169–179
67 Henriques, S. T. and Castanho, M. A. (2005) Environmental factors that enhance the action of the cell penetrating peptide pep-1. A spectroscopic study using lipidic vesicles. Biochim. Biophys. Acta **1669**, 75–86
68 Boisseau, S., Mabrouk, K., Ram, N., Garmy, N., Collin, V., Tadmouri, A., Mikati, M., Sabatier, J. M., Ronjat, M., Fantini, J. and De Waard, M. (2006) Cell penetration properties of maurocalcine, a natural venom peptide active on the intracellular ryanodine receptor. Biochim. Biophys. Acta **1758**, 308–319

69 Nakase, I., Niwa, M., Takeuchi, T., Sonomura, K., Kawabata, N., Koike, Y., Takehashi, M., Tanaka, S., Ueda, K., Simpson, J. C., Jones, A. T. et al. (2004) Cellular uptake of arginine-rich peptides: roles for macropinocytosis and actin rearrangement. Mol. Ther. **10**, 1011–1022

70 Cudic, M. and Otvos, Jr, L. (2002) Intracellular targets of antibacterial peptides. Curr. Drug Targets **3**, 101–106

71 Pouny, Y., Rapaport, D., Mor, A., Nicolas, P. and Shai, Y. (1992) Interaction of antimicrobial dermaseptin and its fluorescently labeled analogues with phospholipid membranes. Biochemistry **31**, 12416–12423

72 Shai, Y. (1999) Mechanism of the binding, insertion and destabilization of phospholipid bilayer membranes by α-helical antimicrobial and cell non-selective membrane-lytic peptides. Biochim. Biophys. Acta **1462**, 55–70

73 Lee, M. T., Chen, F. Y. and Huang, H. W. (2004) Energetics of pore formation induced by membrane active peptides. Biochemistry **43**, 3590–3599

74 Yang, L., Harroun, T. A., Weiss, T. M., Ding, L. and Huang, H. W. (2001) Barrel-stave model or toroidal model? A case study on melittin pores. Biophys. J. **81**, 1475–1485

75 Heerklotz, H. and Seelig, J. (2001) Detergent-like action of the antibiotic peptide surfactin on lipid membranes. Biophys. J. **81**, 1547–1554

76 Strahilevitz, J., Mor, A., Nicolas, P. and Shai, Y. (1994) Spectrum of antimicrobial activity and assembly of dermaseptin-b and its precursor form in phospholipid membranes. Biochemistry **33**, 10951–10960

77 He, K., Ludtke, S. J., Worcester, D. L. and Huang, H. W. (1996) Neutron scattering in the plane of membranes: structure of alamethicin pores. Biophys. J. **70**, 2659–2666

78 Duclohier, H. (2006) Bilayer lipid composition modulates the activity of dermaseptins, polycationic antimicrobial peptides. Eur. Biophys. J. **35**, 401–409

79 Friedrich, C. L., Moyles, D., Beveridge, T. J. and Hancock, R. E. (2000) Antibacterial action of structurally diverse cationic peptides on Gram-positive bacteria. Antimicrob. Agents Chemother. **44**, 2086–2092

80 Wu, M., Maier, E., Benz, R. and Hancock, R. E. (1999) Mechanism of interaction of different classes of cationic antimicrobial peptides with planar bilayers and with the cytoplasmic membrane of *Escherichia coli*. Biochemistry **38**, 7235–7242

81 Zhang, L., Dhillon, P., Yan, H., Farmer, S. and Hancock, R. E. (2000) Interactions of bacterial cationic peptide antibiotics with outer and cytoplasmic membranes of *Pseudomonas aeruginosa*. Antimicrob. Agents Chemother. **44**, 3317–3321

82 Park, C. B., Kim, H. S. and Kim, S. C. (1998) Mechanism of action of the antimicrobial peptide buforin II: buforin II kills microorganisms by penetrating the cell membrane and inhibiting cellular functions. Biochem. Biophys. Res. Commun. **244**, 253–257

83 Kobayashi, S., Takeshima, K., Park, C. B., Kim, S. C. and Matsuzaki, K. (2000) Interactions of the novel antimicrobial peptide buforin 2 with lipid bilayers: proline as a translocation promoting factor. Biochemistry **39**, 8648–8654

84 Kobayashi, S., Chikushi, A., Tougu, S., Imura, Y., Nishida, M., Yano, Y. and Matsuzaki, K. (2004) Membrane translocation mechanism of the antimicrobial peptide buforin 2. Biochemistry **43**, 15610–15616

85 Takeshima, K., Chikushi, A., Lee, K. K., Yonehara, S. and Matsuzaki, K. (2003) Translocation of analogues of the antimicrobial peptides magainin and buforin across human cell membranes. J. Biol. Chem. **278**, 1310–1315

86 Li, W. F., Ma, G. X. and Zhou, X. X. (2006) Apidaecin-type peptides: biodiversity, structure–function relationships and mode of action. Peptides **27**, 2350–2359

87 Casteels, P., Romagnolo, J., Castle, M., Casteels-Josson, K., Erdjument-Bromage, H. and Tempst, P. (1994) Biodiversity of apidaecin-type peptide antibiotics. Prospects of manipulating the antibacterial spectrum and combating acquired resistance. J. Biol. Chem. **269**, 26107–26115

88 Sadler, K., Eom, K. D., Yang, J. L., Dimitrova, Y. and Tam, J. P. (2002) Translocating proline-rich peptides from the antimicrobial peptide bactenecin 7. Biochemistry **41**, 14150–14157

89 Staubitz, P., Peschel, A., Nieuwenhuizen, W. F., Otto, M., Gotz, F., Jung, G. and Jack, R. W. (2001) Structure–function relationships in the tryptophan-rich, antimicrobial peptide indolicidin. J. Peptide Sci. **7**, 552–564

90 Skerlavaj, B., Romeo, D. and Gennaro, R. (1990) Rapid membrane permeabilization and inhibition of vital functions of Gram-negative bacteria by bactenecins. Infect. Immun. **58**, 3724–3730

91 Palm, C., Netzereab, S. and Hallbrink, M. (2006) Quantitatively determined uptake of cell-penetrating peptides in non-mammalian cells with an evaluation of degradation and antimicrobial effects. Peptides **27**, 1710–1716

92 Magzoub, M., Eriksson, L. E. and Gräslund, A. (2002) Conformational states of the cell-penetrating peptide penetratin when interacting with phospholipid vesicles: effects of surface charge and peptide concentration. Biochim. Biophys. Acta **1563**, 53–63

93 Hallbrink, M., Floren, A., Elmquist, A., Pooga, M., Bartfai, T. and Langel, U. (2001) Cargo delivery kinetics of cell-penetrating peptides. Biochim. Biophys. Acta **1515**, 101–109

94 Kim, J., Mosior, M., Chung, L. A., Wu, H. and McLaughlin, S. (1991) Binding of peptides with basic residues to membranes containing acidic phospholipids. Biophys. J. **60**, 135–148

95 Tamm, L. K. (1991) Membrane insertion and lateral mobility of synthetic amphiphilic signal peptides in lipid model membranes. Biochim. Biophys. Acta **1071**, 123–148

96 Vaz Gomes, A., de Waal, A., Berden, J. A. and Westerhoff, H. V. (1993) Electric potentiation, cooperativity, and synergism of magainin peptides in protein-free liposomes. Biochemistry **32**, 5365–5372

97 Scheller, A., Wiesner, B., Melzig, M., Bienert, M. and Oehlke, J. (2000) Evidence for an amphipathicity independent cellular uptake of amphipathic cell-penetrating peptides. Eur. J. Biochem. **267**, 6043–6050

98 Ludtke, S., He, K. and Huang, H. (1995) Membrane thinning caused by magainin 2. Biochemistry **34**, 16764–16769

99 Deshayes, S., Gerbal-Chaloin, S., Morris, M. C., Aldrian-Herrada, G., Charnet, P., Divita, G. and Heitz, F. (2004) On the mechanism of non-endosomial peptide-mediated cellular delivery of nucleic acids. Biochim. Biophys. Acta **1667**, 141–147

100 Fischer, R., Fotin-Mleczek, M., Hufnagel, H. and Brock, R. (2005) Break on through to the other side – biophysics and cell biology shed light on cell-penetrating peptides. ChemBioChem **6**, 2126–2142

101 Zasloff, M. (1987) Magainins, a class of antimicrobial peptides from *Xenopus* skin: isolation, characterization of two active forms, and partial cDNA sequence of a precursor. Proc. Natl. Acad. Sci. U.S.A. **84**, 5449–5453

102 Park, C. B., Kim, M. S. and Kim, S. C. (1996) A novel antimicrobial peptide from *Bufo bufo gargarizans*. Biochem. Biophys. Res. Commun. **218**, 408–413

103 Casteels, P., Ampe, C., Jacobs, F., Vaeck, M. and Tempst, P. (1989) Apidaecins: antibacterial peptides from honeybees. EMBO J. **8**, 2387–2391

104 Castle, M., Nazarian, A., Yi, S. S. and Tempst, P. (1999) Lethal effects of apidaecin on *Escherichia coli* involve sequential molecular interactions with diverse targets. J. Biol. Chem. **274**, 32555–32564

Received 19 July 2006/4 August 2006; accepted 4 August 2006
Published on the Internet 13 September 2006, doi:10.1042/BJ20061100

6.3. *How to address CPP and AMP translocation? Methods to detect and quantify peptide internalization in vitro and in vivo?*

To guarantee that a specific peptide works as a CPP, its ability to cross the membrane is of first importance. Despite the fact that most AMPs exert their activity at the membrane level, translocation of some of them has been shown. The experimental methods to evaluate and quantify peptide translocation are of first importance in CPP and AMP field. Several methods for the assessment of membrane translocation have been reported in the last decades; however the information is scarse and spread over the literature. In the paper titled: *How to address CPP and AMP translocation? Methods to detect and quantify peptide internalization in vitro and in vivo?* we review the different methodologies described in the literature. Advantages and disadvantages associated to each methodology are presented in order to help others to find the most appropriate method for their studies.

6.3.1. Declaration on authorship of published manuscript: *How to address CPP and AMP translocation? Methods to detect and quantify peptide internalization in vitro and in vivo?*

I, Sónia Troeira Henriques declare that the manuscript preparation was carried on by me, Manuel N. Melo and Dr. Miguel ARB Castanho.

I, Miguel ARB Castanho, as Sónia T Henriques supervisor, hereby acknowledge and confirm the information above is correct.

_____	_____
Sónia Troeira Henriques	Miguel ARB Castanho

Molecular Membrane Biology, May–June 2007; 24(3): 173–184

informa
healthcare

How to address CPP and AMP translocation? Methods to detect and quantify peptide internalization *in vitro* and *in vivo* (Review)

SÓNIA TROEIRA HENRIQUES, MANUEL NUNO MELO, &
MIGUEL A. R. B. CASTANHO

Centro de Química e Bioquímica, Faculdade de Ciências da Universidade de Lisboa, Lisbon, Portugal

(Received 22 June 2006 and in revised form 13 October 2006)

Abstract
Membrane translocation is a crucial issue when addressing the activity of both cell-penetrating and antimicrobial peptides. Translocation is responsible for the therapeutic potential of cell-penetrating peptides as drug carriers and can dictate the killing mechanisms, selectivity and efficiency of antimicrobial peptides. It is essential to evaluate if the internalization of cell-penetrating peptides is mediated by endocytosis and if it is able to internalize attached cargoes. The mode of action of an antimicrobial peptide cannot be fully understood if it is not known whether the peptide acts exclusively at the membrane level or also at the cytoplasm. Therefore, experimental methods to evaluate and quantify translocation processes are of first importance. In this work, over 20 methods described in the literature for the assessment of peptide translocation *in vivo* and *in vitro*, with and without attached macromolecular cargoes, are discussed and their applicability, advantages and disadvantages reviewed. In addition, a classification of these methods is proposed, based on common approaches to detect translocation.

Keywords: *Cell-penetrating peptides, antimicrobial peptides, membrane translocation, peptide uptake, evaluation of peptide internalization*

Introduction

The introduction of hydrophilic molecules into mammalian cells has become a key strategy for the investigation of intracellular processes and drug therapy. Several methods have been devised to achieve this goal, but they all have limitations [1]. Some peptides are able to translocate across cell membranes with low toxicity [2–5] and to mediate cellular uptake of proteins [3] and other macromolecules [6,7]. These peptides are known as cell-penetrating peptides (CPPs) but the CPP designation is now generalized for all the peptides with the ability to translocate across membranes even when cargo uptake properties are unknown. They include natural, newly synthesized and chimeric peptides [8]. Beside the ability to translocate through cell membrane, these peptides are normally characterized as short, cationic, water-soluble peptides with high efficiency and low cytotoxicity [9]. The mechanism used by CPPs to pass the membrane is not well understood and is a controversial topic in the literature. At the beginning the internalization mechanism of CPPs was generalized and considered to be endocytosis-independent [2,5]. Nowadays there is experimental evidence for both endocytic and non-endocytic routes (for further information see [9,10]). Considering the information available in the literature a unique mechanism for all the peptides does not seem reasonable and more than one mechanism can operate for a single peptide [10].

Ribosomal antimicrobial peptides, or AMPs, are efficient antibiotics against a variety of microbial pathogens [11–14]. These peptides are usually short and cationic [15] such as CPPs, but they are also characterized by a strong interaction with cellular membranes, and by the ability to selectively attack pathogens without disturbing host cell integrity [16,17]. AMPs are potential candidates of a new antibiotic generation against multiresistant bacterial strains [16].

Despite the fact that most AMPs exert their principal activity at the membrane level [15,17], translocation processes have been shown to occur for many of them [18,19]. Considering this, AMPs are natural templates for designing cell-penetrating

Correspondence: Miguel A. R. B. Castanho, Centro de Química e Bioquímica, Faculdade de Ciências da Universidade de Lisboa, Ed. C8, Campo Grande, 1749-016 Lisbon, Portugal. Tel: +35 1217500931; Fax: +35 1217500088. E-mail: castanho@fc.ul.pt

ISSN 0968-7688 print/ISSN 1464-5203 online
DOI: 10.1080/09687860601102476

molecules, which can be developed into carriers [9,20]. AMPs and their derivatives are thus very promising molecules to use both as antibiotics and as drug transporters.

To guarantee that a specific peptide works as a CPP, its ability to cross the membrane and the capacity to transport attached cargoes is of first importance. Regarding AMPs, internalization is not a prerequisite and the biological efficiency of AMPs can be evaluated without translocation assessment. However the characterization of such membrane processes is of great value both in the development of new antibiotics and in the design of templates for CPPs [10].

In this paper we will review methods that are available to evaluate peptide uptake into cells or vesicular model membranes.

Methods used to evaluate peptide uptake

Assessment of peptide translocation without attached cargo or labelled with a fluorescent probe

In vivo *methods.* The CPPs internalization mechanism is a matter of vibrant discussion in the literature. To evaluate if CPPs are internalized by endocytosis the dependence of translocation on temperature, or in the presence of specific endocytic inhibitors must be assessed *in vivo*. The intrinsic fluorescence of Trp or Tyr residues cannot be used to investigate peptide internalization *in vivo*, due to the relatively large cellular background fluorescence in the near-UV. Therefore, CPPs are normally derivatized with fluorophores such as Rhodamine B (Rh) [21–24], Fluorescein [5,25–32] and Nitrobenzoxadiazole (NBD) [24,33]. Alternatively, the properties of macromolecular cargoes can be used. In most of the methods described in this section, peptide fluorescence is the experimentally measured signal. However the need to derivatize a peptide can be a limitation not only due to experimental and costly requirements but also because the presence of a dye may alter its properties [34].

Available methods for the *in vivo* detection of peptide internalization can be divided into three categories: quantification of cytosolic concentration, direct visualization of internalization and peptide activity analysis.

Quantification of cytoplasmic concentration. Quantification of cytoplasmic concentration is usually carried out by means of direct measurement of fluorescence emission of peptides. In these methods, elimination of the non-internalized and cell-adsorbed peptide fractions is required to avoid an overestimation of peptide internalization; consequently, extensive washing procedures, including trypsinization and centrifugation, are required [21,22,29,30,35,36]. Quenching of peptide fluorescence is an alternative to annihilate non-internalized peptide signal [24,33,37].

A cell lysate should be prepared and the fluorescence intensity of labelled-CPP in supernatant measured [29,32]. The washing procedures can be responsible for a signal reduction, due to sample loss and fluorescence bleaching. An additional limitation is the necessity to distinguish the peptide fluorescence from the cell background fluorescence; to assure a good signal/noise ratio the fluorophore should be chosen carefully to avoid overlap with intrinsic cellular fluorescence emissions and to circumvent a fast fading of fluorescence. For instance, Trp fluorescence of peptide can hardly be used due to the intrinsic fluorescence of cellular proteins. The fluorescence of cellular NAD(P)H (~460 nm) and FAD (~530 nm) is an additional concern. A high amount of cellular sample should be used to provide a good emission signal and controls without fluorophore in the same conditions (e.g., cell number and washing procedures) must also be used; a calibration curve should be prepared to allow quantification of internalization. In this case, absolute quantification of the internal peptide concentration may also require information on the total cellular volume.

Oehlke et al. developed a method to discriminate membrane surface-bound, membrane-inserted and internalized peptide fractions [38]. To obtain quantitative information on the peptide fraction associated with plasma membrane and the peptide fraction actually internalized, the exposed peptide was treated with diazotized 2-nitroaniline. This procedure modifies the peptide fraction bounded to the surface, without damaging the cell [39]. Bound and internalized fractions were detected by HPLC analysis of cell lysates and quantified by spectrofluorimetry (5(6)-carboxyfluorescein-N-hydroxysuccinilmide ester–labelled peptide detected with excitation at 445 nm and emission at 520 nm). The fraction of surface bound peptide is strongly modified by the diazo reagent which renders the peptide completely undetectable in HPLC chromatogram (there is a strong retention of highly hydrophobic modified products on the stationary phase of the HPLC column). The fraction of peptide inserted into plasma membrane is slightly protected from the attack of the diazo reagent, so this fraction is only partially modified. The fraction of peptide inaccessible to the diazo reagent is the internalized fraction [38].

Flow cytometry analysis by fluorescence activated Cell Sorter (FACS) is a tool to quantify cellular

association of a fluorophore-labelled peptide. A large number of cells are analysed and dead cells are identified by propidium iodide staining [21,22,30, 32,33,35,40]. The cell subpopulation displaying significant fluorescence emission is identified and quantified, and the CPP uptake is measured as the cell-associated fluorescence intensity. An absolute quantification of the internalized amount of peptide requires either a comparison with a standard [41] or the use of additional methods, such as the ones described above. The need to wash/quench the membrane-bound peptide fraction, also applies for flow cytometry analysis.

A kinetic evaluation of the translocation process has been obtained by testing the inaccessibility of externally added trypan blue to fluorescein-labelled peptides [42]; the rationale behind this approach is shared by many methods described for *in vitro* translocation studies (see below).

Matrix-assisted laser desorption ionization-time-of-flight mass spectroscopy (MALDI-TOF MS) has been used to evaluate the exit of internalized peptides from cells into the culture medium [32,43], to detect peptide internalization and to investigate intracellular degradation [32,36,43–45]. This method allows the direct detection of the peptide and uptake quantification [44]. The sample (extracellular or intracellular supernatant) has to be concentrated to improve the signal. Elmquist and Langel proposed a procedure where samples are zip-tipped, analysed by MALDI-TOF MS and compared with synthetic peptides for a quantitative analysis [32,43]. Instead of synthetic peptides the quantification of the internalized CPP can be achieved with an internal standard with the same sequence but labelled with deuterium. Peptides are biotinylated and, after cell lysis, they are captured by streptavidin-coated magnetic beads. Finally, beads are washed and analyzed by MALDI-TOF MS and the absolute amount of internalized peptide is determined. This procedure is also adequate to know if the peptide has been degraded during sample preparation or inside the cell [44]. Inherent disadvantages in this method are the necessity for specialized and expensive procedures, and equipment to obtain peptide quantification. Moreover, it is rather time-consuming.

Direct visualization of internalization. In early studies, CPP internalization into cells was studied by fluorescence microscopy or in fixed cells where the fluorescence emission of a peptide-derivatized probe was directly visualized [5,26,33,46]. Internalization of some AMPs has also been identified by a fluorescent label and visualized under the confocal microscope. For instance, biotin-labelled polyphemusin I [47] and FITC-labelled buforin II [48] were detected in the cytoplasm of *E. coli* without damaging the membrane; FITC-labelled magainin 2 was detected on the *E. coli* cell wall [48]. Internalization in mammalian cells was also observed with biotin-labelled LL-37 and localization in the perinuclear region was detected [49]. Alternatively, the presence of peptides in cells can be detected by immunofluorescence; for example, the localization of LL-37 was visualized with a specific antibody [49].

Fixation procedures can bias the location of peptides in cells as the illusionary presence of peptides inside cells can arise from the high affinity of cationic peptides to cell surface [50]. Therefore, peptide internalization in cells has to be compared in fixed and non-fixed conditions [27,30]. Cell treatment with trypsin to digest the peptide at cell surface [27,30,32], or quenching of peptide fluorescence has to be performed to remove the interference of the membrane-bound fraction. In these conditions it is possible to distinguish a deep localization inside the cell from membrane adsorption [24]. With confocal microscopy different cellular plans can be used to confirm, or refute, peptide internalization.

Peptide activity analysis. In this class of methodologies, the effect of the peptides in the cytosol or in the membrane is evaluated. AMP translocation *in vivo* has been inferred from observations of intracellular damage (e.g., [51]) or morphological alterations of bacteria [52–54].

In other reports, the peptide interaction with membranes was evaluated by electrophysiological transmembrane current measurements in oocytes [55,56]. With this setup it is possible to have access to both sides of lipidic membranes and it is not necessary to derivatize the peptide with a fluorophore. However, this detection can be ambiguous because transbilayer current can arise from the activation of endogenous channels in oocyte membranes. In order to rule out this possibility these experiments should be repeated on artificial lipid membranes [57]. In addition, only qualitative information about translocation can be obtained unless a quantitative relationship between transmembrane current and internalization is assumed. Lastly, the occurrence of membrane destabilizations induced by peptides is not a proof of their ability to translocate across the membrane and reach the cytoplasm.

In vitro *methods*. Various biophysical approaches have been used to study peptide-lipid interaction in model bilayers. When CPPs are internalized by a physically-driven translocation mechanism, peptide-lipid interactions are truly important. Application of

in vitro methods to evaluate the internalization of CPP is, however, scarce; on the other hand, AMP translocation has been essentially studied using model membranes. Nevertheless, *in vitro* studies face some difficulties and limitations. Large unilamellar vesicles (LUV), or small unilamellar vesicles (SUV), are the most used membrane models for the *in vitro* study of peptide-bilayer interactions. But, detection of peptide entry into the vesicular lumen is not easy. Theoretically, in a simple setup, it is possible to encapsulate an aqueous phase entity that could report peptide proximity or interaction (a quencher, or a fluorescence resonance energy transfer (FRET) acceptor for Trp fluorescence for example) and use it to probe the translocation event. However, the feasibility of this task can be hampered by several factors (see worked examples in part 1 of the Supplementary material in the online version). Several methods have been proposed to overcome these limitations, for instance peptide-lipid FRET (e.g., between Trp-labelled peptide and Dansyl-PE-labelled lipidic vesicles) and/or permanent alteration of the peptide either in or out of the vesicles (e.g., peptide digestion by trypsin) [18,19]. A classification of methods can be devised regarding the peptide location with respect to the bilayer: (i) detection of entrapped peptide lack of accessibility from the outer phase, (ii) detection of inward peptide positioning within the membrane, (iii) direct detection of peptide in the inner phase, and (iv) detection of encapsulated peptide escape. Because of the many possible combinations of techniques and experimental setups some reported methods do not fall within the given categories, therefore, a fifth group of 'unclassified methods' is also presented. This classification differs from the one used for the *in vivo* methods mostly because for *in vitro* a wider range of approaches to the assessment of translocation have been described.

A schematic representation of *in vitro* methods from all the classes, with focus on the fluorescence methodologies, is depicted in Figure 1.

Detection of entrapped peptide lack of accessibility from the outer phase. A semi-quantitative determination of translocation can be performed by detection of peptide inaccessibility to a non-translocating entity [19,24,58–60] after incubation with the model membranes (see Figure 1, panel A). For example, translocation of AMP magainin 2 was identified by the observation that the percentage of inaccessible peptide increases with peptide-lipid incubation time [19]. To perform this experiment trypsin was used to digest peptide after interaction with acceptor-labelled lipid vesicles. It was shown that proteolysis-dependent FRET reduction decreases with incubation time before trypsin addition. It was thus concluded that the peptide becomes inaccessible to trypsin with time. This is consistent with peptide translocation.

This concept can be used with different external components, for instance non-labelled vesicles to desorb the peptide from the labelled vesicles [19,60]. An inverted setup has also been reported where the peptide (in this case, labelled with NBD or bimane fluorophores) was incubated with the non-labelled vesicles and desorption was induced by addition of acceptor-labelled anionic vesicles [59] (a FRET increase, rather than a decrease, was detected in this case). The use of NBD-labelled peptides and addition of dithionite ion as the non-translocating entity is another possibility; in this case, the NBD fluorescence intensity was measured without the need to label the vesicles [24,59]; dithionite acts in a way similar to digestion by trypsin in that the NBD reduction/quenching is permanent. In all these approaches, an estimation of the translocation kinetics can be obtained by adding the non-translocating component at different incubation times [24,59].

It should be noted that in all these methods a time-dependent measurement is required to determine the degree of peptide inaccessibility (as explained in detail in section 2 in the Supplementary material online).

These methods have a number of disadvantages: first, they are unable to discriminate membrane-bound and internalized peptide; second, in the case of lysis, which can occur for AMPs, peptide populations in inner and outer layers could be accounted as accessible, resulting in a low extent of apparent translocation; finally, not all of these methods are compatible with all peptides: for instance some AMPs are resistant to trypsin proteolysis (e.g., Polymixin B and Gramicidin S) [18]. In addition, when using trypsin, extents of translocation may be overestimated if the peptide fragments also interact with the membrane.

Detection of inward peptide positioning within the membrane. In this category, the passage of the peptide to the inner leaflet of the bilayer is monitored. In all the reports where this method is used [19,61,62], internalization is evaluated by the use of vesicles with asymmetric labelling. The fluorophore in membranes is a FRET acceptor for Trp-containing peptides (see Figure 1, panel B).

Wimley and White developed a methylcoumarin derivatized lysophospholipid (LysoMC). This lipid is easily incorporated into bilayers (into both bilayers or only into the outer one) and is able to act as an efficient Trp-fluorescence acceptor/quencher [63].

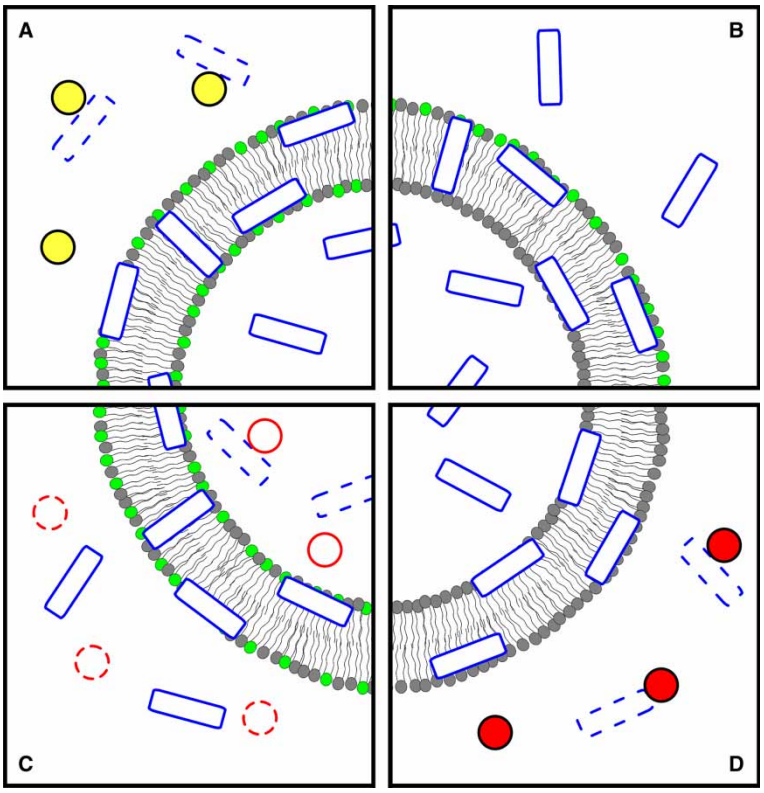

Figure 1. *In vitro* methods for translocation assessment, using FRET and quenching methodologies. Peptide molecules are represented by empty rectangles and additional non-translocating compounds by circles; peptide molecules that have interacted with those compounds are dashed; phospholipids labelled with an acceptor for the peptide's fluorescence are indicated by light grey headgroups. (A) Measurement of the inaccessibility of the peptide to a non-translocating entity with the ability to digest, sequester or permanently quench it; the interaction between the two prevents the peptide from acting as a FRET donor to the labelled phospholipids; small FRET reductions will indicate that the peptide was protected from that interaction; this indicates that the peptide is buried in the membrane or is located in lumen. (B) Detection of inward peptide movement; after the initial adsorption interaction of the peptide with asymmetrically acceptor-labelled vesicles (despite the representation, both inner-leaflet and outer-leaflet labelling can be used), translocation or membrane penetration processes causes the mean distance between peptide and labelled phospholipids to increase (assuming an outer-leaflet labelling) and a concomitant reduction of FRET. If the peptide has quenching capabilities, a quenchable probe can be used to symmetrically label the vesicles; translocation can then be identified by full probe quenching, which is only possible if the peptide reaches the inner bilayer surface. (C) Detection of peptide in the inner phase; in the case of translocation, digestion by encapsulated trypsin (solid circles) reduces the overall amount of peptide available for membrane interaction and, consequently, FRET between peptide and labelled-membrane; trypsin inhibition (dashed circles) is required in the outer phase, prior to peptide addition. (D) Detection of encapsulated peptide escape; in the event of translocation, the peptide fluorescence decreases as it becomes accessible to an externally added, non-translocating quencher; the quencher can, alternatively, be co-encapsulated with the peptide, and the quenching reduction monitored instead. The figure is reproduced in colour in *Molecular Membrane Biology* online.

This probe was initially used to characterize the in-depth membrane distribution of Trp-containing peptides [63], but more recently, Norden and co-workers have developed a method in which LysoMC is used to specifically test translocation; in addition, they described a procedure where is possible to use LysoMC to selectively label the inner layers [61,62]. Experimentally, translocation information is obtained by comparison of emission spectra of inner leaflet LysoMC-labelled vesicles in the presence and absence of the peptide. The Trp residues are donors for FRET. An increase in FRET efficiency in the presence of the peptide means internalization; however, because some outer-to-inner bilayer FRET may occur, it becomes necessary to compare the obtained results with controls where translocating (tryptophan octyl esther [63]) or non-translocating (Ac-18A-NH_2: Ac-DWLKAFYDKVAEKLKEAF-NH_2 [63]) Trp-containing molecules are used [61,62].

Matsuzaki and co-workers had already described a similar method to assess peptide translocation in which vesicles are labelled only on the outer leaflet, with the tryptophan FRET acceptor DNS-PE [19]. With this method it is possible to follow the FRET change during time with a single sample and an end-point approach for each incubation time is not required. Experimentally, after peptide addition, there is an initial increase in FRET efficiency (this corresponds to a peptide partitioning to the outer

leaflet); with time, a decrease in FRET efficiency is observed (which corresponds to translocation where peptide is no longer close to the FRET acceptor in the outer leaflet). With this method, a kinetic analysis of the translocation event can be carried out. Quantitative information may be obtained if additional methods are used to quantitatively relate FRET intensity to luminal peptide concentration.

With these methodologies, peptides do not need to be derivatized and small peptide and lipid concentrations can be used (0.7μM and 100μM respectively [61]). With these methods, in-depth location of peptide can be erroneously measured as translocation; inaddition, they cannot be used with peptides that induce lipid flip flop (FRET acceptor bilayer asymmetry is lost). So far this methodology has been applied only to Trp-containing peptides, although the use of others donor/acceptor pairs is also possible.

Direct detection of peptide in the inner aqueous phase. Methods based on this principle are able to detect the presence of peptides in the inner luminal aqueous phase. With this approach actual translocation, rather than just membrane internalization, is measured (see Figure 1, panel C).

Three different approaches fit in this class of methods. In the first, described by Matsuzaki and co-workers [19], encapsulated trypsin and a peptide-lipid FRET system (Trp-containing peptide and Dansyl chromophore incorporated in vesicles) is used: trypsin is added at the hydration stage of the preparation of symmetrically labelled vesicles; after extrusion, non-encapsulated trypsin is inhibited by a trypsin inhibitor. Upon addition of the peptide to this system, an increase in acceptor fluorescence through FRET is expected as the peptide enters the bilayer; if the peptide is not internalized afterwards, the fluorescence intensity is expected to remain constant after the initial increase. However, if the peptide translocates into the vesicle lumen, it becomes accessible to the uninhibited trypsin and is digested; assuming that the resulting fragments do not interact with the membrane, this degradation of the peptide will lead to a decrease of the amount of peptide in the bilayer and consequent reduction of FRET. A quantitative analysis of the extent of translocation can be easily carried out considering that 100% translocation implies the digestion of all the peptide molecules and absence of FRET; the fluorescence intensity of the system should be the same as in the absence of the peptide. Conversely, 0% translocation will correspond to the maximum fluorescence intensity right after the peptide addition [18,19]. This method cannot be applied to proteolysis-resistent peptide and/or without Trp residues (e.g., Polymixin B and Gramicidin S) [18]. At high translocation efficiency, membrane perturbation caused by peptide fragment accumulation inside vesicles can cause difficulties in internalization quantification. In addition, there is the possibility of digested fragments re-entering the membrane, which can lead to a translocation underestimation.

A second method that detects the presence of the peptide in the inner aqueous phase was recently developed by Bárány-Wallje et al. In this method the experiment is performed with planar lipid membranes (PLMs) and the distribution of fluorescently-labelled peptides, between the two compartments and partitioned in PLM, is followed by confocal fluorescence spectroscopy [64]. This powerful method allows the direct scanning of fluorescence intensity and quantification of peptide in each compartment. Another advantage is the possibility to easily generate asymmetric aqueous phase conditions: a transmembrane potential can be set without the need for ionophores [64]. Besides the need to label the studied peptides (and care must be taken to choose a photostable label), this method has the disadvantage of requiring an uncommon setup with a custom PLM trough.

Another possible method to evaluate peptide translocation with model membranes is to follow peptide interaction with giant vesicles (GVs). With this method direct visualization of peptide interaction with membranes is possible by confocal microscopy. The translocation of peptide across these vesicles can be confirmed by the presence of the fluorophore inside the vesicles [64,65]; in this case, just as with the methodology described for fluorescence imaging of *in vivo* internalization, the use of confocal analysis is crucial to distinguish whether the peptide is inside the vesicle or only adsorbed at the membrane surface. As with the PLM method described above, the peptide has to be derivatized with a fluorophore, which should be carefully chosen to avoid photobleaching.

With GVs it is possible not only to directly visualize the peptide inside the vesicles but also to evaluate its effect on membrane properties: membrane integrity can be followed with a labelled lipid such as N-Rh-PE (the fluorochrome has to be different from the one used to label the peptide), and the possibility of pore formation can be evaluated in GVs loaded with two similar dyes attached to other molecules of very different sizes (for instance Alexa^{488}-Dextran (MW 10000) and Alexa^{546}-maleimide (MW ~1300)). This experimental setup enables direct observation of changes in the membrane permeability during the course of observations and in the case of pore formation to

have information on pore size due to sequential escape of the dyes from the GVs [66,67].

Detection of encapsulated peptide escape. Using a fluorescence quenching assay, Magzoub et al. had developed methodologies in which the escape of a CPP from liposomes is determined in the presence and absence of a pH gradient [68] (see Figure 1, Panel D). To track the peptide escape two assays based on encapsulation were carried out: (i) vesicles were prepared with the peptide inside and the Trp quencher acrylamide was added to the outer phase (the escape of peptide from liposomes was followed by fluorescence quenching of peptide Trp residues caused by acrylamide); (ii) fluorescein-labelled peptides were encapsulated with a quencher (iodide) and, in the case of translocation, a de-quenching of the fluorescein label was observed. The fluorescence intensity corresponding to 100% peptide escape was determined by vesicle lyses with Triton X-100 and the fraction of peptide escape was calculated at different incubation times [68].

Both these approaches allow the quantification of translocation as well as the determination of membrane crossing kinetics. Under certain situations, however, both methods can lead to misleading conclusions: in method (i) acrylamide is excluded from membranes, so only the fraction of peptide that reaches the outer aqueous environment is accounted for (if the peptide remains essentially partitioned in the outer leaflet after crossing the membrane, a lower translocation extent is measured); in method (ii) if the peptide does not translocate but has a deep location in the bilayer, it becomes inaccessible to the encapsulated quencher and is counted as having crossed the membrane.

In these methods if the peptide translocates very efficiently a significant amount of peptide can escape from the liposome during the gel filtration step (used to remove non-encapsulated peptide); therefore, these methods are only applicable to peptides that require special conditions to translocate (such as pH or potential membrane gradients), so that membrane crossing can be triggered only after the separation procedure.

Another peptide escape assay was described by Bárány-Wallje et al. in which vesicles uniformly preloaded with peptide both in the lumen and outer medium are dialysed so that any peptide outside of the liposomes is washed away [64]. If any peptide absorption/fluorescence remains after the dialysis, it can be concluded that translocation from the lumen/inner leaflet to the outer side did not occur; conversely, the occurrence of translocation can be inferred from the absence of any peptide signal. Due to the very simple setup and instrumentation requirements, this seems a good option to begin a translocation study with; however, there are a number of disadvantages that are addressed in section 3 of the Supplementary material online.

Other methods. A methodology based on a particular peptide property was developed in reference [69]. For this purpose, the specific fluorescence quenching of Rh by the CPP pep-1 was taken advantage of. Vesicles labelled symmetrically with N-Rh-PE were used to evaluate fluorescence emission quenching of Rh by pep-1 in the presence and absence of a transmembrane potential. After the peptide is added to LUVs, Rh fluorescence in the outer layer is quenched. If translocation occurs, it can be identified by a further reduction in Rh fluorescence due to contact of the peptide with Rh in the inner leaflet. The effect can be improved by using labelled multilamellas vesicles (MLVs): the fraction of Rh-PE available for peptide access is smaller than if LUVs are used, therefore a much larger relative increase in quenching is expected if the peptide translocates and accesses all the phospholipids [69]. Alternatively, soluble Rh can be encapsulated in vesicles and its fluorescence followed after peptide addition [69].

This method allows measurements to be taken during a time course, enabling the kinetic evaluation of the translocation process. Its main disadvantage is that it is only applicable to peptides that are able to quench a given fluorophore.

Another method using MLVs has been reported [60,70]: dithionite ion was externally added to NBD-PE-doped MLVs, resulting in quenching of the fluorophores in the outermost leaflet; upon the addition of a pore-forming peptide the dithionite ion will have access to the first intramembranar space of the MLVs, resulting in an increase in quenching; full NBD quenching, however, will only be attained if the peptide can translocate and form pores in the inner bilayers because only then will all the fluorophore become accessible to the dithionite ion.

This method does not require any peptide labelling or intrinsic fluorescence but, on the other hand, this can only be applied to peptides that perturb the membrane to an extent where dithionite can cross it (by a pore or otherwise). Kinetic information can be extracted but it is necessary to take into consideration the multiple membrane crossing steps.

Assessment of peptide translocation with attached cargo

The translocation process of CPPs may vary if the peptide is in free form or attached to a cargo. Differences in peptide kinetics and cell localization can occur [71–73]. In the above described methodologies the only attached 'cargoes' were

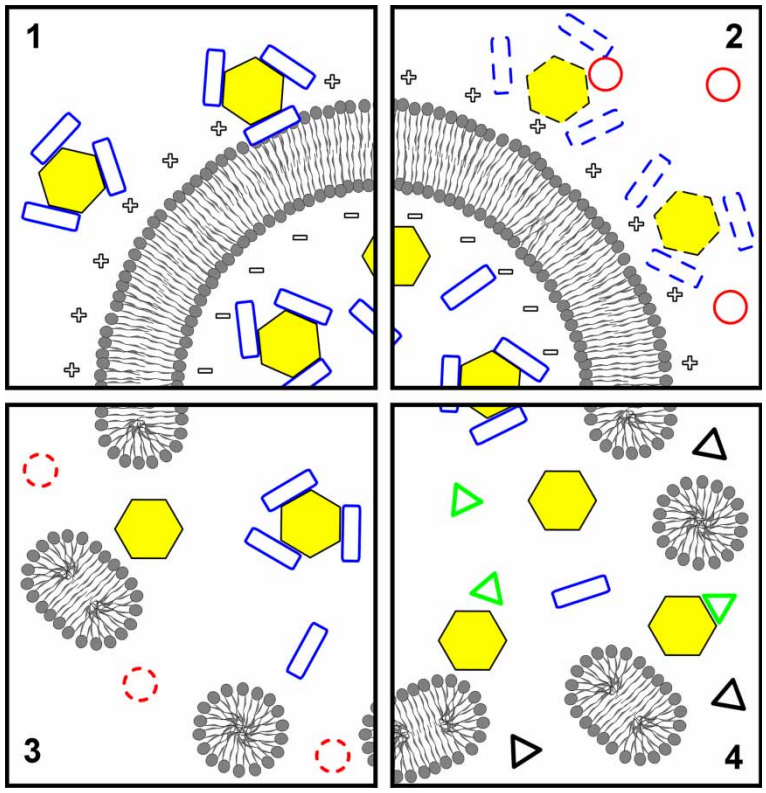

Figure 2. To evaluate the translocation of β-Gal/pep-1 (hexagons/rectangles) complexes across model membranes the following steps were reported [81]: (1) valinomycin was added to K^+-loaded vesicles in Na^+-buffer to create a negative transmembrane potential; the complex was added to the solution and translocated across bilayer; (2) trypsin (circles) was added to digest non-incorporated complex and free pep-1 or β-Gal (dashed hexagons/rectangles); (3) after digestion, trypsin was inhibited (dashed circles) with phenylmethylsulfonyl fluoride and TX-100 was then added to facilitate the release of internalized β-Gal and allow its quantification (digestion debris were excluded from the last two panels, and inhibited trypsin from the last, to avoid image crowding); (4) β-Gal activity was assayed by MUG (black triangles) hydrolysis to a fluorescent product, 4-MU (lighter triangles). The figure is reproduced in colour in *Molecular Membrane Biology* online.

fluorophores. The nature and size of the cargoes and the nature of attachment to the peptide (whether covalent [3,74] or weaker [7,75]) can also be a determinant for the translocation mechanism. Given these differences, development of consistent methods to evaluate the capacity to translocate/deliver proteins across artificial/natural membranes would be fruitful to systematically confirm (or refute) vector properties of CPPs. Practically all methods described above for *in vivo* or *in vitro* testing can, in principle, be extended to assess the translocation of CPP-cargo complexes, although no reports on such usage were found; however, some properties of the macromolecule attached to the peptide are additional advantages to detect and quantify translocation, opening the possibility for more sensitive methodologies. Three methods that have been reported for the *in vivo* studies and one for the *in vitro* studies of the internalization of CPP-cargo complexes are discussed here; while these can easily fit into the above classification, they are presented separately to underscore their importance in confirming the vector properties of a CPP.

Morris et al. had observed the efficiency of pep-1 to deliver GFP [75] and a similar approach demonstrated the ability of the AMP buforin 2 to translocate across bilayers with a macromolecular cargo [76]. Recombinant proteins with CPP and GFP domains have also been produced [77–79]. Instead of GFP, Wadia et al. labelled TAT-Cre recombinase by coupling it to Alexa 488 or Alexa 546 fluorophores [80]. GFP or Cre recombinase translocation is followed by its intrinsic fluorescence; this is in all aspects identical to what was previously described for the *in vivo* direct visualization of internalization. Another possibility to measure Cre recombinase translocation mediated by TAT is by recombination reporter assay, where the expression of enhanced GFP (EGFP) is dependent on TAT-Cre transduction into cells, followed by nuclear import. The signal of EGFP is followed and measured as a consequence of TAT-Cre import [80].

Detection of β-Gal delivery into cells was also reported. Translocation was assessed by monitoring the X-Gal staining enzymatic activity of β-Gal [75]. The detection of the enzymatic activity of the cargo not only allows a sensitive detection of the

Table I. Classification of available methods for *in vivo* and *in vitro* translocation assessment, and respective advantages and disadvantages.

			Advantages			Disadvantages			
		Refs	Can provide kinetic information	Can use intrinsic peptide fluorescence	Can quantify the internalized peptide	Cannot identify translocation with certainty	Peptide derivatization is an absolute requirement	Complex/lengthy experimental setup	Not applicable to all peptides
in vivo methods	*Quantification of cytoplasmic concentration*								
	Fluorescence spectroscopy	[29,32,33,37]			●		●	●	
	Mass spectrometry	[32,36,43–45]			●		●	●	
	Flow cytometry	[30,41,42]	●		●		●	●	
	Direct visualization of internalization								
	Confocal microscopy	[5,27,30,50]	●				●	●	
	Peptide activity analysis								
	Visualization of cytoplasmic damage	[51–54]				●			●
	Channel detection	[55,56]				●			●
	Methods used for peptides with attached cargo								
	Visualization of attached GFP	[75–77]	●						
	Measurement of cargo enzymatic activity	[37,75,81]			●				
	Immunofluorescence visualization (antibodies raised against cargo)	[81]							
in vivo methods	*Measurement of peptide inaccessibility from the outer phase*								
	FRET within the membrane; trypsin addition	[19]	●	●		●			●
	FRET within the membrane; vesicle addition	[19,59,60]	●	●		●			
	Quenching of NBD-derivatized peptides by added dithionite	[24,59]	●			●	●		
	Detection of inward peptide positioning within the membrane								
	Asymmetrical labeling of vesicles with LysoMC or DNS-PE	[19,61,62]	●	●		●	●		●
	Detection of peptide in the inner phase								
	Trypsin digestion in the vesicular lumen	[19]	●	●	●				●
	PLM assembly visualized by confocal microscopy	[64]	●		●		●	●	
	Detection of encapsulated peptide escape								
	External quencher addition to encapsulated peptide	[68]	●	●				●	●
	Co-encapsulation of quencher and peptide	[68]	●	●				●	●
	Dialysis of peptide-LUV mixtures	[64]		●				●	●
	Other methods								
	Rh quenching by the peptide	[69]	●		●				●
	Peptide-promoted NBD-PE quenching by dithionite in MLVs	[60,70]	●						●
in vivo methods	*Methods used for peptides with attached cargo*								
	Measurement of cargo enzymatic activity	[80,81]			●				

internalized CPP-cargo complex, but also tests whether CPP-mediated translocation can occur without cargo damage/denaturation. A quantification of β-Gal internalization was developed by means of its enzymatic activity on the substrate 4-methylumbelliferone β-D-galactopyranoside (MUG), a non fluorescent substrate that is converted to 4-methylumbelliferone (4-MU), which is a fluorescent product. 4-MU production enables quantification of protein internalization from its activity [37,81].

Another possibility to evaluate protein delivery efficiency is by immunofluorescence, using a primary antibody raised against the carried protein and a fluorescently labelled secondary antibody, as was preformed with β-Gal [81]. This method is independent of particular cargo properties; therefore, it is suited to study the transport of cargoes that do not have intrinsic fluorescence or detectable enzymatic activity. With these methodologies it is possible to obtain cell transfection efficiency, but not the quantification of peptide/protein internalization.

Protein uptake was also evaluated *in vitro* with pep-1/β-Gal, by taking advantage of the β-Gal enzymatic activity and 4-MU fluorescent properties (see Figure 2). Briefly, after peptide/protein incubation with LUVs, trypsin was added externally to digest the non-incorporated peptide and β-Gal; afterwards, phenylmethanesulfonyl fluoride (PMSF) was added to inhibit trypsin. To induce LUV permeabilization and leakage of the incorporated β-Gal, Triton X-100 was added, and enzymatic activity of β-Gal was determined by MUG hydrolysis [81]. Intrinsic cargo fluorescence and/or enzymatic activity are specific properties that can be used for application of a similar methodology to other peptides/proteins complexes.

The classification and the general advantages and disadvantages of the application of each reviewed method are summarized in Table I.

For all the methods presented here, it is possible to conclude about the ability of peptides to translocate. When further information is sought, quantitative analysis should always be carefully carried out; for this, several different complementing methodologies should be conjugated, regarding not only the actual evaluation of translocation but also to quantify the peptide distribution between the membrane and aqueous environments and to characterize the membrane topology upon peptide interaction (occurrence of membrane thinning, pore formation, lysis, etc.).

Concluding remarks

Because most methods for the assessment of membrane translocation have only been reported during the last decade, it is understandable that this field is regarded as being underdeveloped, methodology-wise [18]. In addition, the description of new methods has not always been given the due emphasis by their authors, which further contributed to the lack of visibility of these procedures. Yet, over 20 methods that address the assessment of membrane translocation have been found. The authors of this work hope that the gathering of this knowledge will help others find and use the most appropriate methods for their studies. On the other hand, this compilation should by no means be regarded as an ultimate source for information on translocation assessment methodologies in a way that the development of new methods, or the improvement of already described ones, is discouraged. Rather, by exposing the strengths and weaknesses of several methodologies, it is hoped that the development of newer and better methods is encouraged and facilitated.

References

[1] Wadia JS, Becker-Hapak M, Dowdy SF. 2002. Protein transport. In: Langel Ü, editor. Cell-penetrating peptides, processes and applications. 1st ed. New York: CRC Press. p. 365–375.
[2] Derossi D, Joliot AH, Chassaing G, Prochiantz A. 1994. The third helix of the Antennapedia homeodomain translocates through biological membranes. J Biol Chem 269:10444–10450.
[3] Fawell S, Seery J, Daikh Y, Moore C, Chen LL, Pepinsky B, Barsoum J. 1994. Tat-mediated delivery of heterologous proteins into cells. Proc Natl Acad Sci USA 91:664–668.
[4] Schwarze SR, Ho A, Vocero-Akbani A, Dowdy SF. 1999. In vivo protein transduction: delivery of a biologically active protein into the mouse. Science 285:1569–1572.
[5] Vives E, Brodin P, Lebleu B. 1997. A truncated HIV-1 Tat protein basic domain rapidly translocates through the plasma membrane and accumulates in the cell nucleus. J Biol Chem 272:16010–16017.
[6] Allinquant B, Hantraye P, Mailleux P, Moya K, Bouillot C, Prochiantz A. 1995. Downregulation of amyloid precursor protein inhibits neurite outgrowth in vitro. J Cell Biol 128:919–927.
[7] Morris MC, Vidal P, Chaloin L, Heitz F, Divita G. 1997. A new peptide vector for efficient delivery of oligonucleotides into mammalian cells. Nucleic Acids Res 25:2730–2736.
[8] Lindgren M, Hallbrink M, Prochiantz A, Langel U. 2000. Cell-penetrating peptides. Trends Pharmacol Sci 21:99–103.
[9] Magzoub M, Graslund A. 2004. Cell-penetrating peptides: from inception to application. Q Rev Biophys 37:147–195.
[10] Henriques ST, Melo MN, Castanho MA. 2006. Cell-penetrating peptides and antimicrobial peptides: how different are they? Biochem J 399:1–7.
[11] Koczulla AR, Bals R. 2003. Antimicrobial peptides: current status and therapeutic potential. Drugs 63:389–406.
[12] Tossi A, Mitaritonna N, Tarantino C, Giangaspero A, Sandri L, Winterstein KA. 2003. Antimicrobial Sequences Database.

[13] Powers JP, Hancock RE. 2003. The relationship between peptide structure and antibacterial activity. Peptides 24: 1681–1691.
[14] Hancock RE. 2001. Cationic peptides: effectors in innate immunity and novel antimicrobials. Lancet Infect Dis 1:156–164.
[15] Hancock RE. 1997. Peptide antibiotics. Lancet 349:418–422.
[16] Zasloff M. 2002. Antimicrobial peptides of multicellular organisms. Nature 415:389–395.
[17] Yeaman MR, Yount NY. 2003. Mechanisms of antimicrobial peptide action and resistance. Pharmacol Rev 55:27–55.
[18] Zhang L, Rozek A, Hancock RE. 2001. Interaction of cationic antimicrobial peptides with model membranes. J Biol Chem 276:35714–35722.
[19] Matsuzaki K, Murase O, Fujii N, Miyajima K. 1995. Translocation of a channel-forming antimicrobial peptide, magainin 2, across lipid bilayers by forming a pore. Biochemistry 34:6521–6526.
[20] Fischer R, Fotin-Mleczek M, Hufnagel H, Brock R. 2005. Break on through to the other side-biophysics and cell biology shed light on cell-penetrating peptides. Chembiochem 6:2126–2142.
[21] Mano M, Teodosio C, Paiva A, Simoes S, Pedroso de Lima MC. 2005. On the mechanisms of the internalization of S4(13)-PV cell-penetrating peptide. Biochem J 390:603–612.
[22] Jones SW, Christison R, Bundell K, Voyce CJ, Brockbank SM, Newham P, Lindsay MA. 2005. Characterisation of cell-penetrating peptide-mediated peptide delivery. Br J Pharmacol 145:1093–1102.
[23] Fuchs SM, Raines RT. 2004. Pathway for polyarginine entry into mammalian cells. Biochemistry 43:2438–2444.
[24] Drin G, Cottin S, Blanc E, Rees AR, Temsamani J. 2003. Studies on the internalization mechanism of cationic cell-penetrating peptides. J Biol Chem 278:31192–31201.
[25] Wender PA, Mitchell DJ, Pattabiraman K, Pelkey ET, Steinman L, Rothbard JB. 2000. The design, synthesis, and evaluation of molecules that enable or enhance cellular uptake: peptoid molecular transporters. Proc Natl Acad Sci USA 97:13003–13008.
[26] Vives E, Granier C, Prevot P, Lebleu B. 1997. Structure-activity relationship study of the plasma membrane translocating potential of a short peptide from HIV-1 Tat protein. Lett Pept Sci 4:429–436.
[27] Thoren PE, Persson D, Isakson P, Goksor M, Onfelt A, Norden B. 2003. Uptake of analogs of penetratin, Tat(48-60) and oligoarginine in live cells. Biochem Biophys Res Commun 307:100–107.
[28] Suzuki T, Futaki S, Niwa M, Tanaka S, Ueda K, Sugiura Y. 2002. Possible existence of common internalization mechanisms among arginine-rich peptides. J Biol Chem 277:2437–2443.
[29] Saalik P, Elmquist A, Hansen M, Padari K, Saar K, Viht K, Langel U, Pooga M. 2004. Protein cargo delivery properties of cell-penetrating peptides. A comparative study. Bioconjug Chem 15:1246–1253.
[30] Richard JP, Melikov K, Vives E, Ramos C, Verbeure B, Gait MJ, Chernomordik LV, Lebleu B. 2003. Cell-penetrating peptides. A reevaluation of the mechanism of cellular uptake. J Biol Chem 278:585–590.
[31] Potocky TB, Menon AK, Gellman SH. 2003. Cytoplasmic and nuclear delivery of a TAT-derived peptide and a beta-peptide after endocytic uptake into HeLa cells. J Biol Chem 278:50188–50194.
[32] Fischer R, Kohler K, Fotin-Mleczek M, Brock R. 2004. A stepwise dissection of the intracellular fate of cationic cell-penetrating peptides. J Biol Chem 279:12625–12635.
[33] Drin G, Mazel M, Clair P, Mathieu D, Kaczorek M, Temsamani J. 2001. Physico-chemical requirements for cellular uptake of pAntp peptide. Role of lipid-binding affinity. Eur J Biochem 268:1304–1314.
[34] Szeto HH, Schiller PW, Zhao K, Luo G. 2005. Fluorescent dyes alter intracellular targeting and function of cell-penetrating tetrapeptides. Faseb J 19:118–120.
[35] Boisseau S, Mabrouk K, Ram N, Garmy N, Collin V, Tadmouri A, Mikati M, Sabatier JM, Ronjat M, Fantini J, De Waard M. 2006. Cell penetration properties of maurocalcine, a natural venom peptide active on the intracellular ryanodine receptor. Biochim Biophys Acta 1758:308–319.
[36] Balayssac S, Burlina F, Convert O, Bolbach G, Chassaing G, Lequin O. 2006. Comparison of penetratin and other homeodomain-derived cell-penetrating peptides: interaction in a membrane-mimicking environment and cellular uptake efficiency. Biochemistry 45:1408–1420.
[37] Henriques ST, Costa J, Castanho MA. 2005. Re-evaluating the role of strongly charged sequences in amphipathic cell-penetrating peptides: a fluorescence study using Pep-1. FEBS Lett 579:4498–4502.
[38] Oehlke J, Scheller A, Wiesner B, Krause E, Beyermann M, Klauschenz E, Melzig M, Bienert M. 1998. Cellular uptake of an alpha-helical amphipathic model peptide with the potential to deliver polar compounds into the cell interior non-endocytically. Biochim Biophys Acta 1414:127–139.
[39] Oehlke J, Brudel M, Blasig IE. 1994. Benzoylation of sugars, polyols and amino acids in biological fluids for high-performance liquid chromatographic analysis. J Chromatogr B Biomed Appl 655:105–111.
[40] Richard JP, Melikov K, Brooks H, Prevot P, Lebleu B, Chernomordik LV. 2005. Cellular uptake of unconjugated TAT peptide involves clathrin-dependent endocytosis and heparan sulfate receptors. J Biol Chem 280:15300–15306.
[41] Raucher D, Chilkoti A. 2001. Enhanced uptake of a thermally responsive polypeptide by tumor cells in response to its hyperthermia-mediated phase transition. Cancer Res 61:7163–7170.
[42] Massodi I, Bidwell GL, 3rd, Raucher D. 2005. Evaluation of cell penetrating peptides fused to elastin-like polypeptide for drug delivery. J Control Release 108:396–408.
[43] Elmquist A, Langel U. 2003. In vitro uptake and stability study of pVEC and its all-D analog. Biol Chem 384:387–393.
[44] Burlina F, Sagan S, Bolbach G, Chassaing G. 2005. Quantification of the cellular uptake of cell-penetrating peptides by MALDI-TOF mass spectrometry. Angew Chem Int Ed Engl 44:4244–4247.
[45] Aussedat B, Sagan S, Chassaing G, Bolbach G, Burlina F. 2006. Quantification of the efficiency of cargo delivery by peptidic and pseudo-peptidic Trojan carriers using MALDI-TOF mass spectrometry. Biochim Biophys Acta 1758:375–383.
[46] Futaki S, Suzuki T, Ohashi W, Yagami T, Tanaka S, Ueda K, Sugiura Y. 2001. Arginine-rich peptides. An abundant source of membrane-permeable peptides having potential as carriers for intracellular protein delivery. J Biol Chem 276: 5836–5840.
[47] Powers JP, Martin MM, Goosney DL, Hancock RE. 2006. The antimicrobial peptide polyphemusin localizes to the cytoplasm of *Escherichia coli* following treatment. Antimicrob Agents Chemother 50:1522–1524.

[48] Park CB, Kim HS, Kim SC. 1998. Mechanism of action of the antimicrobial peptide buforin II: buforin II kills microorganisms by penetrating the cell membrane and inhibiting cellular functions. Biochem Biophys Res Commun 244: 253–257.

[49] Lau YE, Rozek A, Scott MG, Goosney DL, Davidson DJ, Hancock RE. 2005. Interaction and cellular localization of the human host defense peptide LL-37 with lung epithelial cells. Infect Immun 73:583–591.

[50] Lundberg M, Johansson M. 2001. Is VP22 nuclear homing an artifact? Nat Biotechnol 19:713–714.

[51] Friedrich CL, Moyles D, Beveridge TJ, Hancock RE. 2000. Antibacterial action of structurally diverse cationic peptides on gram-positive bacteria. Antimicrob Agents Chemother 44:2086–2092.

[52] Boman HG, Agerberth B, Boman A. 1993. Mechanisms of action on Escherichia coli of cecropin P1 and PR-39, two antibacterial peptides from pig intestine. Infect Immun 61:2978–2984.

[53] Shi J, Ross CR, Chengappa MM, Sylte MJ, McVey DS, Blecha F. 1996. Antibacterial activity of a synthetic peptide (PR-26) derived from PR-39, a proline-arginine-rich neutrophil antimicrobial peptide. Antimicrob Agents Chemother 40:115–121.

[54] Subbalakshmi C, Sitaram N. 1998. Mechanism of antimicrobial action of indolicidin. FEMS Microbiol Lett 160:91–96.

[55] Deshayes S, Heitz A, Morris MC, Charnet P, Divita G, Heitz F. 2004. Insight into the mechanism of internalization of the cell-penetrating carrier peptide Pep-1 through conformational analysis. Biochemistry 43:1449–1457.

[56] Deshayes S, Gerbal-Chaloin S, Morris MC, Aldrian-Herrada G, Charnet P, Divita G, Heitz F. 2004. On the mechanism of non-endosomial peptide-mediated cellular delivery of nucleic acids. Biochim Biophys Acta 1667:141–147.

[57] Chaloin L, De E, Charnet P, Molle G, Heitz F. 1998. Ionic channels formed by a primary amphipathic peptide containing a signal peptide and a nuclear localization sequence. Biochim Biophys Acta 1375:52–60.

[58] Pouny Y, Rapaport D, Mor A, Nicolas P, Shai Y. 1992. Interaction of antimicrobial dermaseptin and its fluorescently labeled analogues with phospholipid membranes. Biochemistry 31:12416–12423.

[59] Terrone D, Sang SL, Roudaia L, Silvius JR. 2003. Penetratin and related cell-penetrating cationic peptides can translocate across lipid bilayers in the presence of a transbilayer potential. Biochemistry 42:13787–13799.

[60] Drin G, Demene H, Temsamani J, Brasseur R. 2001. Translocation of the pAntp peptide and its amphipathic analogue AP-2AL. Biochemistry 40:1824–1834.

[61] Persson D, Thoren PE, Esbjorner EK, Goksor M, Lincoln P, Norden B. 2004. Vesicle size-dependent translocation of penetratin analogs across lipid membranes. Biochim Biophys Acta 1665:142–155.

[62] Thoren PE, Persson D, Esbjorner EK, Goksor M, Lincoln P, Norden B. 2004. Membrane binding and translocation of cell-penetrating peptides. Biochemistry 43:3471–3489.

[63] Wimley WC, White SH. 2000. Determining the membrane topology of peptides by fluorescence quenching. Biochemistry 39:161–170.

[64] Barany-Wallje E, Keller S, Serowy S, Geibel S, Pohl P, Bienert M, Dathe M. 2005. A critical reassessment of penetratin translocation across lipid membranes. Biophys J 89:2513–2521.

[65] Thoren PE, Persson D, Karlsson M, Norden B. 2000. The antennapedia peptide penetratin translocates across lipid bilayers – the first direct observation. FEBS Lett 482:265–268.

[66] Ambroggio EE, Kim DH, Separovic F, Barrow CJ, Barnham KJ, Bagatolli LA, Fidelio GD. 2005. Surface behavior and lipid interaction of Alzheimer beta-amyloid peptide 1-42: a membrane-disrupting peptide. Biophys J 88:2706–2713.

[67] Ambroggio EE, Separovic F, Bowie JH, Fidelio GD, Bagatolli LA. 2005. Direct visualization of membrane leakage induced by the antibiotic peptides: maculatin, citropin, and aurein. Biophys J 89:1874–1881.

[68] Magzoub M, Pramanik A, Graslund A. 2005. Modeling the endosomal escape of cell-penetrating peptides: transmembrane pH gradient driven translocation across phospholipid bilayers. Biochemistry 44:14890–14897.

[69] Henriques ST, Castanho MA. 2004. Consequences of nonlytic membrane perturbation to the translocation of the cell penetrating peptide pep-1 in lipidic vesicles. Biochemistry 43:9716–9724.

[70] Matsuzaki K, Yoneyama S, Murase O, Miyajima K. 1996. Transbilayer transport of ions and lipids coupled with mastoparan X translocation. Biochemistry 35:8450–8456.

[71] Rejman J, Oberle V, Zuhorn IS, Hoekstra D. 2004. Size-dependent internalization of particles via the pathways of clathrin- and caveolae-mediated endocytosis. Biochem J 377:159–169.

[72] De Coupade C, Fittipaldi A, Chagnas V, Michel M, Carlier S, Tasciotti E, Darmon A, Ravel D, Kearsey J, Giacca M, Cailler F. 2005. Novel human-derived cell-penetrating peptides for specific subcellular delivery of therapeutic biomolecules. Biochem J 390:407–418.

[73] Silhol M, Tyagi M, Giacca M, Lebleu B, Vives E. 2002. Different mechanisms for cellular internalization of the HIV-1 Tat-derived cell penetrating peptide and recombinant proteins fused to Tat. Eur J Biochem 269:494–501.

[74] Pooga M, Soomets U, Hallbrink M, Valkna A, Saar K, Rezaei K, Kahl U, Hao JX, Xu XJ, Wiesenfeld-Hallin Z, Hokfelt T, Bartfai T, Langel U. 1998. Cell penetrating PNA constructs regulate galanin receptor levels and modify pain transmission in vivo. Nat Biotechnol 16:857–861.

[75] Morris MC, Depollier J, Mery J, Heitz F, Divita G. 2001. A peptide carrier for the delivery of biologically active proteins into mammalian cells. Nat Biotechnol 19:1173–1176.

[76] Takeshima K, Chikushi A, Lee KK, Yonehara S, Matsuzaki K. 2003. Translocation of analogues of the antimicrobial peptides magainin and buforin across human cell membranes. J Biol Chem 278:1310–1315.

[77] Tyagi M, Rusnati M, Presta M, Giacca M. 2001. Internalization of HIV-1 tat requires cell surface heparan sulfate proteoglycans. J Biol Chem 276:3254–3261.

[78] Fittipaldi A, Ferrari A, Zoppe M, Arcangeli C, Pellegrini V, Beltram F, Giacca M. 2003. Cell membrane lipid rafts mediate caveolar endocytosis of HIV-1 Tat fusion proteins. J Biol Chem 278:34141–34149.

[79] Ferrari A, Pellegrini V, Arcangeli C, Fittipaldi A, Giacca M, Beltram F. 2003. Caveolae-mediated internalization of extracellular HIV-1 tat fusion proteins visualized in real time. Mol Ther 8:284–294.

[80] Wadia JS, Stan RV, Dowdy SF. 2004. Transducible TAT-HA fusogenic peptide enhances escape of TAT-fusion proteins after lipid raft macropinocytosis. Nat Med 10:310–315.

[81] Henriques ST, Costa J, Castanho MA. 2005. Translocation of beta-galactosidase mediated by the cell-penetrating peptide pep-1 into lipid vesicles and human HeLa cells is driven by membrane electrostatic potential. Biochemistry 44:10189–10198.

Supplementary Material

Problems associated with the detection of entry of peptide into vesicles

At usual lipid concentrations, used to perform *in vitro* studies, the volume occupied by the vesicles is very small when compared to the bulk aqueous phase: for 100 nm diameter LUVs, produced at a total lipid concentration of 1 mM, and assuming a mean membrane surface area of 0.7 nm^2 per phospholipid [1], the ratio of luminal volume over the total volume will be about $r = 0.003$ v/v. Another problem arises from the fact that these peptides usually have large molar ratio partition constants towards lipidic membranes (about 10^3 to 10^4, e.g., [2,3]). This means that only a small concentration of peptide will be in the aqueous phase unless relatively low lipid concentrations are used. Given the above-mentioned obstacles, it is clear that methods based on the detection of the concentration of internalized peptide will have to deal with very low signal intensities that will likely lie below instrumental detection limit.

Comments on time-dependent measurements

It should be noted that in all the methods presented in the section *Measurement of peptide inaccessibility from the outer phase* a time-dependent measurement is required to determine the degree of peptide inaccessibility: because the amount of free peptide in the outer phase will decrease – as it is digested, sequestered or permanently quenched – the internalized peptide will equilibrate back to the outer phase. Consequently, two stages are expected: in the first, signal magnitude increases (here 'signal', in a very broad sense, can be FRET reduction, FRET increase or fluorescence reduction, depending on the particular method used), detecting the adsorbed/non-internalized peptide fraction; then a second stage ensues with a usually slower signal increase [4,5], which corresponds to the detection of the internalized peptide molecules that are returning to the outer phase. At equilibrium, the signal magnitude should be approximately the same whether translocation has occurred or not. The percentage of accessible peptide is usually obtained by comparing the end of the first stage with a control where peptide, membrane and the non-translocating entity are added simultaneously [4, 5]. From this, it can be seen that, in a hypothetical situation where the translocation kinetics were of the same magnitude of the desorption kinetics, this method would be very difficult to apply as both stages would have the same approximate slopes and the end of the first stage would be hard to detect. On the other hand, information about translocation kinetics could, in principle, be obtained from the rate at which the peptide molecules return to the outer phase, in the second stage.

Advantages and disadvantages associated with the dialysis method

Due to the very simple setup and instrumentation requirements for this experiment (see the section *Detection of encapsulated peptide escape*) this seems a good option to begin a translocation study with, because membrane crossing may be ruled out immediately avoiding the need to use more complex and costly methodologies. However, in order for this method to provide a measurable absorbance/fluorescence peptide signal in the absence of translocation it is required that the amount of internalized peptide be relatively large, to compensate for the effect of the small encapsulation volume. This is only possible to attain if the peptide partitions strongly towards the bilayer and the lipid concentration is high enough: under these conditions, upon vesicle preparation, the peptide molecules can be expected to be equally distributed by the inner and outer leaflets and very few to be left in the aqueous phase; in the absence of translocation, roughly one half of the peptide signal will remain, correspondent to the peptide molecules partitioned in the inner leaflet. Should the peptide partition weakly to the membrane or there be a small lipid concentration, the inner leaflet peptide fraction could be undetected in the absence of translocation, which would generate a false positive. This limitation has to be accounted for by quantifying the extent of membrane interaction. Other disadvantages include the lengthy dialysis process and the lack of any kind of translocation characterization, which makes this method more suited to rule out, rather than ascertain, peptide translocation.

References

[1] Marsh D. 1990. CRC handbook of lipid bilayers. Boca Raton: CRC Press.

[2] Heerklotz H, Seelig J. 2001. Detergent-like action of the antibiotic peptide surfactin on lipid membranes. Biophys J 81:1547–1554.

[3] Strahilevitz J, Mor A, Nicolas P, Shai Y. 1994. Spectrum of antimicrobial activity and assembly of dermaseptin-b and its precursor form in phospholipid membranes. Biochemistry 33:10951–1060.

[4] Terrone D, Sang SL, Roudaia L, Silvius JR. 2003. Penetratin and related cell-penetrating cationic peptides can translocate across lipid bilayers in the presence of a transbilayer potential. Biochemistry 42:13787–13799.

[5] Matsuzaki K, Murase O, Fujii N, Miyajima K. 1995. Translocation of a channel-forming antimicrobial peptide, magainin 2, across lipid bilayers by forming a pore. Biochemistry 34:6521–6526.

Chapter 7

Annex II

Chapter 7.

Annex II

7.1. *Neurotoxicity of PrP(106-126) revisited. A biophysical study with model membranes.*

During this PhD project other peptide was studied, PrP(106-126), a prion protein fragment considered to be responsible for toxicity in prion disease. The exact mechanism behind PrP(106-126) toxicity is largely unknown. In similarity with pep-1, PrP(106-126) has an amphiphatic structure. In this work the possibility of PrP(106-126) to translocate across the membrane by a related mechanism was studied. Once inside the cell, PrP(106-126) could become toxic. This was the hypothesis tested. Fluorescence and UV-vis spectroscopies, CD spectroscopy and surface Plasmon resonance were used to carry on these studies.

Fluorescence and UV-Vis methodologies were used at the Molecular Biophysics laboratory in FCUL, while CD spectroscopy and surface plasmon resonance were carried out at Monash University in Victoria, Australia.

Part of the obtained results are presented in a first version of the manuscript, titled: *Neurotoxicity of PrP(106-126) revisited. A biophysical study with model membranes*. This will be shortly submitted.

7.1.1. Declaration on authorship of the manuscript: *Neurotoxicity of PrP(106-126) revisited. A biophysical study with model membranes.*

I, Sónia Troeira Henriques declare that the experimental design, the laboratory work, the data analysis, discussion and manuscript preparation were carried out by me under guidance of Dr. Miguel ARB Castanho, Dr. Mibel Aguilar and Dr. Leonard Patenden. Fluorescence and UV-Vis studies were carried at Faculdade de Ciências and supervised by Dr. Miguel ARB Castanho while studies with surface plasmon resonance and CD spectroscopy were carried at Monash University, Victoria, Australia, under supervision of Dr. Mibel Aguilar and Dr. Leonard Patenden.

I, Miguel ARB Castanho, as Sónia T Henriques supervisor, hereby acknowledge and confirm the information above is correct.

_____ _____

Sónia Troeira Henriques Miguel ARB Castanho

Neurotoxicity of PrP(106-126) revisited. A biophysical study with model membranes.

Sónia Troeira Henriques[1], Leonard Pattenden[2], Marie-Isabel Aguilar[2], Miguel A.R.B. Castanho[1,*]

[1]*Centro de Química e Bioquímica, Faculdade de Ciências da Universidade de Lisboa, Ed. C8, Campo Grande, 1749-016 Lisboa, Portugal*
[2]*Department of Biochemistry & Molecular Biology, Monash University, Victoria, 3800 Clayton, Australia*

* Corresponding author

Short title: Does PrP(106-126) form pores?

ABSTRACT

Transmissible spongiform encephalopathies are neurodegenerative diseases with characteristic accumulation of an abnormal isoform of the prion protein, PrP^{Sc}. Its fragment 106-126 was reported to maintain most of the pathological features of PrP^{Sc} and a role in neurodegeneration has been proposed based on the modulation of membrane properties and channel formation. Nevertheless, this issue is quite controversial in the literature. In the case channels are formed the peptide-membrane interactions should be the key feature to explain the toxicity of PrP^{Sc}. In the present work we examined the interaction of PrP(106-126) with model membranes by surface plasmon resonance and fluorescence methodologies. A comprehensive study where different conditions, such as: membrane charge, viscosity, lipid composition, presence of ganglioside, pH and ionic strength, were tested, modulated, and compared. PrP(106-126) has a very low affinity for lipidic membranes at physiological conditions. Only in extreme conditions, where strong electrostatic interactions are operative, insertion in lipid bilayer and leakage were detected. These results support the hypothesis of the requirement PrP^{C} to mediate PrP(106-126) toxic effects in neuronal cells.

Keywords: Prion Disease, Fluorescence methodologies, Model membranes, Surface Plasmon resonance, Pore formation.

INTRODUCTION

Prion diseases, also known as transmissible spongiform encephalopathies (TSE), are human and animal diseases, characterized by progressive neuronal loss often accompanied by a spongiform brain alteration and the deposition of amyloid fibrils. These diseases appear in sporadic, familial and infectiously acquired forms and are invariably fatal without evoking in the host any inflammatory or immune response [1]. The interest in prion diseases has grown from the emergence of bovine spongiform encephalopathy and the possible infection of human beings [2].

This pathology is initiated by a post-translational modification of a glycoprotein called prion protein (PrP) abundantly expressed in the central nervous system (CNS) of mammalian species. A pathological scrapie form, PrP^{Sc}, interacts with the physiological form, PrP^{C}, which is converted into another scrapie form molecule ($PrP^{Sc} + PrP^{C} \rightarrow 2\ PrP^{C}$). This conversion occurs by a mechanism not well understood and is likely to take place at cell surface, more specifically in rafts domains, where the PrP^{C} is preferentially located due to its glycosylphosphatidylinositol (GPI)-anchor (see [3, 4] and references therein).

These two PrP isoforms possess different physico-chemical properties: PrP^{C} has an α-helical structure susceptible to enzymatic digestion, while PrP^{Sc} has a large amount of β-structure contribution and is resistant to proteolysis. With this conformation, highly insoluble aggregates are formed within the brain and seem to be responsible for the neurological damages that occur in this disease [5].

PrP^{Sc} aggregates are not the only cause of pathology and the time course of its accumulation is not coincident with the time course of neurodegeneration [6]. The observation of PrP^{Sc} accumulation in intracellular compartments and the identification of some other forms of PrP (transmembrane forms [6] and a cytosolic form [7]) suggest that the endosomal pathway can also be involved in disease propagation where all these forms can be involved and take part on the propagation of the disease (see [6] and references therein).

Among all the synthetic peptides that have been tested, the fragment spanning human PrP region 106-126 (KTNMKHMAGAAAAGAVVGGLG) was identified as the most highly amyloidogenic region, with the capacity to readily form fibrils [8, 9], with neurotoxic activity [10] and partially resistant to proteolysis [11]. Regarding these

observations it was postulated that the PrP(106-126) may be a major contributor to the physico-chemical and pathogenic properties of PrP^{Sc} [12] with a role in amyloid formation and in the nerve cell degeneration occurring in prion-related encephalopathies, therefore it was proposed as a model peptide of PrP infectious form [11]. PrP(106-126) sequence is present in all abnormal PrP isoforms accumulated in the patients brain [12] suggesting that this region may possess the ability to trigger or enable a fundamental pathogenic mechanism common to different forms of Prion disease [13].

The amphiphatic primary structure of PrP(106-126), characterized by two domains, one hydrophilic (KTNMKHM) and other hydrophobic (AGAAAAGAVVGGLG), suggests an ability to interact with cell membrane [14]. Previous studies of the interaction of PrP (106-126) with model membranes show that the pH and ionic strength are of first importance both on secondary structure and interaction with membranes [8, 15]. An increased affinity for membranes at acidic pH together with a concomitant increase in β-sheet content support the hypothesis of endosomal pathway involment in PrP^{Sc} formation/propagation through the neuronal cells and a possible effect of PrP(106-126) fragment in the Prion disease toxicity. Not only the formation of fibril aggregates but also membrane pore induced by PrP(106-126) may be a possible explanation for PrP toxicity, as shown by electrophysiological studies [16, 17]. However, pore formation [18] and neurotoxicity [19] were not confirmed by other groups. Moreover Fioriti et al, had not found evidences for PrP(106-126) infection or ability for conversion of PrP^{C} to PrP^{Sc} or to any other toxic PrP species [13]. Furthermore, it was suggested that PrP(106-126) is not toxic by itself, it becomes toxic only in the presence of PrP^{C} form [13, 20]. It was proposed that it toxicity results from an alteration of physiological functions of PrP^{C} instead of an effect induced by the PrP(106-126) fragment *per si* [13].

Therefore, the existence of a physiological role for this peptide remains unclear in the literature. If a toxic effect in fact exists, peptide-membrane interactions are the key feature to explain it effects. This prompt us to perform a study of the interaction of PrP(106-126) with model membranes. These experiments were carried out by Surface Plasmon Resonance (SPR) with supported lipid bilayers and by fluorescence spectroscopy methodologies with large unilamellar vesicles (LUVs). Peptide affinity to membranes, kinetics of peptide interaction, effects on membrane stability, and the possibility of pore formation were addressed. Different conditions such as: membrane

charge, viscosity, lipid composition, pH, and ionic strength were studied. The interaction with membranes appears to be relevant only at low ionic strength and high anionic-phospholipids contents, which are non-physiological conditions, and no evidence for pore formation was detected. This supports the hypothesis that PrP(106-126) toxicity can be explained by a loss/modification of biological PrP^{C} function within neuronal cells in opposition to this peptide being toxic by itself.

MATERIALS AND METHODS

Materials

PrP(106-126) with purity higher than 95% was obtained from Genscript corporation (piscataway, New Jersey); 2-(4-(2-Hydroxyethul)-1-piperazinyl)ethanesulfonic acid (HEPES), sodium chloride, L-Tryptophan, acrylamide, ethanol and chloroform spectroscopic were obtained from Merk (Darmstadt, Germany); 1-Palmitoyl-2-Oleoyl-*sn*-Glycero-3-Phosphocholine (POPC), 1-Palmitoyl-2-Oleoyl-*sn*-Glycero-3-(Phospho-rac-(1-glycerol)) (POPG), 1-Palmitoyl-2-Oleoyl-*sn*-Glycero-3-(Phospho-rac-(1-serine)) (POPS), 1,2-Dipalmitoyl-*sn*-Glycero-3-phosphocholine (DPPC) and 1-Palmitoyl-2-Oleoyl-*sn*-Glycero-3-(phospho-L-serine) (POPS), 1,2dipalmitoyl-*sn*-glycero-3-phosphoethanolamine-N(7-nitro-2-1,3-benzoxadiazol-4-yl) (N-NBD-PE), and monoganglioside GM1 were obtained from Avanti Polar-Lipids (Alabaster, Alabama); congo red (CR), Thioflavin T (ThT), (3-[3-Cholamidpropy)-dimethyl-ammonio]-1-propanesulfonate (CHAPS) and Cholesterol (chol) were obtained from sigma (St. Louis, Missouri); tris-(2-cyanoethyl)phosphine (phosphine), 1-anilinonaphthalene-8-sulfonic acid (ANS) and 4-(2-[6-(dioctylamino)-2-naphthalenyl]ethenyl)-1-(3-sulfopropyl)-pyridinium (Di-8-ANEPPS) were obtained from molecular probes (Eugene, Oregon).

Working conditions and apparatus

PrP(106-126) was dissolved in sterile water with 2mg/mL (1.05mM). Throughout this study, pH effect was evaluated comparing cytoplasmatic physiological conditions (10 mM HEPES, pH7.4 containing 150mM NaCl) with pH5 to mimic endosomal medium (20mM Sodium Acetate, pH 5 containing 150 mM NaCl). The effect of low ionic strength was evaluated at pH5 (20mM Sodium Acetate, 10mM NaCl). Assays were performed at room temperature (25ºC). UV-vis spectrophotometer Jasco V-560 was used for UV-vis measurements. Steady-state fluorescence measurements were carried out in a Spex ® FluoroLog-3 (Horiba Jobin Yvon) with double excitation and emission monochromators and a 450W xenon lamp. SPR measurements were performed in a Biacore T100 (GE Healthcare) with a series S sensor chip L1. Circular Dichroism (CD) measurements were done on a Jasco J-810 spectropolarimeter equipped with a temperature unit control.

Intermolecular β-structures determined by Thioflavin T and Congo Red

The presence of β-structures was analysed by fluorescence emission of ThT [21] and CR absorbance [22, 23]. Titration of 15μM ThT with PrP(106-126) was followed by fluorescence spectra with $\lambda_{excitation}$=450nm.

CR absorption was followed by titration of 5μM CR with PrP(106-126) stock solution for final peptide concentrations in the range 0-50μM.

Peptide aggregation followed by ANS fluorescence

The effect of peptide concentration on PrP(106-126) aggregation was followed by means of ANS fluorescence emission [24-26] with excitation at 369nm; 12.8μM ANS (A_{369}~0.1) was used through the experiments.

Lipid vesicles preparation for peptide-membrane studies

Large unilamellar vesicles (LUVs) are good model membranes due to their large radii of curvature and because they are equilibrium structures [27]. With these model membranes different properties can be modulated (e.g. lipid charge, membrane viscosity, the presence of a sterol, the effect of pH and ionic strength). Using different lipidic mixtures is possible to explore selected membrane properties on peptide insertion. LUVs were prepared by extrusion method as previously stated [28]. Briefly, lipid solutions in chloroform were dried under a stream of N2 and residual organic solvent was removed in vacuum chamber overnight. The lipidic film was hydrated with buffer and subject to eight freeze-thaw cycles to produce multilamellar vesicles (MLVs). MLVs were extruded through polycarbonate filters (400nm and 100nm pore size filter two and eight times, respectively), to obtain LUVs. For SPR measurements vesicles were prepared by the same procedure but extruded with a 50nm pore size in order to obtain smaller vesicles, more unstable and easier to fuse at chip surface.

Peptide affinity for lipidic membranes followed by SPR

Interaction of PrP(106-126) with lipidic bilayers was studied by SPR. Liposomes composed by different lipidic mixtures (POPC, POPC/POPG (20% POPG molar), POPC/Chol (33% Chol molar) and POPC/GM1 (10% GM1 molar)) were prepared as stated above. For lipid deposition on chip surface, LUVs (1mM lipid concentration)

were injected across the L1 chip for 40min at a flow rate of 2μL/min; with this procedure an equilibrium level was reached. The signal obtained varied with lipidic composition, but was reproduced for each composition though the assays.

A short injection of 10mM NaOH (36s at a flow rate of 50μL/min) was used to remove loosely bound LUVs with a final stabilization period of 300s, which resulted in a stable baseline. The response units of lipid membranes immobilized on the chip were in the range 5000-11000, depending on the liposome lipidic composition.

Peptide solutions with different concentrations (0-50μM) were injected over the lipid surface for 180s at 20μL/min, and dissociation was followed for 600s. The sensor chip surface was washed with injection of 20mM CHAPS (60s, 5μL/min), 10mM NaOH in 20% MeOH (36s, 50μL/min) and 10mM NaOH (36s, 50μL/min), with a final stabilization period of 600s. All solutions were freshly prepared and filtered through 0.22μm pores. The operating temperature was 25ºC. The procedure was followed maintaining the conditions to ensure that the experimental conditions are comparable between experiments as far as possible.

The affinity of peptide for the lipid bilayer membrane was determined from analysis and curve fitting of a series of response curves collected with different peptide concentrations. When appropriate, association and dissociation rate constants were globally fitted using BIAevaluation version 3.0.

Secondary structure by CD spectroscopy

CD measurements were performed to have insights on PrP(106-126) secondary structure. CD spectra in absence and presence of LUVs composed by POPC/POPG (20% POPG molar percentage) (2mM final lipid concentration) were carried out with 100μM PrP(106-126) in a quartz cell with an optical path of 0.1cm at 25ºC. For this particular experiment, samples were prepared in buffer containing NaF instead of NaCl. Wavelengths from 260 to 190nm were recorded with a 0.1nm step and 20nm/min speed. Spectra were collected and averaged over 5 scans and corrected for background contribution.

A peptide lipid/ratio of 1:20 was used. Lower peptide lipid ratios are normally advised (e.g. 1:100) however in this particular case it was not possible (10mM of lipid would be necessary which would greatly contribute for dispersion). In the case of alteration of

secondary structure upon interaction with lipid, an effect on CD spectrum should be evident.

Membrane effects induced by the presence of PrP(106-126)

Pore formation was tested for different lipid compositions with 100μM final lipid concentration and was evaluated with a methodology based on NBD fluorescence quenching by Co^{2+} ions (see ref [29] and references therein). To follow permeability to Co^{2+} ions, vesicles doped with 1% of N-NBD-PE were prepared with or without 20mM Co^{2+} inside and outside (positive control). For positive control, lipid was hydrated with buffer containing 20mM Co^{2+}; therefore, quencher is accessible to NBD in the outer and in the inner layer. This control was compared with samples where Co^{2+} was added after vesicle preparation; in this case Co^{2+} is accessible only to outer layer. In the case of pore formation, after peptide addition, Co^{2+} will become accessible to the NBD fluorophores in the inner layer. Addition of different PrP(106-126) concentrations was carried out (0-50μM). Controls with the different peptide concentrations were performed. PrP(106-126) was left to incubate for 30 min and Co^{2+} was added to the samples. NBD fluorescence emission spectrum was followed with $\lambda_{excitation}$ = 460 nm before and after PrP(106-126) addition. Data were corrected for the inner filter effect [30]. Control samples with Co^{2+} outside and inside vesicles were carried out at the same conditions. For this particular assay MLVs were used instead of LUVs. Usage of MLVs enables a gradual effect in case of translocation after pore formation and therefore a more reliable reading of the spectroscopic signal. Several lipid mixtures were used: POPC/POPG (0, 5, 10, 20 and 50% molar POPG); POPC/Chol (33% molar chol) and POPC/POPG/Chol (47, 20 and 33 molar respectively).

Dipolar potential in the presence of PrP(106-126) and the pH gradient effect

Membrane dipolar potential is dependent on the orientation of dipoles in the membrane/water interface. Variations of the membrane dipole potential can be used to report membrane binding and insertion of molecules by recording fluorescence excitation spectra of di-8-ANEPPS-labelled vesicles which are particularly sensitive to dipolar potential variations [31]. 25μM PrP(106-126) was added to LUVs with 200μM lipid and 4μM of dye (di-8-ANEPPS is not fluorescent in aqueous medium). To detect spectral variations in di-8-ANEPPS excitation the spectrum ($\lambda_{emission}$=570nm) in the

absence of the peptide was subtracted from the spectrum in the presence of 25μM PrP(106126) (both spectra were normalized to total integrated area). This differential spectrum enables detection of peptide-induced changes on the membrane dipolar potential [31, 32]. Fresh solutions and aging peptides (48h, 37ºC) were used in these experiments. Several lipid compositions were used: POPC/POPG (0, 20, 30, 40, 50 and 100% molar POPG) to evaluate the charge effect; POPC/POPS (20% molar POPS) to test any particular effect with serine; POPC/Chol (0, 18 and 33% molar Chol) to evaluate the effects of the presence of cholesterol; POPC/GM1 (0, 5, 10, 20 and 50% molar GM1) and a mixture of POPC/POPG/Chol/GM1 (37, 20, 33, 10% molar, respectively) was also used to test if the mixture would improve the interaction with membranes. Liposomes with a pH gradient (pH=5.0 inside and pH=7.4 outside liposomes) were prepared in order to mimetize the environment at the liposome/cytoplasm interface. POPC/POPG (50% molar percentage) vesicles were tested. Controls with pH=7.4/pH=5 (in/out); pH=7.4 (in/out) and pH=5 (in/out) were performed.

RESULTS

It has been suggested that PrP(106-126) has a role in PrP^{Sc}- PrP^{C} association and also in prion disease propagation and amplification [6], which is dictated by its physico-chemical properties. Several activities have been attributed to this peptide but so far its contribution in Prion disease is not clarified (see references [6, 13] and references therein). In this study it is our main goal to elucidate the membrane role on the activity of this PrP fragment.

The endosomal pathway may be implicated on PrP^{Sc} synthesis and propagation [3, 33-35]. PrP^{Sc} synthesis is likely to occur during PrP recycling through the endosomal pathway. Exogenous prions could initiate infection by entry through the endosomal pathway to induce the conversion of PrP^{C} molecules from cell surface to PrP^{Sc} [35]. Moreover toxic forms of PrP have been identified in endosomal pathway and have been suggested to play a role in neurotoxicity which cannot be explained solely by fibril formation [6]. In this regard, PrP(106-126) interaction with membranes was studied not only at pH7.4, but also at pH5 to evaluate pH effect on peptide-membrane interaction and possible differences in cytoplasm/endosomal environment.

PrP(106-126) aggregates in aqueous solution and forms amyloid fibrils

Previous studies had shown that PrP(106-126) tends to aggregate and to form β-structures as the scrapie PrP isoform [9, 10]. In order to verify if the same occurs in conditions of the present study, the formation of β-structures aggregates was tested by the fluorescence of ThT and also by the absorbance of CR. These two dyes are widely used to detect the formation of amyloid structures [25].

In the absence of β-sheet aggregates, the ThT dye has an excitation and fluorescence emission maxima at 350 and 438nm, respectively. In the presence of amyloid fibrils the ThT spectra shift to 450nm and 482nm, respectively [21]. During titration of ThT with PrP(106-126) a slight increase in the fluorescence intensity at 482nm, characteristic of ThT interacting with β-sheet structures was observed (data not shown). This effect is not strong, but some β-sheet-rich proteins are unable to induce the characteristic ThT fluorescence [36]. CR absorbance was used to further study if this peptide has a significant β-sheet conformation. In the case of amyloid fibrils formation a red-shift in CR absorbance spectrum at physiological pH is expected [22, 23]. At pH 7.4, 150mM NaCl the CR maximum appears at 489nm. When CR was titrated with PrP(106-126) a red shift in absorbance spectra was observed (Figure1A), due to an increase of the component at 535nm (see differential spectra inset in Figure1A). At pH 5, 150mM NaCl, the CR absorbance spectrum peaks at 502nm which is blue shifted in the presence of PrP(106-126) (Figure1B). An increase at 496nm is detected in differential spectra (see inset in Figure1B). The direct comparison of the effects on CR absorbance at pH5 and pH7.4 is not straightforward because CR absorbance properties change with pH [15]. However it is possible to conclude that at pH7.4 and pH5 PrP(106-126) is able to interact with CR and this strongly suggests β-sheet conformation.

As a final test, the possibility of peptide aggregation was also followed by ANS fluorescence. This dye is sensitive to the polarity of its micro-environment and is frequently used to identify the presence of hydrophobic "pockets" in proteins and peptides [24-26]. In the presence of hydrophobic "pockets", ANS fluorescence emission intensity increases and concomitantly blue-shifts.

Titration of ANS with PrP(106-126) causes an increase in the fluorescence intensity and a significant blue shift (59nm) on the maxima of ANS emission (Figure 2), which is

indicative of the presence of aggregates in solution. This was detected at pH7.4 and pH5 both for low and physiologic ionic strength.

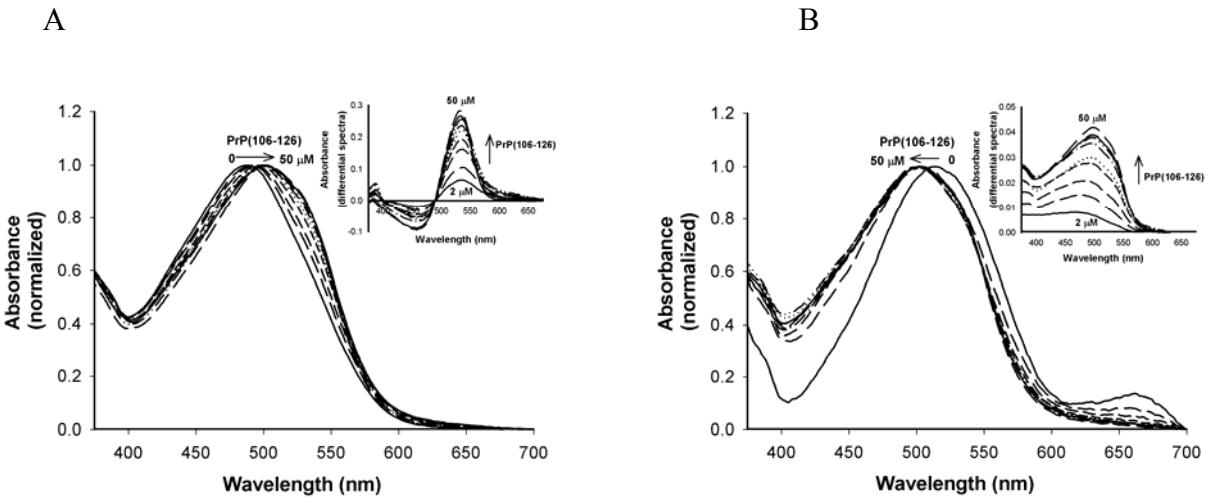

Figure 1. Identification of β-structures in the PrP(106-126) by Congo Red absorbance. Absorbance spectra of 5μM CR in the presence of PrP(106-126) 0-50μM (A) at pH7.4, 150 mM NaCl or (B) at pH5, 150mM NaCl. Absorbance was normalized to highlight the red shift at pH7.4 and the blue shift at pH5.0 upon peptide addition. *Inset*: initial CR absorbance spectrum was subtracted to all the spectra obtained after peptide addition at pH 7.4 or pH5. At pH 7.4 is possible to identify an increase in the CR absorbance at 535nm with peptide concentration and at pH5 there is an increase at 496nm. This indicates that PrP(106-126) is interacting with CR, suggesting β-structures. This effect is stronger at pH7.4 than at pH5.

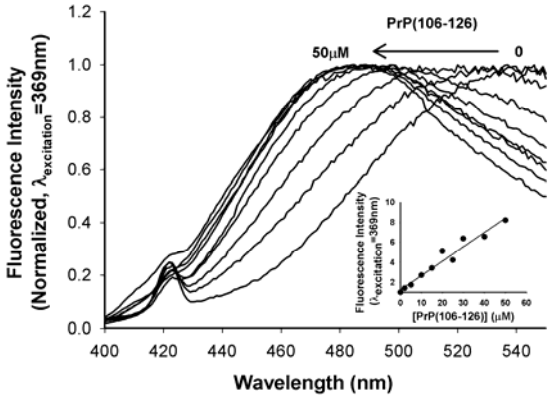

Figure 2. Aggregation of PrP(106-126) evaluated by ANS fluorescence properties. A) The effect of peptide concentration in 12.5 μM ANS fluorescence emission spectrum ($\lambda_{excitation}$=369nm, pH7.4, 150mM NaCl). Spectra were normalized to highlight ANS blue shift upon interaction with PrP. *Inset*: Dependence of integrated fluorescence intensity of ANS with peptide concentration. A significant blue shift and a concomitant increase in ANS fluorescence intensity indicates that this peptide is in an aggregated form.

PrP(106-126) interaction with membranes – kinetic and affinity

The interaction and affinity of PrP(106-126) to lipidic bilayers was studied by SPR with lipid membranes onto a sensor chip L1 (which contains a carboxymethylated dextran

matrix with lipophilic alkyl chains giving the surface amphiphilic properties). SPR has proven to be a valuable experimental approach to study the interaction of peptides with lipidic bilayers, which allows the real-time monitoring of peptide binding to and dissociation from the lipidic bilayers, and has the advantage of overcoming the need to use labelled peptides [37]. Liposomes are immobilized on the surface of the sensor chip and the peptide is passed across membrane. SPR detects changes in the optical properties of the sensor surface caused by the association/dissociation of the peptide to/from the lipid immobilized onto the sensor surface. The sensor surface response is proportional to the adsorbed mass on the sensor surface [37].

In this study we have examined the association/dissociation of PrP(106-126) to/from lipidic membranes with different lipid compositions to get more insights on the parameters that govern peptide affinities and membrane preferences.

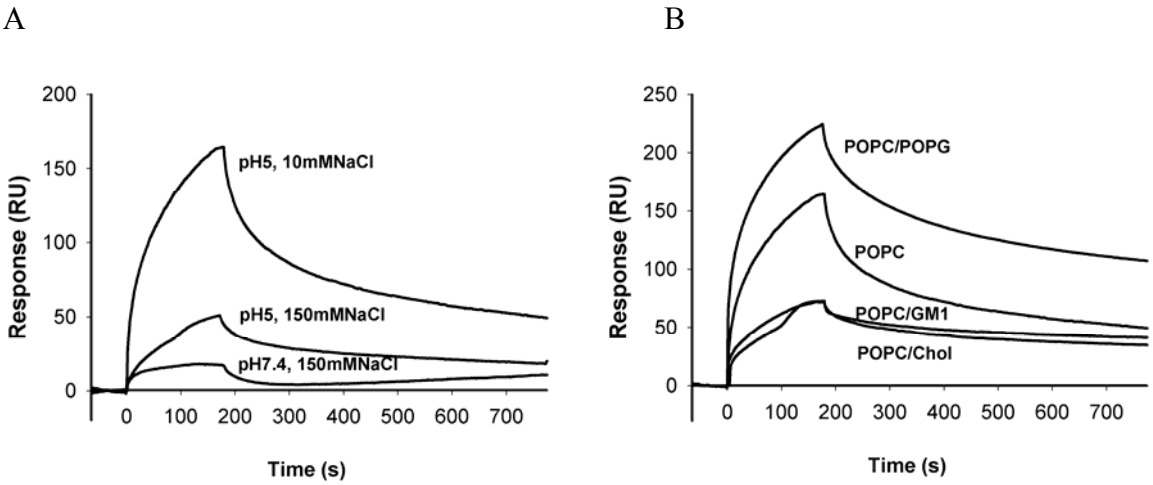

Figure 3. Lipidic composition and buffer effects on peptide affinity for lipidic membranes. (A) pH and ionic strength effect on PrP(106-126) (25μM) interaction with POPC membranes immobilized on the surface of L1 chip. HEPES buffer pH7.4, 150mM NaCl, Acetate buffer pH5, 150mM NaCl and Acetate buffer pH5, 10mM NaCl were used. The peptide does not have a detectable affinity for physiological membranes. At acidic pH a slightly increase in the peptide fraction bound occurs, which is enhanced at low ionic strength. (B) 25μM PrP(106-126) affinity for lipidic membranes immobilized on the surface of L1 chip at pH5, 10mM NaCl is represented for different lipidic composition: POPC, POPC/POPG (20% molar POPG), POPC/Chol (33% molar Chol) and POPC/GM1 (10% molar GM1). PrP(106-126) has higher affinity for membranes when anionic phospholipids are present. The Peptide does not bind significantly to POPC/Chol and POPC/GM1 lipidic membranes.

After bulk shift correction and evaluation of possible mass transport effect (see supporting information for this subject) it was possible to compare different sets of sensorgrams obtained in different conditions. The effect of pH and ionic strength on PrP(106-126) interaction with POPC is represented in Figure 3A. It is possible to conclude that in physiological conditions (pH7.4, 150mM NaCl) the peptide does not have a significant affinity for POPC membranes (see Figure 3A and Figure S.1.A in supporting information). A weak peptide interaction was detected for POPC at pH5, 150mM NaCl (see Figure 3A and Figure S.1.B in supporting information). With acidic pH and low ionic strength (pH5, 10mMNaCl) an increase of RU signal intensity is observed (see Figure 3A and Figure S.1.C in supporting information). By comparison of POPC membranes with the ones containing POPG a charge effect is evident; an increase of peptide bound occurs in the presence of anionic phospolipid (Figure 3B). Interaction with POPC/Chol (33% molar chol) and POPC/GM1 (10% molar GM1) is not significant whatever the conditions tested (Figure 3B).

A kinetic analysis was performed only with sensorgrams obtained with concentrations up to 25μM with POPC and POPC/POPG (20% molar POPG) surfaces in pH5 10mM NaCl (see Figure 4). These were the conditions where peptide/membrane interactions are more notorious. Using the simplest 1:1 Langmuir binding model resulted in a poor fit of the sensorgrams. The two-step binding model, which assumes a change in the structure of the peptide after initial binding to the membrane, leads to a significant improvement in fit quality. In this model the first step is the initial peptide interaction with membranes and is described by k_{a1} and k_{d1}. Peptide binding is followed by reorientation and/or insertion of the peptide into the hydrophobic core (step two, described by k_{a2} and k_{d2}) (for further details see references [37, 38] and references therein). Association rates (k_{a1}, k_{a2}), dissociation rates (k_{d1}, k_{d2}) and affinity constant obtained are present in Table 1. The most significant outcome of this kinetics analysis is the higher affinity constant for this peptide on the POPC/POPG membranes.

TABLE 1 Association (k_{a1} and k_{a2}), dissociation (k_{d1} and k_{d2}) and affinity constant (K) of PrP(106-126) binding to POPC and POPC/POPG (20% POPG molar percentage) lipidic bilayers in Acetate buffer, pH5 containing 10mM NaCl[a]

Lipid type	k_{a1} ($\times 10^2$ 1/Ms)	k_{d1} ($\times 10^{-2}$ 1/s)	k_{a2} ($\times 10^{-3}$ 1/s)	k_{d2} ($\times 10^{-3}$ 1/s)	K ($\times 10^4$ 1/s)	χ^2
POPC	5.05	1.35	5.30	1.56	1.26	5.14
POPC/POPG	2.14	5.69	1.37	1.17	4.39	13.9

[a] Binding constants were obtained after fitting the SPR data from Figure 5 to a two-step binding model with BIAevaluation version 3.0. Experimental conditions are described in the legend of Figure 4.

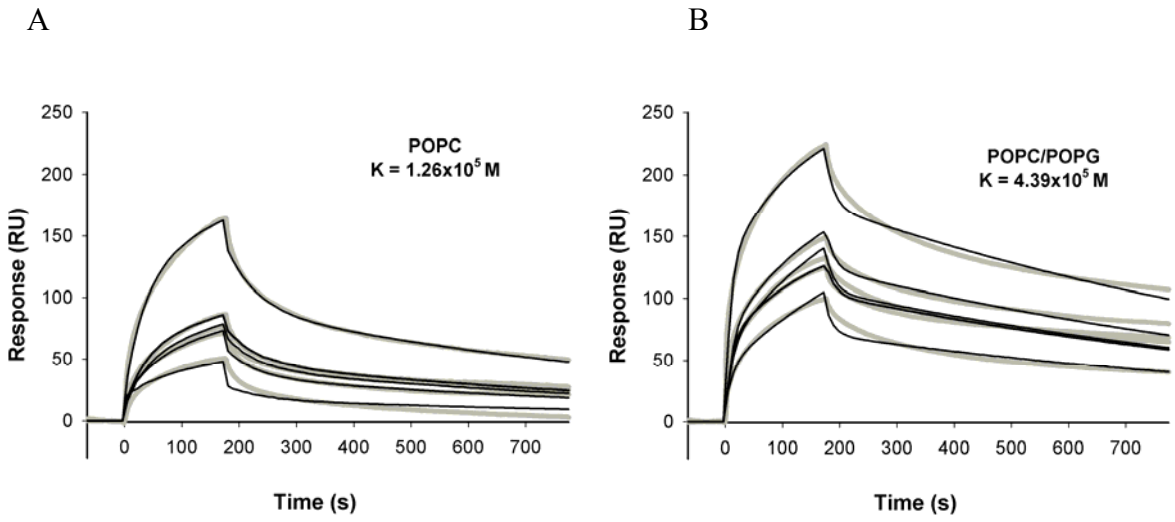

Figure 4. Global analysis of SPR data PrP(106-126) in the presence of POPC and POPC/POPG (20% molar POPG) membranes immobilized onto a L1 chip surface. Peptide samples (5, 10, 15, 20 and 25μM) prepared in acetate buffer, pH5, 10mM NaCl were injected at 20μL/min flow rate. Sensorgrams were corrected for bulk shift effect (grey lines) and a two-step binding model was fitted to data with BIAevaluation version 3.0 (black lines). All the parameters were fitted globally. K is the global affinity constant. Other kinetic constants are presented in table 1.

CD spectroscopy for PrP(106-126) – secondary structure

Regarding the previous results with ThT and CR dyes and previous publications [8] on PrP(106-126) secondary structure there are evidences for the contribution of β-sheet secondary structure in solution. In order to study the implications of the secondary structure of the peptide upon interaction with membranes, CD spectroscopy was used.

There are three major secondary structures identifiable by CD: a random coil structure which is characterized by the well defined poli(Pro)II (PPII) CD spectral form with a strong negative band around 195nm; a α-helix conformation with minima bands at 208 and 222nm and a positive band at 192nm; and β-sheet with a positive band below 200nm but with a single negative band at ~ 220nm [39]. The CD signal for β-sheet conformation is weaker than the other two. β-rich proteins, depending on the interference of random coil signal can have a CD spectra that resemble those of model β-sheets or a CD spectra mainly dominated by random coil conformation domains, depending on the total random coil contribution. [39, 40].

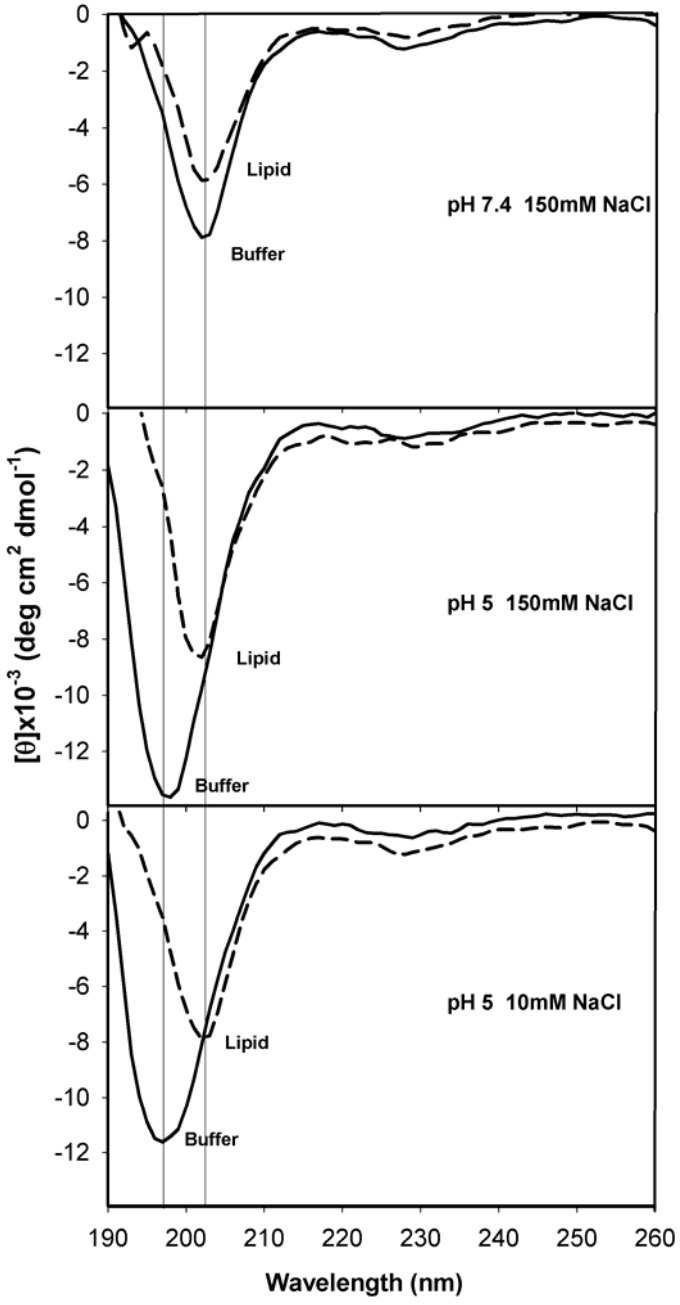

Figure 5. CD spectra of 100μM PrP(106-126) in the absence and in the presence of POPC/POPG (20% molar POPG) LUVs ([Lipid]=2mM). Three conditions were tested: 10mM HEPES buffer, pH7.4, 150mM NaCl; 20mM Acetate buffer, pH5, 150mM NaCl and 20mM acetate buffer, pH5, 10mM NaCl.

Figure 5 show no α-helix signal. At pH5, PrP(106-126) CD spectra have a strong negative band around 198nm which suggests that at acidic pH the peptide has a high contribution of random coil structure. This characteristic band is in agreement with previous results obtained in similar conditions [15], where the hydrophobic core (AGAAAAGAVVGGLG) seems to be important in the magnitude of this negative band (Ala was identified as the aminoacid with more propensity to have this random-like structure spectrum [41]).

Upon interaction with membranes, the effect of the positive β band convoluted with the 198nm random coil signal causes an apparent shift to lower energies and a concomitant decrease in intensity (see references [41-43]). This effect can only be ascertained to an increase in β content because the strong α-helix component at 222nm is absent. At physiological condition alteration in the band position was not detected in the presence of liposomes. Alteration in PrP(106-126) convoluted spectra after lipid addition, at pH 5 and not at pH 7.4 is in agreement with SPR results.

PrP(106-126) does not form ionic channel in physiological conditions

One possible explanation for PrP(106-126) toxicity is channel formation across cell membranes. To test pore formation we took advantage of Co^{2+} properties as quencher of NBD fluorophores (for further details see material and methods section). SPR results showed that PrP(106-126) prefers vesicles with negatively-charged phospholipids. PrP(106-126) was not able to make vesicles permeable to Co^{2+} ions, regardless of the POPG percentages (0, 5, 10, 20 and 50% molar) at physiological conditions. At acidic pH it was only possible to have a noteworthy effect with low ionic strength (10mM NaCl) and high POPG percentage (50% molar – Figure 6). These are extreme conditions, and Co^{2+} permeability can only be achieved if electrostatic interactions force PrP(106-126) to interact with negatively charged vesicles. To rule out the possibility of a specific effect of phospholipid headgroup, experiments with POPS instead of POPG were also performed and no difference was noticed in the capacity to induce channel formation.

The presence of cholesterol, and GM1 was also tested by the use of liposomes composed by POPC/Chol (33% molar chol) and POPC/GM1 (10% molar GM1). No leakage was observed in these liposomes neither in POPC/POPG/Chol (47:20:33 molar) in any of the buffers tested.

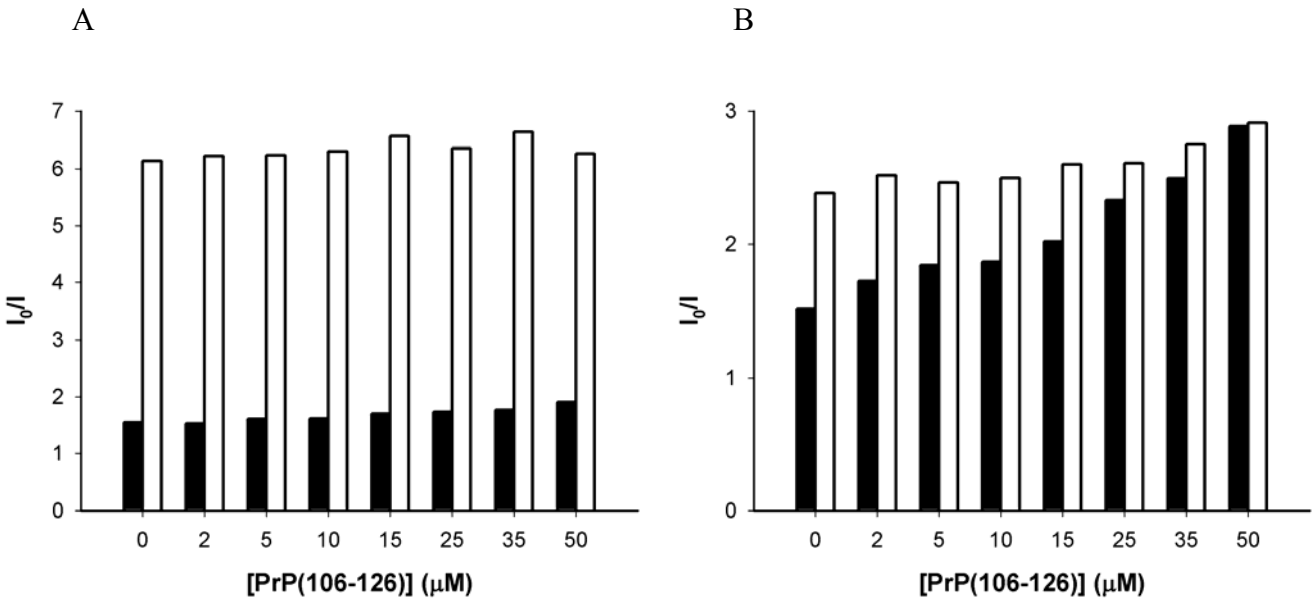

Figure 6. Cross-bilayer channel formation induced by PrP(106-126) in 100 μM POPC/POPG (50% molar POPG) vesicles followed by NBD quenching by Co^{2+}. The ratio of NBD fluorescence emission ($\lambda_{excitation}$ = 460nm) in the absence of quencher (I_0) and in presence of 20mM Co^{2+} (I), for the vesicles with Co^{2+} accessible to both layers (white columns) and for the vesicles where Co^{2+} is only accessible to the outer layer (black columns), is presented for different peptide concentrations. These experiments where carried at pH5 containing A) 150mM NaCl or B) 10mM NaCl. Comparing the results (black columns) with the positive control (white columns) is possible to conclude that at 150mM NaCl PrP(106126) does not form pores even at high peptide/lipid ratio (1:2, for 50μM PrP(106-126)). At 10mM NaCl leakage increases is evident with peptide concentration.

The effect of PrP(106-126) on membrane potential and the pH gradient

Peptide insertion in lipidic bilayers is likely to perturb membrane dipolar potential which can be monitored by means of spectral shift in the excitation spectra of Di-8-ANEPPS [32]. This dye is located in lipid headgroup region, where is sensitive to the local electric field [31]. In order to screen PrP(106-126) interaction with membranes, 25μM PrP(106-126) fresh solution or aged solution was added to liposomes with different lipid compositions: POPC/POPG (0, 20, 30, 40, 50 and 100% molar POPG); POPC/POPS (20% molar POPS); POPC/Chol (0, 18 and 33% molar Chol); POPC/GM1 (0, 5, 10, 20 and 50% molar GM1) and a mixture of POPC/POPG/Chol/GM1 (37:20:33:10 molar). A noticeable shift in Di-8-ANEPPS was only observed with pH5 10mM NaCl in lipidic vesicles composed by POPC/POPG (50% molar POPG) (Figure 7).

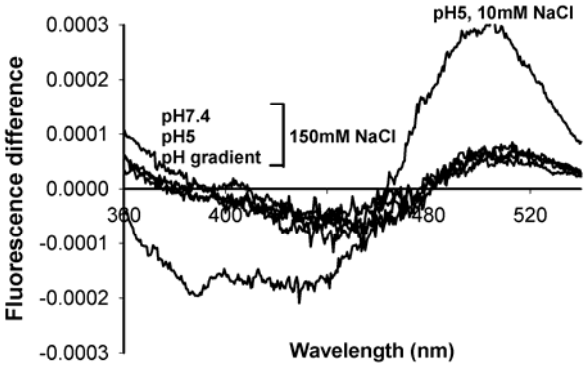

Figure 7. PrP(106-126) effect in the dipolar potential of POPC/POPG (50% molar POPG) vesicles followed by fluorescence difference spectra of Di-8-ANEPPS-labelled vesicles. Excitation spectrum obtained in the absence of peptide was subtracted to the spectrum obtained in the presence of 25μM PrP(106-126); both spectra were normalized to the integrated areas to reflect only the spectral shift. The difference spectrum obtained in acetate buffer, pH5 10mM NaCl has a more pronounced shift than the other four difference spectra obtained with 150mM NaCl: pH 7.4, pH5 or with a pH gradient pH7.4/pH5 (in/out) and pH5/pH7.4 (in/out). PrP(106-126) effect on dipolar potential is independent on pH or pH gradient but depends on ionic strength.

A pH gradient can promote translocation across membrane of some peptides [44]. In the present work we have tested if pH gradient across endosomes/cytoplasm can promote PrP(106-126) interaction with membranes and induce membrane translocation. With a constant ionic strength (150mM NaCl), a pH gradient across membranes was created in POPC/POPG (50% molar POPG). Liposomes with pH5/pH7.4 (in/out) were compared with pH7.4/pH5 (in/out), pH7.4 (in/out) and pH5 (in/out) 150mM NaCl. No significant differences were detected between the samples with pH gradient and the controls (see Figure 7).

DISCUSSION

In the present work our main goal is to understand if PrP(106-126) interacts with biological membranes and if this possible interaction can or cannot explain toxic effect due to PrP(106-126). The study was carried on in model membranes and different membrane properties were modulated and three different buffers were tested: pH7.4 containing 150mM NaCl to evaluate PrP(106-126) features at physiological conditions; pH5 containing 150mM NaCl to have insights in the possible interaction with

endosomes where some toxic PrP species were identified and possible PrP^{Sc} propagation has been suggested. A third condition, pH5 with low ionic strength (10 mM NaCl) was also studied for a better evaluation of charge effect and possible electrostatic interactions driving events.

PrP(106-126) aggregation and secondary structure dependence on pH

The existence of aggregates for PrP(106-126) was confirmed (Figure 2). CD spectra show a random coil organization without contribution of α-helix (Figure 5). Peptides/protein with different secondary structures (α-helix, α + β contributions) are able to interact with CR, while unfolded proteins are unable to interact with CR [45]. Due to lack of α-helix, binding of PrP(106-126) to CR (Figure 1) is explained by the presence of β-sheet structures. The relative contribution of random coil and β-sheet conformation in PrP(106-126) is dependent on pH and ionic strength (Figure 5). A higher β-sheet contribution is present at pH7.4 than at pH5.

PrP(106-126) does not interact strongly with lipid membranes at physiological conditions

PrP(106-126) interaction with membrane could be involved in cytotoxicity mechanisms by perturbation of membrane functions [46]. Interaction of PrP(106-126) with lipid membranes was evaluated by SPR and using fluorescence methodologies related to the variation of dipolar potential at the membrane. In an attempt to screen different lipidic systems in order to evaluate the effect of a specific phospholipid or other membrane components, model membranes of POPC were compared with membranes with more complex lipidic compositions such as POPC/POPG (20% molar POPG), POPC/Chol (33% molar Chol) or POPC/GM1(10% molar GM1).

Phospholipids with a phosphatidylcholine (PC) headgroup are the major component in animal cell membranes [47]. This lipid forms bilayers in fluid phase at room temperature and can be used to represent the bulk phase in cell membrane. Negatively-charged phospholipids are mainly present in the inner leaflet of plasma membrane [47] and have been implicated in amyloid fibril stimulation *in vivo* whatever the acidic headgroup [46]. This was been tested by means of membranes composed by POPC/POPG.

Rafts are specialized plasma membrane domains enriched in cholesterol and have been implicated in conversion of PrP^{C} to PrP^{Sc}, where both isoform are localized. A chol depletion induces a decrease in PrP^{C}-PrP^{Sc} conversion in prion infected cellular lines [48, 49]. The possible interaction of PrP(106-126) with these domains within plasma membrane was tested with vesicles composed by POPC/Chol.

GM1 is a ganglioside abundantly expressed in neurons and concentrated in caveolae and lipid rafts regions and has been identified to bind specifically to Aβ peptide leading to the induction of β-structure [50-52] and also to induce membrane disruption [53]. The similarities between Aβ peptide amyloid formation in Alzheimer disease and Prion disease prompt us to study the effect of GM1 in PrP(106-126) membrane affinity with vesicles composed by POPC/GM1.

At physiological conditions no interaction of PrP(106-126) with any of these lipidic membranes was detected. A lack of affinity for membranes at physiological buffer conditions was confirmed by membrane dipolar potential studies and leakage measurements. Moreover POPC/POPS was also tested, to exclude a possible specific interaction with PS and also a mixture of POPC/POPG/GM1/Chol. In none of these conditions PrP(106-126) insertion or membrane leakage was identified.

PrP(106-126) only interacts with membranes at conditions where strong electrostatic interactions are operative

At pH5, His residue in PrP(106-126) sequence is ionized and the formal net charge of peptide increases from +2 to +3 [6]. With pH5, 150mM NaCl a slight increase in membrane affinity was detected by SPR for POPC membranes. This affinity was greatly increased in the presence of POPG (negatively-charged phospholipid) and with low ionic strength. In such conditions, electrostatic interactions are enhanced due to electrostatic interactions between the positively charged peptide and negatively charged membrane. Even though, the RU obtained by SPR are lower than values verified for other peptides known to interact with membranes (values between 1000-10000 were obtained for peptides with similar length with the same sensor chip, [54, 55] compared to 100-250 for PrP(106-126) – Figure 4B). Nevertheless no insertion or pore formation was detected.

It was suggested that amyloid formation is stimulated in the presence of hydrophobic environment at acidic pH [56]. PrP(106-126) at acidic pH and low ionic strength has a

lower propensity for β-sheet conformation, although an increase in β-structures was verified in the presence of lipidic vesicles (see Figure 6). SPR shows that a two state model kinetics of PrP(106-126) interaction with membranes at pH5 10mM NaCl are adequate to describe the data. Based on the results obtained, the two states may be identified: 1st) peptide interaction with membrane interface (governed by electrostatic interactions between peptide and membrane) and 2nd) the peptide undergoes a secondary structure modification at the bilayer surface; no insertion was detected.

PrP(106-126) does not bind specifically with ganglioside GM1. GM1 has tendency to form microdomains in PC membranes [57, 58]. These domains are probably hindering the interaction of PrP(106-126) with POPC due to sugar headgroups stearic constraints, which explains the lower affinity for POPC/GM1 than to POPC at acidic pH (see Figure 3B).

The presence of Chol also reduces the affinity of PrP(106-126) to POPC membranes. A decrease in peptide affinity can arise from an increase in membrane viscosity due to Chol presence [59].

Membrane insertion and channel formation was only detected with model membranes composed by POPC/POPG (50% molar POPG) at pH5 containing 10mM NaCl. In these conditions the membrane is strongly negatively charged and the low ionic strength is not enough to prevent a strong electrostatic attraction to the positively charged peptide.

Regarding the possible importance of endosomes in PrP propagation we decided to mimic the pH gradient in cytoplasm/endosome environment. The pH gradient: pH7.4/5 (in/out) or pH 5/7.4 (in/out) could eventually be a driving force for peptide insertion in the membrane, as observed for other peptides [44]. However for PrP(106-126) the pH gradient does not lead insertion (see Figure 7).

Altogether peptide membrane studies show that PrP does not have affinity for lipidic membranes at conditions similar to the cytoplasmatic environment. At conditions similar to endosomal environment PrP(106-126) has weak interaction with membrane and in these conditions insertion or pore formation were not detected. Only in extreme conditions insertion and leakage were detected.

The lack of affinity for lipid membrane can be understood based on thermodynamics of lipid-peptide interactions [60] and the interfacial hydrophobicity scale published by White and Wimley [61]. The interaction of a peptide with the lipid membrane can be

divided into three thermodynamic steps governed by electrostatic forces, hydrogen bond formation and hydrophobic interactions. The first step is initiated by the electrostatic attraction between peptide and membranes; the second step involves a transition of the peptide into the plane of binding, which depends on the hydrophobic/hydrophilic balance of the molecules groups and forces involved; and the third step involves a conformation modification of the bound peptide [60]. Electrostatic attraction is responsible for increasing the peptide concentration in membrane vicinity, however, even in conditions were PrP(160-126) charge can be prominent and a concentration of peptide occurs, the interfacial partitioning, mainly governed by hydrophobic effect, is not favourable considering the free energy for interfacial transfer of the overall PrP(106-126) sequence (see Figure 8). An increase in partition at low ionic strength results from the increase in peptide concentration close to membrane environment.

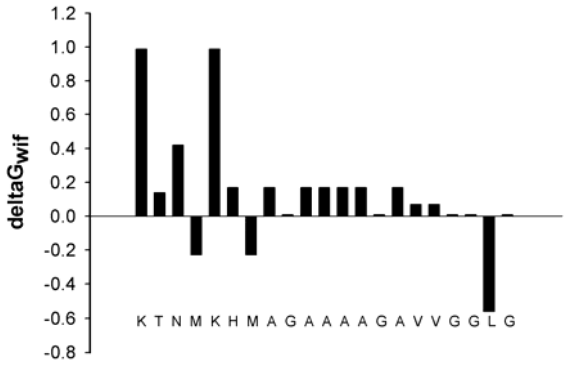

Figure 8. Theoretical analysis of PrP(106-126) partition into interfacial membrane region based free energy change ΔG_{wif} from water transfer to lipid membrane interface (see reference [61]). Residues with Values $\Delta G_{wif} < 0$ have tendency to the membrane water-interface.

Contextualization of present results and biological relevance of PrP(106-126)

Prion disease is initiated by conversion of physiological PrP^{C}, a protein abundantly expressed in mammalian brain, into a pathological isoform PrP^{Sc}, which accumulates within the brain as highly toxic insoluble aggregates [1]. The neurodegeneration rate verified in Prion disease cannot be explained solely by PrP^{Sc} formation and deposition [6]; some other PrP toxic species have been identified inside the cells, which seem to have an important role in disease propagation and transmission after infection by PrP^{Sc} [6]. A neurotoxic PrP fragment, PrP(106-126) with physico-chemical properties similar to PrP^{Sc} and present in all abnormal toxic species within the patient brain, has been used as a model of PrP^{Sc} and to study the possible mechanism in disease propagation and transmission [8-13].

PrP(106-126) toxicity remains controversial in literature. A mechanism by a non-selective pore formation responsible for ionic gradient destabilization was proposed to explain PrP(106-126) neurotoxicity [16]. However channel formation was not reproduced in some reports [18] and neurotoxicity of this peptide was verified only in the presence of PrP^C [62, 63].

The present work shows that PrP(106-126), in conditions that mimic cytoplasmic environment, lacks propensity to interact with lipidic membranes and to form pores, whatever the lipid composition tested. Such observation indicates that toxic effects of PrP(106-126) cannot be explained by cell membrane leakage. Alternatively, it can be hypothesized that the PrP(106126) toxic effects occur inside the cell. Such suggestion implies PrP(106-126) cellular internalization, which is a phenomenon that has been verified for some peptides belonging to the cell-penetrating peptides (CPPs) family (for further information see reference [64]). The uptake of CPP can follow two routes: one is physically-mediated and the other is dependent on endosomal pathway. Both routes require peptide-membrane interactions as the first step [65] . With the lack of affinity of PrP(106-126) for lipid membranes both routes for cell entry are discarded, unless PrP(106-126) cellular internalization occurs via a mechanism mediated by the presence of a physiological PrP (e.g. mediated by caveolae or rafts where PrP is localized in cell surface). The N-terminal domain of PrP with a non-cleaved signal sequence has CPP properties and can be responsible by internalization of sizeable cargo into cells [66]. Implication in PrP trafficking as well as in prion infectivity has been suggested [66]. A possible internalization of PrP(106-126) in cells mediated by this N-terminal domain of PrP could explain possible toxic effects inside cells after internalization.

In the present work we have tested if at endosomal environment PrP(106-126) has affinity for the membrane. An increased propensity to interact with lipid bilayer (see Figure 3A) and to form β-sheet structures in membrane vicinity (see Figure 5) was shown, however this does not represent a significant membrane insertion (see Figure 7) or an improved tendency to form transmembrane pore. This is in agreement with previous finding that the fibrilogenic properties alone are not sufficient for neurotoxicity as verified by other PrP fragments able to assemble into filaments but with lack of toxic effects [10]. Moreover, even with a pH gradient across membrane, similar to endosomal/cytoplasmic interface, insertion in membrane was not identified. Therefore, in the case PrP(106-126) fragment endosomal internalization, the toxic effect cannot be

explained by acidic pH. Altogether is possible to rule out the pore formation/or any direct effect on membrane properties to explain PrP(106-126) toxicity.

Our results corroborate with previous reports where pore formation was not detected [18] reinforcing the hypothesis that PrP^{C} is necessary to mediate PrP(106-126) toxicity [13]. One possible explanation is the formation of heterodimers of PrP^{C} with PrP(106-126) that stimulate PrP^{Sc} conversion into a pathological channel formation and manifest neurotoxicity or induce formation of abnormal PrP species upon interaction with PrP^{C}. Formation of abnormal PrP species induced by PrP(106-126) was not confirmed [13]. Instead, it was suggested that this peptide may kill neurons by modification/inhibition of a physiological function of PrP^{C}. In this hypothesis PrP(106-126) toxicity is related to a loss of PrP function instead of a gain of toxic properties in the presence of PrP(106-126) [13].

Physiological function of PrP is still in debate in literature. A SOD activity has been attributed to PrP^{C} [67, 68] and recent reports suggest that PrP(106-126) inhibits SOD activity of PrP^{C} [69]. Other hypothesis is that PrP^{C} is important on β-secretase activity, which is responsible for Aβ peptide formation as in Alzheimer disease [70]. PrP^{C} has been implicated in signal pathway, namely a possible blockage of a signal mediated by PrP^{C} was also proposed to explain PrP(106-126) toxic effects [13].

ACKNOWLEDGMENTS

Fundação para a Ciência e Tecnologia (Portugal) is acknowledged for the grant SFRH/BD/14337/2003 to S. T. Henriques. IUBMB is acknowledged for financial support to S. T. Henriques for a short-term visit to Dr. Marie-Isabel Aguilar laboratory at Monash University, Victoria, Australia.

REFERENCES

1 Prusiner, S. B. (1998) Prions. Proc Natl Acad Sci U S A **95**, 13363-13383

2 Johnson, R. T. (2005) Prion diseases. Lancet Neurol **4**, 635-642

3 Naslavsky, N., Shmeeda, H., Friedlander, G., Yanai, A., Futerman, A. H., Barenholz, Y. and Taraboulos, A. (1999) Sphingolipid depletion increases formation of the scrapie prion protein in neuroblastoma cells infected with prions. J Biol Chem **274**, 20763-20771

4 Pinheiro, T. J. (2006) The role of rafts in the fibrillization and aggregation of prions. Chem Phys Lipids **141**, 66-71

5 Thellung, S., Florio, T., Corsaro, A., Arena, S., Merlino, M., Salmona, M., Tagliavini, F., Bugiani, O., Forloni, G. and Schettini, G. (2000) Intracellular mechanisms mediating the neuronal death and astrogliosis induced by the prion protein fragment 106-126. Int J Dev Neurosci **18**, 481-492

6 Kourie, J. I. (2001) Mechanisms of prion-induced modifications in membrane transport properties: implications for signal transduction and neurotoxicity. Chem Biol Interact **138**, 1-26

7 Mironov, A., Jr., Latawiec, D., Wille, H., Bouzamondo-Bernstein, E., Legname, G., Williamson, R. A., Burton, D., DeArmond, S. J., Prusiner, S. B. and Peters, P. J. (2003) Cytosolic prion protein in neurons. J Neurosci **23**, 7183-7193

8 De Gioia, L., Selvaggini, C., Ghibaudi, E., Diomede, L., Bugiani, O., Forloni, G., Tagliavini, F. and Salmona, M. (1994) Conformational polymorphism of the amyloidogenic and neurotoxic peptide homologous to residues 106-126 of the prion protein. J Biol Chem **269**, 7859-7862

9 Tagliavini, F., Prelli, F., Verga, L., Giaccone, G., Sarma, R., Gorevic, P., Ghetti, B., Passerini, F., Ghibaudi, E., Forloni, G. and et al. (1993) Synthetic peptides homologous to prion protein residues 106-147 form amyloid-like fibrils in vitro. Proc Natl Acad Sci U S A **90**, 9678-9682

10 Forloni, G., Angeretti, N., Chiesa, R., Monzani, E., Salmona, M., Bugiani, O. and Tagliavini, F. (1993) Neurotoxicity of a prion protein fragment. Nature **362**, 543-546

11 Selvaggini, C., De Gioia, L., Cantu, L., Ghibaudi, E., Diomede, L., Passerini, F., Forloni, G., Bugiani, O., Tagliavini, F. and Salmona, M. (1993) Molecular characteristics of a protease-resistant, amyloidogenic and neurotoxic peptide homologous to residues 106-126 of the prion protein. Biochem Biophys Res Commun **194**, 1380-1386

12 Florio, T., Thellung, S., Amico, C., Robello, M., Salmona, M., Bugiani, O., Tagliavini, F., Forloni, G. and Schettini, G. (1998) Prion protein fragment 106-126 induces apoptotic cell death and impairment of L-type voltage-sensitive calcium channel activity in the GH3 cell line. J Neurosci Res **54**, 341-352

13 Fioriti, L., Quaglio, E., Massignan, T., Colombo, L., Stewart, R. S., Salmona, M., Harris, D. A., Forloni, G. and Chiesa, R. (2005) The neurotoxicity of prion protein (PrP) peptide 106-126 is independent of the expression level of PrP and is not mediated by abnormal PrP species. Mol Cell Neurosci **28**, 165-176

14 Salmona, M., Forloni, G., Diomede, L., Algeri, M., De Gioia, L., Angeretti, N., Giaccone, G., Tagliavini, F. and Bugiani, O. (1997) A neurotoxic and gliotrophic fragment of the prion protein increases plasma membrane microviscosity. Neurobiol Dis **4**, 47-57

15 Jobling, M. F., Stewart, L. R., White, A. R., McLean, C., Friedhuber, A., Maher, F., Beyreuther, K., Masters, C. L., Barrow, C. J., Collins, S. J. and Cappai, R. (1999) The hydrophobic core sequence modulates the neurotoxic and secondary structure properties of the prion peptide 106-126. J Neurochem **73**, 1557-1565

16 Lin, M. C., Mirzabekov, T. and Kagan, B. L. (1997) Channel formation by a neurotoxic prion protein fragment. J Biol Chem **272**, 44-47

17 Kourie, J. I. and Culverson, A. (2000) Prion peptide fragment PrP[106-126] forms distinct cation channel types. J Neurosci Res **62**, 120-133

18 Manunta, M., Kunz, B., Sandmeier, E., Christen, P. and Schindler, H. (2000) Reported channel formation by prion protein fragment 106-126 in planar lipid bilayers cannot be reproduced. FEBS Lett **474**, 255-256

19 Kunz, B., Sandmeier, E. and Christen, P. (1999) Neurotoxicity of prion peptide 106-126 not confirmed. FEBS Lett **458**, 65-68

20 Brown, D. R., Herms, J. and Kretzschmar, H. A. (1994) Mouse cortical cells lacking cellular PrP survive in culture with a neurotoxic PrP fragment. Neuroreport **5**, 2057-2060

21 LeVine, H., 3rd (1993) Thioflavine T interaction with synthetic Alzheimer's disease beta-amyloid peptides: detection of amyloid aggregation in solution. Protein Sci **2**, 404-410

22 Klunk, W. E., Jacob, R. F. and Mason, R. P. (1999) Quantifying amyloid beta-peptide (Abeta) aggregation using the Congo red-Abeta (CR-abeta) spectrophotometric assay. Anal Biochem **266**, 66-76

23 Sabate, R. and Estelrich, J. (2003) Pinacyanol as effective probe of fibrillar beta-amyloid peptide: comparative study with Congo Red. Biopolymers **72**, 455-463

24 Bertsch, M., Mayburd, A. L. and Kassner, R. J. (2003) The identification of hydrophobic sites on the surface of proteins using absorption difference spectroscopy of bromophenol blue. Anal Biochem **313**, 187-195

25 McParland, V. J., Kad, N. M., Kalverda, A. P., Brown, A., Kirwin-Jones, P., Hunter, M. G., Sunde, M. and Radford, S. E. (2000) Partially unfolded states of beta(2)-microglobulin and amyloid formation in vitro. Biochemistry **39**, 8735-8746

26 Veiga, S., Yuan, Y., Li, X., Santos, N. C., Liu, G. and Castanho, M. A. (2006) Why are HIV-1 fusion inhibitors not effective against SARS-CoV? Biophysical evaluation of molecular interactions. Biochim Biophys Acta **1760**, 55-61

27 Ladokhin, A. S., Jayasinghe, S. and White, S. H. (2000) How to measure and analyze tryptophan fluorescence in membranes properly, and why bother? Anal Biochem **285**, 235-245

28 Mayer, L. D., Hope, M. J. and Cullis, P. R. (1986) Vesicles of variable sizes produced by a rapid extrusion procedure. Biochim Biophys Acta **858**, 161-168

29 Henriques, S. T. and Castanho, M. A. (2004) Consequences of nonlytic membrane perturbation to the translocation of the cell penetrating peptide pep-1 in lipidic vesicles. Biochemistry **43**, 9716-9724

30 Caputo, G. A. and London, E. (2003) Using a novel dual fluorescence quenching assay for measurement of tryptophan depth within lipid bilayers to determine hydrophobic alpha-helix locations within membranes. Biochemistry **42**, 3265-3274

31 Gross, E., Bedlack, R. S., Jr. and Loew, L. M. (1994) Dual-wavelength ratiometric fluorescence measurement of the membrane dipole potential. Biophys J **67**, 208-216

32 Cladera, J. and O'Shea, P. (1998) Intramembrane molecular dipoles affect the membrane insertion and folding of a model amphiphilic peptide. Biophys J **74**, 2434-2442

33 Vey, M., Pilkuhn, S., Wille, H., Nixon, R., DeArmond, S. J., Smart, E. J., Anderson, R. G., Taraboulos, A. and Prusiner, S. B. (1996) Subcellular colocalization of the cellular and scrapie prion proteins in caveolae-like membranous domains. Proc Natl Acad Sci U S A **93**, 14945-14949

34 Caughey, B. and Raymond, G. J. (1991) The scrapie-associated form of PrP is made from a cell surface precursor that is both protease- and phospholipase-sensitive. J Biol Chem **266**, 18217-18223

35 Borchelt, D. R., Taraboulos, A. and Prusiner, S. B. (1992) Evidence for synthesis of scrapie prion proteins in the endocytic pathway. J Biol Chem **267**, 16188-16199

36 Groenning, M., Olsen, L., van de Weert, M., Flink, J. M., Frokjaer, S. and Jorgensen, F. S. (2007) Study on the binding of Thioflavin T to beta-sheet-rich and non-beta-sheet cavities. J Struct Biol **158**, 358-369

37 Mozsolits, H. and Aguilar, M. I. (2002) Surface plasmon resonance spectroscopy: an emerging tool for the study of peptide-membrane interactions. Biopolymers **66**, 3-18

38 Kamimori, H., Hall, K., Craik, D. J. and Aguilar, M. I. (2005) Studies on the membrane interactions of the cyclotides kalata B1 and kalata B6 on model membrane systems by surface plasmon resonance. Anal Biochem **337**, 149-153

39 Sreerama, N. and Woody, R. W. (2003) Structural composition of betaI- and betaII-proteins. Protein Sci **12**, 384-388

40 Wu, J., Yang, J. T. and Wu, C. S. (1992) Beta-II conformation of all-beta proteins can be distinguished from unordered form by circular dichroism. Anal Biochem **200**, 359-364

41 Shi, Z., Chen, K., Liu, Z., Ng, A., Bracken, W. C. and Kallenbach, N. R. (2005) Polyproline II propensities from GGXGG peptides reveal an anticorrelation with beta-sheet scales. Proc Natl Acad Sci U S A **102**, 17964-17968

42 Gokce, I., Woody, R. W., Anderluh, G. and Lakey, J. H. (2005) Single peptide bonds exhibit poly(pro)II ("random coil") circular dichroism spectra. J Am Chem Soc **127**, 9700-9701

43 Schweitzer-Stenner, R. and Measey, T. J. (2007) The alanine-rich XAO peptide adopts a heterogeneous population, including turn-like and polyproline II conformations. Proc Natl Acad Sci U S A **104**, 6649-6654

44 Magzoub, M., Pramanik, A. and Graslund, A. (2005) Modeling the endosomal escape of cell-penetrating peptides: transmembrane pH gradient driven translocation across phospholipid bilayers. Biochemistry **44**, 14890-14897

45 Khurana, R., Uversky, V. N., Nielsen, L. and Fink, A. L. (2001) Is Congo red an amyloid-specific dye? J Biol Chem **276**, 22715-22721

46 Zhao, H., Tuominen, E. K. and Kinnunen, P. K. (2004) Formation of amyloid fibers triggered by phosphatidylserine-containing membranes. Biochemistry **43**, 10302-10307

47 Gennis, R. B. (1989) Biomembranes molecular structure and function Spreinger-Verlag, New york

48 Taraboulos, A., Scott, M., Semenov, A., Avrahami, D., Laszlo, L. and Prusiner, S. B. (1995) Cholesterol depletion and modification of COOH-terminal targeting sequence of the prion protein inhibit formation of the scrapie isoform. J Cell Biol **129**, 121-132

49 Bate, C., Salmona, M., Diomede, L. and Williams, A. (2004) Squalestatin cures prion-infected neurons and protects against prion neurotoxicity. J Biol Chem **279**, 14983-14990

50 Choo-Smith, L. P., Garzon-Rodriguez, W., Glabe, C. G. and Surewicz, W. K. (1997) Acceleration of amyloid fibril formation by specific binding of Abeta-(1-40) peptide to ganglioside-containing membrane vesicles. J Biol Chem **272**, 22987-22990

51 Choo-Smith, L. P. and Surewicz, W. K. (1997) The interaction between Alzheimer amyloid beta(1-40) peptide and ganglioside GM1-containing membranes. FEBS Lett **402**, 95-98

52 Kakio, A., Nishimoto, S., Yanagisawa, K., Kozutsumi, Y. and Matsuzaki, K. (2002) Interactions of amyloid beta-protein with various gangliosides in raft-like membranes: importance of GM1 ganglioside-bound form as an endogenous seed for Alzheimer amyloid. Biochemistry **41**, 7385-7390

53 Chi, E. Y., Frey, S. L. and Lee, K. Y. (2007) Ganglioside G(M1)-mediated amyloid-beta fibrillogenesis and membrane disruption. Biochemistry **46**, 1913-1924

54 Kamimori, H., Blazyk, J. and Aguilar, M. I. (2005) Lipid membrane-binding properties of tryptophan analogues of linear amphipathic beta-sheet cationic antimicrobial peptides using surface plasmon resonance. Biol Pharm Bull **28**, 148-150

55 Mozsolits, H., Lee, T. H., Clayton, A. H., Sawyer, W. H. and Aguilar, M. I. (2004) The membrane-binding properties of a class A amphipathic peptide. Eur Biophys J **33**, 98-108

56 Whittingham, J. L., Scott, D. J., Chance, K., Wilson, A., Finch, J., Brange, J. and Guy Dodson, G. (2002) Insulin at pH 2: structural analysis of the conditions promoting insulin fibre formation. J Mol Biol **318**, 479-490

57 Matsubara, T., Iijima, K., Nakamura, M., Taki, T., Okahata, Y. and Sato, T. (2007) Specific binding of GM1-binding peptides to high-density GM1 in lipid membranes. Langmuir **23**, 708-714

58 Yuan, C. and Johnston, L. J. (2001) Atomic force microscopy studies of ganglioside GM1 domains in phosphatidylcholine and phosphatidylcholine/cholesterol bilayers. Biophys J **81**, 1059-1069

59 de Almeida, R. F., Fedorov, A. and Prieto, M. (2003) Sphingomyelin/phosphatidylcholine/cholesterol phase diagram: boundaries and composition of lipid rafts. Biophys J **85**, 2406-2416

60 Seelig, J. (2004) Thermodynamics of lipid-peptide interactions. Biochim Biophys Acta **1666**, 40-50

61 White, S. H. and Wimley, W. C. (1998) Hydrophobic interactions of peptides with membrane interfaces. Biochim Biophys Acta **1376**, 339-352

62 Hope, J., Shearman, M. S., Baxter, H. C., Chong, A., Kelly, S. M. and Price, N. C. (1996) Cytotoxicity of prion protein peptide (PrP106-126) differs in mechanism from the cytotoxic activity of the Alzheimer's disease amyloid peptide, A beta 25-35. Neurodegeneration **5**, 1-11

63 Pietri, M., Caprini, A., Mouillet-Richard, S., Pradines, E., Ermonval, M., Grassi, J., Kellermann, O. and Schneider, B. (2006) Overstimulation of PrPC signaling pathways by prion peptide 106-126 causes oxidative injury of bioaminergic neuronal cells. J Biol Chem **281**, 28470-28479

64 Magzoub, M. and Graslund, A. (2004) Cell-penetrating peptides: [corrected] from inception to application. Q Rev Biophys **37**, 147-195

65 Henriques, S. T., Melo, M. N. and Castanho, M. A. (2006) Cell-penetrating peptides and antimicrobial peptides: how different are they? Biochem J **399**, 1-7

66 Magzoub, M., Sandgren, S., Lundberg, P., Oglecka, K., Lilja, J., Wittrup, A., Goran Eriksson, L. E., Langel, U., Belting, M. and Graslund, A. (2006) N-terminal peptides from unprocessed prion proteins enter cells by macropinocytosis. Biochem Biophys Res Commun **348**, 379-385

67 Choi, C. J., Anantharam, V., Saetveit, N. J., Houk, R. S., Kanthasamy, A. and Kanthasamy, A. G. (2007) Normal cellular prion protein protects against manganese-induced oxidative stress and apoptotic cell death. Toxicol Sci **98**, 495-509

68 Sakudo, A., Lee, D. C., Saeki, K., Nakamura, Y., Inoue, K., Matsumoto, Y., Itohara, S. and Onodera, T. (2003) Impairment of superoxide dismutase activation by N-terminally truncated prion protein (PrP) in PrP-deficient neuronal cell line. Biochem Biophys Res Commun **308**, 660-667

69 Sakudo, A., Nakamura, I., Lee, D. C., Saeki, K., Ikuta, K. and Onodera, T. (2007) Neurotoxic prion protein (PrP) fragment 106-126 requires the N-terminal half of the hydrophobic region of PrP in the PrP-deficient neuronal cell line. Protein Pept Lett **14**, 1-6

70 Parkin, E. T., Watt, N. T., Hussain, I., Eckman, E. A., Eckman, C. B., Manson, J. C., Baybutt, H. N., Turner, A. J. and Hooper, N. M. (2007) Cellular prion protein regulates beta-secretase cleavage of the Alzheimer's amyloid precursor protein. Proc Natl Acad Sci U S A **104**, 11062-11067

71 BIACORE (2001) Biacore concentration analysis handbook. Version AA. Biacore AB, Upsala

72 Goldstein, B., Coombs, D., He, X., Pineda, A. R. and Wofsy, C. (1999) The influence of transport on the kinetics of binding to surface receptors: application to cells and BIAcore. J Mol Recognit **12**, 293-299

SUPPORTING INFORMATION

Bulk shift correction

Equivalent buffer composition in the sample and in running buffer is required, although exact matching was difficult to achieve due to varying peptide concentrations in the samples. Peptide samples were prepared by diluting stock solution in the running buffer. Because stock solution was in H_2O sterile, the final concentration of buffer varies with peptide concentration, which results in different refractive indexes and thus vertical jumps in the responses upon peptide addition are observed in sensorgram curves (see Figure S.1). In order to compare the data analysis for the different peptide concentrations in different buffers studied, a bulk shift correction was applied to all sets of sensorgrams as suggested by good practice guidelines [71]. Examples of this effect and the correction of sensorgrams obtained with POPC are shown in Figure S.1.

Figure S.1. Bulk refractive index effect on sensorgrams obtained in the study of PrP(106-126) interaction with POPC membranes immobilized on the surface of L1 chip**.** Sensorgrams obtained for PrP(106-126) interaction with lipidic membranes are affected by bulk refractive index, the response observed during injection sample in Biacore results from a combination of peptide binding to the sensor and differences between refractive index between samples and running buffer. To correct this effect, refractive indexes were calculated by the signal difference between the end of injection and a report point clear of bulk effects (in this case 2s after injection end). Refractive indexes were subtracted from the association curve. Sensograms obtained with different PrP(10-126) samples (0-50μM) injections onto POPC lipidic membrane at three different conditions are represented: A) HEPES buffer, pH7.4 with 150mM NaCl; B) Acetate buffer, pH5 with 150mMNaCl and C) Acetate buffer, pH5 with 10mMNaCl. At pH7.4 with 150mM NaCl there is not a concentration effect, the signal is low and comparable with buffer signal. Peptide binding in this buffer is neglected.

A) pH7.4, 150mM NaCl

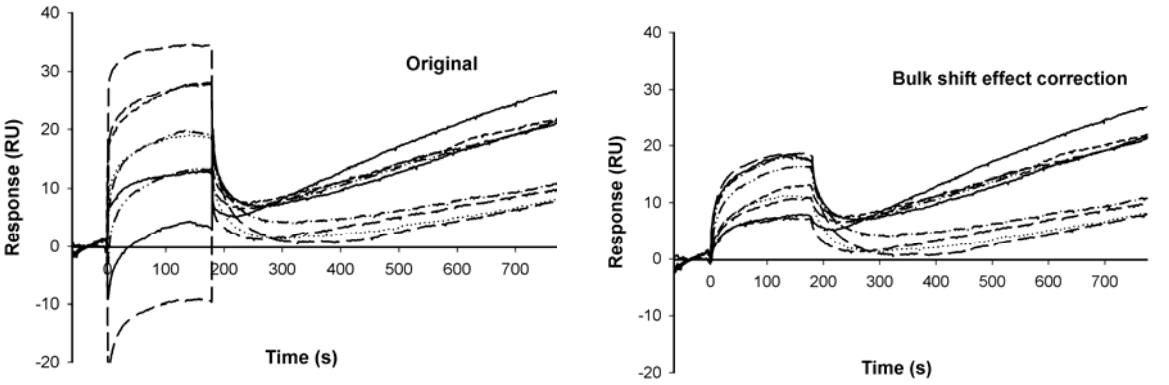

B) pH5 150mM NaCl

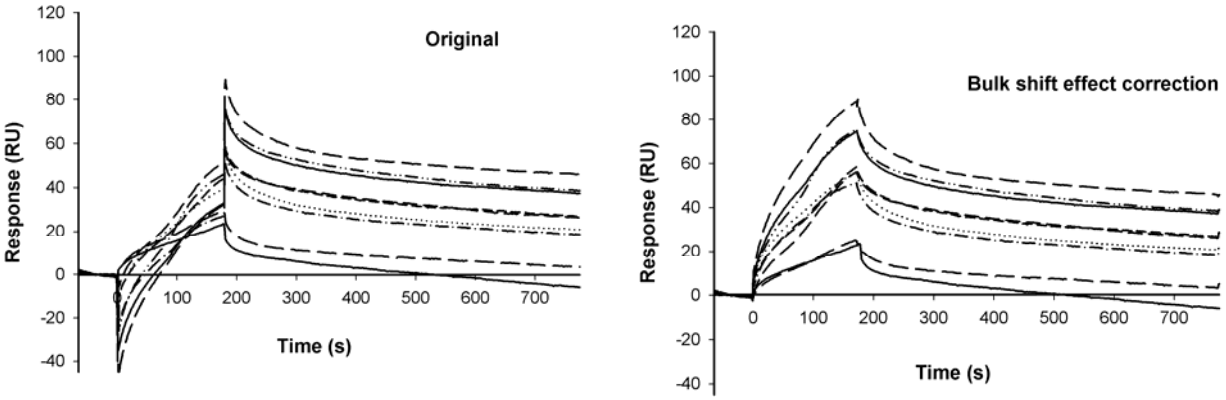

C) pH510mMNaCl

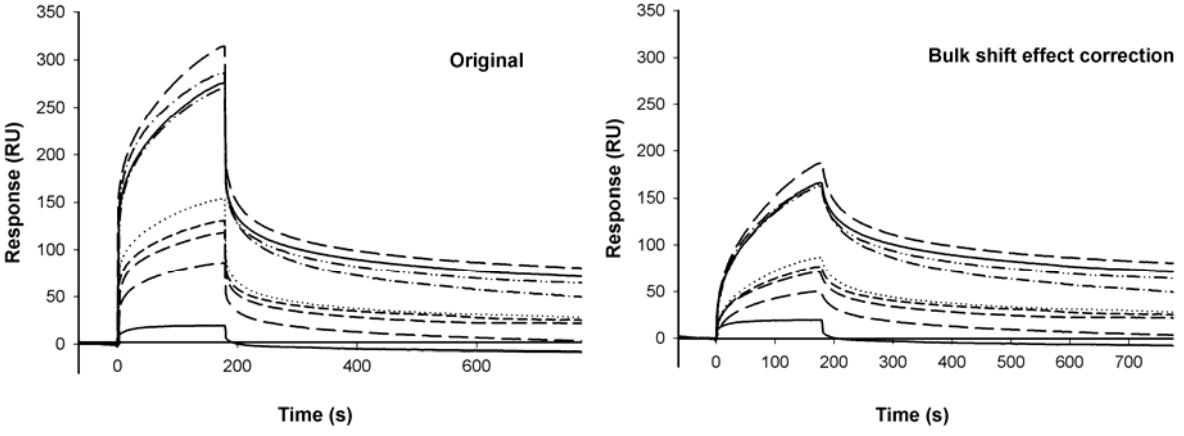

Evaluation of mass transport effect on SPR sensorgrams

The kinetic in a sensorgram is a result of peptide molecules diffusion from the bulk solution to the surface and the peptide-membrane binding rate. The ideal situation is when the transport is faster than the binding and kinetic is not affected by molecule diffusion [72]. When the peptide/membrane binding rate is faster than peptide diffusion to the surface, or when the rate of these two processes are of similar magnitude kinetic an accurate binding rate constant is not possible to calculate unless this diffusion effect is accounted for. This effect is commonly designated by mass transport effect and its magnitude is dependent on the peptide flow rate [71]. In order to evaluate if kinetics is or not affected by this effect, sensograms obtained at different flow rates should be compared. In this particular case, peptide injections at 5μL/min and 20μL/min flow rates were compared. Peptide-membrane binding rate is highest at the beginning of the injection, while mass transport rate is constant through the injection since the peptide concentration is constant in solution. The relative contribution of mass transport rate on biochemical interaction varies during peptide injection. Diffusion effects have a higher contribution to the overall kinetics immediately after injection start. Comparing the initial rates for the sensograms obtained at 5μL/min vs. 20μL/min (Figure S.2) it was possible to conclude that the flow rate does not affect the kinetic. Binding rate for this system is not affected by mass transport effect; even though, the faster flow rate was chosen to carry on the experiments in order to avoid unspecific interactions or other effects.

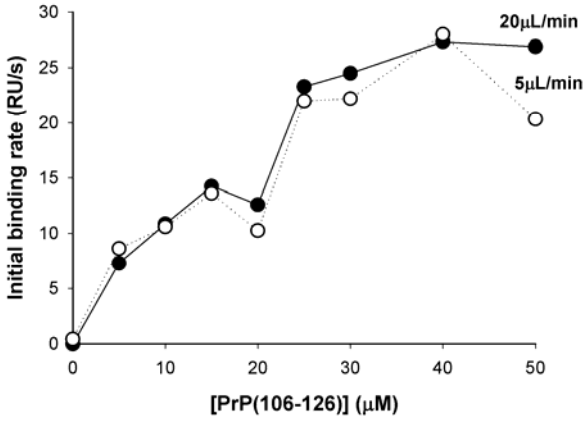

Figure S.2. Evaluation of mass transport effect on PrP(106-126) interaction with POPC/POPG(4:1) membranes immobilized on the surface of L1 chip, pH 5 with 10mM NaCl. Two peptide injection flow rates, 5μL/min and 20μL/min, were compared to test if kinetic binding is affected by mass transport. Initial peptide binding rate was calculated in sensorgrams (corrected for bulk refractive index effect) by the initial slope of the sensogram using a report point placed shortly after the injection start (2s). By calculation of initial binding rates obtained within a peptide range concentration of 0-50μM it was possible to verify that initial binding is dependent on peptide concentration but independent on flow rate. No mass transport effects were detected for PrP(106-126).

REFERENCES

1 BIACORE (2001) Biacore concentration analysis handbook. Version AA. Biacore AB, Upsala

2 Goldstein, B., Coombs, D., He, X., Pineda, A. R. and Wofsy, C. (1999) The influence of transport on the kinetics of binding to surface receptors: application to cells and BIAcore. J Mol Recognit **12**, 293-299

Chapter 8

Bibliography

Chapter 8.

Bibliography

1 Wadia, J. S., Becker-Hapak, M. and Dowdy, S. F. (2002) Protein Transport. In Cell-penetrating peptides, processes and applications (Langel, Ü., ed.), pp. 365-375, CRC Press, New York

2 Gao, X., Kim, K. S. and Liu, D. (2007) Nonviral gene delivery: what we know and what is next. Aaps J **9**, E92-104

3 Burton, E. A., Fink, D. J. and Glorioso, J. C. (2002) Gene delivery using herpes simplex virus vectors. DNA Cell Biol **21**, 915-936

4 Lai, C. M., Lai, Y. K. and Rakoczy, P. E. (2002) Adenovirus and adeno-associated virus vectors. DNA Cell Biol **21**, 895-913

5 Quinonez, R. and Sutton, R. E. (2002) Lentiviral vectors for gene delivery into cells. DNA Cell Biol **21**, 937-951

6 Smyth Templeton, N. (2002) Liposomal delivery of nucleic acids in vivo. DNA Cell Biol **21**, 857-867

7 Celis, J. E. (1984) Microinjection of somatic cells with micropipettes: comparison with other transfer techniques. Biochem J **223**, 281-291

8 Stephens, D. J. and Pepperkok, R. (2001) The many ways to cross the plasma membrane. Proc Natl Acad Sci U S A **98**, 4295-4298

9 Neumann, E., Schaefer-Ridder, M., Wang, Y. and Hofschneider, P. H. (1982) Gene transfer into mouse lyoma cells by electroporation in high electric fields. Embo J **1**, 841-845

10 Henshaw, J. W. and Yuan, F. (2007) Field distribution and DNA transport in solid tumors during electric field-mediated gene delivery. J Pharm Sci

11 Felgner, P. L., Gadek, T. R., Holm, M., Roman, R., Chan, H. W., Wenz, M., Northrop, J. P., Ringold, G. M. and Danielsen, M. (1987) Lipofection: a highly efficient, lipid-mediated DNA-transfection procedure. Proc Natl Acad Sci U S A **84**, 7413-7417

12 Hashida, M., Kawakami, S. and Yamashita, F. (2005) Lipid carrier systems for targeted drug and gene delivery. Chem Pharm Bull (Tokyo) **53**, 871-880

13 Frankel, A. D. and Pabo, C. O. (1988) Cellular uptake of the tat protein from human immunodeficiency virus. Cell **55**, 1189-1193

14 Joliot, A., Pernelle, C., Deagostini-Bazin, H. and Prochiantz, A. (1991) Antennapedia homeobox peptide regulates neural morphogenesis. Proc Natl Acad Sci U S A **88**, 1864-1868

15 Vives, E., Brodin, P. and Lebleu, B. (1997) A truncated HIV-1 Tat protein basic domain rapidly translocates through the plasma membrane and accumulates in the cell nucleus. J Biol Chem **272**, 16010-16017

16 Derossi, D., Joliot, A. H., Chassaing, G. and Prochiantz, A. (1994) The third helix of the Antennapedia homeodomain translocates through biological membranes. J Biol Chem **269**, 10444-10450

17 Theodore, L., Derossi, D., Chassaing, G., Llirbat, B., Kubes, M., Jordan, P., Chneiweiss, H., Godement, P. and Prochiantz, A. (1995) Intraneuronal delivery of protein kinase C pseudosubstrate leads to growth cone collapse. J Neurosci **15**, 7158-7167

18 Fawell, S., Seery, J., Daikh, Y., Moore, C., Chen, L. L., Pepinsky, B. and Barsoum, J. (1994) Tat-mediated delivery of heterologous proteins into cells. Proc Natl Acad Sci U S A **91**, 664-668

19 Ezhevsky, S. A., Nagahara, H., Vocero-Akbani, A. M., Gius, D. R., Wei, M. C. and Dowdy, S. F. (1997) Hypo-phosphorylation of the retinoblastoma protein (pRb) by cyclin D:Cdk4/6 complexes results in active pRb. Proc Natl Acad Sci U S A **94**, 10699-10704

20 Lindgren, M., Hallbrink, M., Prochiantz, A. and Langel, U. (2000) Cell-penetrating peptides. Trends Pharmacol Sci **21**, 99-103

21 Prochiantz, A. (2000) Messenger proteins: homeoproteins, TAT and others. Curr Opin Cell Biol **12**, 400-406

22 Schwarze, S. R. and Dowdy, S. F. (2000) In vivo protein transduction: intracellular delivery of biologically active proteins, compounds and DNA. Trends Pharmacol Sci **21**, 45-48

23 Schwarze, S. R., Ho, A., Vocero-Akbani, A. and Dowdy, S. F. (1999) In vivo protein transduction: delivery of a biologically active protein into the mouse. Science **285**, 1569-1572

24 Elmquist, A., Lindgren, M., Bartfai, T. and Langel, U. (2001) VE-cadherin-derived cell-penetrating peptide, pVEC, with carrier functions. Exp Cell Res **269**, 237-244

25 Elliott, G. and O'Hare, P. (1997) Intercellular trafficking and protein delivery by a herpesvirus structural protein. Cell **88**, 223-233

26 Hallbrink, M., Floren, A., Elmquist, A., Pooga, M., Bartfai, T. and Langel, U. (2001) Cargo delivery kinetics of cell-penetrating peptides. Biochim Biophys Acta **1515**, 101-109

27 Futaki, S., Suzuki, T., Ohashi, W., Yagami, T., Tanaka, S., Ueda, K. and Sugiura, Y. (2001) Arginine-rich peptides. An abundant source of membrane-permeable peptides having potential as carriers for intracellular protein delivery. J Biol Chem **276**, 5836-5840

28 Langel, U., Pooga, M., Kairane, C., Zilmer, M. and Bartfai, T. (1996) A galanin-mastoparan chimeric peptide activates the Na+,K(+)-ATPase and reverses its inhibition by ouabain. Regul Pept **62**, 47-52

29 Morris, M. C., Vidal, P., Chaloin, L., Heitz, F. and Divita, G. (1997) A new peptide vector for efficient delivery of oligonucleotides into mammalian cells. Nucleic Acids Res **25**, 2730-2736

30 Scheller, A., Oehlke, J., Wiesner, B., Dathe, M., Krause, E., Beyermann, M., Melzig, M. and Bienert, M. (1999) Structural requirements for cellular uptake of alpha-helical amphipathic peptides. J Pept Sci **5**, 185-194

31 Mitchell, D. J., Kim, D. T., Steinman, L., Fathman, C. G. and Rothbard, J. B. (2000) Polyarginine enters cells more efficiently than other polycationic homopolymers. J Pept Res **56**, 318-325

32 Hariton-Gazal, E., Feder, R., Mor, A., Graessmann, A., Brack-Werner, R., Jans, D., Gilon, C. and Loyter, A. (2002) Targeting of nonkaryophilic cell-permeable peptides into the nuclei of intact cells by covalently attached nuclear localization signals. Biochemistry **41**, 9208-9214

33 Chaloin, L., Vidal, P., Lory, P., Mery, J., Lautredou, N., Divita, G. and Heitz, F. (1998) Design of carrier peptide-oligonucleotide conjugates with rapid membrane translocation and nuclear localization properties. Biochem Biophys Res Commun **243**, 601-608

34 Magzoub, M. and Graslund, A. (2004) Cell-penetrating peptides: from inception to application. Q Rev Biophys **37**, 147-195

35 Harada, H., Hiraoka, M. and Kizaka-Kondoh, S. (2002) Antitumor effect of TAT-oxygen-dependent degradation-caspase-3 fusion protein specifically stabilized and activated in hypoxic tumor cells. Cancer Res **62**, 2013-2018

36 Klekotka, P. A., Santoro, S. A., Ho, A., Dowdy, S. F. and Zutter, M. M. (2001) Mammary epithelial cell-cycle progression via the alpha(2)beta(1) integrin: unique and synergistic roles of the alpha(2) cytoplasmic domain. Am J Pathol **159**, 983-992

37 Rojas, M., Donahue, J. P., Tan, Z. and Lin, Y. Z. (1998) Genetic engineering of proteins with cell membrane permeability. Nat Biotechnol **16**, 370-375

38 Borsello, T., Clarke, P. G., Hirt, L., Vercelli, A., Repici, M., Schorderet, D. F., Bogousslavsky, J. and Bonny, C. (2003) A peptide inhibitor of c-Jun N-terminal kinase protects against excitotoxicity and cerebral ischemia. Nat Med **9**, 1180-1186

39 Giorello, L., Clerico, L., Pescarolo, M. P., Vikhanskaya, F., Salmona, M., Colella, G., Bruno, S., Mancuso, T., Bagnasco, L., Russo, P. and Parodi, S. (1998) Inhibition of cancer cell growth and c-Myc transcriptional activity by a c-Myc helix 1-type peptide fused to an internalization sequence. Cancer Res **58**, 3654-3659

40 Rojas, M., Yao, S., Donahue, J. P. and Lin, Y. Z. (1997) An alternative to phosphotyrosine-containing motifs for binding to an SH2 domain. Biochem Biophys Res Commun **234**, 675-680

41 Cutrona, G., Carpaneto, E. M., Ulivi, M., Roncella, S., Landt, O., Ferrarini, M. and Boffa, L. C. (2000) Effects in live cells of a c-myc anti-gene PNA linked to a nuclear localization signal. Nat Biotechnol **18**, 300-303

42 Moulton, H. M., Hase, M. C., Smith, K. M. and Iversen, P. L. (2003) HIV Tat peptide enhances cellular delivery of antisense morpholino oligomers. Antisense Nucleic Acid Drug Dev **13**, 31-43

43 Allinquant, B., Hantraye, P., Mailleux, P., Moya, K., Bouillot, C. and Prochiantz, A. (1995) Downregulation of amyloid precursor protein inhibits neurite outgrowth in vitro. J Cell Biol **128**, 919-927

44 Pooga, M., Soomets, U., Hallbrink, M., Valkna, A., Saar, K., Rezaei, K., Kahl, U., Hao, J. X., Xu, X. J., Wiesenfeld-Hallin, Z., Hokfelt, T., Bartfai, T. and Langel, U. (1998) Cell penetrating PNA constructs regulate galanin receptor levels and modify pain transmission in vivo. Nat Biotechnol **16**, 857-861

45 Simeoni, F., Morris, M. C., Heitz, F. and Divita, G. (2003) Insight into the mechanism of the peptide-based gene delivery system MPG: implications for delivery of siRNA into mammalian cells. Nucleic Acids Res **31**, 2717-2724

46 Simeoni, F., Morris, M. C., Heitz, F. and Divita, G. (2005) Peptide-based strategy for siRNA delivery into mammalian cells. Methods Mol Biol **309**, 251-260

47 Ignatovich, I. A., Dizhe, E. B., Pavlotskaya, A. V., Akifiev, B. N., Burov, S. V., Orlov, S. V. and Perevozchikov, A. P. (2003) Complexes of plasmid DNA with basic domain 47-57 of the HIV-1 Tat protein are transferred to mammalian cells by endocytosis-mediated pathways. J Biol Chem **278**, 42625-42636

48 Rudolph, C., Plank, C., Lausier, J., Schillinger, U., Muller, R. H. and Rosenecker, J. (2003) Oligomers of the arginine-rich motif of the HIV-1 TAT protein are capable of transferring plasmid DNA into cells. J Biol Chem **278**, 11411-11418

49 Lewin, M., Carlesso, N., Tung, C. H., Tang, X. W., Cory, D., Scadden, D. T. and Weissleder, R. (2000) Tat peptide-derivatized magnetic nanoparticles allow in vivo tracking and recovery of progenitor cells. Nat Biotechnol **18**, 410-414

50 Torchilin, V. P., Rammohan, R., Weissig, V. and Levchenko, T. S. (2001) TAT peptide on the surface of liposomes affords their efficient intracellular delivery even at low temperature and in the presence of metabolic inhibitors. Proc Natl Acad Sci U S A **98**, 8786-8791

51 Bucci, M., Gratton, J. P., Rudic, R. D., Acevedo, L., Roviezzo, F., Cirino, G. and Sessa, W. C. (2000) In vivo delivery of the caveolin-1 scaffolding domain inhibits nitric oxide synthesis and reduces inflammation. Nat Med **6**, 1362-1367

52 Rousselle, C., Clair, P., Lefauconnier, J. M., Kaczorek, M., Scherrmann, J. M. and Temsamani, J. (2000) New advances in the transport of doxorubicin through the blood-brain barrier by a peptide vector-mediated strategy. Mol Pharmacol **57**, 679-686

53 Derossi, D., Calvet, S., Trembleau, A., Brunissen, A., Chassaing, G. and Prochiantz, A. (1996) Cell internalization of the third helix of the Antennapedia homeodomain is receptor-independent. J Biol Chem **271**, 18188-18193

54 Suzuki, T., Futaki, S., Niwa, M., Tanaka, S., Ueda, K. and Sugiura, Y. (2002) Possible existence of common internalization mechanisms among arginine-rich peptides. J Biol Chem **277**, 2437-2443

55 Lundberg, M. and Johansson, M. (2001) Is VP22 nuclear homing an artifact? Nat Biotechnol **19**, 713-714

56 Lundberg, M. and Johansson, M. (2002) Positively charged DNA-binding proteins cause apparent cell membrane translocation. Biochem Biophys Res Commun **291**, 367-371

57 Melan, M. A. and Sluder, G. (1992) Redistribution and differential extraction of soluble proteins in permeabilized cultured cells. Implications for immunofluorescence microscopy. J Cell Sci **101 (Pt 4)**, 731-743

58 Thoren, P. E., Persson, D., Isakson, P., Goksor, M., Onfelt, A. and Norden, B. (2003) Uptake of analogs of penetratin, Tat(48-60) and oligoarginine in live cells. Biochem Biophys Res Commun **307**, 100-107

59 Drin, G., Cottin, S., Blanc, E., Rees, A. R. and Temsamani, J. (2003) Studies on the internalization mechanism of cationic cell-penetrating peptides. J Biol Chem **278**, 31192-31201

60 Richard, J. P., Melikov, K., Vives, E., Ramos, C., Verbeure, B., Gait, M. J., Chernomordik, L. V. and Lebleu, B. (2003) Cell-penetrating peptides. A reevaluation of the mechanism of cellular uptake. J Biol Chem **278**, 585-590

61 Potocky, T. B., Menon, A. K. and Gellman, S. H. (2003) Cytoplasmic and nuclear delivery of a TAT-derived peptide and a beta-peptide after endocytic uptake into HeLa cells. J Biol Chem **278**, 50188-50194

62 Fittipaldi, A., Ferrari, A., Zoppe, M., Arcangeli, C., Pellegrini, V., Beltram, F. and Giacca, M. (2003) Cell membrane lipid rafts mediate caveolar endocytosis of HIV-1 Tat fusion proteins. J Biol Chem **278**, 34141-34149

63 Console, S., Marty, C., Garcia-Echeverria, C., Schwendener, R. and Ballmer-Hofer, K. (2003) Antennapedia and HIV transactivator of transcription (TAT) "protein transduction domains" promote endocytosis of high molecular weight cargo upon binding to cell surface glycosaminoglycans. J Biol Chem **278**, 35109-35114

64 Lundberg, M., Wikstrom, S. and Johansson, M. (2003) Cell surface adherence and endocytosis of protein transduction domains. Mol Ther **8**, 143-150

65 Fischer, R., Kohler, K., Fotin-Mleczek, M. and Brock, R. (2004) A stepwise dissection of the intracellular fate of cationic cell-penetrating peptides. J Biol Chem **279**, 12625-12635

66 Fuchs, S. M. and Raines, R. T. (2004) Pathway for polyarginine entry into mammalian cells. Biochemistry **43**, 2438-2444

67 Nakase, I., Niwa, M., Takeuchi, T., Sonomura, K., Kawabata, N., Koike, Y., Takehashi, M., Tanaka, S., Ueda, K., Simpson, J. C., Jones, A. T., Sugiura, Y. and Futaki, S. (2004) Cellular uptake of arginine-rich peptides: roles for macropinocytosis and actin rearrangement. Mol Ther **10**, 1011-1022

68 Wadia, J. S., Stan, R. V. and Dowdy, S. F. (2004) Transducible TAT-HA fusogenic peptide enhances escape of TAT-fusion proteins after lipid raft macropinocytosis. Nat Med **10**, 310-315

69 Vendeville, A., Rayne, F., Bonhoure, A., Bettache, N., Montcourrier, P. and Beaumelle, B. (2004) HIV-1 Tat enters T cells using coated pits before translocating from acidified endosomes and eliciting biological responses. Mol Biol Cell **15**, 2347-2360

70 Richard, J. P., Melikov, K., Brooks, H., Prevot, P., Lebleu, B. and Chernomordik, L. V. (2005) Cellular uptake of unconjugated TAT peptide involves clathrin-dependent endocytosis and heparan sulfate receptors. J Biol Chem **280**, 15300-15306

71 Renigunta, A., Krasteva, G., Konig, P., Rose, F., Klepetko, W., Grimminger, F., Seeger, W. and Hanze, J. (2006) DNA transfer into human lung cells is improved with Tat-RGD peptide by Caveoli-mediated endocytosis. Bioconjug Chem **17**, 327-334

72 Vives, E., Granier, C., Prevot, P. and Lebleu, B. (1997) Structure-activity relationship study of the plasma membrane translocating potential of a short peptide from HIV-1 Tat protein. Lett Pept Sci **4**, 429-436

73 Wender, P. A., Mitchell, D. J., Pattabiraman, K., Pelkey, E. T., Steinman, L. and Rothbard, J. B. (2000) The design, synthesis, and evaluation of molecules that enable or enhance cellular uptake: peptoid molecular transporters. Proc Natl Acad Sci U S A **97**, 13003-13008

74 Ghibaudi, E., Boscolo, B., Inserra, G., Laurenti, E., Traversa, S., Barbero, L. and Ferrari, R. P. (2005) The interaction of the cell-penetrating peptide penetratin with heparin, heparansulfates and phospholipid vesicles investigated by ESR spectroscopy. J Pept Sci **11**, 401-409

75 Letoha, T., Gaal, S., Somlai, C., Venkei, Z., Glavinas, H., Kusz, E., Duda, E., Czajlik, A., Petak, F. and Penke, B. (2005) Investigation of penetratin peptides. Part 2. In vitro uptake of penetratin and two of its derivatives. J Pept Sci **11**, 805-811

76 Letoha, T., Kusz, E., Papai, G., Szabolcs, A., Kaszaki, J., Varga, I., Takacs, T., Penke, B. and Duda, E. (2006) In vitro and in vivo NF-{kappa}B inhibitory effects of the cell-penetrating penetratin Mol Pharmacol **69**, 2027-2036

77 Magzoub, M., Pramanik, A. and Graslund, A. (2005) Modeling the endosomal escape of cell-penetrating peptides: transmembrane pH gradient driven translocation across phospholipid bilayers. Biochemistry **44**, 14890-14897

78 Terrone, D., Sang, S. L., Roudaia, L. and Silvius, J. R. (2003) Penetratin and related cell-penetrating cationic peptides can translocate across lipid bilayers in the presence of a transbilayer potential. Biochemistry **42**, 13787-13799

79 Thoren, P. E., Persson, D., Karlsson, M. and Norden, B. (2000) The antennapedia peptide penetratin translocates across lipid bilayers - the first direct observation. FEBS Lett **482**, 265-268

80 Mann, D. A. and Frankel, A. D. (1991) Endocytosis and targeting of exogenous HIV-1 Tat protein. Embo J **10**, 1733-1739

81 Rothbard, J. B., Jessop, T. C., Lewis, R. S., Murray, B. A. and Wender, P. A. (2004) Role of membrane potential and hydrogen bonding in the mechanism of translocation of guanidinium-rich peptides into cells. J Am Chem Soc **126**, 9506-9507

82 Abes, S., Turner, J. J., Ivanova, G. D., Owen, D., Williams, D., Arzumanov, A., Clair, P., Gait, M. J. and Lebleu, B. (2007) Efficient splicing correction by PNA conjugation to an R6-Penetratin delivery peptide. Nucleic Acids Res **35**, 4495-4502

83 Bogoyevitch, M. A., Kendrick, T. S., Ng, D. C. and Barr, R. K. (2002) Taking the cell by stealth or storm? Protein transduction domains (PTDs) as versatile vectors for delivery. DNA Cell Biol **21**, 879-894

84 Morris, M. C., Depollier, J., Mery, J., Heitz, F. and Divita, G. (2001) A peptide carrier for the delivery of biologically active proteins into mammalian cells. Nat Biotechnol **19**, 1173-1176

85 Peluso, J. J., Pappalardo, A. and Fernandez, G. (2001) Basic fibroblast growth factor maintains calcium homeostasis and granulosa cell viability by stimulating calcium efflux via a PKC delta-dependent pathway. Endocrinology **142**, 4203-4211

86 Zhou, J. and Hsieh, J. T. (2001) The inhibitory role of DOC-2/DAB2 in growth factor receptor-mediated signal cascade. DOC-2/DAB2-mediated inhibition of ERK phosphorylation via binding to Grb2. J Biol Chem **276**, 27793-27798

87 Zhang, Q., Nottke, A. and Goodman, R. H. (2005) Homeodomain-interacting protein kinase-2 mediates CtBP phosphorylation and degradation in UV-triggered apoptosis. Proc Natl Acad Sci U S A **102**, 2802-2807

88 Jurney, W. M., Gallo, G., Letourneau, P. C. and McLoon, S. C. (2002) Rac1-mediated endocytosis during ephrin-A2- and semaphorin 3A-induced growth cone collapse. J Neurosci **22**, 6019-6028

89 Bandichhor, R., Petrescu, A. D., Vespa, A., Kier, A. B., Schroeder, F. and Burgess, K. (2006) Synthesis of a new water-soluble rhodamine derivative and application to protein labeling and intracellular imaging. Bioconjug Chem **17**, 1219-1225

90 Jiang, J., Borisenko, G. G., Osipov, A., Martin, I., Chen, R., Shvedova, A. A., Sorokin, A., Tyurina, Y. Y., Potapovich, A., Tyurin, V. A., Graham, S. H. and Kagan, V. E. (2004) Arachidonic acid-induced carbon-centered radicals and phospholipid peroxidation in cyclo-oxygenase-2-transfected PC12 cells. J Neurochem **90**, 1036-1049

91 Sebbagh, M., Hamelin, J., Bertoglio, J., Solary, E. and Breard, J. (2005) Direct cleavage of ROCK II by granzyme B induces target cell membrane blebbing in a caspase-independent manner. J Exp Med **201**, 465-471

92 Wu, Y., Wood, M. D., Tao, Y. and Katagiri, F. (2003) Direct delivery of bacterial avirulence proteins into resistant Arabidopsis protoplasts leads to hypersensitive cell death. Plant J **33**, 131-137

93 Jain, A., Brady-Kalnay, S. M. and Bellamkonda, R. V. (2004) Modulation of Rho GTPase activity alleviates chondroitin sulfate proteoglycan-dependent inhibition of neurite extension. J Neurosci Res **77**, 299-307

94 Buster, D., McNally, K. and McNally, F. J. (2002) Katanin inhibition prevents the redistribution of gamma-tubulin at mitosis. J Cell Sci **115**, 1083-1092

95 Coulpier, M., Anders, J. and Ibanez, C. F. (2002) Coordinated activation of autophosphorylation sites in the RET receptor tyrosine kinase: importance of tyrosine 1062 for GDNF mediated neuronal differentiation and survival. J Biol Chem **277**, 1991-1999

96 Gallo, G., Yee, H. F., Jr. and Letourneau, P. C. (2002) Actin turnover is required to prevent axon retraction driven by endogenous actomyosin contractility. J Cell Biol **158**, 1219-1228

97 Ikari, A., Nakano, M., Kawano, K. and Suketa, Y. (2002) Up-regulation of sodium-dependent glucose transporter by interaction with heat shock protein 70. J Biol Chem **277**, 33338-33343

98 Remacle, A. G., Rozanov, D. V., Baciu, P. C., Chekanov, A. V., Golubkov, V. S. and Strongin, A. Y. (2005) The transmembrane domain is essential for the microtubular trafficking of membrane type-1 matrix metalloproteinase (MT1-MMP). J Cell Sci **118**, 4975-4984

99 Tisdale, E. J. (2002) Glyceraldehyde-3-phosphate dehydrogenase is phosphorylated by protein kinase Ciota /lambda and plays a role in microtubule dynamics in the early secretory pathway. J Biol Chem **277**, 3334-3341

100 Aoshiba, K., Yokohori, N. and Nagai, A. (2003) Alveolar wall apoptosis causes lung destruction and emphysematous changes. Am J Respir Cell Mol Biol **28**, 555-562

101 Maron, M. B., Folkesson, H. G., Stader, S. M. and Walro, J. M. (2005) PKA delivery to the distal lung air spaces increases alveolar liquid clearance after isoproterenol-induced alveolar epithelial PKA desensitization. Am J Physiol Lung Cell Mol Physiol **289**, L349-354

102 Fernandez-Carneado, J., Kogan, M. J., Pujals, S. and Giralt, E. (2004) Amphipathic peptides and drug delivery. Biopolymers **76**, 196-203

103 Yeaman, M. R. and Yount, N. Y. (2003) Mechanisms of antimicrobial peptide action and resistance. Pharmacol Rev **55**, 27-55

104 Oehlke, J., Krause, E., Wiesner, B., Beyermann, M. and Bienert, M. (1996) Nonendocytic, amphipathicity dependent cellular uptake of helical model peptides. Protein Peptide Lett **3**, 393-398

105 Chaloin, L., Vidal, P., Heitz, A., Van Mau, N., Mery, J., Divita, G. and Heitz, F. (1997) Conformations of primary amphipathic carrier peptides in membrane mimicking environments. Biochemistry **36**, 11179-11187

106 Edidin, M. (2003) Lipids on the frontier: a century of cell-membrane bilayers. Nat Rev Mol Cell Biol **4**, 414-418

107 Gennis, R. B. (1989) Biomembranes molecular structure and function Spreinger-Verlag, New york

108 Tanford, C. (1978) The hydrophobic effect and the organization of living matter. Science **200**, 1012-1018

109 Kranenburg, M. and Smit, B. (2005) Phase behavior of model lipid bilayers. J Phys Chem B **109**, 6553-6563

110 Sankaram, M. B. and Thompson, T. E. (1990) Modulation of phospholipid acyl chain order by cholesterol. A solid-state 2H nuclear magnetic resonance study. Biochemistry **29**, 10676-10684

111 Singer, S. J. and Nicolson, G. L. (1972) The fluid mosaic model of the structure of cell membranes. Science **175**, 720-731

112 Simons, K. and Ikonen, E. (1997) Functional rafts in cell membranes. Nature **387**, 569-572

113 de Almeida, R. F., Fedorov, A. and Prieto, M. (2003) Sphingomyelin/phosphatidylcholine/cholesterol phase diagram: boundaries and composition of lipid rafts. Biophys J **85**, 2406-2416

114 Chiantia, S., Kahya, N. and Schwille, P. (2007) Raft domain reorganization driven by short- and long-chain ceramide: a combined AFM and FCS study. Langmuir **23**, 7659-7665

115 Op den Kamp, J. A. (1979) Lipid asymmetry in membranes. Annu Rev Biochem **48**, 47-71

116 Depierre, J. W. and Dallner, G. (1975) Structural aspects of the membrane of the endoplasmic reticulum. Biochim Biophys Acta **415**, 411-472

117 Pomorski, T., Hrafnsdottir, S., Devaux, P. F. and van Meer, G. (2001) Lipid distribution and transport across cellular membranes. Semin Cell Dev Biol **12**, 139-148

118 Bretscher, M. S. (1972) Phosphatidyl-ethanolamine: differential labelling in intact cells and cell ghosts of human erythrocytes by a membrane-impermeable reagent. J Mol Biol **71**, 523-528

119 Crain, R. C. and Zilversmit, D. B. (1980) Two nonspecific phospholipid exchange proteins from beef liver. 2. Use in studying the asymmetry and transbilayer movement of phosphatidylcholine, phosphatidylethanolamine, and sphingomyelin in intact rat erythrocytes. Biochemistry **19**, 1440-1447

120 Verkleij, A. J., Zwaal, R. F., Roelofsen, B., Comfurius, P., Kastelijn, D. and van Deenen, L. L. (1973) The asymmetric distribution of phospholipids in the human red cell membrane. A combined study using phospholipases and freeze-etch electron microscopy. Biochim Biophys Acta **323**, 178-193

121 Daleke, D. L. (2003) Regulation of transbilayer plasma membrane phospholipid asymmetry. J Lipid Res **44**, 233-242

122 Hill, W. G. and Zeidel, M. L. (2000) Reconstituting the barrier properties of a water-tight epithelial membrane by design of leaflet-specific liposomes. J Biol Chem **275**, 30176-30185

123 Zachowski, A. (1993) Phospholipids in animal eukaryotic membranes: transverse asymmetry and movement. Biochem J **294 (Pt 1)**, 1-14

124 O'Shea, P. (2003) Intermolecular interactions with/within cell membranes and the trinity of membrane potentials: kinetics and imaging. Biochem Soc Trans **31**, 990-996

125 Izumida, Y., Seiyama, A. and Maeda, N. (1991) Erythrocyte aggregation: bridging by macromolecules and electrostatic repulsion by sialic acid. Biochim Biophys Acta **1067**, 221-226

126 McLaughlin, S. (1989) The electrostatic properties of membranes. Annu Rev Biophys Biophys Chem **18**, 113-136

127 Cladera, J. and O'Shea, P. (1998) Intramembrane molecular dipoles affect the membrane insertion and folding of a model amphiphilic peptide. Biophys J **74**, 2434-2442

128 Shapovalov, V. L., Kotova, E. A., Rokitskaya, T. I. and Antonenko, Y. N. (1999) Effect of gramicidin A on the dipole potential of phospholipid membranes. Biophys J **77**, 299-305

129 Skerjanc, I. S., Shore, G. C. and Silvius, J. R. (1987) The interaction of a synthetic mitochondrial signal peptide with lipid membranes is independent of transbilayer potential. Embo J **6**, 3117-3123

130 Wall, J., Ayoub, F. and O'Shea, P. (1995) Interactions of macromolecules with the mammalian cell surface. J Cell Sci **108 (Pt 7)**, 2673-2682

131 Wall, J., Golding, C. A., Van Veen, M. and O'Shea, P. (1995) The use of fluoresceinphosphatidylethanolamine (FPE) as a real-time probe for peptide-membrane interactions. Mol Membr Biol **12**, 183-192

132 Veiga, A. S. and Castanho, M. A. (2006) The membranes' role in the HIV-1 neutralizing monoclonal antibody 2F5 mode of action needs re-evaluation. Antiviral Res **71**, 69-72

133 Bangham, A. D., Standish, M. M. and Watkins, J. C. (1965) Diffusion of univalent ions across the lamellae of swollen phospholipids. J Mol Biol **13**, 238-252

134 Mayer, L. D., Hope, M. J. and Cullis, P. R. (1986) Vesicles of variable sizes produced by a rapid extrusion procedure. Biochim Biophys Acta **858**, 161-168

135 Huang, C. (1969) Studies on phosphatidylcholine vesicles. Formation and physical characteristics. Biochemistry **8**, 344-352

136 Ladokhin, A. S., Jayasinghe, S. and White, S. H. (2000) How to measure and analyze tryptophan fluorescence in membranes properly, and why bother? Anal Biochem **285**, 235-245

137 Wieprecht, T., Beyermann, M. and Seelig, J. (2002) Thermodynamics of the coil-alpha-helix transition of amphipathic peptides in a membrane environment: the role of vesicle curvature. Biophys Chem **96**, 191-201

138 Lakowicz, J. R. (1999) Principles of fluorescence spectroscopy. Kluwer Academis, New York

139 Santos, N. C. and Castanho, M. (2002) Fluorescence spectroscopy methodologies on the study of proteins and peptides. On the 150th anniversary of protein fluorescence. Trends Applied Spectroscopy **4**, 113-125

140 Santos, N. C., Prieto, M. and Castanho, M. A. (2003) Quantifying molecular partition into model systems of biomembranes: an emphasis on optical spectroscopic methods. Biochim Biophys Acta **1612**, 123-135

141 Fernandes, M. X., Garcia de la Torre, J. and Castanho, M. A. (2002) Joint determination by Brownian dynamics and fluorescence quenching of the in-depth location profile of biomolecules in membranes. Anal Biochem **307**, 1-12

142 Caputo, G. A. and London, E. (2003) Using a novel dual fluorescence quenching assay for measurement of tryptophan depth within lipid bilayers to determine hydrophobic alpha-helix locations within membranes. Biochemistry **42**, 3265-3274

143 Buser, C. A., Sigal, C. T., Resh, M. D. and McLaughlin, S. (1994) Membrane binding of myristylated peptides corresponding to the NH2 terminus of Src. Biochemistry **33**, 13093-13101

144 Murray, D., Hermida-Matsumoto, L., Buser, C. A., Tsang, J., Sigal, C. T., Ben-Tal, N., Honig, B., Resh, M. D. and McLaughlin, S. (1998) Electrostatics and the membrane association of Src: theory and experiment. Biochemistry **37**, 2145-2159

145 Parasassi, T., Di Stefano, M., Loiero, M., Ravagnan, G. and Gratton, E. (1994) Influence of cholesterol on phospholipid bilayers phase domains as detected by Laurdan fluorescence. Biophys J **66**, 120-132

146 Reyes Mateo, C., Ulises Acuna, A. and Brochon, J. C. (1995) Liquid-crystalline phases of cholesterol/lipid bilayers as revealed by the fluorescence of trans-parinaric acid. Biophys J **68**, 978-987

147 Persson, D., Thoren, P. E. and Norden, B. (2001) Penetratin-induced aggregation and subsequent dissociation of negatively charged phospholipid vesicles. FEBS Lett **505**, 307-312

148 Khlebtsov, B. N., Burygin, G. L., Matora, L. Y., Shchyogolev, S. Y. and Khlebtsov, N. G. (2004) A method for studying insoluble immune complexes. Biochim Biophys Acta **1670**, 199-207

149 Basanez, G. (2002) Membrane fusion: the process and its energy suppliers. Cell Mol Life Sci **59**, 1478-1490

150 Nir, S. and Nieva, J. L. (2000) Interactions of peptides with liposomes: pore formation and fusion. Prog Lipid Res **39**, 181-206

151 Pecheur, E. I., Martin, I., Ruysschaert, J. M., Bienvenue, A. and Hoekstra, D. (1998) Membrane fusion induced by 11-mer anionic and cationic peptides: a structure-function study. Biochemistry **37**, 2361-2371

152 Huebsch, N. D. and Mooney, D. J. (2007) Fluorescent resonance energy transfer: A tool for probing molecular cell-biomaterial interactions in three dimensions. Biomaterials **28**, 2424-2437

153 Henriques, S. T. and Castanho, M. A. (2005) Environmental factors that enhance the action of the cell penetrating peptide pep-1 A spectroscopic study using lipidic vesicles. Biochim Biophys Acta **1669**, 75-86

154 Dupont, E., Joliot, A. and Prochiantz, A. (2002) Penetratins. In Cell-Penetrating Peptides. Processes and Applications. (Langel, U., ed.), pp. 23-51, CRC press, New York

155 Matsuzaki, K., Yoneyama, S. and Miyajima, K. (1997) Pore formation and translocation of melittin. Biophys J **73**, 831-838

156 Papo, N. and Shai, Y. (2003) Exploring peptide membrane interaction using surface plasmon resonance: differentiation between pore formation versus membrane disruption by lytic peptides. Biochemistry **42**, 458-466

157 Matsuzaki, K., Murase, O., Fujii, N. and Miyajima, K. (1995) Translocation of a channel-forming antimicrobial peptide, magainin 2, across lipid bilayers by forming a pore. Biochemistry **34**, 6521-6526

158 Kobayashi, S., Chikushi, A., Tougu, S., Imura, Y., Nishida, M., Yano, Y. and Matsuzaki, K. (2004) Membrane translocation mechanism of the antimicrobial peptide buforin 2. Biochemistry **43**, 15610-15616

159 Chattopadhyay, A. and London, E. (1988) Spectroscopic and ionization properties of N-(7-nitrobenz-2-oxa-1,3-diazol-4-yl)-labeled lipids in model membranes. Biochim Biophys Acta **938**, 24-34

160 Fattal, E., Nir, S., Parente, R. A. and Szoka, F. C. (1994) Pore-Forming Peptides Induce Rapid Phospholipid Flip-Flop in Membranes. Biochemistry **33**, 6721-6731

161 Kol, M. A., de Kroon, A. I. P. M., Rijkers, D. T. S., Killian, J. A. and de Kruijff, B. (2001) Membrane-spanning peptides induce phospholipid flop: A model for

phospholipid translocation across the inner membrane of E-coli. Biochemistry **40**, 10500-10506

162 Matsuzaki, K., Murase, O., Fujii, N. and Miyajima, K. (1996) An antimicrobial peptide, magainin 2, induced rapid flip-flop of phospholipids coupled with pore formation and peptide translocation. Biochemistry **35**, 11361-11368

163 John, K., Schreiber, S., Kubelt, J., Herrmann, A. and Muller, P. (2002) Transbilayer movement of phospholipids at the main phase transition of lipid membranes: implications for rapid flip-flop in biological membranes. Biophys J **83**, 3315-3323

164 Marx, U., Lassmann, G., Holzhutter, H. G., Wustner, D., Muller, P., Hohlig, A., Kubelt, J. and Herrmann, A. (2000) Rapid flip-flop of phospholipids in endoplasmic reticulum membranes studied by a stopped-flow approach. Biophys J **78**, 2628-2640

165 Maier, O., Oberle, V. and Hoekstra, D. (2002) Fluorescent lipid probes: some properties and applications (a review). Chemistry and Physics of Lipids **116**, 3-18

166 Abdalah, R., Wei, L., Francis, K. and Yu, S. P. (2006) Valinomycin-induced apoptosis in Chinese hamster ovary cells. Neurosci Lett **405**, 68-73

167 Rose, L. and Jenkins, A. T. (2007) The effect of the ionophore valinomycin on biomimetic solid supported lipid DPPTE/EPC membranes. Bioelectrochemistry **70**, 387-393

168 Drin, G., Mazel, M., Clair, P., Mathieu, D., Kaczorek, M. and Temsamani, J. (2001) Physico-chemical requirements for cellular uptake of pAntp peptide. Role of lipid-binding affinity. Eur J Biochem **268**, 1304-1314

169 Herbig, M. E., Weller, K., Krauss, U., Beck-Sickinger, A. G., Merkle, H. P. and Zerbe, O. (2005) Membrane surface-associated helices promote lipid interactions and cellular uptake of human calcitonin-derived cell penetrating peptides. Biophys J **89**, 4056-4066

170 Deshayes, S., Gerbal-Chaloin, S., Morris, M. C., Aldrian-Herrada, G., Charnet, P., Divita, G. and Heitz, F. (2004) On the mechanism of non-endosomial peptide-mediated cellular delivery of nucleic acids. Biochim Biophys Acta **1667**, 141-147

171 Zasloff, M. (2002) Antimicrobial peptides of multicellular organisms. Nature **415**, 389-395

172 Shai, Y. (1999) Mechanism of the binding, insertion and destabilization of phospholipid bilayer membranes by alpha-helical antimicrobial and cell non-selective membrane-lytic peptides. Biochim Biophys Acta **1462**, 55-70

173 Ludtke, S., He, K. and Huang, H. (1995) Membrane thinning caused by magainin 2. Biochemistry **34**, 16764-16769

174 Chen, F. Y., Lee, M. T. and Huang, H. W. (2002) Sigmoidal concentration dependence of antimicrobial peptide activities: a case study on alamethicin. Biophys J **82**, 908-914

175 Toke, O. (2005) Antimicrobial peptides: new candidates in the fight against bacterial infections. Biopolymers **80**, 717-735

176 Baumann, G. and Mueller, P. (1974) A molecular model of membrane excitability. J Supramol Struct **2**, 538-557

177 Ojcius, D. M. and Young, J. D. (1991) Cytolytic pore-forming proteins and peptides: is there a common structural motif? Trends Biochem Sci **16**, 225-229

178 Shai, Y. (1995) Molecular recognition between membrane-spanning polypeptides. Trends Biochem Sci **20**, 460-464

179 Zemel, A., Ben-Shaul, A. and May, S. (2005) Perturbation of a lipid membrane by amphipathic peptides and its role in pore formation. Eur Biophys J **34**, 230-242

180 Yang, L., Harroun, T. A., Weiss, T. M., Ding, L. and Huang, H. W. (2001) Barrel-stave model or toroidal model? A case study on melittin pores. Biophys J **81**, 1475-1485

181 Pouny, Y., Rapaport, D., Mor, A., Nicolas, P. and Shai, Y. (1992) Interaction of antimicrobial dermaseptin and its fluorescently labeled analogues with phospholipid membranes. Biochemistry **31**, 12416-12423

182 Shai, Y. (2002) Mode of action of membrane active antimicrobial peptides. Biopolymers **66**, 236-248

183 Seelig, J. (2004) Thermodynamics of lipid-peptide interactions. Biochim Biophys Acta **1666**, 40-50

184 Blondelle, S. E., Lohner, K. and Aguilar, M. (1999) Lipid-induced conformation and lipid-binding properties of cytolytic and antimicrobial peptides: determination and biological specificity. Biochim Biophys Acta **1462**, 89-108

185 Deshayes, S., Heitz, A., Morris, M. C., Charnet, P., Divita, G. and Heitz, F. (2004) Insight into the mechanism of internalization of the cell-penetrating carrier peptide Pep-1 through conformational analysis. Biochemistry **43**, 1449-1457

186 Henriques, S. T. and Castanho, M. A. (2004) Consequences of nonlytic membrane perturbation to the translocation of the cell penetrating peptide pep-1 in lipidic vesicles. Biochemistry **43**, 9716-9724

187 Kelly, S. M. and Price, N. C. (2000) The use of circular dichroism in the investigation of protein structure and function. Curr Protein Pept Sci **1**, 349-384

188 Greenfield, N. J. (1996) Methods to estimate the conformation of proteins and polypeptides from circular dichroism data. Anal Biochem **235**, 1-10

189 Sreerama, N. and Woody, R. W. (2003) Structural composition of betaI- and betaII-proteins. Protein Sci **12**, 384-388

190 van Mierio, C. P. M., de Jongh, H. H. J. and Visser, A. J. W. G. (2000) Circular dichroism of proteins in solution and at interfaces. Applied spectroscopy reviews **35**, 277-313

191 Kelly, S. M., Jess, T. J. and Price, N. C. (2005) How to study proteins by circular dichroism. Biochim Biophys Acta **1751**, 119-139

192 Miles, A. J. and Wallace, B. A. (2006) Synchrotron radiation circular dichroism spectroscopy of proteins and applications in structural and functional genomics. Chem Soc Rev **35**, 39-51

193 Goormaghtigh, E., Raussens, V. and Ruysschaert, J. M. (1999) Attenuated total reflection infrared spectroscopy of proteins and lipids in biological membranes. Biochim Biophys Acta **1422**, 105-185

194 Vigano, C., Manciu, L., Buyse, F., Goormaghtigh, E. and Ruysschaert, J. M. (2000) Attenuated total reflection IR spectroscopy as a tool to investigate the structure, orientation and tertiary structure changes in peptides and membrane proteins. Biopolymers **55**, 373-380

195 Tatulian, S. A. (2003) Attenuated total reflection Fourier transform infrared spectroscopy: a method of choice for studying membrane proteins and lipids. Biochemistry **42**, 11898-11907

196 Goormaghtigh, E., Cabiaux, E. and Ruysschaert, J. M. (1994) Determination of soluble and membrane protein structure by Fourier transform infrared soectroscopy. I. Assignments and model compounds. In Subcellular Biochemistry. Volume 23: Physicochemical methods in the study of Biomembranes (Herwig, J. and Ralston, G. B., eds.), pp. 329-362, Plenum Press, New York

197 Arrondo, J. L. and Goni, F. M. (1999) Structure and dynamics of membrane proteins as studied by infrared spectroscopy. Prog Biophys Mol Biol **72**, 367-405

198 Barth, A. and Zscherp, C. (2002) What vibrations tell us about proteins. Q Rev Biophys **35**, 369-430

199 Torrecillas, A., Martinez-Senac, M. M., Goormaghtigh, E., de Godos, A., Corbalan-Garcia, S. and Gomez-Fernandez, J. C. (2005) Modulation of the membrane orientation and secondary structure of the C-terminal domains of Bak and Bcl-2 by lipids. Biochemistry **44**, 10796-10809

200 Oberg, K. A., Ruysschaert, J. M. and Goormaghtigh, E. (2004) The optimization of protein secondary structure determination with infrared and circular dichroism spectra. Eur J Biochem **271**, 2937-2948

201 Bechinger, B., Ruysschaert, J. M. and Goormaghtigh, E. (1999) Membrane helix orientation from linear dichroism of infrared attenuated total reflection spectra. Biophys J **76**, 552-563

202 Montal, M. and Mueller, P. (1972) Formation of bimolecular membranes from lipid monolayers and a study of their electrical properties. Proc Natl Acad Sci U S A **69**, 3561-3566

203 Bivas, I. and Danelon, C. (2004) Fields and forces acting on a planar membrane with a conducting channel. Phys Rev E Stat Nonlin Soft Matter Phys **69**, 041901

204 Fuks, B. and Homble, F. (1994) Permeability and electrical properties of planar lipid membranes from thylakoid lipids. Biophys J **66**, 1404-1414

205 Micelli, S., Gallucci, E., Meleleo, D., Stipani, V. and Picciarelli, V. (2002) Mitochondrial porin incorporation into black lipid membranes: ionic and gating contribution to the total current. Bioelectrochemistry **57**, 97-106

206 Fidorra, M., Duelund, L., Leidy, C., Simonsen, A. C. and Bagatolli, L. A. (2006) Absence of fluid-ordered/fluid-disordered phase coexistence in ceramide/POPC mixtures containing cholesterol. Biophys J **90**, 4437-4451

207 Angelova, M. I. and Dimitrov, D. S. (1986) Liposome electroformation. Faraday Discuss. Chem. Soc. **81**, 303-311

208 Ambroggio, E. E., Separovic, F., Bowie, J. H., Fidelio, G. D. and Bagatolli, L. A. (2005) Direct visualization of membrane leakage induced by the antibiotic peptides: maculatin, citropin, and aurein. Biophys J **89**, 1874-1881

209 Ambroggio, E. E., Kim, D. H., Separovic, F., Barrow, C. J., Barnham, K. J., Bagatolli, L. A. and Fidelio, G. D. (2005) Surface behavior and lipid interaction of Alzheimer beta-amyloid peptide 1-42: a membrane-disrupting peptide. Biophys J **88**, 2706-2713

210 Bagatolli, L. A. and Gratton, E. (1999) Two-photon fluorescence microscopy observation of shape changes at the phase transition in phospholipid giant unilamellar vesicles. Biophys J **77**, 2090-2101

211 Nichols, B. J. and Lippincott-Schwartz, J. (2001) Endocytosis without clathrin coats. Trends Cell Biol **11**, 406-412

212 Stryer, L. (1996) Biochemistry. W. H. Freeman and company, New York

213 Cardelli, J. (2001) Phagocytosis and macropinocytosis in Dictyostelium: phosphoinositide-based processes, biochemically distinct. Traffic **2**, 311-320

214 Conner, S. D. and Schmid, S. L. (2003) Regulated portals of entry into the cell. Nature **422**, 37-44

215 Soldati, T. and Schliwa, M. (2006) Powering membrane traffic in endocytosis and recycling. Nat Rev Mol Cell Biol **7**, 897-908

216 Mayor, S. and Pagano, R. E. (2007) Pathways of clathrin-independent endocytosis. Nat Rev Mol Cell Biol **8**, 603-612

217 Meier, O. and Greber, U. F. (2003) Adenovirus endocytosis. J Gene Med **5**, 451-462

218 Swanson, J. A. and Watts, C. (1995) Macropinocytosis. Trends Cell Biol **5**, 424-428

219 Lewin, B. (2000) Genes VII. Oxford University Press, Oxford

220 Hammond, A. T. and Glick, B. S. (2000) Dynamics of transitional endoplasmic reticulum sites in vertebrate cells. Mol Biol Cell **11**, 3013-3030

221 Sousa, V. L., Brito, C. and Costa, J. (2004) Deletion of the cytoplasmic domain of human alpha3/4 fucosyltransferase III causes the shift of the enzyme to early Golgi compartments. Biochim Biophys Acta **1675**, 95-104

222 Zhao, X., Lasell, T. K. and Melancon, P. (2002) Localization of large ADP-ribosylation factor-guanine nucleotide exchange factors to different Golgi compartments: evidence for distinct functions in protein traffic. Mol Biol Cell **13**, 119-133

223 Griffith, K. L. and Wolf, R. E., Jr. (2002) Measuring beta-galactosidase activity in bacteria: cell growth, permeabilization, and enzyme assays in 96-well arrays. Biochem Biophys Res Commun **290**, 397-402

224 McGuire, J. B., James, T. J., Imber, C. J., St Peter, S. D., Friend, P. J. and Taylor, R. P. (2002) Optimisation of an enzymatic method for beta-galactosidase. Clin Chim Acta **326**, 123-129

225 Remani, P., Ostapenko, V. V., Akagi, K., Bhattathiri, V. N., Nair, M. K. and Tanaka, Y. (1999) Relation of transmembrane potential to cell survival following hyperthermia in HeLa cells. Cancer Lett **144**, 117-123

226 Li, Y., Um, S. Y. and McDonald, T. V. (2006) Voltage-gated potassium channels: regulation by accessory subunits. Neuroscientist **12**, 199-210

227 Iliev, I. G. and Marino, A. A. (1993) Potassium channels in epithelial cells. Cell Mol Biol Res **39**, 601-611

228 Chifflet, S., Hernandez, J. A., Grasso, S. and Cirillo, A. (2003) Nonspecific depolarization of the plasma membrane potential induces cytoskeletal modifications of bovine corneal endothelial cells in culture. Exp Cell Res **282**, 1-13

229 Sheline, C. T., Takata, T., Ying, H., Canzoniero, L. M., Yang, A., Yu, S. P. and Choi, D. W. (2004) Potassium attenuates zinc-induced death of cultured cortical astrocytes. Glia **46**, 18-27

230 Henriques, S. T., Costa, J. and Castanho, M. A. (2005) Translocation of beta-galactosidase mediated by the cell-penetrating peptide pep-1 into lipid vesicles and human HeLa cells is driven by membrane electrostatic potential. Biochemistry **44**, 10189-10198

231 Scheller, A., Wiesner, B., Melzig, M., Bienert, M. and Oehlke, J. (2000) Evidence for an amphipathicity independent cellular uptake of amphipathic cell-penetrating peptides. Eur J Biochem **267**, 6043-6050

232 Kramer, S. D. and Wunderli-Allenspach, H. (2003) No entry for TAT(44-57) into liposomes and intact MDCK cells: novel approach to study membrane permeation of cell-penetrating peptides. Biochim Biophys Acta **1609**, 161-169

233 Takeshima, K., Chikushi, A., Lee, K. K., Yonehara, S. and Matsuzaki, K. (2003) Translocation of analogues of the antimicrobial peptides magainin and buforin across human cell membranes. J Biol Chem **278**, 1310-1315

234 Thoren, P. E., Persson, D., Esbjorner, E. K., Goksor, M., Lincoln, P. and Norden, B. (2004) Membrane binding and translocation of cell-penetrating peptides. Biochemistry **43**, 3471-3489

235 Barany-Wallje, E., Keller, S., Serowy, S., Geibel, S., Pohl, P., Bienert, M. and Dathe, M. (2005) A critical reassessment of penetratin translocation across lipid membranes. Biophys J **89**, 2513-2521

236 Esteve, E., Mabrouk, K., Dupuis, A., Smida-Rezgui, S., Altafaj, X., Grunwald, D., Platel, J. C., Andreotti, N., Marty, I., Sabatier, J. M., Ronjat, M. and De Waard, M. (2005) Transduction of the scorpion toxin maurocalcine into cells. Evidence that the toxin crosses the plasma membrane. J Biol Chem **280**, 12833-12839

237 Farrera-Sinfreu, J., Giralt, E., Castel, S., Albericio, F. and Royo, M. (2005) Cell-penetrating cis-gamma-amino-l-proline-derived peptides. J Am Chem Soc **127**, 9459-9468

238 Holm, T., Netzereab, S., Hansen, M., Langel, U. and Hallbrink, M. (2005) Uptake of cell-penetrating peptides in yeasts. FEBS Lett **579**, 5217-5222

239 Jones, S. W., Christison, R., Bundell, K., Voyce, C. J., Brockbank, S. M., Newham, P. and Lindsay, M. A. (2005) Characterisation of cell-penetrating peptide-mediated peptide delivery. Br J Pharmacol **145**, 1093-1102

240 Mae, M., Myrberg, H., Jiang, Y., Paves, H., Valkna, A. and Langel, U. (2005) Internalisation of cell-penetrating peptides into tobacco protoplasts. Biochim Biophys Acta **1669**, 101-107

241 Maiolo, J. R., Ferrer, M. and Ottinger, E. A. (2005) Effects of cargo molecules on the cellular uptake of arginine-rich cell-penetrating peptides. Biochim Biophys Acta **1712**, 161-172

242 Mano, M., Teodosio, C., Paiva, A., Simoes, S. and Pedroso de Lima, M. C. (2005) On the mechanisms of the internalization of S4(13)-PV cell-penetrating peptide. Biochem J **390**, 603-612

243 Parenteau, J., Klinck, R., Good, L., Langel, U., Wellinger, R. J. and Elela, S. A. (2005) Free uptake of cell-penetrating peptides by fission yeast. FEBS Lett **579**, 4873-4878

244 Rennert, R., Wespe, C., Beck-Sickinger, A. G. and Neundorf, I. (2006) Developing novel hCT derived cell-penetrating peptides with improved metabolic stability. Biochim Biophys Acta **1758**, 347-354

245 Veach, R. A., Liu, D., Yao, S., Chen, Y., Liu, X. Y., Downs, S. and Hawiger, J. (2004) Receptor/transporter-independent targeting of functional peptides across the plasma membrane. J Biol Chem **279**, 11425-11431

246 Bjorklund, J., Biverstahl, H., Graslund, A., Maler, L. and Brzezinski, P. (2006) Real-time transmembrane translocation of penetratin driven by light-generated proton pumping. Biophys J **91**, L29-31

247 Bodor, N., Toth-Sarudy, E., Holm, T., Pallagi, I., Vass, E., Buchwald, P. and Langel, U. (2007) Novel, cell-penetrating molecular transporters with flexible backbones and permanently charged side-chains. J Pharm Pharmacol **59**, 1065-1076

248 Duchardt, F., Fotin-Mleczek, M., Schwarz, H., Fischer, R. and Brock, R. (2007) A comprehensive model for the cellular uptake of cationic cell-penetrating peptides. Traffic **8**, 848-866

249 D'Ursi, A. M., Giusti, L., Albrizio, S., Porchia, F., Esposito, C., Caliendo, G., Gargini, C., Novellino, E., Lucacchini, A., Rovero, P. and Mazzoni, M. R. (2006) A membrane-permeable peptide containing the last 21 residues of the G alpha(s) carboxyl terminus inhibits G(s)-coupled receptor signaling in intact cells: correlations between peptide structure and biological activity. Mol Pharmacol **69**, 727-736

250 Fernandez-Carneado, J., Kogan, M. J., Van Mau, N., Pujals, S., Lopez-Iglesias, C., Heitz, F. and Giralt, E. (2005) Fatty acyl moieties: improving Pro-rich peptide uptake inside HeLa cells. J Pept Res **65**, 580-590

251 Fretz, M. M., Penning, N. A., Al-Taei, S., Futaki, S., Takeuchi, T., Nakase, I., Storm, G. and Jones, A. T. (2007) Temperature-, concentration- and cholesterol-dependent translocation of L- and D-octa-arginine across the plasma and nuclear membrane of CD34+ leukaemia cells. Biochem J **403**, 335-342

252 Mabrouk, K., Ram, N., Boisseau, S., Strappazzon, F., Rehaim, A., Sadoul, R., Darbon, H., Ronjat, M. and De Waard, M. (2007) Critical amino acid residues of maurocalcine involved in pharmacology, lipid interaction and cell penetration. Biochim Biophys Acta **1768**, 2528-2540

253 Palm, C., Netzereab, S. and Hallbrink, M. (2006) Quantitatively determined uptake of cell-penetrating peptides in non-mammalian cells with an evaluation of degradation and antimicrobial effects. Peptides **27**, 1710-1716

254 Rhee, M. and Davis, P. (2006) Mechanism of uptake of C105Y, a novel cell-penetrating peptide. J Biol Chem **281**, 1233-1240

255 Wu, R. P., Youngblood, D. S., Hassinger, J. N., Lovejoy, C. E., Nelson, M. H., Iversen, P. L. and Moulton, H. M. (2007) Cell-penetrating peptides as transporters for morpholino oligomers: effects of amino acid composition on intracellular delivery and cytotoxicity. Nucleic Acids Res **35**, 5182-5191

256 Marinova, Z., Vukojevic, V., Surcheva, S., Yakovleva, T., Cebers, G., Pasikova, N., Usynin, I., Hugonin, L., Fang, W., Hallberg, M., Hirschberg, D., Bergman, T., Langel, U., Hauser, K. F., Pramanik, A., Aldrich, J. V., Graslund, A., Terenius, L. and Bakalkin, G. (2005) Translocation of dynorphin neuropeptides across the plasma membrane. A putative mechanism of signal transmission. J Biol Chem **280**, 26360-26370

257 Mano, M., Henriques, A., Paiva, A., Prieto, M., Gavilanes, F., Simoes, S. and Pedroso de Lima, M. C. (2006) Cellular uptake of S4(13)-PV peptide occurs upon

conformational changes induced by peptide-membrane interactions. Biochim Biophys Acta **1758**, 336-346

258 Boisseau, S., Mabrouk, K., Ram, N., Garmy, N., Collin, V., Tadmouri, A., Mikati, M., Sabatier, J. M., Ronjat, M., Fantini, J. and De Waard, M. (2006) Cell penetration properties of maurocalcine, a natural venom peptide active on the intracellular ryanodine receptor. Biochim Biophys Acta **1758**, 308-319

259 Szeto, H. H., Schiller, P. W., Zhao, K. and Luo, G. (2005) Fluorescent dyes alter intracellular targeting and function of cell-penetrating tetrapeptides. Faseb J **19**, 118-120

260 Haugland, R. P. (2002) Handbook of fliorescent probes and research products. Molecular Probes, Inc., Eugene

261 Rink, T. J., Montecucco, C., Hesketh, T. R. and Tsien, R. Y. (1980) Lymphocyte membrane potential assessed with fluorescent probes. Biochim Biophys Acta **595**, 15-30

262 Wan, C. P., Park, C. S. and Lau, B. H. (1993) A rapid and simple microfluorometric phagocytosis assay. J Immunol Methods **162**, 1-7

263 Schwartz, J. W., Blakely, R. D. and DeFelice, L. J. (2003) Binding and transport in norepinephrine transporters. Real-time, spatially resolved analysis in single cells using a fluorescent substrate. J Biol Chem **278**, 9768-9777

264 Wang, Z., Leisner, T. M. and Parise, L. V. (2003) Platelet alpha2beta1 integrin activation: contribution of ligand internalization and the alpha2-cytoplasmic domain. Blood **102**, 1307-1315

265 Rejman, J., Oberle, V., Zuhorn, I. S. and Hoekstra, D. (2004) Size-dependent internalization of particles via the pathways of clathrin- and caveolae-mediated endocytosis. Biochem J **377**, 159-169

266 Mosiman, V. L., Patterson, B. K., Canterero, L. and Goolsby, C. L. (1997) Reducing cellular autofluorescence in flow cytometry: an in situ method. Cytometry **30**, 151-156

267 Zuhorn, I. S., Kalicharan, R. and Hoekstra, D. (2002) Lipoplex-mediated transfection of mammalian cells occurs through the cholesterol-dependent clathrin-mediated pathway of endocytosis. J Biol Chem **277**, 18021-18028

268 Henriques, S. T. and Castanho, M. A. (2007) Translocation or membrane disintegration? Implication of peptide-membrane interactions in pep-1 activity. J Pept Sci **In press**

269 Henriques, S. T., Quintas, A., Bagatolli, L. A., Homble, F. and Castanho, M. A. (2007) Energy-independent translocation of cell-penetrating peptides occurs without formation of pores. A biophysical study with pep-1. Mol Membr Biol **24**, 282-293

270 Weller, K., Lauber, S., Lerch, M., Renaud, A., Merkle, H. P. and Zerbe, O. (2005) Biophysical and biological studies of end-group-modified derivatives of Pep-1. Biochemistry **44**, 15799-15811

271 Zhu, W. L., Lan, H., Park, I. S., Kim, J. I., Jin, H. Z., Hahm, K. S. and Shin, S. Y. (2006) Design and mechanism of action of a novel bacteria-selective antimicrobial peptide from the cell-penetrating peptide Pep-1. Biochem Biophys Res Commun **349**, 769-774

272 Deshayes, S., Plenat, T., Charnet, P., Divita, G., Molle, G. and Heitz, F. (2006) Formation of transmembrane ionic channels of primary amphipathic cell-penetrating peptides. Consequences on the mechanism of cell penetration. Biochim Biophys Acta **1758**, 1846-1851

273 Killian, J. A. and von Heijne, G. (2000) How proteins adapt to a membrane-water interface. Trends Biochem Sci **25**, 429-434

274 Yau, W. M., Wimley, W. C., Gawrisch, K. and White, S. H. (1998) The preference of tryptophan for membrane interfaces. Biochemistry **37**, 14713-14718

275 Vives, E., Richard, J. P., Rispal, C. and Lebleu, B. (2003) TAT peptide internalization: seeking the mechanism of entry. Curr Protein Pept Sci **4**, 125-132

276 Henriques, S. T., Costa, J. and Castanho, M. A. (2005) Re-evaluating the role of strongly charged sequences in amphipathic cell-penetrating peptides: a fluorescence study using Pep-1. FEBS Lett **579**, 4498-4502

277 Henriques, S. T., Melo, M. N. and Castanho, M. A. (2006) Cell-penetrating peptides and antimicrobial peptides: how different are they? Biochem J **399**, 1-7

278 Christiaens, B., Symoens, S., Verheyden, S., Engelborghs, Y., Joliot, A., Prochiantz, A., Vandekerckhove, J., Rosseneu, M. and Vanloo, B. (2002) Tryptophan fluorescence study of the interaction of penetratin peptides with model membranes. Eur J Biochem **269**, 2918-2926

279 Magzoub, M., Kilk, K., Eriksson, L. E., Langel, U. and Graslund, A. (2001) Interaction and structure induction of cell-penetrating peptides in the presence of phospholipid vesicles. Biochim Biophys Acta **1512**, 77-89

280 Thoren, P. E., Persson, D., Lincoln, P. and Norden, B. (2005) Membrane destabilizing properties of cell-penetrating peptides. Biophys Chem **114**, 169-179

281 Ziegler, A., Nervi, P., Durrenberger, M. and Seelig, J. (2005) The cationic cell-penetrating peptide CPP(TAT) derived from the HIV-1 protein TAT is rapidly transported into living fibroblasts: optical, biophysical, and metabolic evidence. Biochemistry **44**, 138-148

282 Tunnemann, G., Martin, R. M., Haupt, S., Patsch, C., Edenhofer, F. and Cardoso, M. C. (2006) Cargo-dependent mode of uptake and bioavailability of TAT-containing proteins and peptides in living cells. Faseb J **20**, 1775-1784

283 Mano, M., Henriques, A., Paiva, A., Prieto, M., Gavilanes, F., Simoes, S. and de Lima, M. C. (2007) Interaction of S413-PV cell penetrating peptide with model membranes: relevance to peptide translocation across biological membranes. J Pept Sci **13**, 301-313

284 Hallbrink, M., Oehlke, J., Papsdorf, G. and Bienert, M. (2004) Uptake of cell-penetrating peptides is dependent on peptide-to-cell ratio rather than on peptide concentration. Biochim Biophys Acta **1667**, 222-228

285 Binder, H. and Lindblom, G. (2003) Charge-dependent translocation of the Trojan peptide penetratin across lipid membranes. Biophys J **85**, 982-995

286 Henriques, S. T., Melo, M. N. and Castanho, M. A. (2007) How to address CPP and AMP translocation? Methods to detect and quantify peptide internalization in vitro and in vivo (Review). Mol Membr Biol **24**, 173-184